VOLUME II
OF
TECHNICAL REPORT

ON

ANALYSIS OF NUCLEAR WASTE DISPOSAL IN SPACE--PHASE III

TO

NATIONAL AERONAUTICS AND
SPACE ADMINISTRATION
MARSHALL SPACE FLIGHT CENTER
(Contract Number NAS8-32391)
DPD No. 580, DR No. 4

March 31, 1980

Eric E. Rice
E. E. Rice, Program Manager
Battelle's Columbus Laboratories
Columbus, Ohio

C. C. Priest
C. C. Priest, COR
NASA/Marshall Space Flight Center
Huntsville, Alabama

BATTELLE
Columbus Laboratories
505 King Avenue
Columbus, Ohio 43201

FOREWORD

The study summarized in this report is a part of an ongoing analysis to determine the feasibility and preferred approaches for disposal of selected high-level nuclear wastes in space. The Battelle Columbus Laboratory (BCL) study is an integral part of the ongoing Office of Nuclear Waste Isolation (ONWI) managed DOE/NASA program for study of nuclear waste disposal in space, and was conducted in parallel with efforts at NASA Marshall Space Flight Center (MSFC); Science Applications, Inc. (SAI--under subcontract to Battelle and reported here); Battelle's Human Affairs Research Centers (HARC); Bechtel National, Inc.; and Oak Ridge National Laboratory (ORNL). The research effort reported here (Phase III) was performed by Battelle's Columbus Laboratories (with SAI being a subcontractor for Task 4) under NASA Contract NAS8-32391 from June 1979 through March 1980. The study objective was to provide NASA and DOE with additional technical data and information in specialized areas as a basis for developing space disposal concept definitions, requirements, and program plans.

The information developed during the study period is contained in this two-volume final report. The title of each volume is listed below.

Volume I Executive Summary
Volume II Technical Report

Inquiries regarding this study should be addressed to:

C. C. (Pete) Priest, COR
NASA/Marshall Space Flight Center
Attention: PS04
Huntsville, Alabama 35812
Telephone: (205) 453-2769

Eric E. Rice, Program Manager
Battelle's Columbus Laboratories
505 King Avenue
Columbus, Ohio 43201
Telephone: (614) 424-5103

ACKNOWLEDGMENTS

The principal authors, Eric E. Rice, Neil E. Miller, Kenneth R. Yates, William E. Martin, and Alan L. Friedlander (SAI) acknowledge the generous assistance of the following individuals who provided significant contributions to the technical content of this report:

Michael E. Balmert	Richard G. Jung
Sanford G. Bloom	Kenneth D. Kok
David P. Boerschlein	Philip M. Lindsey
Anthony A. Boiarski	Albert E. Weller
Donald S. Edgecombe	William C. Wells (SAI)
Ira M. Grinberg	Gale R. Whitacre

Acknowledgment is also made to the outstanding guidance and cooperation by the NASA/MSFC study monitor, Mr. Claude C. (Pete) Priest, and by various members of the MSFC staff, particularly Robert F. Nixon, William E. Galloway, Rowland E. Burns, and Wilber A. Riehl. Also, special thanks must go to Ralph E. Best, Manager of Alternative Concepts at the Department of Energy (DOE) Office of Nuclear Waste Isolation (ONWI), Columbus, Ohio, and Philip R. Compton, Energy Systems Division, Office of Aeronautics and Space Technology, NASA/Headquarters, Washington, D.C. for their guidance throughout the study.

TABLE OF CONTENTS

TABLE OF CONTENTS
(Continued)

TABLE OF CONTENTS
(Continued)

TABLE OF CONTENTS
(Continued)

TABLE OF CONTENTS
(Continued)

TABLE OF CONTENTS
(Continued)

TABLE OF CONTENTS
(Continued)

TABLE OF CONTENTS
(Continued)

APPENDIXES

TABLE OF CONTENTS
(Continued)

APPENDIXES (continued)

LIST OF FIGURES

TABLE OF CONTENTS
(Continued)

Page

LIST OF FIGURES
(Continued)

TABLE OF CONTENTS
(Continued)

Page

LIST OF FIGURES
(Continued)

TABLE OF CONTENTS
(Continued)

Page

LIST OF FIGURES
(Continued)

TABLE OF CONTENTS
(Continued)

Page

LIST OF FIGURES
(Continued)

TABLE OF CONTENTS
(Continued)

Page

LIST OF FIGURES
(Continued)

TABLE OF CONTENTS
(Continued)

Page

LIST OF FIGURES
(Continued)

LIST OF TABLES

TABLE OF CONTENTS
(Continued)

Page

LIST OF TABLES
(Continued)

TABLE OF CONTENTS
(Continued)

Page

LIST OF TABLES
(Continued)

TABLE OF CONTENTS
(Continued)

Page

LIST OF TABLES
(Continued)

TABLE OF CONTENTS
(Continued)

LIST OF TABLES
(Continued)

TABLE OF CONTENTS
(Continued)

Page

LIST OF TABLES
(Continued)

1.0 INTRODUCTION

This volume (Volume II) summarizes the results of the 1979-1980 Phase III Battelle Columbus Laboratory study of nuclear waste disposal in space. The study objective was to provide NASA and DOE with additional technical data and information in specialized areas as a basis for developing space disposal concept definitions, requirements, and program plans. To accomplish the objective of the study, five basic tasks were defined:

- Nuclear Waste Payload Characterization (Task 1)
- Safety Assessment (Task 2)
- Health Effects Assessment (Task 3)
- Long-Term Risk Assessment (Task 4)
- Program Planning Support Analysis (Task 5)

Tasks 1, 2, 3 and 5 were conducted by Battelle; Task 4 was performed by Science Applications, Inc. (SAI) under subcontract. During the study, a considerable amount of interaction existed among the study tasks and with NASA and DOE. Figure 1-1 illustrates this interaction. Table 1-1 relates the study tasks to sections contained (also page number) in this Technical Report. The following paragraphs briefly describe the contents of this volume. Volume I is the Executive Summary of Volume II.

Section 2 summarizes the current reference concept for nuclear waste disposal in space, and is based upon the Concept Definition Document developed for NASA/Marshall Space Flight Center as a part of this study. Aspects covered in this section include: (1) major concept options; (2) a reference concept overview; (3) a reference concept mission description; (4) reference mission element characteristics; (5) system safety design requirements; (6) major contingency plans for accidents and/or malfunctions; (7) a reference launch traffic model, system hardware and propellant requirements; and (8) an advanced space disposal concept that employs a heavy lift launch vehicle.

Section 3 reports the work accomplished under the commercial and defense waste payload characterization activity (Task 1). The waste form evaluation and selection process is documented (Section 3.1) along with the physical characteristics of the chosen reference waste form (iron/nickel-based cermet matrix). The radionuclide inventories for the reference commercial waste (BNWL PW-4b) and defense waste (Hanford) are defined in detail (Section 3.2). A draft Containment Requirements Document was prepared during the study and is presented in Section 3.3. Section 3.4 presents the results of a parametric shielding and cooling analysis; data are presented for both commercial and defense waste. Section 3.5 describes waste processing and payload fabrication for the reference space disposal concept.

The safety assessment (Task 2) is summarized in Section 4.0. The review of various safety studies for space nuclear payloads was conducted. The documents reviewed, including safety aspects of ratioisotope thermal generators (RTGS), the General Purpose Heat Source (GPHS), and Lewis Research Center concept for space disposal, as well as some other discussions of interest, are

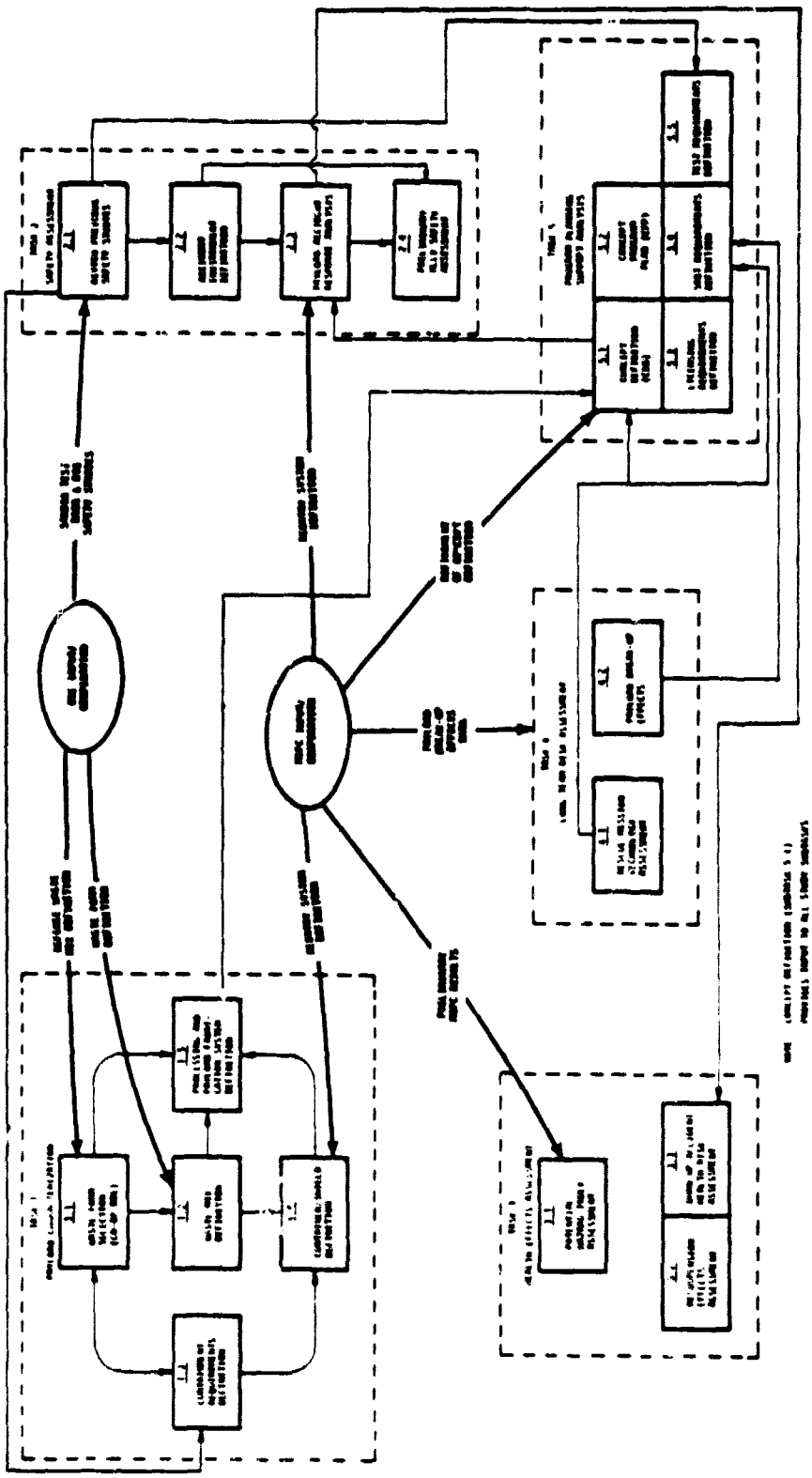

FIGURE 1-1. TASK SUMMARY AND INTERRELATIONSHIPS--PHASE III STUDY

TABLE 1-1. RELATIONSHIP BETWEEN STUDY TASKS AND SECTIONS OF THIS THIS TECHNICAL REPORT FOR THE BCL PHASE III STUDY

Study Task	Final Report Section	Page Number
Task 1 - Payload Characterization	3.0	3-1
1.1 Waste Form Selection	3.1	3-2
1.2 Waste Mix Definition	3.2	3-9
1.3 Containment Requirements Definition	3.3	3-22
1.4 Container/Shield Definition	3.4	3-33
1.5 Processing and Payload Fabrication Definition	3.5	3-51
Task 2 - Safety Assessment	4.0	4-1
2.1 Safety Study Review	4.1	4-2
2.2 Accident Environment Definition	4.2	4-13
2.3 Payload Accident Response Analysis	4.3	4-55
2.4 Preliminary HLLV Safety Assessment	4.4	4-82
Task 3 - Health Effects Assessment	5.0	5-1
3.1 Hazard Index Evaluation	5.1	5-2
3.2 Resuspension Effects	5.2	5-8
3.3 Burnup Accident Analysis	5.3	5-13
Task 4 - Long-Term Risk Assessment (conducted by SAI)	6.0	6-1
4.1 Rescue Mission Technology Assessment	6.2	6-26
4.2 Payload Breakup Effects	6.1	6-3
Task 5 - Program Planning Support Analysis	7.0	7-1
5.1 Concept Definition	7.1,2.0	7-2
5.2 Concept Definition & Evaluation Program Plan	7.2*	7-3
5.3 Licensing Requirements Definition	7.3	7-6
5.4 SR&T Requirements	7.4	7-15
5.5 Safety Test Requirements	7.5	7-24

* Note: The major output for this activity resulted in the "Concept Definition and Evaluation Program Plan for the Space Disposal of Nuclear Waste, 1980-1983," dated January 28, 1980.

presented in Section 4.1. The on-pad catastrophic accident environments for the Uprated Space Shuttle (see Section 2.4.8 for definition) and the heavy lift launch vehicle (HLLV--see Section 2.8.5 for definition) are described in Section 4.2. These accident environments have been characterized in terms of blast overpressures and impulses, fragment sizes and velocities, liquid propellant fireball temperatures and heat fluxes, and residual fire temperatures and heat fluxes. This information will be useful in future payload response studies. The thermal accident environments for on-pad booster failures formed the basis for: (1) a limited survivability analysis that is described in Section 4.3; and (2) the preliminary conclusions related to the HLLV safety assessment (Section 4.4). Section 4.3 also presents the analyses for the inadvertent reentry of the payload containers. Design changes to the reference concept have also been recommended. Section 4.4 provides the results of a preliminary safety assessment for using the HLLV as the boost vehicle for the space disposal option.

Section 5 summarizes the results of the health effects assessment. The ORIGEN dilution hazard index model was exercised in an attempt to aid in the determination of the radionuclides that contribute most to the long-term risk of terrestrial disposal. The results from an EPA pathway hazard model were also evaluated. Discussions of these are presented in Section 5.1. The effects of resuspension of fallout particles from an accidental release of waste material is discussed in Section 5.2. A resuspension model was chosen for use in the health effects model. A health effects assessment (upper atmospheric burnup) was conducted (see section 5.3) employing data developed in the payload response analysis (described in Section 4.3). Design changes to the reference concept have been motivated, based upon upon this health effects assessment (see Section 4.3).

Section 6.0 presents the results of the payload breakup analysis (Task 4.2) and rescue technology assessment (Task 4.1) conducted by SAI, under subcontract. Section 6.1 describes the assumptions and considerations made in the deep space payload breakup analysis. The analysis was conducted for both calcine powder and cermet matrix waste forms and two solar orbit disposal regions were considered. Section 6.2 presents the results of a preliminary rescue technology assessment for the nuclear waste disposal mission. Previous works have been reviewed and certain approaches have been recommended for further consideration.

Section 7 describes the effort on the program planning support analysis task. Sections 7.1 and 7.2 briefly discuss the work performed to prepare two documents: (1) the Concept Definition Document (CDD); and (2) the Concept Definition and Evaluation Program Plan. A slightly modified version of the CDD is presented in Section 2. A very brief discussion of the program plan is presented. Sections 7.3, 7.4 and 7.5 describe the expected requirements for licensing, supporting research and technology (SR&T), and safety testing.

Sections 8 and 9 present the conclusions and recommenations that have resulted from this Phase III study. Appendix A provides definitions of acronyms and abbreviations used in this volume. Appendix B contains appropriate metric to English unit conversion factors. Appendixes C through J,

supporting various aspects of the analyses performed here, are located at the end of this volume.

References indicated in the text are found at the end of each major section.

2.0 REFERENCE CONCEPT DEFINITION AND OPTIONS SUMMARY

The purpose of this section is to summarize the various options, reference definitions and/or requirements currently envisioned for the total nuclear waste disposal in space mission.(2-1)* Many reference definitions and requirements defined in this section were employed in the study and are documented here, but due to the evolving nature of the space disposal option, especially with regard to requirements, many have not been used. It is expected that follow-on studies will use and update these reference definitions and requirements.

Section 2.1 identifies major mission options available for the space disposal of nuclear waste (including alternative waste sources through to the alternate final space destinations), notes the reference and primary alternatives, and identifies options no longer considered viable. Section 2.2 provides a brief overview of the reference space disposal concept by outlining the "single thread" characteristics, all the way from the waste source to the space destination. Section 2.3 defines the reference mission, emphasizing operational or procedural aspects. Definitions for specific reference mission elements (e.g., waste payload characteristics, space systems and facilities) are provided in Section 2.4; emphasis is on hardware and facilities. Section 2.5 describes currently envisioned system safety design requirements. Section 2.6 describes the major contingency plans and systems that have been defined for the overall reference mission to minimize effects caused by possible accidents and/or malfunctions. General space system hardware and propellant requirements for the early years (1990's) of the waste disposal activity are identified in Section 2.7. Section 2.8 defines an advanced disposal concept which employs the use of a Space Power System (SPS)-derived heavy lift launch vehicle for the space booster to low Earth orbit. This concept is believed to be possible in the 2000 to 2010 time period. References are listed in Section 2.9.

---

*Note: This section has been derived from the latest version of the Concept Definition Document, see Reference 2-1. The "reference concept is a space disposal concept that has been defined and documented by the Concept Definition Working Group made up of NASA/Hq, NASA/MSFC, BCL, and SAI personnel. The reference concept is believed to be representative of what could be done to rid the Earth of hazardous nuclear wastes and allows trade-off studies to be performed such that the concept can be properly improved. However, the reference concept is expected to change during the planned 4-year Concept Definition and Evaluation Program (1980-1983).

2.1 Concept Options

The reference concept for the initial space disposal of nuclear waste has been developed from a considerable number of options available at each step along the way from the reactor to the ultimate space disposal destination. A summary of the various options available is shown in Figure 2-1. The reference mission options are shown in the blocks; primary alternatives are indicated by an asterisk; and those options no longer considered viable have lines drawn through them. Discussions of many of these options are available in References 2-2 through 2-13.

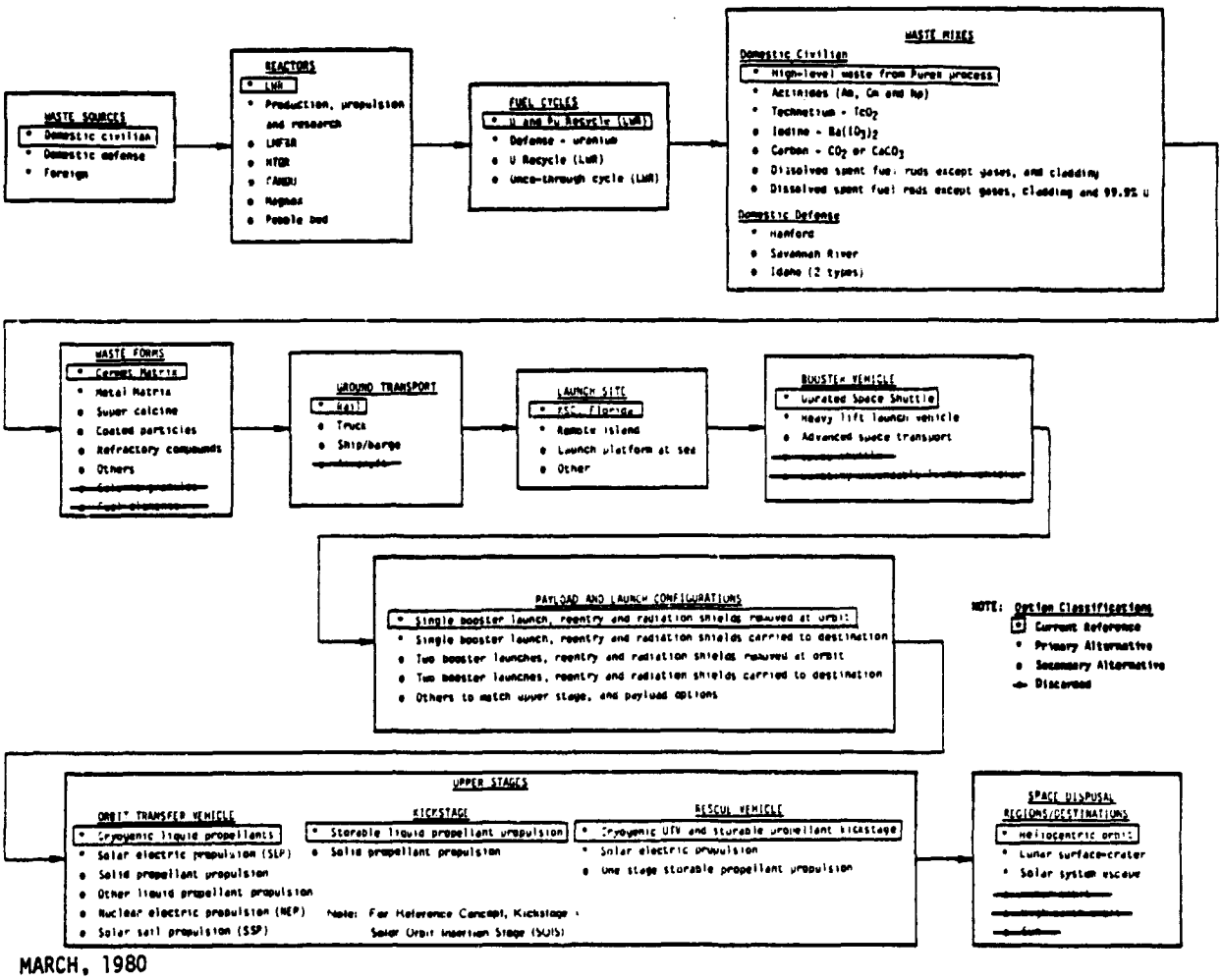

FIGURE 2-1. MAJOR OPTIONS FOR SPACE DISPOSAL OF NUCLEAR WASTE

2.2 Reference Concept Overview

This section provides a brief overview of the reference concept, from the chosen waste source to the final space destination. Reference options for this concept, shown in Figure 2-2, are described in subsequent sections.

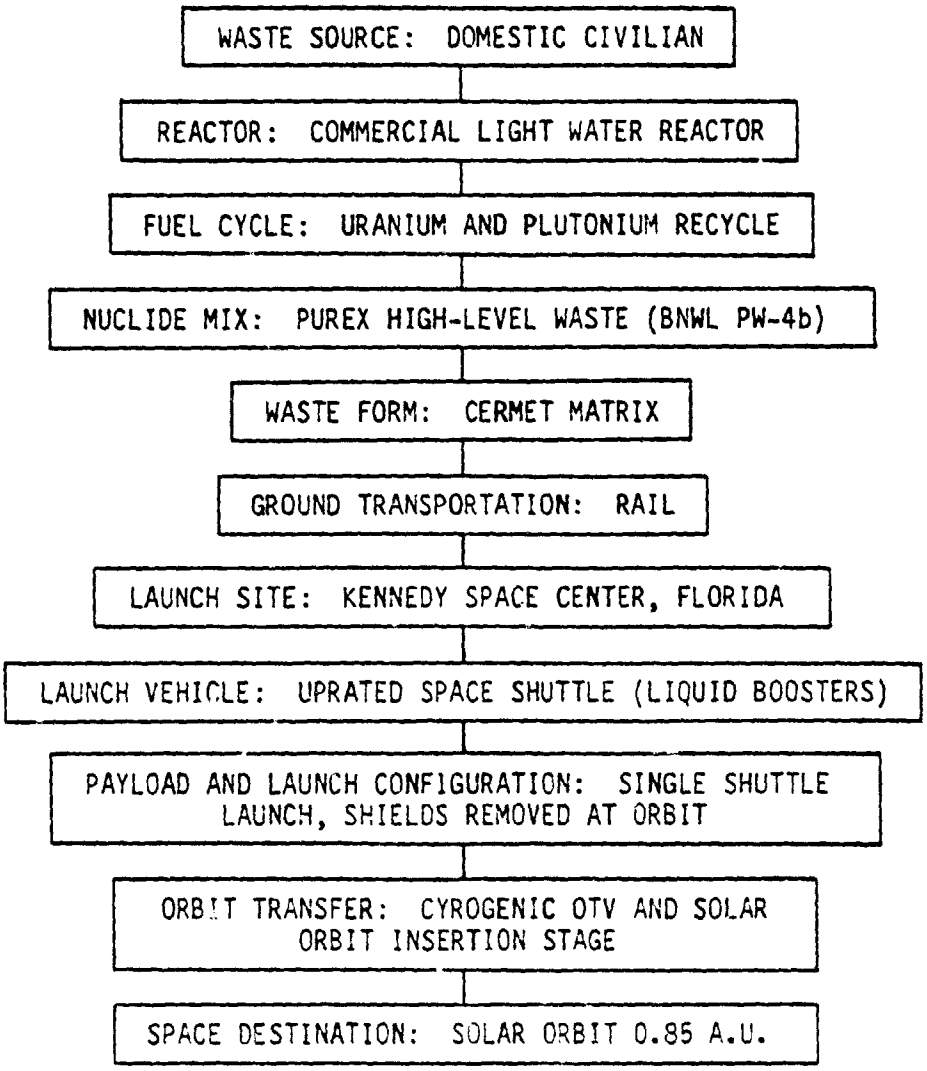

FIGURE 2-2. OVERVIEW OF REFERENCE CONCEPT FOR INITIAL NUCLEAR WASTE DISPOSAL IN SPACE PROGRAM

2.3 Overall Reference Mission

The overall reference mission, described in this section and developed during the course of this study, represents the concept for which most of the analyses in this report and in the NASA/MSFC documentation were conducted. Because of the many possible variations within the space disposal option, one point of reference is necessary. The major aspects of the reference mission are illustrated in Figure 2-3. This mission profile has been divided into seven major activities. The first two are expected to be the responsibility of the Department of Energy (DOE) and the last five are expected to be NASA's. These are:

(1) Nuclear Waste Processing and Payload Fabrication (DOE)
(2) Nuclear Waste Ground Transport (DOE)
(3) Payload Preparation at Launch Site (NASA)
(4) Prelaunch Activities (NASA)
(5) Uprated Space Shuttle Operations (NASA)
(6) Upper Stage Operations (NASA)
(7) Payload Monitoring (NASA).

Considerations of rescue and recovery systems are discussed in Sections 2.4 and 2.6. Also, see Section 6.2 for a detailed discussion of rescue mission technology. More complete definitions for individual system elements are discussed in Section 2.4. The following paragraphs provide the reader with a general overview of the reference mision.

2.3.1 Nuclear Waste Processing and Payload Fabrication (DOE)

Typically, spent fuel rods from domestic power plants would be transported to the waste processing and payload fabrication sites via conventional shipping casks. Using the Purex process, high-level waste containing fission products and actinides, inc'uding 0.1 percent plutonium and 0.1 percent uranium, would be processed from these spent fuel rods (see Section 3.2.1). The high-level waste would be formed into a cermet matrix by a calcination and hydrogen reduction process (see Section 3.1.2). The waste form would then be fabricated into a 5000 kg spherical payload (see Section 3.5). Within a remote shielded cell, the waste payload is loaded into a container; the container is then closed and sealed, inspected, decontaminated, and packaged into a flight-weight gamma radiation shield assembly (see Section 3.4.2). During these operations and subsequent interim storage at the processing site, the waste payload is cooled by an auxiliary cooling system.

2.3.2 Nuclear Waste Ground Transport (DOE)

The shielded waste container would then be loaded into a ground transportation shipping cask (see Figure 2-4). This cask, which provides additional shielding, thermal, and impact protection for the waste container

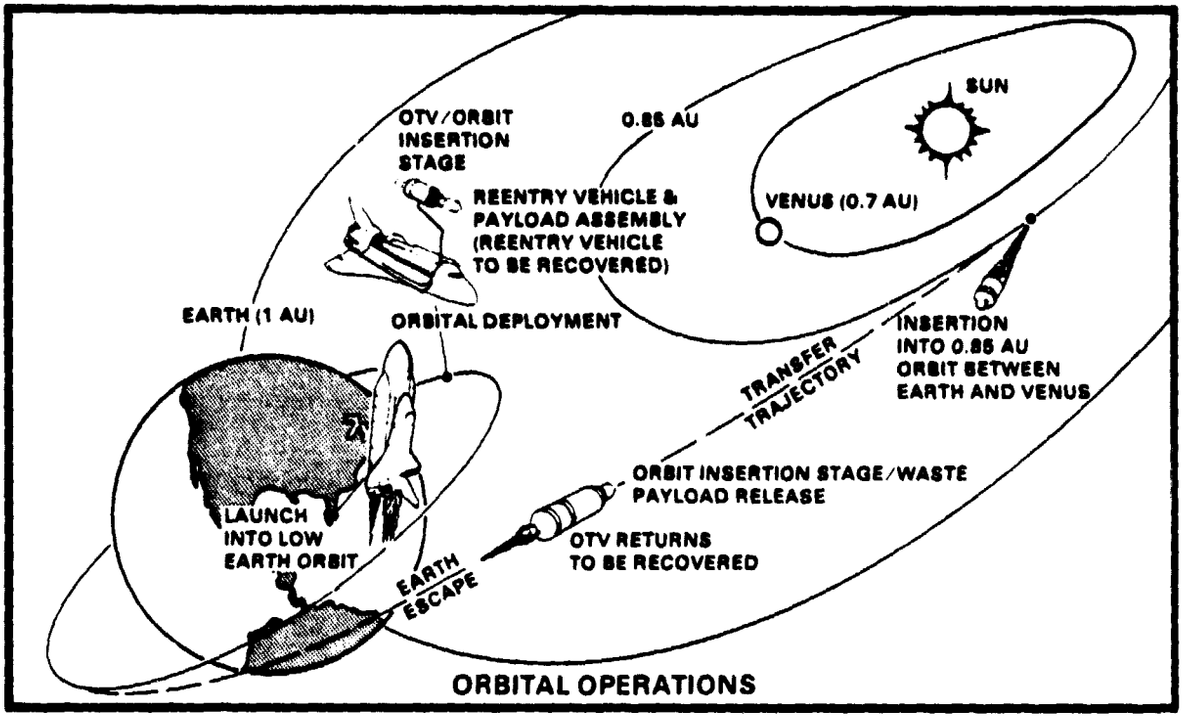

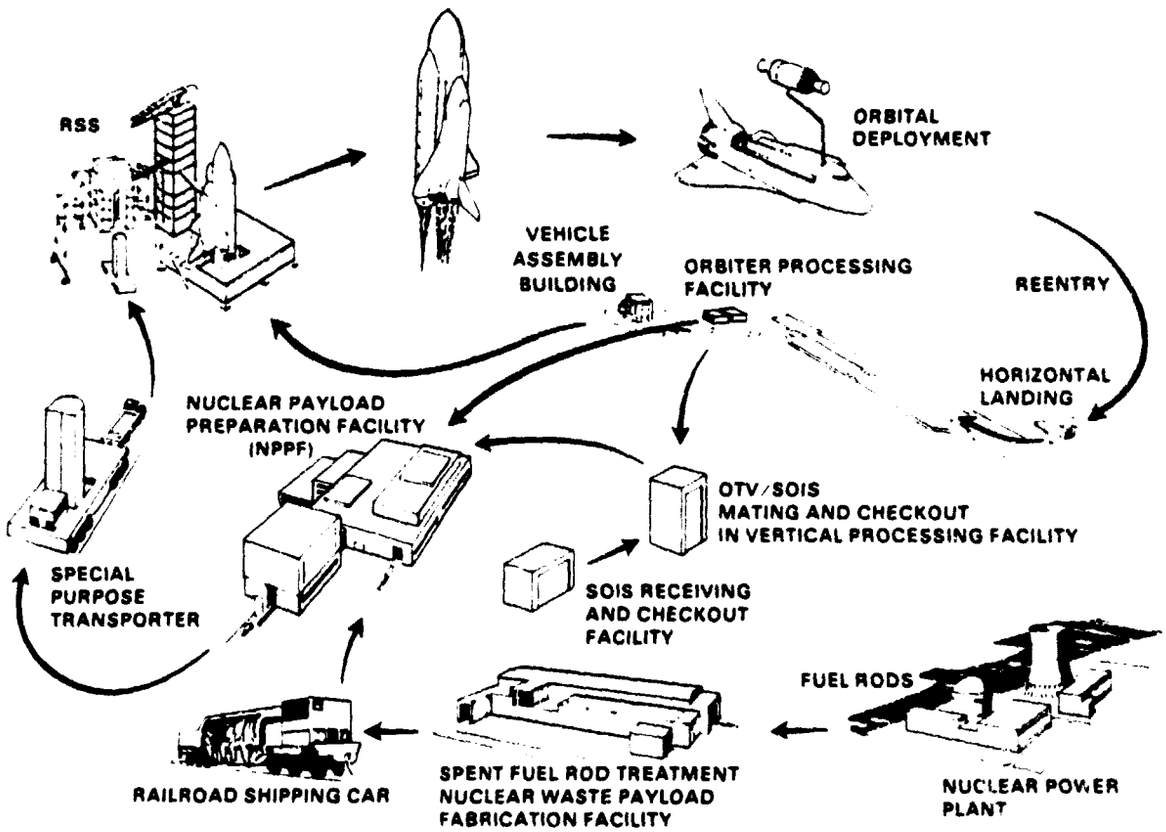

FIGURE 2-3. GROUND AND SPACE OPERATIONS FOR REFERENCE SPACE DISPOSAL MISSION

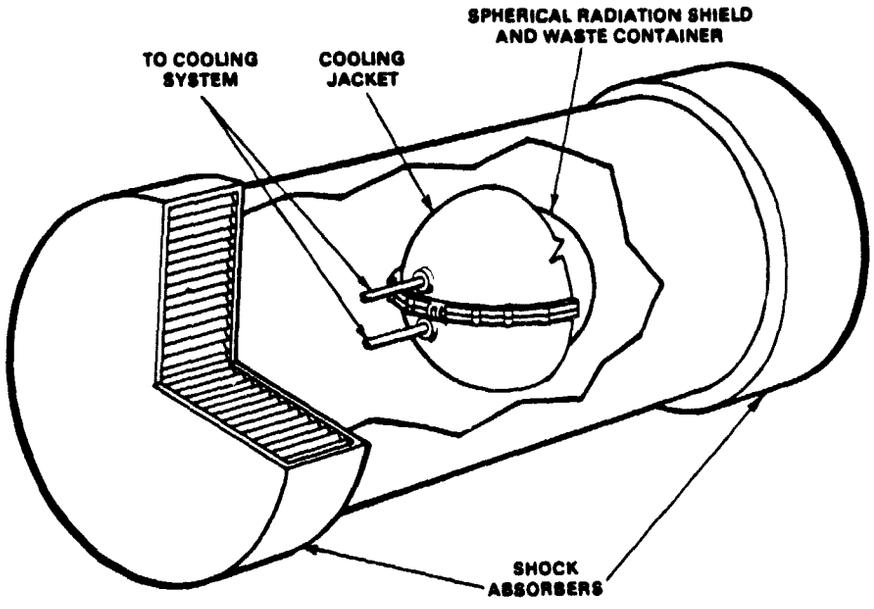

FIGURE 2-4. REFERENCE CONCEPT FOR NUCLEAR WASTE PAYLOAD SHIPPING CASK FOR TERRESTRIAL TRANSPORT

to comply with the Nuclear Regulatory Commission/Department of Transportation regulations, is then loaded onto a specially designed rail car for transporting the waste container from the waste payload fabrication site to the Kennedy Space Center (KSC), Florida launch site. Once the cask reaches the launch site, it is offloaded into the Nuclear Payload Preparation Facility (NPPF).

2.3.3 Payload Preparation at Launch Site (NASA)

The NPPF is expected to provide interim storage capability for up to three shielded waste containers, which affords efficient preparation for launches plus capacity for unplanned delays. During storage, additional radiation shielding, thermal control, monitoring and inspection of the waste container would be provided.

2.3.4 Prelaunch Activities (NASA)

In preparation for launch of the nuclear waste into space, the integrated Space Shuttle waste payload is prelaunch checked in the NPPF. The integrated Shuttle payload consists of: the waste form; the container; the

radiation shield; the reentry vehicle (RV), which protects and structurally supports the waste in the Orbiter cargo bay (see Figure 2-5); the Solar Orbit Insertion Stage (SOIS), which circularizes the waste payload into the solar orbit disposal destination; and the Orbit Transfer Vehicle (OTV), which provides escape from low Earth orbit and insertion into the heliocentric transfer trajectory. Integration and checkout in the NPPF is typical of future ground flow planning at Kennedy Space Center and parallel to the current use of the Vertical Processing Facility (VPF) by the Inertial Upper Stage (IUS). Prelaunch checkout in the NPPF includes verification of the payload and the payload to Orbiter interface systems. The Orbiter interface would be simulated by standardized equipment. Typically, storable propellant loading would occur in the NPPF to minimize the hazard of propellant loading while the payload is in the Shuttle cargo bay on the launch pad.

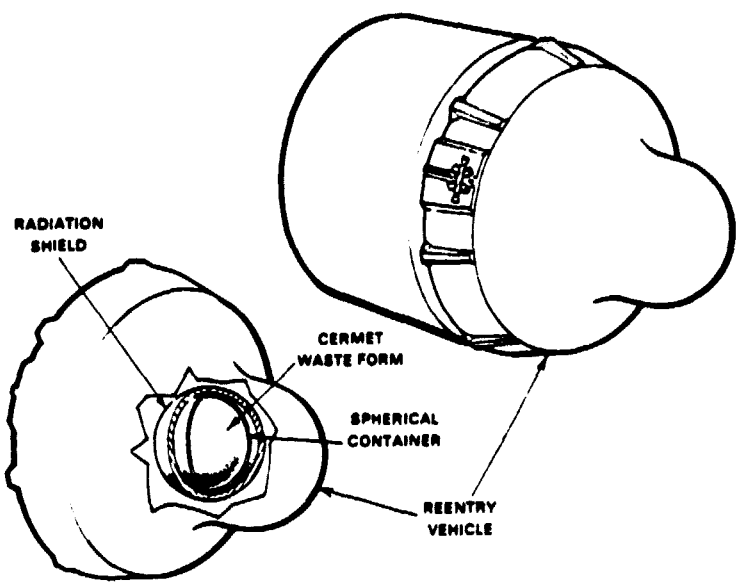

FIGURE 2-5. REFERENCE CONCEPT OF A LOADED REENTRY VEHICLE

Transfer of the payload to the launch pad's Rotating Service Structure (RSS), is accomplished by a special purpose transporter which maintains the Shuttle payload in the proper position for installation in the Orbiter cargo bay (see Figure 2-3). The payload is transferred from the NPPF to the pad after the Shuttle vehicle installation at the launch pad has been completed. The payload is then positioned by the RSS and installed in the Orbiter cargo bay. After payload installation, propellant loading of the OTV, and final systems checkout the decision to launch is made.

2.3.5 Uprated Space Shuttle Operations (NASA)

One Uprated Space Shuttle vehicle would be readied for launch for a given disposal mission. The to-be-constructed Pad C at KSC Launch Complex 39 would be used for this mission. Pad A or B could be used to launch the Shuttle vehicle that carries the rescue OTV, should it be required.

The Uprated Space Shuttle (45,400 kg payload to low Earth orbit), that is to perform the disposal mission, is launched at a 108 degree south azimuth to a 300 km (160 n.mi.) circular orbit inclined 38 degrees to the equator. A small degree of yaw steering is required such that early land overflight of various populated land masses (West Indies and South Africa) is avoided. Once on orbit, the loaded reentry vehicle (RV) in the Shuttle Orbiter cargo bay is remotely translated aft a short distance and structurally latched to the SOIS. Using the OTV payload bay rotation structure, the OTV, SOIS, and loaded RV are deployed from the Orbiter bay. Actual separation from the rotation structure is accomplished by a spring powered deployment system. After the OTV, SOIS, and loaded RV configuration has been stabilized in a fixed attitude, the Orbiter will move to a safe distance away to limit the radiation dose to the crew from the unshielded payload. At this time, the waste payload would be mechanically transferred by remote control to the SOIS payload adapter, and the OTV/SOIS/waste payload is oriented for the Earth escape propulsive burn. The reentry vehicle would remain in orbit and be recovered and returned to KSC by the Shuttle Orbiter.

The waste payload is cooled, while the payload is inside the reentry vehicle, by an auxiliary cooling system that has been integrated into the reentry vehicle. Passive radiative cooling of the waste payload would be adequate after the waste payload has been removed from the reentry vehicle. After the OTV delivers the nuclear waste payload and SOIS to the desired trajectory and returns to a low Earth orbit, the Orbiter would rendezvous with the OTV and return it to the launch site for refurbishment for use on a later flight.

2.3.6 Upper Stage Operations (NASA)

After the OTV/SOIS/waste payload system has passed final systems checkouts, the OTV propulsive burn would place the SOIS and its attached waste payload on the proper Earth escape trajectory. Control of the propulsive burn from low Earth orbit would be from the aft deck payload control station on the Orbiter, with backup provided by a ground control station. After the burn is complete, the SOIS/waste payload is then released. In about 160 days the payload and the storable liquid propellant SOIS would travel to its perihelion at 0.85 A.U. about the Sun. [One astronomical unit (A.U.) is equal to the average distance from the Earth to the Sun.] The SOIS would then place the payload in its final space disposal destination by reducing the aphelion from 1.0 to 0.85 A.U. To aid in obtaining the desired orbital lifetimes, this orbit would be inclined to the ecliptic plane by 1 degree. The recovery burns of the OTV would use the remaining OTV propellant to rendezvous with the

Shuttle Orbiter for its subsequent recovery, refurbishment, and reuse on a later mission. The reference OTV/SOIS mission profile is shown in Figure 2-6.

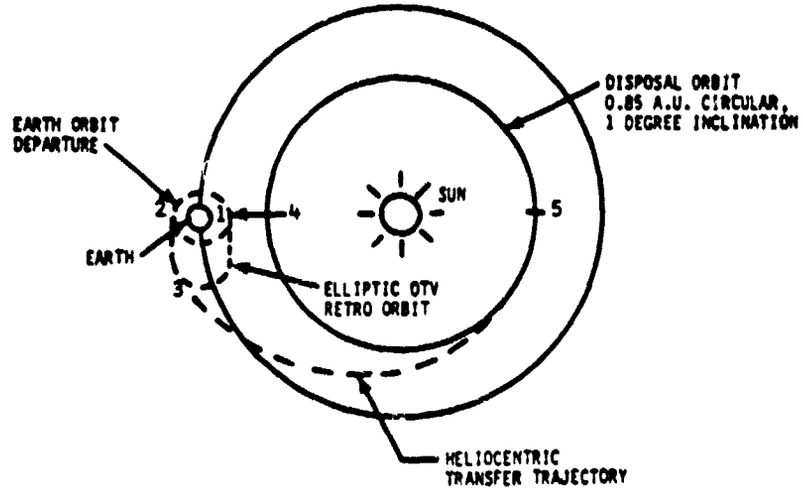

1-2 Uprated Space Shuttle (45,400 kg payload) ascent from Earth to a 300 km circular orbit with a 38° inclination

2-3 Prime OTV burn of approximately 10 min for escape from low-Earth orbit on elliptic solar orbit transfer trajectory with perigee of 0.85 A.U. and 1° inclination to the ecliptic. The ΔV for this maneuver is 3350 m/sec.

3 OTV separation from the SOIS/nuclear waste payload and retro burn to an elliptic Earth orbit. The ΔV for this maneuver is 640 m/sec. The OTV lifetime for return to the Orbiter is approximately 50 hours. The apogee for this orbit is 61,000 km.

4 OTV circularization into the 300 km, 38° inclination recovery orbit. The ΔV is 2770 m/sec.

5 SOIS and payload circularization into 0.85 A.U., 1° inclination to the ecliptic, solar orbit. The ΔV is 1160 m/sec.

FIGURE 2-6. REFERENCE OTV/SOIS MISSION PROFILE

2.3.7 Payload Monitoring (NASA)

The Earth escape trajectory of the SOIS/waste payload would be monitored by ground-based radar systems and telemetry from the SOIS and OTV. The final disposal orbit achieved would be monitored by NASA's Deep Space Network. Once the proper disposal orbit has been verified, no additional monitoring is necessary. However, monitoring could be re-established in the future, if required.

2.4 Reference System Element Definitions

The definitions for reference mission system elements are described below. These definitions have been used in almost all cases for the work documented in this report. Twelve major system elements identified for this definition document are:

(1) Waste Source
(2) Waste Mix
(3) Waste Form
(4) Waste Processing and Fabrication Facilities
(5) Payload Container, Shielding, and Reentry Vehicle
(6) Ground Transport Vehicles and Casks
(7) Launch Site Facilities
(8) Uprated Space Shuttle Vehicle
(9) Upper Stages
(10) Payload Ejection System
(11) Docking System
(12) Space Destination.

Definitions for the reference mission system elements follow.

2.4.1 Waste Source

The primary waste source would be nuclear waste generated by the operation of commercial nuclear power plants (see Section 3.2.1). Table 2-1 provides the most realistic projections of waste generation (assuming 200 GWe by the year 2000) found in the literature.[2-14] By assuming that the waste must be at least 10 years old before it can be disposed of in space, and that reprocessing capacities should be able to process the waste according to the proposed schedule, the annual amount of waste available for disposal is given. Projections of the mass available for space disposal are also given as a function of year. The mass of waste available annually for space disposal, in cermet form, would increase to 310 metric tons (MT) by the year 2000.

2.4.2 Waste Mix

Waste generated using the Purex process (fission products, actinides including approximately 0.1 percent Pu, and 0.1 percent U) is considered to be the reference waste mix composition. The specific reference waste used for the 1979-1980 Space Option study activity was defined as the Battelle Northwest Laboratory PW-4b waste mix (see Section 3.2.1 for details).[2-15] The elemental definition of this waste is given in Table 2-2; isotopic definition is given in Section 3.2.1.

TABLE 2-1. PROJECTED NUCLEAR POWER GENERATION REPROCESSING CAPACITY AND COMMERCIAL HIGH-LEVEL WASTE AVAILABLE FOR SPACE DISPOSAL

Year	Cumulative Power, GWe	Cumulative Waste, MTHM	Annual Nuclear Waste Available for Disposal, MTHM/yr	Annual High-Level Purex Waste in Cermet Form Available for Space Disposal, MT/yr
1979	61.9	5890(c)	0	0
1980	74.8	7690	0	0
1981	87.3	9790	0	0
1982	101.1	12,220	0	0
1983	115.4	14,990	0	0
1984	131.4	18,140	0	0
1985	144.3	21,600	0	0
1986	157.1	25,370	0	0
1987	164.9	29,330	0	0
1988	174.0	33,510	0	0
1989	180.9	37,850	5890(c)	410
1990	186.5	42,330	1800	125
1991	188.9	46,860	2100	146
1992	190.1	51,420	2430	169
1993	192.5	56,040	2770	193
1994	194.0	60,700	3150	219
1995	195.0	65,380	3460	241
1996	196.0	70,080	3500	244
1997	197.0	74,810	3960	275
1998	198.0	79,560	4180	290
1999	199.0	84,340	4340	301
2000	200.0	89,140	4480	310

(a) From: Yates, K. R., and Park, U. Y., "Projections of Commercial Nuclear Capacity and Spent-Fuel Accumulation in the United States", Fuel Reprocessing, pp. 350-352 (June 1979).
(b) MTHM is metric tons heavy metal.
(c) Includes 4400 MTHM PW-4b existing as of 1978.
(d) Assumes 40.8 kg/MT waste for space disposal and a cermet waste form loading of 58.7 percent.
(e) Computed by multiplying 5890 MTHM by 0.0408 MT/MTHM and dividing by 0.587.

TABLE 2-2. REFERENCE WASTE MIX COMPOSITION FOR SPACE DISPOSAL (BNWL PW-4b)

	Constituent	Amount, kg/MTHM		Constituent	Amount, kg/MTHM
Inerts	Na_2O	--	Fission Products (Cont'd.)	TeO_2	0.725
	Fe_2O_3	1.511		Cs_2O	2.880
	Cr_2O_3	0.345		BaO	1.567
	NiO	0.141		La_2O_3	1.480
	P_2O_5	0.672		CeO_2	3.323
	Gd_2O_3	--		Pr_6O_{11}	1.482
				Nd_2O_3	4.522
Fission Products	Rb_2O	0.354		Pm_2O_3	0.123
	SrO	1.059		Sm_2O_3	0.924
	Y_2O_3	0.598		Eu_2O_3	0.200
	ZrO_2	4.944		Gd_2O_3	0.137
	MoO_3	5.176			
	Tc_2O_7	1.291	Actinides	U_3O_8	1.169
	RuO_2	2.972		NpO_2	0.865
	Rh_2O_3	0.480		PuO_2	0.010
	PdO	1.483		Am_2O_3	0.181
	Ag_2O	0.088		Cm_2O_3	0.040
	CdO	0.097			
				TOTAL	40.8

Source: Reference 2-15.

2.4.3 Waste Form

The reference waste form for space disposal is the ORNL iron/nickel-based cermet. It has been chosen over may other waste forms (see Section 3.1.1). A cermet is a dispersion of ceramic particles in a continuous metallic phase. The reference cermet is formed by a process involving dissolution and precipitation from molten urea followed by calcination and hydrogen reduction to produce a continuous metallic phase (see Section 3.1.2). Nonhydrogen reducible oxides form the ceramic portion of the ceramic/metal matrix waste form. This waste form has been shown to have superior properties as compared to other potential waste forms for space disposal. The iron/nickel-based cermet has high waste loading (58.7 percent), a relatively high thermal conductivity (14 Watts/m-C at 300 C), a high density (6.7 g/cc), a good specific heat (0.583 kJ/kg-C), and a high structural integrity.

2.4.4 Waste Processing and Payload Fabrication Facilities

The waste processing and payload fabrication facilities are assumed to be collocated. The reference waste mix requires a waste processing facility utilizing the Purex process. After separation and generation of the aqueous waste stream, approximately 5 years of storage would occur before further processing. The waste would then be put into its final cermet waste form.

The waste payload fabrication facilities would provide a series of interconnected, shielded cells for loading the waste form into containers, closing, sealing, inspecting, decontaminating containers, and ultimate insertion into the flight-weight radiation shield assembly. Each cell would have provisions to connect the waste container to an auxiliary cooling system. Each facility would provide interim storage for a number of shielded waste packages and equipment/systems for cask handling and rail car loading.

2.4.5 Payload Container, Shielding, and Reentry Vehicle Systems

The primary containment for the radioactive waste is a stainless steel spherical container (1.27 cm thick -- see Figure 2-5). This container must provide high integrity containment for the waste during the various defined mechanical and thermal loads to which the total payload is subjected in anticipated normal and accident conditions. These loads would be mitigated in varying degrees by the waste form itself, the gamma radiation shield assembly, by the shipping cask which provides additional gamma radiation shielding for ground transportation, and by the reentry vehicle (RV) system during the prelaunch and boost phase of the disposal mission. The container would be designed to dissipate the heat generated within the waste form by passive cooling to the space environment during the orbital operations. During any normal operation, the maximum temperature of the waste form should not exceed the normal limiting temperature of 1200 C. During launch and on orbit while the waste is in the RV, the temperature is to be controlled with assistance of various auxiliary cooling systems located on the Shuttle Orbiter and the RV. If accidents occur, the temperature of the waste and container material may exceed the normal limit but must not exceed that which would cause loss of containment.

The container would be housed in a flight-weight radiation shield assembly for the period prior to leaving the waste fabrication facility until attached to the OTV in Earth orbit. This flight-weight shielding would be designed to limit the radiation level to 2 rem/hr at 1 meter from its surface (see Section 2.5.2.4). Additional shielding would need to be provided by temporary shielding at the NPPF and RSS, and possibly a shadow shield in the Shuttle Orbiter for the crew (see Section 2.5.1.1). The spherical radiation shield would be of depleted uranium sandwiched between two layers of stainless steel.

The radiation shielded waste container would be enclosed in a protective reentry and impact shield prior to launch and during the boost phase (see Figure 2-7). This system would be designed to minimize the probability of

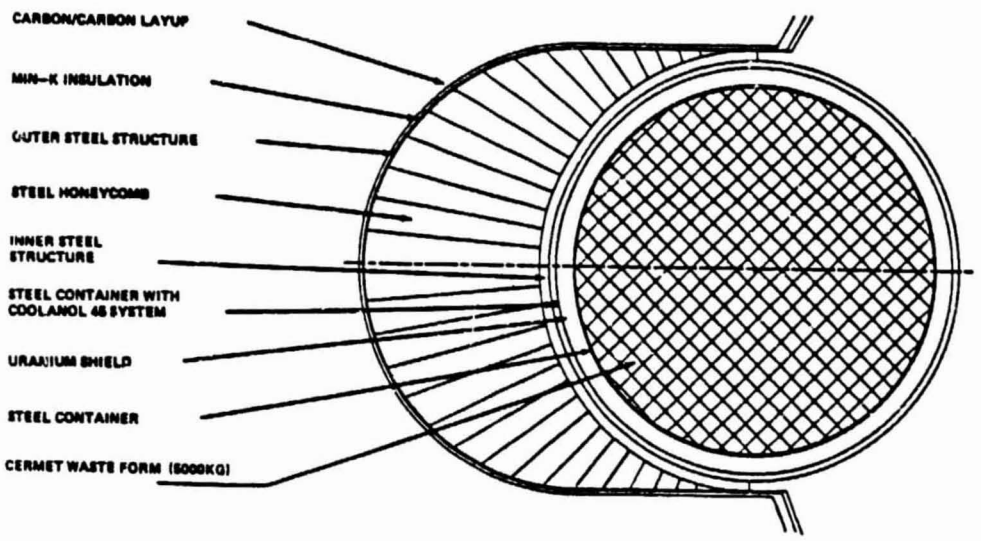

Reentry Vehicle Nose Cross Section

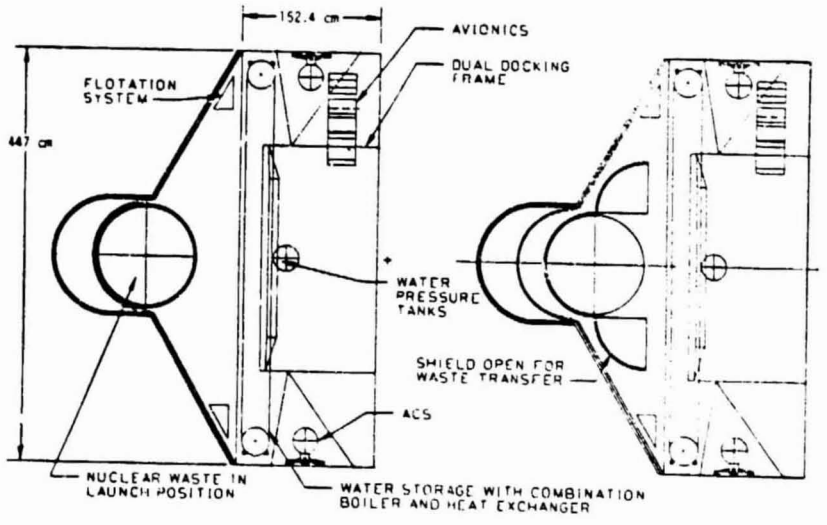

Reentry Vehicle Configuration

FIGURE 2-7. REFERENCE REENTRY VEHICLE CONFIGURATION AND NOSE CROSS SECTION

containment breach as a result of accidents or malfunctions which could occur during the prelaunch, launch, suborbital, orbital, or unplanned reentry phases of the mission. The protection shield would consist of an outer layer of carbon/carbon thermal protection and MIN-K insulation and a 61 cm thick steel honeycomb impact structure (at the nose point). The thermal protection is completely around the payload, whereas, the impact structure covers only the nose of the RV. The waste payload/reentry vehicle/SOIS/OTV configuration, as positioned in the Shuttle Orbiter, is shown in Figure 2-8.

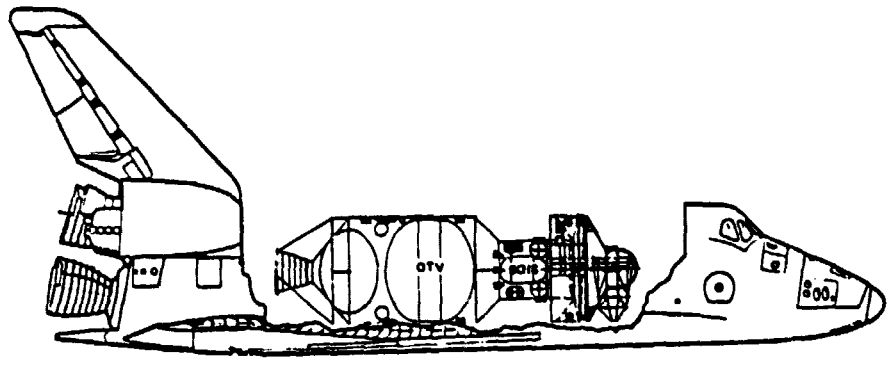

FIGURE 2-8. LOCATION OF PAYLOAD/RV/SOIS/OTV CONFIGURATION IN SHUTTLE ORBITER CARGO BAY

2.4.6 Ground Transport Vehicles and Casks

For transport from the waste fabrication facility to the launch site, the waste containers and associated flight-weight shielding would be housed in a shipping cask affording additional shielding, thermal and impact protection to meet the Nuclear Regulatory Commission/Department of Transportation regulations.(2-16) The cask (see Figure 2-4) is expected to be licensed by the Nuclear Regulatory Commission. The cask would be transported from the payload fabrication facilities to the KSC launch site on a specially designed rail car that adequately supports and distributes the weight of the cask and provides acceptable tie downs. In addition, the rail car would carry an auxiliary cooling system to reliably cool the waste package.

2.4.7 Launch Site Facilities

The reference launch site for launching nuclear waste payloads during the early phase of the program (early-1990's) would be Launch Complex 39 at Kennedy Space Center Florida. New facility construction and equipment expected during this period is noted below.

- A secure, sealed, environmentally controlled, Nuclear Payload Preparation Facility (NPPF) to store, cool, monitor, assemble, and

checkout the waste payload systems from the time the shielded nuclear waste container arrives at KSC until the time the loaded payload reentry vehicle is moved to the launch pad.

- A dedicated, special-purpose transporter to move the nuclear waste payload from the NPPF to the Rotating Service Structure (RSS) at the launch pad. This includes construction of a roadway or tracks for the transporter to use.

The other currently planned Shuttle and upper stage launch facilities may or may not be adequate to support the additional Shuttle launches required by a high launch rate (60 per year) nuclear waste disposal program. Further analysis of the nuclear waste disposal traffic model coupled with the Space Shuttle traffic model and current turnaround time lines is needed. It is expected that additional facilities would likely be needed at the higher launch rates. Facilities envisioned are:

- A dedicated Space Shuttle launch pad (Pad C) for launching nuclear waste payloads. The waste payload would be installed in the Shuttle Orbiter at the pad. A specially designed RSS is required for this mission.

- A third Mobile Launch Platform (MLP) for transporting built-up Shuttles from the Vehicle Assembly Building (VAB) to the launch pads is required.

- A third firing room in the Launch Control Center (LCC) would have to be activated to handle the increased number of Space Shuttle flights dedicated to the nuclear waste disposal program. This firing room would be used exclusively for the waste disposal missions.

2.4.8 Uprated Space Shuttle Vehicle

During the early years of a space disposal program, the Uprated Space Shuttle (45,400 kg payload to low Earth orbit--see Figure 2-9) would represent an ideal vehicle to carry out the boost phase of the space transport. The National Aeronautics and Space Administration is now managing the development of the Space Shuttle (to be operational at Kennedy Space Center in 1981), a new class of space booster that is a highly reliable, reusable, low-cost vehicle that can transport payloads to low Earth orbit and back. It is anticipated that the Space Shuttle vehicle expected to fly space missions will be uprated around 1990. This uprating involves the use of a higher performance and environmentally cleaner Liquid Rocket Booster (LRB) as a replacement for the Solid Rocket Booster (SRB).

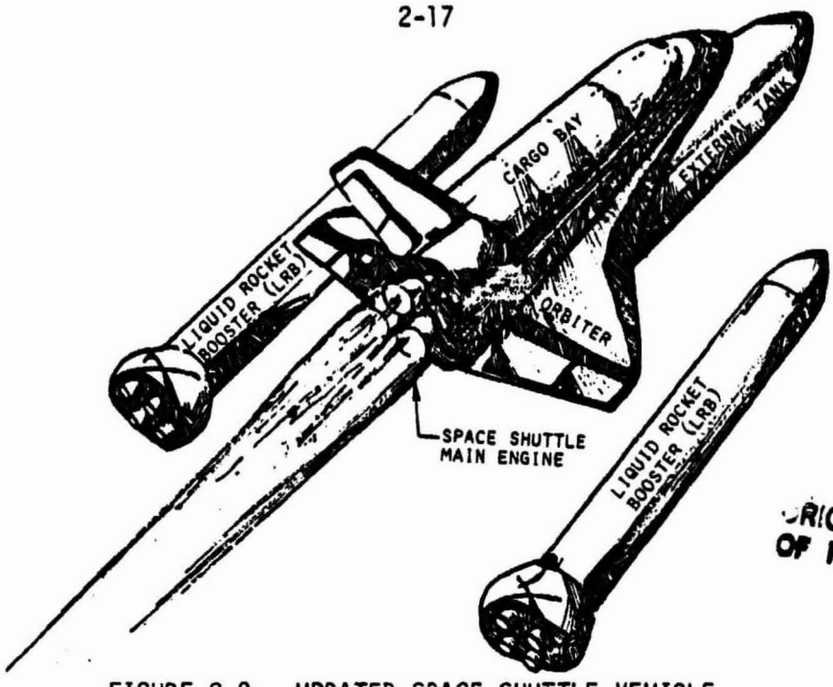

FIGURE 2-9. UPRATED SPACE SHUTTLE VEHICLE

The Uprated Space Shuttle consists of a piloted reusable orbiting vehicle (the Orbiter) mounted on an expendable External Tank (ET) containing hydrogen/oxygen propellants and two recoverable and reusable Liquid Rocket Boosters (LRB's). The propellants for the LRB's are RP-1 (kerosene) and liquid oxygen (LOX), having an oxidizer to fuel ratio of 2.9. The Orbiter will have three main hydrogen/oxygen liquid rocket engines and a cargo bay 18.29 m long and 4.57 m in diameter. At launch, both the LRB's and the Orbiter's three liquid rocket engines would burn simultaneously. After about 140 seconds and after the Space Shuttle vehicle attains an altitude of about 45 km (28 miles), the LRB's would be separated and subsequently recovered from the Atlantic Ocean. The ET is jettisoned before the Orbiter goes into orbit. The Orbital Maneuvering System (OMS) is then propels the Orbiter into the desired Earth orbit. The Orbiter with its crew and payload (weighing up to 45,400 kg) would remain in orbit to carry out its mission, normally from 1 to 7 days, but, when required, as long as 30 days. When the mission is completed, the Orbiter would be deorbited and piloted back to the launch site for an unpowered landing on a runway. The Orbiter and LRB's would subsequently be refurbished and reflown on other space missions. References 2-17, 2-18, and 2-19 provide additional information about the standard Space Shuttle and its capabilities. Reference 2-20 provides data on LRB's for the Uprated Space Shuttle. Table 2-3 provides a reference mass summary for the Uprated Space Shuttle Vehicle.

Small changes to the Space Shuttle system may be required to provide a safer and more reliable launch vehicle. These modifications have not yet been identified.

TABLE 2-3. MASS SUMMARY FOR UPRATED SPACE SHUTTLE VEHICLE

Vehicle Component/Element	Mass, kg	Weight, lb
Orbiter		
Dry (Less Engines)	63,875	140,821
Engines	9,063	19,980
Personnel and Equipment	1,197	2,640
Residuals and Reserves	4,212	9,285
Total Inert	78,347	172,726
OMS/RCS Propellants	12,322	27,166
Total at Liftoff	90,669	199,892
External Tank (ET)		
Dry	32,757	72,217
Residuals and Reserves	4,276	9,428
Total Inert	37,034	81,645
Usable Propellants (LOX/LH_2)	711,196	1,567,918
Total at Liftoff	748,230	1,649,563
Liquid Rocket Boosters (Both)		
Dry	126,269	278,376
Residuals	4,853	10 00
Total Inert	131,122	289,076
Usable Propellants (LOX/RP-1)	1,080,480	2,382,050
Total at Liftoff	1,211,602	2,671,126
Payload	45,360	100,000
Total Vehicle at Liftoff	2,095,861	4,620,581

Source: Reference 2-20.

2.4.9 Upper Stages

Two different upper stages have been defined for use for the nuclear waste disposal mission: (1) an Orbit Transfer Vehicle (OTV), and (2) a storable propellant Solar Orbit Insertion Stage (SOIS). The OTV is a completely reusable and recoverable stage; the SOIS is expendable. Orbital rescue capability would be performed by the OTV and SOIS systems.

The OTV is defined as a reusable LOX/LH_2 chemical propulsion stage similar to the cryogenic OTV defined in the past few years for possible development and use with the Space Shuttle. This vehicle would have separate propellant tanks, an oxidizer/fuel (O/F) mixture ratio of 6 and a delivered specific impulse (I_{sp}) of 470 seconds. It would also have an advanced, redundant, avionics and attitude control system. Figure 2-10 is a pictoral of the OTV.

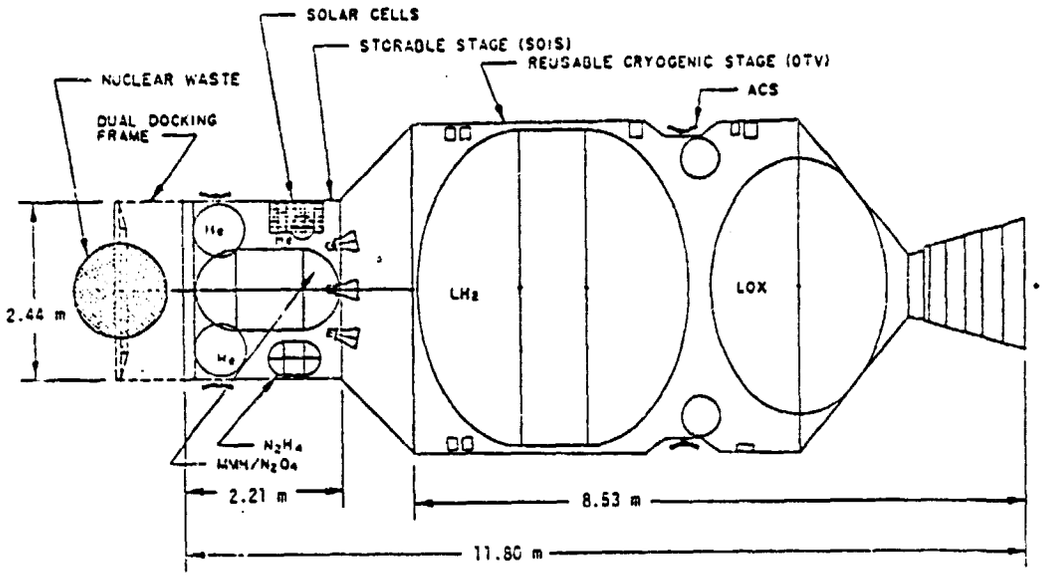

FIGURE 2-10. REFERENCE OTV/SOIS/WASTE PAYLOAD CONFIGURATION

The storable-propellant, pressure-fed SOIS would be sized to provide a specific impulse of 289 sec. The NASA/MSFC scaling relation for the SOIS is given below:

$$M_{B.O.} = 810 + 0.0522\ Mp$$

where $M_{B.O.}$ and Mp are the SOIS stage burnout mass (kg) and propellant loading mass (kg), respectively. The propellant loading includes a 15 percent flight reserve. This stage would have three off-the-shelf (Space Shuttle-Reaction Control System) pressure-fed engines at a thrust level of 3870 N (870 lb) each, monomethylhydrazine/nitrogen tetroxide (MMH/NTO) propellants, a guidance and control system, and a payload docking adapter system compatible with the docking system. The stage would be designed to adequately withstand

the adverse nuclear radiation, and space environments experienced while coasting 160 days before firing.

The rescue vehicle would be a Shuttle launched OTV/SOIS system. It would include appropriate provisions for targeting and docking with the nuclear waste container attached to an OTV/SOIS, the nuclear waste container attached to an SOIS only, a payload reentry vehicle assembly, or an unshielded, separated waste container. It would be reusable or expendable depending upon the rescue mission. This vehicle would be required to have an on-orbit stay time of at least 300 hours with little reduction expected in reliability or performance. The rescue vehicle may be returned to Earth by the Shuttle Orbiter at the end of the cycle for refurbishment, if recoverable. Definition of other rescue requirements are expected as studies progress.

2.4.10 Payload Ejection System

A payload ejection system would be incorporated into the pallet which supports the reentry vehicle (see Figure 2-8). This system would employ 16 small solid propellant rocket motors which would be ignited to eject the loaded reentry vehicle from the Orbiter cargo bay in the event of a serious on-pad or ascent failure. The reentry vehicle would be designed to withstand the expected sea or ground impact environment.

2.4.11 Payload Docking and Transfer System

The payload docking and transfer system would be launched into orbit attached to the reentry vehicle. The docking/transfer system would be used to transfer the waste payload container from the reentry vehicle to the SOIS payload adapter. The payload adapter would be designed to jettison the nuclear payload during the very low probability occurrence of a grossly inaccurate OTV propulsive burn. This action would prevent possible reentry and allow subsequent recovery by a Shuttle or OTV rescue vehicle.

2.4.12 Space Destination

The reference space destination for the nuclear waste disposal mission is an orbital region between the orbits of the Earth and Venus. The nominal circular orbit is defined as 0.85 $\pm$ 0.01 A.U. The orbital inclination about the Sun is specified as 1 degree from the ecliptic plane.

2.5 System Safety Design Requirements for Reference Concept

This section defines system safety design requirements for the reference nuclear waste disposal in space mission (also see Section 3.3 and Appendix C). These requirements provide the guidelines against which nuclear waste payloads may be considered acceptable from a radiological safety point of view. These requirements should be used for future studies, and modified as changes in the concept occur.

The general safety design objectives for the nuclear waste payload and/or its associated system components are: (1) to contain the solid radioactive waste materials and (2) to limit the exposure of humans and the environment to the radioactive waste materials. For normal operations, complete containment and minimum exposure are required; for potential accident situations, the degree of containment and degree of interaction shall result in an acceptable risk to humans and the environment.

The following subsections describe the general and specific system design requirements for the nuclear waste disposal in space mission.

2.5.1 General System Safety Design Requirements

The general system safety design requirements for the nuclear waste disposal in space mission involve considering of the following:

(1) Radiation Exposure
(2) Containment
(3) Accident Environments
(4) Criticality
(5) Postaccident Recovery
(6) Monitoring Systems.

The following paragraphs define the requirements that should be followed for the reference system concept design activity.

2.5.1.1 Radiation Exposure

Radiation exposure limits for normal operations for the public and ground crews will be those contained in ERDA-MC-0524 and shown in Table 2-4. Radiation exposure limits for Space Shuttle crew members during normal operations will be those contained in the Space Shuttle Flight and Ground Specification, JSC 07700, Volume X, Revision A, Chapter 7.4 and shown in Table 2-5.

The normal radiation exposure limits for the current terrestrial transportation of nuclear waste materials would also apply to ground

TABLE 2-4. NORMAL OPERATIONS EXPOSURE LIMITS FOR INDIVIDUALS IN CONTROLLED AND UNCONTROLLED AREAS

INDIVIDUALS IN CONTROLLED AREAS:

Type of Exposure	Exposure Period	Dose Equivalent (Dose or Dose Commitment[a], rem)
Whole body, head and trunk, gonads, lens of the eye[b], red bone marrow, active blood forming organs.	Year	5[c]
	Calendar Quarter	3
Unlimited areas of the skin (except hands and forearms). Other organs, tissues, and organ systems (except bone).	Year	15
	Calendar Quarter	5
Bone.	Year	30
	Calendar Quarter	10
Forearms.[d]	Year	30
	Calendar Quarter	10
Hands[d] and feet.	Year	75
	Calendar Quarter	25

INDIVIDUALS IN UNCONTROLLED AREAS:

Type of Exposure	Annual Dose Equivalent or Dose Commitment (rem)[e]: Based on dose to individuals at points of maximum probable exposure	Based on an average dose to a suitable sample of exposed population
Whole body, gonads, or bone marrow	0.5	0.17
Other organs	1.5	0.5

(a) To meet the above dose commitment standards, operations must be conducted in such a manner that it would be unlikely that an individual would assimilate in a critical organ, by inhalation, ingestion, or absorption, a quantity of a radionuclide(s) that would commit the individual to an organ dose which exceeds the limits specified in the above table.
(b) A beta exposure below an average energy of 700 Kev will not penetrate the lens of the eye; therefore, the applicable limit for these energies would be that for the skin (15 rem/year).
(c) In special cases with the approval of the Director, Division of Operational Safety, a worker may exceed 5 rem/year provided his average exposure per year since age 18 will not exceed 5 rem per year.
(d) All reasonable efforts shall be made to keep exposures of forearms and hands to the general limit for the skin.
(e) In keeping with ERDA policy on lowest practicable exposure, exposures to the public shall be limited to as small a fraction of the respective annual dose limits as is practicable.

Source: See Section 4.5, Reference 4-7.

TABLE 2-5. RADIATION EXPOSURE LIMITS FOR SPACE SHUTTLE FLIGHT CREWS(a)

Constraints, rem	Bone Marrow, 5 cm	Skin, 0.1 mm	Eye, 3 mm	Testes(c)
1 year average daily rate	0.2	0.6	0.3	0.1
30-day maximum	25	75	37	13
Quarterly maximum(b)	35	105	52	18
Yearly maximum	75	225	112	38
Career limit	400	1200	600	200

Notes:

(a) These exposure limits and exposure rate constraints apply to all sources of radiation exposure. In making trade-offs between man-made and natural sources of radiation, adequate allowance must be made for the contingency of unexpected exposure. These data are from Space Shuttle Flight and Ground Specification, JSC 07700, Volume X, Revision A, Chapter 7.4.
(b) May be allowed for two consecutive quarters followed by six months of restriction from further exposure to maintain yearly limit.
(c) These dose and dose rate limits are applicable only where the possibility of oligospermia and temporary infertility are to be avoided. For most manned space flights, the allowable exposure accumulation to the Germinal Epithelium (3 cm) will be the subject of a risk/gain decision for particular program, mission, and individuals concerned.

transportation of nuclear waste payloads. The radiation limits (49CFR 173.393) are given as:

- 1 m from external container surface...1000 mrem/hour
- External surface of transport vehicle...200 mrem/hour
- 2m from external surface of transport vehicle...10mrem/hour
- Normally occupied position of transport vehicle...2mrem/hour.

For accident conditions of terrestrial transport, dose rates are limited to 1000 mrem/hour at 1 meter from the external surface of the waste package. For launch/reentry accidents, higher dose limits are expected because of the anticipated lower probability for these accidents.

2.5.1.2 Containment

The containment requirements (also see Section 3.3) are different for the various portions of the disposal mission. For the current reference

mission, four different types of containment configurations are used: (1) shipping cask/auxiliary shielding/flight-weight radiation shield/container/waste, (2) auxiliary shielding/flight-weight radiation shield/container/waste, (3) reentry shield/impact shield/flight-weight radiation shield/container/waste, and (4) container/waste. For all normal operations, the systems will be designed such that no release of radioactive material occurs. Configuration (1) must survive probable shipping accidents without major release. Configuration (2) must survive probable handling accidents without major containment breach. Configuration (3) must survive all handling, on-pad, booster ascent to orbit, and reentry accidents without major containment breach. Configuration (4) must be designed to survive the two postulated reentry conditions (see Section 2.5.1.3.4) with only minimal release possible. The accident environments for which the designs of these generic configurations must survive are given below.

2.5.1.3 Accident Environments

The accident environments that need to be considered in the design of containment and other auxiliary systems are as follows:

- Shipping accident
- Ground handling accident in NPPF
- On-pad or near-pad Uprated Space Shuttle vehicle failure
- Reentry accidents.

2.5.1.3.1 Shipping Accident Environments (for Configuration 1)

DOT and NRC regulations, as defined in 49 CFR 170 to 179 and 10 CFR 71, will be assumed for the ground shipment of nuclear waste payloads from the waste payload fabrication facility to the launch site. The following sequential test environments for shipping cask accidents are given below. Initial conditions are to be assumed the same as the normal condition.

- A 9-m drop in worst orientation onto an unyielding surface
- A 1-m drop in the worst orientation onto the end of 15-cm-diameter, 20-cm-high bar (mild steel)
- A 30-min. ground fire at 800 C followed by 3 hours of no artificial cooling; with a cask emissivity of 0.9 and cask absorbtivity of 0.8
- An 8-hour emersion in 0.9 m of water.

At the end of this test, surface radiation of the shipping cask should not exceed 1 rem/hour at 1 m from the surface, the contents must remain subcritical, and only minute radioactive material releases are allowed (see 10 CFR 71).

2.5.1.3.2 Handling in NPPF (for Configuration 2)

The payload systems, auxiliary support equipment and facilities must be designed to minimize the occupational radiation exposure to workers (see Table 2-4). Care must also be taken to insure that if certain subsystem failures occur during handing in the NPPF, radiation exposure and contamination is kept to as low as reasonably achievable. The handling area in the NPPF will be designed to be a total containment vessel.

2.5.1.3.3 On- or Near-Pad or Ascent Booster Accident (for Configuration 3)

The payload package must be designed to withstand the following nominal accident environments (developed in Section 4.2) in sequence without a major breach of primary containment. Initial conditions are assumed to be the normal condition.

- A blast side-on overpressure of 250 N/cm^2, a reflected overpressure of 1700 N/cm^2 and side-on and reflected impulses of 2.0 and 15.0 $N-s/cm^2$, respectively, in worst orientation. (Based upon a 10 percent yield of the ET propellants--see Table 4-9, Section 4.2.3)
- A potential edge-on penetration of 1 per m^2 of impacting fragments, assumed to be discs 100 cm in diameter and 0.56 cm thick, having a mass of 12 kg, and moving at 500 meters per second. The worst orientation is assumed. (Based upon data in Section 4.3.4)
- A heat flux of 3500 kW/m^2 for 15 seconds from a liquid propellant fireball. (Based upon results described in Section 4.2.1.3)
- A 60-min. ground fire at 1100 C followed by 2 hours of no artificial cooling. (Based upon results described in Section 4.2.2.3)
- An impact in the worst orientation onto an unyielding surface at 10 percent higher than the predicted terminal velocity.
- An impact in the worst orientation into 25 C water at a velocity 10 percent higher than the predicted terminal velocity.

2.5.1.3.4 Reentry Accidents (for Configuration 4)

The payload container and waste must be able to withstand reentry into the Earth's atmosphere and impact onto the Earth's surface without the dispersion of significant quantities of radioactive material. The reentry environments are defined as follows:

- A decaying reentry trajectory to provide maximum heating energy
- A reentry trajectory which provides the maximum heating flux
- An impact on an unyielding surface and in the ocean at a velocity 10 percent higher than the predicted terminal velocity.

The response of the container and waste to the reentry environments must be calculated after the specific reentry conditions have been determined by analysis.

2.5.1.4 Criticality

The radioactive waste package shall be subcritical (K-effective $\leq$ 0.95) for normal operations or any possible credible accident during processing, fabrication, handling, storage, or transport to the space destination.

2.5.1.5 Postaccident Recovery

Postaccident recovery teams will be made part of the operational disposal system. They will be responsible for all accident recovery operations, including accidents involving processing, payload fabrication and railroad shipment, payload preparation at the launch site, the launch and possible reentry.

2.5.1.6 Monitoring Systems

Monitoring systems will be developed for the overall system such that overall mission safety can be assured. Examples of such systems include devices for measuring radiation, temperature and, possibly, pressure in the waste package, and instruments to provide data for tracking the payload after it is placed into its solar orbit disposal region.

2.5.2 Specific System Safety Design Requirements

The following paragraphs define specific design requirements established for the elements of the reference disposal concept (see Sections 2.3, 2.4, 3.3 and Appendix C). As the reference concept changes, these requirements are also expected to change.

2.5.2.1 Waste Form

For normal conditions, the cermet fabrication temperature of 1200 C shall not be exceeded. For accident conditions, the cermet decomposition temperature of 1450 C shall not be exceeded.

2.5.2.2 Waste Processing and Payload Fabrication Facilities

The design and operation of these facilities will follow current proposed regulations, as specified for reprocessing plants.

2.5.2.3 Payload Primary Container

For normal conditions, the primary stainless steel container shall not exceed the creep limit temperature of 427 C. No chemical and physical interaction will occur between the cermet waste form and the container. For accident conditions, the primary container must not exceed the melt temperature of 1450 C.

2.5.2.4 Flight Radiation Shielding

Radiation shielding for flight systems will be designed to limit radiation to no more than 2 rem per hour at 1 meter from the shield surface under normal conditions. Auxiliary shielding will be designed such that radiation exposure limits (see Tables 2-4 and 2-5) for ground personnel and flight crews are not exceeded during handling or flight operations.

For normal conditions, the temperature limit for the depleted uranium/stainless steel flight radiation shield is 427 C. For accident conditions, the radiation shield must not exceed the uranium melt temperature of 1130 C.

2.5.2.5 Reentry Vehicle Systems

The reentry vehicle systems must include provisions to survive on-pad and reentry environments as stated in Sections 2.5.1.3.3 and 2.5.1.3.4. Also, the system must include: (1) an aerodynamic drag fin to minimize the terminal velocity during reentry; (2) provisions for absorbing the external impact loads; (3) a fire and reentry thermal protection system; (4) provisions for flotation upon ocean entry; (5) a transmitter for recovery; and (6) a redundant reaction control system for attitude control in space.

2.5.2.6 Shipping Casks and Ground Transport Vehicles

Shipping casks and ground transport vehicles will comply with DOT and NRC regulations (see Section 2.5.1.1). The maximum outside diameter of the shipping cask will be 3.05 meters (10 feet). When required for heat rejection, a redundant cooling system for the shipping cask will be required.

2.5.2.7 Launch Site Facilities

The launch pad used for the reference nuclear waste disposal traffic model (see Table 2-6) will be a dedicated pad.

2.5.2.8 Uprated Space Shuttle Launch Vehicle

The Uprated Space Shuttle launch vehicle design will reflect considerations of keeping on-pad accident environments as low as possible. The overall vehicle launch reliability goal will be greater than 0.999 (meaning one chance in 1000 that the vehicle will be catastrophically lost during ascent). The External Tank and liquid rocket booster design will include destruct systems, properly located, which provide for a minimum explosive yield of the liquid propellants when a catastrophic event is expected.

2.5.2.9 Earth Parking Orbits

Intermediate Earth parking orbits shall be incorporated into the flight profiles of space transportation systems to allow a minimum of 6 months before orbital decay of the nuclear waste payload could occur.

2.5.2.10 Upper Stages

All upper stages will have delivery reliabilities greater than 0.99. Achievement of delivery is defined as being within the bounds of the following: 0.85 $\pm$ .01 A.U. and 1.00 $\pm$ 0.20 degrees inclination.

2.5.2.11 Payload Ejection System

The reliability of this system must be established such that it is truly beneficial in keeping the radiological hazard to a minimum.

2.5.2.12 Space Destination

The nominal space destination will insure, at a minimum, an expected isolation time of one million years.

2.6 Accident and Malfunction Contingency Plans for Reference Concept

Accident and malfunction contingency plans for the reference space disposal concept have been developed over the last 2 years of study. The philosophy contained in this section is important to the future development of the space option concepts. Accident and malfunction contingency plans for the general phases of the space disposal mission are listed and addressed below:

- Ground transportation from the payload fabrication sites to KSC
- Preflight operations prior to ignition of the Shuttle's engines
- Launch operations from the launch pad to achieving parking orbit
- Orbital operations.

2.6.1 Ground Transportation

Ground transport (via rail) of the shipping cask will be assigned to the Department of Energy (DOE) which will supply the necessary accident recovery plans and systems. At least two types of incidents must be considered: loss of cooling to the waste container and possible breach of the waste container with a loss of radioactive material.

In case of cooling loss, provisions must be made to have self-contained, auxiliary cooling units available within 3 hours (see Section 2.5.1.3.1). Monitoring equipment for both container temperature and radiation will be required during all ground transport operations.

A continuous capability to cope with a container breach will be necessary. A specially trained accident recovery crew will always be ready to act, if necessary.

2.6.2 Preflight Operations

Contingency plans must be provided for potential malfunctions and accidents that could occur while the waste payload is in the NPPF, being transported to the launch pad, being transferred from the pad RSS to the Space Shuttle cargo bay, and awaiting liftoff in the Shuttle. Accidents and contingency plans would be similar to those discussed in Section 2.6.1, above.

2.6.3 Launch Operations

Contingency plans, procedures and systems envisioned to minimize the hazard caused by on-or near-pad failure are given below. These plans, procedures and systems would minimize the effects of severe blast wave, high velocity fragments, fire, and possible high velocity impact (see Section 2.5.1.3.3).

- **A system to eject the loaded reentry vehicle system** (contains nuclear waste) from the Orbiter's cargo bay and away from ensuing adverse environments.

- **A destruct system** on the External Tank and LRB's properly designed to minimize the blast wave and fragment environments caused by the exploding hydrogen/oxygen and RP-1/oxygen propellants. This would aid in minimizing the effect on the containment systems.

- **Stringent containment systems designs** (e.g., container, shielding and reentry vehicle systems) to maximize the probability of surviving the possible hostile environments. The reentry vehicle will contain flotation gear and locator beacons to assist in the recovery of the payload.

- **The use of a waste form** not easily dispersed under adverse conditions.

- **The application of appropriate launch constraints** (e.g., wind direction) to reduce human radiological exposure resulting from a potential containment breach.

- **The use of a recovery team** ready to rescue the payload at sea or on land.

- **Engine shutdown** is an important factor in total vehicle reliability. For the Uprated Space Shuttle, all booster engines are liquid fueled, and as such, they can be shut down if a failure occurs during the engine start-up process, and prior to actual liftoff. This capability would greatly reduce the probability of an on-pad catastrophic vehicle failure.

Systems and procedures, in addition to some of those mentioned above, which would minimize the hazard caused by subsystem failures during the boost phase are:

- **Intact aborts** can be implemented after a few seconds into the flight. Three types of intact aborts are possible for the Uprated Space Shuttle. These are: the return-to-launch-site (RTLS), abort-once-around (AOA) and abort-to-orbit (ATO).

- **Contingency aborts** could lead to either a return to land or to ditching at sea.

- **Design of the boost trajectory** to avoid land overflight, for example the 38° inclination orbit, should help in reducing overall risk for the early portion of the flight.

2.6.4 Orbital Operations

The OTV propulsion phase provides for transportation from low Earth orbit to the intermediate destination. In the initial years* of the disposal mission the OTV would be a high-thrust, chemical propulsion (liquid hydrogen/liquid oxygen) stage (see Section 2.4.9). To minimize possible failures the following systems, procedures and design requirements are envisioned:

- **The use of command OTV engine shutdown** in the event of a grossly inaccurate propulsive burn
- **The capability to separate the SOIS and attached payload from the OTV** and the use of the SOIS to place the payload in a safe orbit for eventual recovery by a rescue vehicle or Shuttle Orbiter
- **A jettison system** incorporated into the SOIS payload adapter to separate the waste payload from the OTV/SOIS configuration when necessary to preclude a possible reentry
- **The use of a rescue vehicle** to retrieve a waste payload stranded in any given orbit
- **The use of redundant systems** where feasible to ensure high reliability
- **On-orbit OTV launch crew** to obtain instantaneous visual and telemetric status of the OTV propulsive burn (from the Orbiter)
- **The proper design of trajectories** and propulsive burns of the OTV to reduce the probability for reentry if a failure occurs
- **A waste form** which helps insure intact reentry of the waste container, should an unplanned reentry occur
- **The application of thermal protection material** on the outside of the container to reduce the risk of atmospheric dispersal.
- **The use of a high melting point container material** to reduce the risk of atmospheric disposal.

The SOIS provides for transportation from an intermediate to the final destination. For the reference concept, the SOIS is used to reduce the aphelion from 1.0 to 0.85 A.U. (see Section 2.4.9). Systems, procedures and design requirements envisioned to minimize hazards due to SOIS failures are:

---

*Later on, low-thrust technology (e.g., solar electric propulsion) might be used. With low-thrust systems, both the probability and magnitude of an explosion are decreased. In addition, there is a much longer decision and response time available in case of a malfunction of the low-thrust propulsion systems.

- The use of a rescue vehicle to retrieve a cooperative or non-cooperative payload stranded in any orbit in heliocentric space
- The use of redundant SOIS systems where feasible to ensure high reliability
- The proper use of trajectories and orbits inclined to the ecliptic plane that exhibit long-term orbital stability
- The use of tracking systems on board the SOIS to aid in deep space rescue operations.

2.6.5 Rescue Operations

Provisions must be made to rescue the SOIS and the nuclear waste payload in Earth orbit in the event of a failure of the OTV during the Earth escape burn. The approach is to rendezvous and dock the rescue OTV with the SOIS and continue the mission from the failed orbit. The rescue mission is based on the premise that, with proper control of the OTV launch, any failure of the OTV will result in an elliptic orbit about Earth. The mission profile for payload rescue, summarized in Figure 2-11, is to deliver a rescue OTV to low Earth orbit in the Shuttle, transfer by a burn of the OTV to a phase-adjust orbit, and transfer from the phase-adjust orbit at the proper time for rendezvous and docking with the failed system. The lifetime of the rescue OTV, considering the coast time in the phase-adjust orbit, must be as much as 300 hours, compared to the 50 hours for OTV lifetime on the nominal reference mission. Locating failed systems and docking with noncooperative systems is discussed in Section 6.2.

After injection into deep space, the nuclear waste payload could fail to achieve its stable destination orbit, because of a premature shut-down of the OTV engine beyond Earth-escape conditions or a failure of the SOIS to ignite at solar orbit conditions. Studies that address the probability of Earth reentry under these failure conditions have recommended the use of a deep space rescue mission capability as a way of further reducing the overall risk during this phase of the mission (see Section 6.2). A deep space rescue mission capability is defined as the ability to send another propulsion system (e.g., OTV and SOIS) to rendezvous with the failed payload in solar orbit and to place it into the desired stable orbit (circular 0.85-A.U. solar orbit).

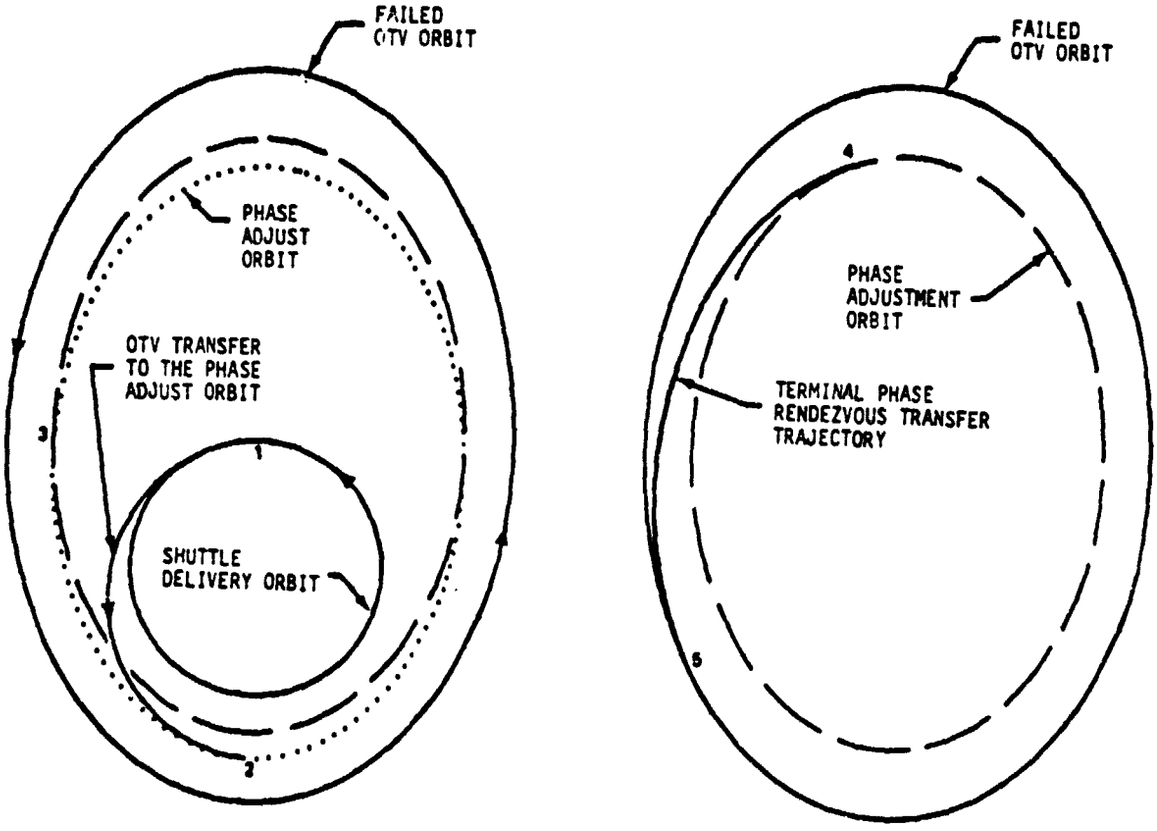

1-2 OTV Transfer to Phase Adjust Orbit

2-3 Coast in Phase Adjust Orbit

4-5 Transfer from Phase Adjust Orbit to Rendezvous Position in Target Orbit

FIGURE 2-11. EARTH ORBITAL PAYLOAD RESCUE MISSION PROFILE

2.7 Reference Projected Traffic Model, Hardware, and Propellant Requirements

The projected traffic model, hardware, and propellant requirements for major reference mission elements have been estimated for the period from 1992 to 2003.

For the reference mission definition, an upper bound of 580 Uprated Space Shuttle flights are required to dispose of all of the available U.S. high-level commercial nuclear wastes (PW-4B cermet) through the year 2000 (see Table 2-1). One Uprated Space Shuttle flight would be required for each disposal mission--5000 kg of cermet waste form per payload. Consideration of development flights and aborted missions would be expected to increase this number somewhat. Table 2-6 provides the projected Uprated Space Shuttle traffic model required to support the space disposal mission.

TABLE 2-6. PROJECTED UPRATED SPACE SHUTTLE TRAFFIC MODEL FOR COMMERCIAL HIGH-LEVEL NUCLEAR WASTE DISPOSAL MISSIONS (1992-2003)

	Year												
	92	93	94	95	96	97	98	99	00	01	02	03	Total
Uprated Space Shuttle Flights	10	20	50	50	50	50	50	60	60	60	60	60	580

Table 2-7 shows the major mission elements, the hardware use factor assumed and the total hardware requirements. No impact is expected on the Space Shuttle traffic model for the decade of the 1980's (see Reference 2-2), as the nuclear waste disposal activity is not expected to be operational before 1992.

TABLE 2-7. MAJOR HARDWARE REQUIREMENTS ESTIMATES DURING 1992-2003 TIME PERIOD FOR HIGH-LEVEL COMMERCIAL NUCLEAR WASTE DISPOSAL IN SPACE

Hardware Element	Use Factor	Number Required
Uprated Space Shuttle Hardware		
- Orbiters	100	6
- ET's	1	580
- LRB's (2 LRB's Per Flight)	20	58
Upper Stage Hardware		
- OTV's	20	29
- SOIS's	1	580
Waste Payload Systems		
- Containers	1	580
- Gamma Radiation Shields	20	29
- Payload Reentry Vehicles	20	29
- Crew Shields (flight)	100	6
- Cooling Systems (flight)	100	6
- Rail Cars and Casks	200	3

NOTE: Table assumes 580 Uprated Space Shuttle flights to dispose of high-level commercial nuclear waste (PW-4b cermet), one Shuttle flight per mission.

The onboard propellant requirements per Uprated Space Shuttle disposal mission are given in Table 2-8. Total requirements can be estimated by multiplying these data by the number of flights/year as given in Table 2-6. Actual propellant requirements will be somewhat higher than shown due to losses from propellant transfer and cryogenic propellant boil-off.

TABLE 2-8. ON-BOARD, PER FLIGHT, PROPELLANT REQUIREMENTS FOR REFERENCE NUCLEAR WASTE DISPOSAL MISSION

	Propellants, metric tons				
Vehicle	Liquid Hydrogen (LH_2)	Liquid Oxygen (LOX)	RP-1 (Kerosene) (RP)	Nitrogen Tetroxide (NTO)	Monomethyl Hydrazine (MMH)
Uprated Shuttle External Tank (ET)	102	610	--	--	--
Uprated Shuttle Liquid Rocket Booster (LRB)	--	803	277	--	--
Uprated Shuttle Orbiter	--	--	--	7.58	4.74
Orbit Transfer Vehicle (OTV)	2.59	15.6	--	--	--
Solar Orbit nsertion Stage (SOIS)	--	--	--	1.74	2.79
Totals	104.59	1428.6	277	9.32	7.53

2.8 Advanced Concept for Space Disposal of Nuclear Waste

The advanced concept for space disposal of nuclear waste is similar in many respects to the reference concept defined in Sections 2.3 and 2.4. The advanced concept is based upon the availability of a heavy lift launch vehicle (HLLV) that may be developed by NASA for future space missions beyond the year 2000. The major differences between the advanced and reference concepts are discussed in the paragraphs below that pertain to each major portion of the mission. The differences are summarized in Table 2-9.

TABLE 2-9. COMPARISON OF REFERENCE AND ADVANCED SPACE DISPOSAL CONCEPTS

Mission Elements	Reference Concept	Advanced Concept
Waste Mix	PW-4b	Modified PW-4b (90% and Cs Sr removed)
Waste Form Mass/Payload, kg	5000	9500
Number of Payloads/Mission	1	3
Number of OTVs/Mission	1	3
Number of SOIS's/Mission	1	3
Ground Transportation	Rail	Rail/Sea
Launch Site	KSC, Florida	Remote Island
Launch Vehicle	Uprated Space Shuttle	HLLV
Launch Vehicle Payload, kg	45,400	231,000

2.8.1 Nuclear Waste Processing and Payload Fabrication

Spent fuel rods from domestic power plants would be transported to a waste processing and payload fabrication facility via conventional shipping casks. Using a modified Purex process (Modified PW-4b) high-level waste containing fission products (less 90 percent of the Cs and Sr) and actinides, including 0.1 percent plutonium and 0.1 percent uranium, will be processed from these spent fuel rods (see Section 3.4.4 and Appendix F). The 90 percent of the Cs and Sr would be disposed of via terrestrial disposal. These two elements have been removed from the PW-4b mix to meet thermal requirements for the fabrication of 9500 kg sized spheres of cermet waste form (see Section 2.3.1). Other activities are the same as the reference concept (see Section 2.3.1).

2.8.2 Nuclear Waste Ground Transport

Once the spherical waste form (9500 kg) has been fabricated and placed in its primary container and flight radiation shield, it would be

loaded into a transportation shipping cask for travel by rail and then by escorted ship to the remote island launch site. Once the cask reaches the launch site the cask would be off-loaded into an Advanced Nuclear Payload Preparation Facility (ANPPF).

2.8.3 Payload Preparation at Launch Site

The remote island located ANPPF will provide interim storage capability for up to 18 shielded waste containers, which affords efficient preparation for launches plus capacity for unplanned delays. During storage, additional radiation shielding, thermal control, monitoring and inspection of the waste container will be provided.

2.8.4 Prelaunch Activities

In preparation for launch of the nuclear waste into space on board a HLLV, three-9500 kg waste payloads will be prepared (see Figure 2-12). Each (including its own container and flight shield) will be integrated with a reentry vehicle, a Solar Orbit Insertion Stage (SOIS) and an Orbit Transfer Vehicle (OTV). The three integrated payloads would then be placed in the cargo bay of the HLLV orbiter.

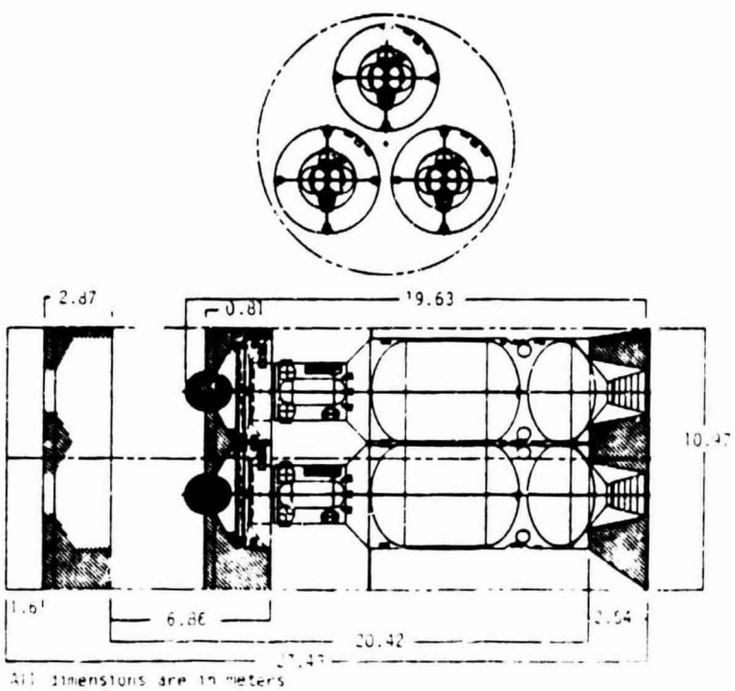

FIGURE 2-12. HLLV LAUNCH CONFIGURATION WITH NUCLEAR WASTE PAYLOADS AND SPACE VEHICLES

2.8.5 HLLV Booster Operations

One HLLV will be readied for launch for a given disposal mission. The HLLV is a fully reusable vertical takeoff, two-stage vehicle (see Figure 2-13). The booster and orbiter stages have a common body diameter, wing and vertical stabilizer; however, the overall length of the orbiter is 5 meters greater than the booster. The vehicle gross liftoff mass is 7.1 million kg.

The HLLV booster is shown in the landing configuration in Figure 2-14. The vehicle is 91.4 meters in length with a wing span of 56 meters. The nominal body diameter is 12 meters. The vehicle has a dry mass of 0.47 million kg. Seven high pressure gas generator driven LOX/RP-1 engines mounted in the aft fuselage provide a nominal sea-level thrust of 10.2 million Newtons (N) each. Eight turbojet engines are mounted on the upper portion of the aft fuselage with a nominal thrust of 89,000 N each.

The HLLV orbiter is depicted in Figure 2-15. The vehicle is 96.6 meters long with the same wing span, vertical height, and nominal body diameter as the booster. The orbiter employs four high-pressure staged combustion LOX/LH_2 rocket engines with a nominal sea level thrust of 5.29 million Newtons each. The cargo bay is located in the mid-fuselage in a manner similar to the Space Shuttle Orbiter and is about 27.4 meters long. The HLLV, with its 231,000 kg payload is launched to a 487 km circular orbit inclined 38 degrees to the equator. Once on orbit, the three payload configurations would be deployed from the HLLV orbiter cargo bay. The three reentry vehicles would be remotely removed from the OTV/SOIS/Payload configurations and loaded back into the HLLV orbiter cargo bay for reuse.

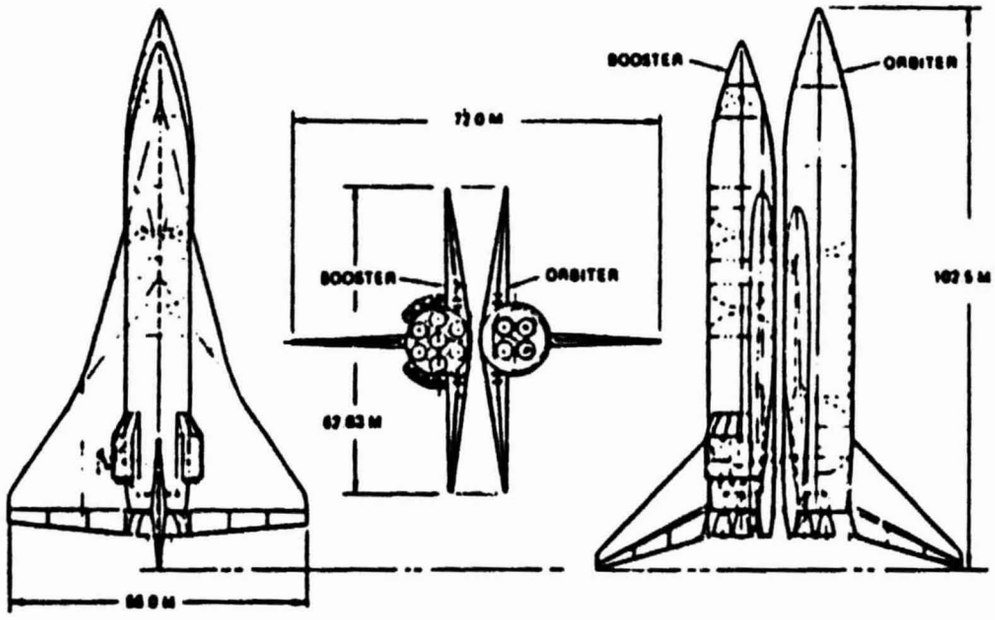

FIGURE 2-13. HLLV LAUNCH CONFIGURATION

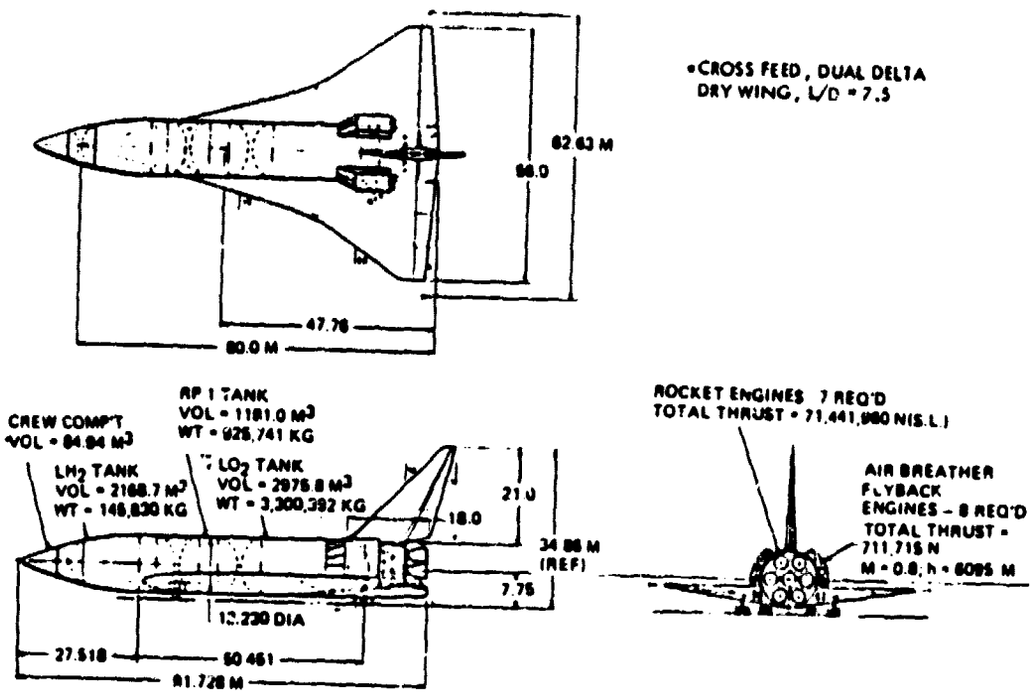

FIGURE 2-14. HLLV FIRST STAGE (BOOSTER) LANDING CONFIGURATION

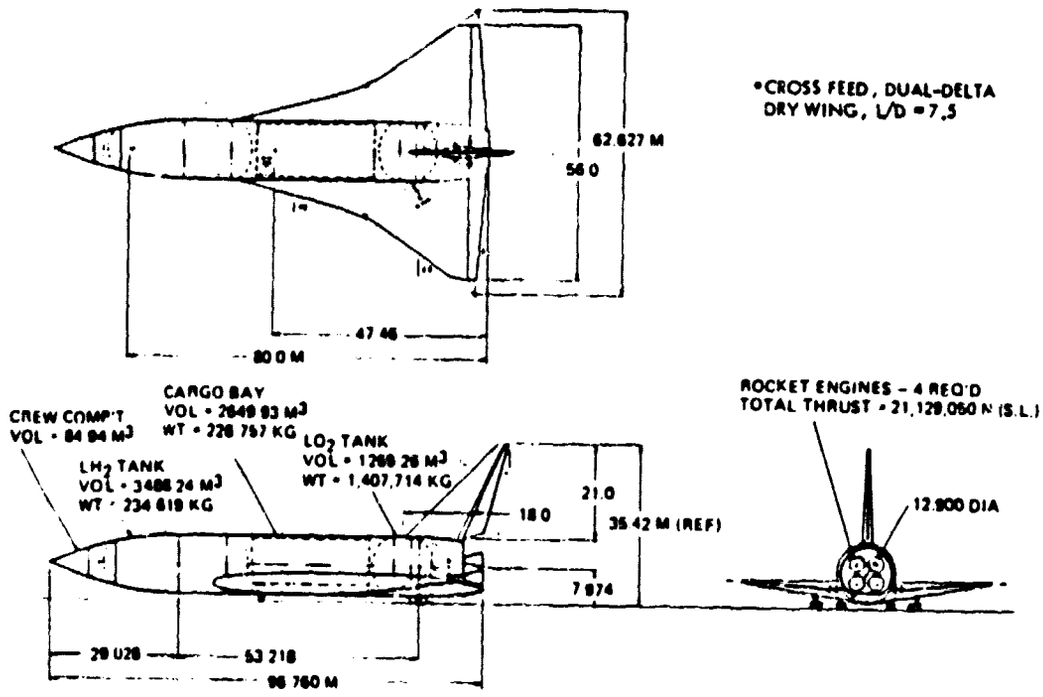

FIGURE 2-15. HLLV SECOND STAGE (ORBITER) LANDING CONFIGURATION

2.8.6 Upper Stage Operations

Operations of upper stages for the advanced concept are identical to those described in Section 2.3.6. The three OTV's employed during each mission would be recovered by the single HLLV orbiter.

2.9 References

2-1. "Concept Definition Document for Nuclear Waste Disposal in Space," NASA/Marshall Space Flight Center, Huntsville, Alabama (January 1980).

2-2. "NASA Payload Model," JSC 13829, NASA/JSC, Houston, Texas (January 1978).

2-3. Burns, R. E., et al., "Nuclear Waste Disposal in Space," NASA-TP-1225, NASA/MSFC, Huntsville, Alabama (May 1978).

2-4. Pardue, W. M., Rice, E. E., Miller, N. E., and Davis, D.K., "Preliminary Evaluation of the Space Disposal of Nuclear Waste," 8-32391(100), Battelle Memorial Institute, Columbus, Ohio (August 1977).

2-5. Brown, B. G., et al., "Nuclear Waste Disposal Mission Analysis," TR-223-1874, Northrop Services, Inc., Huntsville, Alabama (November 1977).

2-6. Friedlander, A. L., et al., "Analysis of Long-Term Safety Associated with Space Disposal of Hazardous Material," SAI-1-120-676-T11, Science Applications, Inc., Schaumburg, Illinois (December 1977).

2-7. Friedlander, A. L., et al., "Aborted Space Disposal of Hazardous Material: The Long-Term Risk of Earth Reencounter," SAI-1-120-676-T8, Science Applications, Inc., Rolling Meadows, Illinois (February 1977).

2-8. "Feasibility of Space Disposal of Radioactive Nuclear Waste," NASA-TM-X-2912, NASA/LeRC, Cleveland, Ohio (May 1974).

2-9. Priest, C. C., et al., "Nuclear Waste Management (Space Option) - Mission and Design Analysis," NASA/MSFC, Huntsville, Alabama (December 1978).

2-10. Edgecombe, D. S., Rice, E. E., Miller, N. E., Yates, K. R., and Conlon, R. J., "Evaluation of the Space Disposal of Defense Nuclear Waste -Phase II," Volumes I, II, and III, Battelle's Columbus Laboratories, Columbus, Ohio (January 1979).

2-11. "Draft Environmental Impact Statement for the Management of Commercially Generated Radioactive Waste," DOE/EIS-0046 D, U.S. Department of Energy, Washington, D.C. (April 1979).

2-12. Friedlander, A. L., and Davis, D. R., "Long-Term Risk Analysis Associated with Nuclear Waste Disposal in Space," Report No. SAI-1-120-062-T12, Science Applications, Inc., Schaumburg, Illinois (December 1978).

2-13. Priest, C. C., "Nuclear Waste Management (Space Option) - Historical Activity Summary," NASA/MSFC, Huntsville, Alabama (June 1979).

2-14. Yates, K. R., and Park, U. Y., "Projections of Commercial Nuclear Capacity and Spent-Fuel Accumulation in the United States," Fuel Reprocessing, pp. 350-352 (June 1979).

2-15. Mendel, J. E., et al., "Annual Report on the Characteristics of High-Level Waste Glass," BWNL-2252, Battelle Northwest Laboratories, Richland, Washington (June 1977).

2-16. United States Nuclear Regulatory Commission, Rules and Regulations, Title 10, Part 71, Code of Federal Regulations--Energy (September 1978).

2-17. "Final Environmental Impact Statement for the Space Shuttle Program," NASA Headquarters, Washington, D.C. (April 1978).

2-18. "Space Shuttle," NASA SP407, NASA Headquarters, Washington, D.C. (1976).

2-19. "Space Shuttle System Payload Accommodations," NASA/JSC 07700, Volume XIV - Revision F, NASA/JSC, Houston, Texas (March 1979).

2-20. Sanders, J., et al., "Shuttle Liquid Rocket Booster Study--A Conceptual Design/Feasibility Analysis Study," NASA/MSFC, Huntsville, Alabama (April 1979).

3.0 NUCLEAR WASTE PAYLOAD CHARACTERIZATION

The objective of the Nuclear Waste Payload Characterization Task was to define the commercial and defense nuclear waste payload in terms of waste form, waste mix, containment system requirements, container and shield definitions, and waste processing and payload fabrication operations.

The major goal of this activity was to identify a new waste form with properties appropriate for the accident and normal conditions identified for the disposal in space of both commercial and defense high-level wastes. Although commercial and defense wastes have been considered in previous space disposal studies, a new effort was made to define, in terms of the most recent information, the quantities and availability of each of these waste types. In addition, the composition and concentration of each waste type was reevaluated to update the radiation and heat source terms for the waste package. The data were used for parametric studies of the radiation shield definition and thermal design for a range of waste payload sizes from a small RTG-size sphere to a large HLLV package. A 5.5 MT sized payload was defined as a design basis for the Uprated Space Shuttle case.

This section is composed of six subsections. Section 3.1 discusses the efforts made to define a new waste form, the present state of technical development of that waste form, and its thermophysical properties. Section 3.2 describes the updated information on the commercial and defense high-level waste compositions and the quantities of these wastes projected to be available for space disposal. Section 3.3 discusses preliminary specifications for the waste package. Section 3.4 presents the results of the radiation shielding, payload mass, and thermal analyses performed for the range of waste package sizes. Section 3.5 presents a general discussion of the waste treatment and packaging facility, which will be necessary for preparing the waste payload for disposal in space. Section 3.6 is a list of references for Section 3.0.

3.1 Waste Form Selection

3.1.1 Waste Form Evaluation and Selection

During the Phase I[3-1] and Phase II studies of[3-2] nuclear waste disposal in space, a constraint was placed on waste form selection by specifying that waste form technology be available on an industrial scale by the early 1980's. This constraint limited the waste form selection to calcine or glass. Because of its higher waste loading and better thermal stability, calcine was selected over glass during the Phase I and II studies. It was recognized during these previous studies that calcine had problems of its own, i.e., it is easily dispersed and leached, and that it has poor thermal conductivity.

For the Phase III study, the waste form technology-availability constraint was shifted to the early 1990's. Because of this, waste forms such as supercalcine, cermet, metal matrix with coated particles, glass ceramic, and titanate ceramic could be evaluated along with calcine and glass for potential use as a waste form for space disposal.

To insure proper credibility a careful and objective waste form evaluation and selection had to be undertaken. The plan used to evaluate and select the waste form for the current study consisted of:

- Selecting waste form experts from DOE facilities in which waste forms are actually being made and tested
- Providing the waste form experts with: general background information on the space disposal concept; descriptions of the failure modes and accident environments; and preliminary waste form parameters considered to be important for the safe and reliable performance of the disposal mission
- Having the waste form experts visit BCL for a meeting to discuss and evaluate waste forms for space disposal
- Obtaining concurrence among all parties involved (NASA, BCL, DOE experts, ONWI) on final waste form selection.

The waste form evaluation and selection plan was implemented during July and August 1979. A meeting was held at BCL on July 19, 1979 to evaluate waste forms for the space disposal of commercial and defense high-level waste (HLW). Participants included ONWI, NASA, BCL, and DOE-Richland Operations personnel and waste form experts from Battelle Northwest Laboratories, Oak Ridge National Laboratories, Idaho Chemical Processing Plant, and Sandia Laboratories. During that meeting, the following set of parameters was determined to be applicable to the space disposal waste form evaluation:

1. **High waste loading** - This is an important parameter when considering the disposal of the large mass of commercial or defense

HLW. Waste forms having high waste loadings will require fewer launches. Fewer launches not only lower operational costs but also yield lower construction costs for dedicated launch facilities. Rating: primary importance.

2. **High thermal conductivity** - Commercial HLW, especially in waste forms having high waste loadings, generates a significant quantity of heat. To prevent central regions from becoming excessively hot, the waste form should possess a relatively high heat transfer coefficient. Similarly, upon unplanned reentry of an unprotected waste package, the waste form should be capable of rapidly conducting heat away from the surface. Rating: primary importance.

3. **Resistance to thermal shock** - The waste form should be resistant to shattering which may be caused by thermal shock. This is a property that will help in achieving low dispersibility of the waste form; e.g., during impact of an unprotected package into the oceans. Rating: secondary importance.

4. **Thermochemical stability** - In launch pad or reentry accidents, the waste form should remain chemically stable. It should not degrade, decompose, or otherwise be altered in its chemical form in such a way that a significant release of radionuclides occurs during such postulated accidents. Rating: primary importance.

5. **Resistance to leaching** - A low leach rate is important if the unprotected waste form package impacts into water during an unplanned reentry. During a preorbital launch abort, however, the waste package will reenter with reentry protection and possibly a floatation collar. While leach rate is important, it is not as important as in terrestrial disposal where radionuclide transport by groundwater is considered the most probable mechanism for loss of isolation. Rating: secondary importance.

6. **Toughness** - Another aspect of dispersion resistance is material toughness. The waste form should be shatter and abrasion resistant upon impact, and should deform to absorb impact. Retrieval of the waste form as a single piece rather than many fragmented parts is desirable. Rating: primary importance.

7. **Applicability to both commercial (PW-4b) and defense (Hanford) HLW mixes** - The waste form should be generally capable of accomodating both commercial and defense HLW. Commercial HLW as defined in this study is the PW-4b mix (as discussed in Section 3.2.1). This waste mix has a relatively small quantity of inert reprocessing chemicals and has a high concentration of waste radionuclides. Defense waste considered for this study is the Hanford HLW, which has been subjected to the proposed radionuclide removal process and which has had additional inert material removed. However, the Hanford mix is considerably diluted by ZrO_2 and other inert materials associated with it. Rating: primary importance.

8. **Fabrication** - The waste form fabrication process should be available on the industrial scale by the mid-1990's. It should be capable of producing a relatively large shape (1-meter-diameter sphere or "square" right circular cylinder) by remote processing in a reliable fashion. Rating: primary importance.

9. **Economics and resource utilization** - Waste form materials and fabrication processes should not be prohibitively expensive. Also, waste form materials should not severely deplete valuable raw materials. Since the cost of a booster launch is expected to be the major part of the total cost, waste form material and process costs will not be overly important. Rating: secondary importance.

10. **Resistance to oxidation** - Another aspect of dispersion resistance is waste form resistance to oxidation. If an unplanned reentry of the unprotected waste package occurred, the surface of the waste form should not rapidly oxidize and break away from the main body of the waste package. Rating: secondary importance.

Following the determination of the important parameters for waste form evaluation, a matrix was developed to rate various HLW forms versus these ten parameters. The waste forms chosen for evaluation were: borosilicate glass, hotpressed supercalcine, ORNL cermet, ICPP glass ceramic, Sandia titanate ceramic, and metal matrix with coated particles. Calcine was excluded from evaluation because it is highly dispersible and easily leachable. SYNROC was excluded from evaluation because of its very low waste loading. Table 3-1 presents the qualitative ratings (high, moderate, or low) as agreed to by the waste form experts for the various waste forms for each of the ten parameters.

TABLE 3-1. COMPARISON OF ADVANCED WASTE FORMS FOR SPACE DISPOSAL

	ORNL CERMET	ICPP GLASS CERAMIC	SANDIA TITANATE CERAMIC	BORO-SILICATE GLASS	METAL MATRIX (COATED PARTICLE)	HOT-PRESSED SUPERCALCINE
HIGH WASTE LOADING	M[a]	M	M	L	L	H
HIGH THERMAL CONDUCTIVITY	H	L	L	L	H	L
RESISTANCE TO THERMAL SHOCK	H	H	H	L	H	H
THERMOCHEMICAL STABILITY (FABRICATION TEMP., C)	1450	1100	1100	1100	1000[b]	1100
RESISTANCE TO LEACHING	H	H	H	H	H	H
TOUGHNESS	H	M	M	L	H	M
APPLICABILITY TO COMMERCIAL (PW-4b) AND DEFENSE (HANFORD) MIXES	H	L	L	L	H	L
FABRICATION OF WASTE FORM INTO DESIRED SHAPE AND SIZE	M	L	L	H	M	L
ECONOMICS	M	M	M	H	L	M
RESISTANCE TO OXIDATION	L	H	H	H	L	H

NOTES: (a) H = HIGH, M = MODERATE, AND L = LOW.
(b) COPPER.

An important part of the waste form evaluation was the determination of the relative importance of the parameters. After the waste form expert meeting, BCL personnel met and determined (with concurrence from the waste form experts) that the following parameters are of primary importance: high waste loading, high thermal conductivity, thermochemical stability, toughness, applicability to both waste mixes, and fabrication. Parameters of secondary importance are: resistance to thermal shock, resistance to leaching, economics, and resistance to oxidation. With respect to the parameters deemed to be of greatest importance, ORNL cermet (iron-nickel based) and metal matrix (copper) with coated particles appear clearly superior. The ORNL cermet can achieve generally higher waste loadings and better thermochemical stability than metal matrix with coated particles. Therefore, ORNL cermet was selected (with the concurrence of the waste form experts, NASA, ONWI and the BCL Project Team) as the reference waste form for use in the study.

The only parameter in which cermet (iron-nickel based) or metal matrix (copper) received a significantly lower rating than the ceramic-type other waste forms was for resistance to oxidation. However, since both cermet or metal matrix each have significantly higher thermal conductivity than the other waste forms, their surface temperature may not rise as high as that of the other waste forms during an unplanned reentry. Currently, it is unclear what will actually happen to a waste form with respect to rapid oxidation during a shallow reentry. Because of this uncertainty, the low rating of cermet or metal matrix with respect to oxidation resistance should not be viewed with significant concern at this time. In any event, the waste form and container would likely be encased in a protective wrap to effectively preclude such an occurrence (see Section 4.3.4).

3.1.2 Cermet Characterization

ORNL cermet is a metallic appearing waste form in which the majority of the HLW radionuclides are uniformly distributed as micron-sized particles of crystalline ceramic oxides, aluminosilicates, and/or titanates in a hydrogen reducible metal matrix.[3-3] The metal matrix is composed of chemically reducible metals and fission products already in the waste (Fe, Ni, Cu, Te, etc.) and reducible metal additives necessary to formulate a particular alloy composition.

Cermet fabrication presently consists of four basic steps.[3-3] First, the waste and additives are dissolved in molten urea. Next a calcination of the solution of waste plus additives is accomplished utilizing a spray calciner. The resulting material may then be compacted and formed into a desirable shape by a variety of processes (hot pressing, isostatic pressing, etc.). Finally, the fabricated shape is reduced and sintered in hydrogen. These four steps may require modification as the process is scaled up in size and as it is applied to fabricating a waste form for space disposal.

Reference concept cermet compositions have been recommended by ORNL for both commercial (PW-4b) and defense (Hanford) HLW and are presented in Table 3-2. The densities, waste loadings, thermal conductivities, specific heats, and heat generation rates for commercial and defense HLW are presented in Table 3-3.

TABLE 3-2. ORNL REFERENCE CERMET COMPOSITION FOR COMMERCIAL AND DEFENSE HIGH-LEVEL WASTE

	Reference Commercial HLW Cermet (PW-4b), kg/MTHM	Reference Defense HLW Cermet (Hanford), mass percent
Composition at Start of Form Processing		
Oxide	40.8	40.0
Metal Additives (Fe, Ni, and Cu)	25.2	52.2
TiO_2, SiO_2 and Al_2O_3	3.5	7.8
Total	69.5	100.0*
Composition After Reduction in Hydrogen		
Waste Oxides, Including Ti, Si and Al	34.8	43.0
Reduced Waste Metals	9.5	4.8
Metal Additives	25.2	52.2
Total	69.5	100.0*

*Note: Units in mass percent.

TABLE 3-3. REFERENCE CERMET CHARACTERISTICS (ESTIMATED) FOR COMMERCIAL AND DEFENSE HIGH-LEVEL WASTE

Characteristic	Reference Commercial HLW Cermet (PW-4b)	Reference Defense HLW Cermet (Hanford)
Density, g/cc	6.7	6.7
Waste Loading, percent**	58.7	40.0
Thermal Conductivity, W/m-C	14	20.5
Specific Heat, cal/g-C	0.14	0.20
Heat Generation, kW/MT	19.2	0.23

**Note: Calcine powder defined as 100 percent.

Since any hydrogen-reducible metal can be used for the metal additive in cermet fabrication, a brief assessment was conducted to determine the viability of a few alternatives. ORNL suggested Mo, Nb, and Ta as possible substitutes for Fe-Ni-Cu. Parameters considered in the assessment were resource availability, density, shielding, and heat transfer performance. The results of the assessment are summarized below.

- Molybdenum (Mo)
  - Approximately 0.8% of present U.S. consumption or 0.21-0.27% of U.S. estimated consumption by the year 2000[3-4,3-5]
  - Density (and shielding) not much different than Fe, Ni
  - Heat transfer better than Fe, Ni
- Niobium (Nb)
  - Approximately 13% of present U.S. consumption or 1.5-2.9% of U.S. estimated consumption by the year 2000[3-4,3-5]
  - Density (and shielding) not much different than Fe, Ni
  - Heat transfer better than Fe, Ni
- Tantalum (Ta)
  - Approximately 29% of present U.S. consumption or 8.3% of U.S. estimated consumption by the year 2000[3-4,3-5]
  - Density (and shielding) significantly greater than Fe, Ni

In addition, a brief shielding analysis was conducted using the QAD computer code to determine the effect on the waste form shield mass for the alternative metal additives. The results of the QAD shielding analysis[3-6] are shown in Table 3-4. The heavier (more dense) metal additives resulted in a greater overall waste form shield mass than the reference Fe-Ni-Cu case. This effect is to be expected since the uranium shield is attenuating radiation which is generated primarily in the outermost portion of the largely self-shielded cermet waste form. In other words, the addition of metal additives, more dense, and having a higher atomic number than Fe, Ni, or Cu, accomplishes very little with respect to a reduction in shielding requirements and creates a large penalty in payload mass.

TABLE 3-4. EFFECT OF CERMET METAL PHASE ON SHIELDING DOSE

Cermet Concept	Composition of Metal Phase	Bulk Density, g/cc	Cermet Mass,(a) kg	Uranium Shield Mass,(b) kg	Payload Total Mass,(c) kg
Reference	55% Fe 15% Ni 18% Cu 13% Mo	6.70	5500	4200	9,700
Alternate-1	100% Mo	7.72	6340	3910	10,200
Alternate-2	100% Ta	10.30	8460	3070	11,530

Notes: (a) Equal waste mass (3230 kg) per payload sphere, homogeneous mixture based on 58.7% waste loading for reference case, 30 year old commercial waste.

(b) OAD shielding code, dose at 1 meter from surface = 2 rem/hour.

(c) Includes only waste form and uranium mass.

If an increase in cermet metal additive density and an increase in atomic number has a negative effect on payload/shield mass, the use of lower density (usually a lower atomic number) additives may result in a payload/shield mass reduction. However, it is not apparent that any metal having a significantly lower density or atomic number than Fe would be compatible with the ORNL cermet fabrication process. If future shielding analysis indicates a mass savings benefit for metal additives lighter than Fe, a survey of cermet fabrication process alternatives should be conducted. It is concluded that the Fe-Ni-Cu metal additive is the most viable cermet composition at this time.

Finally, the cermet waste form may also be a viable waste form for waste mixes other than HLW, namely technetium and the transuranics (see Section 5.1). It is not clear what the waste loadings might be, especially for the transuranics which pose a criticality concern. Additional study is needed on this topic.

3.2 Waste Mix Definition

A realistic evaluation of the thermophysical conditions and possible environmental impact for the waste form package during a space disposal mission required a fairly detailed composition definition of both commercial and defense HLW mixes.

3.2.1 Reference Commercial HLW Mix

It is important that the commercial HLW mix used for the space disposal mission concept be referenced easily and understood by members of the waste management community. Therefore, while the waste form experts met at BCL to select a waste form (see Section 3.1.1), they were asked to recommend a reference commercial HLW mix. These experts, as well as others attending the meeting, agreed that the PW-4b[3-7] mix would be the most appropriate commercial HLW mix for space disposal studies.

Several advantages accrue in choosing the PW-4b mix. It is one of four commercial HLW mixes used by Battelle Northwest Laboratories for HLW form development, and is therefore easily referenced and well known to members of the waste management community. PW-4b corresponds to reprocessed HLW of 33,000 megawatt-days per ton burnup from an optimized reprocessing plant, and in general, represents the type of waste which would be generated from the General Electric Morris Plant and the proposed Exxon Plant. Furthermore, PW-4b contains low quantities of inerts and reprocessing chemicals (Na, Fe, Gd), assumes 99.9 percent U and Pu removal, and has the lowest mass/MTHM reprocessed. The result is a waste mix which can be incorporated into waste forms such as cermet with relatively high waste loadings and which will require fewer launches for a given quantity of reprocessed spent fuel. Table 3-5 presents the elemental composition of the PW-4b mix.[3-7] The radionuclide composition was determined as follows: (1) the ORNL Isotope Generation and Depletion Code (ORIGEN)[3-8] calculation was made for fuel with initial enrichment of 3.2 w/o ^{235}U and a 33,000 MWD/T burnup; (2) the relative percentages of the radioisotopes for each element in PW-4b were determined from the ORIGEN printout for 10-year-old waste; (3) these radioisotope percentages were multiplied by their respective total elemental mass as given by PW-4b elemental composition to derive the mass of each radioisotope. Table 3-6 provides the radionuclide composition and activity of the reference PW-4b mix.

TABLE 3-5. REFERENCE COMMERCIAL ELEMENTAL WASTE MIX COMPOSITION (PW-4b)

	Constituent	Amount, kg/MTHM		Constituent	Amount, kg/MTHM
Inerts	Na_2O	--	Fission Products (Cont'd.)	TeO_2	0.725
	Fe_2O_3	1.511		Cs_2O	2.880
	Cr_2O_3	0.345		BaO	1.567
	NiO	0.141		La_2O_3	1.480
	P_2O_5	0.672		CeO_2	3.323
	Gd_2O_3	--		Pr_6O_{11}	1.482
				Nd_2O_3	4.522
Fission Products	Rb_2O	0.354		Pm_2O_3	0.123
	SrO	1.059		Sm_2O_3	0.924
	Y_2O_3	0.598		Eu_2O_3	0.200
	ZrO_2	4.944		Gd_2O_3	0.137
	MoO_3	5.176			
	Tc_2O_7	1.291	Actinides	U_3O_8	1.169
	RuO_2	2.972		NpO_2	0.865
	Rh_2O_3	0.480		PuO_2	0.010
	PdO	1.483		Am_2O_3	0.181
	Ag_2O	0.088		Cm_2O_3	0.040
	CdO	0.097			
				TOTAL	40.839

Source: Reference 3-7.

An important consideration for the space disposal of commercial HLW is the number of launches required for disposal. Recent estimates[3-9] project a nuclear electric generation capacity of 200 GWe by the year 2000. Table 3-7 gives the projected nuclear capacity by year from 1979-2000. Based on this projection it is possible to project the quantity of spent fuel discharged from reactors and reprocessed. It has been assumed that the first reprocessing plant begins operation in 1984 and attains full capacity (1500 MTHM/year) by 1986 (see Table 3-8), and that a second reprocessing plant begins operation in 1989 and attains full capacity (2000 MTHM/year) by 1991. A third plant would be on line in 1997, reaching a full capacity of 2000 MTHM/year by 1999. Table 3-8 presents the annual spent fuel discharge, annual processing capability, and unreprocessed spent fuel backlog.

Additional assumptions must be made regarding the cooling time necessary between discharge and processing. It is also necessary to assume the length of time required between reprocessing, waste solidification, and launch. Two alternatives require consideration:

TABLE 3-6. RADIONUCLIDE COMPOSITION OF COMMERCIAL WASTE (PW-4b)

Isotope	Nuclide Mass, kg/MTHM	Payload[a] Nuclide Mass, kg	Oxide Mass, kg/MTHM	Activity, Ci/MTHM	Payload[a] Activity, Ci
Rb-85	0.092	7.821	0.101	0	0
Rb-87	0.232	18.360	0.253	1.90E-5	1.50E-3
Total	0.324	26.181	0.354(Rb_2O)	1.90E-5	1.50E-3
Sr-88	0.406	32.129	0.480	0	0
Sr-90	0.492	38.935	0.579	6.95E+4	5.50E+6
Total	0.898	71.064	1.059(SrO)	6.95E+4	5.50E+6
Y-89	0.471	37.273	0.598	0	0
Y-90	<0.001	<0.079	<0.001	<6.97E+4	<5.52E+6
Total	0.471	37.352	0.599(Y_2O_3)	6.97E+4	5.52E+6
Zr-90	0.142	11.237	0.193	0	0
Zr-91	0.587	46.453	0.793	0	0
Zr-92	0.641	50.727	0.864	0	0
Zr-93	0.715	56.583	0.961	1.83E+0	1.45E+2
Zr-94	0.774	61.252	1.037	0	0
Zr-96	0.822	65.050	1.096	0	0
Total	3.681	291.302	4.944(ZrO_2)	1.83E+0	1.45E+2
Mo-95	0.066	5.223	0.094	0	0
Mo-97	1.060	83.885	1.590	0	0
Mo-98	1.140	90.216	1.626	0	0
Mo-100	1.260	99.712	1.866	0	0
Total	3.526	279.036	5.176(MoO_3)	0	0
Tc-99	0.976	77.237	1.291	1.66E+1	1.31E+3
Total	0.976	77.237	1.291(Tc_2O_7)	1.66E+1	1.31E+3
Ru-100	0.061	4.827	0.080	0	0
Ru-101	0.806	63.784	1.062	0	0
Ru-102	0.808	63.942	1.061	0	0
Ru-104	0.588	46.532	0.769	0	0
Total	2.263	179.085	2.972(RuO_2)	0	0
Rh-103	0.389	30.784	0.480	0	0
Total	0.389	30.784	0.480(Rh_2O_3)	0	0

(a) For 5500 kg cermet payload.

TABLE 3-6. RADIONUCLIDE COMPOSITION OF COMMERCIAL WASTE (PW-4b) (CONTINUED)

Isotope	Nuclide Mass, kg/MTHM	Payload[a] Nuclide Mass, kg	Oxide Mass, kg/MTHM	Activity, Ci/MTHM	Payload[a] Activity, Ci
Pd-104	0.197	15.590	0.257	0	0
Pd-105	0.233	18.439	0.304	0	0
Pd-106	0.366	28.964	0.476	0	0
Pd-107	0.188	14.878	0.244	8.98E-2	7.11E+0
Pd-108	0.128	10.129	0.166	0	0
Pd-110	0.027	2.137	0.035	0	0
Total	1.139	90.137	1.482(PdO)	8.98E-2	7.11E+0
Ag-109	0.082	6.489	0.088	0	0
Total	0.082	6.489	0.088(Ag_2O)	0	0
Cd-110	0.043	3.403	0.049	0	0
Cd-111	0.018	1.424	0.020	0	0
Cd-112	0.009	0.712	0.011	0	0
Cd-114	0.012	0.950	0.014	0	0
Cd-116	0.003	0.237	0.004	0	0
Total	0.085	6.726	0.098(CdO)	0	0
Te-125	0.011	0.871	0.014	0	0
Te-125	0.138	10.921	0.173	0	0
Te-130	0.428	33.871	0.535	0	0
Total	0.577	45.663	0.722(TeO_2)	0	0
Cs-133	1.200	94.964	1.257	0	0
Cs-134	0.007	0.554	0.007	8.55E+3	6.77E+5
Cs-135	0.370	29.281	0.392	3.27E-1	2.59E+1
Cs-137	1.160	91.799	1.224	1.01E+5	7.99E+6
Total	2.737	216.598	2.880(Cs_2O)	1.10E+5	8.71E+6
Ba-134	0.202	15.986	0.226	0	0
Ba-136	0.020	1.583	0.022	0	0
Ba-137	0.241	19.072	0.269	9.45E-4	7.48E+6
Ba-138	0.940	74.388	1.049	0	0
Total	1.403	111.029	1.566(BaO)	9.45E+4	7.43E+6
La-139	1.260	99.712	1.480	0	0
Total	1.260	99.712	1.480(La_2O_3)	0	0

(a) For 5500 kg cermet payload.

TABLE 3-6. RADIONUCLIDE COMPOSITION OF COMMERCIAL WASTE (PW-4b) (CONTINUED)

Isotope	Nuclide Mass, kg/MTHM	Payload[a] Nuclide Mass, kg	Oxide Mass, kg/MTHM	Activity, Ci/MTHM	Payload[a] Activity, Ci
Ce-140	1.420	112.374	1.749	0	0
Cs-142	1.280	101.295	1.574	0	0
Total	2.700	213.669	3.323(CeO_2)	0	0
Pr-141	1.230	97.338	1.482	0	0
Total	1.230	97.338	1.482(Pr_6O_{11})	0	0
Nd-142	0.022	1.741	0.026	0	0
Nd-143	0.746	59.036	0.871	0	0
Nd-144	1.270	100.504	1.484	0	0
Nd-145	0.651	51.518	0.759	0	0
Nd-146	0.665	52.626	0.774	0	0
Nd-148	0.354	28.014	0.411	0	0
Nd-150	0.171	13.532	0.198	0	0
Total	3.879	306.971	4.523(Nd_2O_3)	0	0
Pm-147	0.106	8.388	0.123	9.82E+4	7.77E+6
Total	0.106	8.388	0.123(Pm_2O_3)	9.82E+4	7.77E+6
Sm-147	0.078	6.173	0.090	0	0
Sm-148	0.087	6.885	0.101	0	0
Sm-149	0.354	28.014	0.411	0	0
Sm-150	0.191	15.115	0.221	0	0
Sm-151	0.021	1.662	0.024	5.63E+2	4.46E+4
Sm-152	0.048	3.799	0.055	0	0
Sm-154	0.019	1.504	0.022	0	0
Total	0.798	63.152	0.924(Sm_2O_3)	5.63E+2	4.46E+4
Eu-151	0.003	0.237	0.004	0	0
Eu-153	0.137	10.842	0.158	0	0
Eu-154	0.033	2.612	0.038	4.78E+3	3.78E+5
Total	0.173	13.691	0.200(Eu_2O_3)	4.78E+3	3.78E+5
Gd-154	0.016	1.266	0.019	0	0
Gd-155	0.005	0.396	0.006	0	0
Gd-156	0.084	6.647	0.097	0	0
Gd-158	0.012	0.950	0.014	0	0
Gd-160	0.001	0.079	0.001	0	0
Total	0.118	9.338	0.137(Gd_2O_3)	0	0

(a) For 5500 kg cermet payload.

TABLE 3-6. RADIONUCLIDE COMPOSITION OF COMMERCIAL WASTE (PW-4b) (CONTINUED)

Isotope	Nuclide Mass, kg/MTHM	Payload[a] Nuclide Mass, kg	Oxide Mass, kg/MTHM	Activity, Ci/MTHM	Payload[a] Activity, Ci
U-235	0.008	0.633	0.010	1.81E-5	1.43E-3
U-236	0.004	0.317	0.005	2.69E-4	2.13E-2
U-238	0.979	77.475	1.154	3.26E-4	2.58E-2
Total	0.991	78.425	1.169(U_3O_8)	6.13E-4	4.85E-2
Np-237	0.762	60.302	0.865	5.37E-1	4.25E-1
Total	0.762	60.302	0.865(NpO_2)	5.37E-1	4.25E-1
Pu-239	0.005	0.396	0.006	3.22E-1	2.55E+1
Pu-240	0.003	0.237	0.003	5.82E-1	4.61E+1
Pu-241	0.001	0.079	0.001	9.80E+1	7.86E+3
Total	0.009	0.712	0.010(PuO_2)	9.89E+1	7.83E+3
Am-241	0.129	10.209	0.142	4.41E+1	3.49E+4
Am-243	0.035	2.770	0.039	6.83E+0	5.41E+2
Total	0.164	12.979	0.181(Am_2O_3)	4.48E+2	3.55E+4
Cm-244	0.036	2.849	0.040	2.94E+3	2.33E+5
Total	0.036	2.849	0.040(Cm_2O_3)	2.94E+3	2.33E+5
Reprocessing Chemicals	--	211.1	2.671	--	--
Totals	30.777	2647.3	40.839	4.50E+5	3.57E+7

(a) For 5500 kg cermet payload.

TABLE 3-7. PROJECTIONS OF NUCLEAR ELECTRICAL GENERATING CAPACITY(3-9)

Year(a)	Annual Addition, GWe	Total Capacity, GWe
1979	9.6	61.9(b)
1980	12.9	74.8
1981	12.5	87.3
1982	13.8	101.1
1983	14.3	115.4
1984	16.0	131.4
1985	12.9	144.3
1986	12.8	157.1
1987	7.8	164.9
1988	9.1	174.0
1989	6.9	180.9
1990	5.6	186.5
1991	2.4	188.9
1992	1.2	190.1
1993	2.4	192.5
1994	1.5	194
1995	1.0	195
1996	1.0	196
1997	1.0	197
1998	1.0	198
1999	1.0	199
2000	1.0	200

Notes: (a) Data given for year end.

(b) Includes 52.3 GWe by the end of 1978.

Source: Reference 3-9.

TABLE 3-8. PROJECTED SPENT FUEL DISCHARGED AND REPROCESSED

Year	Annual Discharge, MTHM	Annual Processing Capability, MTHM	Unprocessed Spent Fuel Backlog, MTHM
1979	1490	0	5,390*
1980	1800	0	7,690
1981	2100	0	9,790
1982	2430	0	12,220
1983	2770	0	14,990
1984	3150	500	17,640
1985	3460	1000	20,100
1986	3770	1500	22,370
1987	3960	1500	24,830
1988	4180	1500	27,510
1989	4340	2200	29,650
1990	4480	2800	31,330
1991	4530	3500	32,360
1992	4560	3500	33,420
1993	4620	3500	34,540
1994	4660	3500	35,700
1995	4680	3500	36,880
1996	4700	3500	38,080
1997	4730	4200	38,610
1998	4750	4800	38,560
1999	4780	5500	37,840
2000	4800	5500	37,140

*Note: Includes about 4400 MTHM existing at the end of 1978.

Alternative I- Assume that even though there is a considerable quantity of spent fuel, no credit will be given for prior cooling. Then assume that when reprocessing begins, 5 years is required between processing and solidification and an additional 5 years is required between solidification and launch.

Alternative II- Assume that credit is given to prior cooling of spent fuel. Assume waste is available for disposal 10 years after discharge. Assume solidification begins in the late 1980's (presently proposed schedule for ONWI for geologic disposal).

For these two alternatives, the cumulative processed backlog of spent fuel, the spent fuel available for annual disposal and the cumulative spent fuel disposal are presented in Table 3-9. Since it is reasonable to assume that credit will be given for spent fuel cooling prior to reprocessing, Alternative II is believed to be more realistic than Alternative I. Alternative II is recommended for the reference space option scenario.

TABLE 3-9. PROJECTED WASTE AMOUNT FOR SPACE DISPOSAL

	Alternate I			Alternate II		
	Cumulative* Processed Backlog	Available for Annual Disposal	Cumulative Disposal	Cumulative Processed Backlog	Available for Annual Disposal	Cumulative Disposal
1979	0	0	--	0	0	--
1980	0	0	--	0	0	--
1981	0	0	--	0	0	--
1982	0	0	--	0	0	--
1983	0	0	--	0	0	--
1984	500	0	--	500	0	--
1985	1,500	0	--	1,500	0	--
1986	3,000	0	--	3,000	0	--
1987	4,500	0	--	4,500	0	--
1988	6,000	0	--	6,000	0	--
1989	8,200	0	--	2,310	5890	5,890
1990	11,000	0	--	3,310	1800	7,690
1991	14,500	0	--	4,710	2100	9,790
1992	18,000	0	--	5,730	2430	12,220
1993	21,500	0	--	6,510	2770	14,990
1994	24,300	500	500	6,860	3150	18,140
1995	27,000	1000	1,500	6,900	3460	21,600
1996	29,000	1500	3,000	6,900	3500	25,100
1997	31,700	1500	4,500	7,140	3960	29,060
1998	34,950	1500	6,000	7,760	4180	33,240
1999	37,530	2200	8,200	8,920	4340	37,580
2000	39,530	2800	11,000	9,940	4480	42,060

*Note: Data are in MTHM.

Finally, combining the information in the aforementioned tables, the cumulative spent fuel discharged, the annual spent fuel available for disposal, and the annual HLW in cermet form available for space disposal are presented in Table 3-10.

TABLE 3-10. PROJECTED NUCLEAR POWER GENERATION AND COMMERCIAL HIGH-LEVEL WASTE AVAILABLE FOR SPACE DISPOSAL

Year	Cumulative[a] Power, GWe	Cumulative[a] Waste, MTHM[b]	Annual Nuclear Waste Available for Disposal, MTHM/yr	Annual High-Level PW-4b Waste in Cermet Form[d] Available for Space Disposal, MT/yr
1979	61.9	5890(c)	0	0
1980	74.8	7690	0	0
1981	87.3	9790	0	0
1982	101.1	12,220	0	0
1983	115.4	14,990	0	0
1984	131.4	18,140	0	0
1985	144.3	21,600	0	0
1986	157.1	25,370	0	0
1987	164.9	29,330	0	0
1988	174.0	33,510	0	0
1989	180.9	37,850	5890(c)	410(e)
1990	186.5	42,330	1800	125
1991	188.9	46,860	2100	146
1992	190.1	51,420	2430	169
1993	192.5	56,040	2770	193
1994	194.0	60,700	3150	219
1995	195.0	65,380	3460	241
1996	196.0	70,080	3500	244
1997	197.0	74,810	3960	275
1998	198.0	79,560	4180	290
1999	199.0	84,340	4340	301
2000	200.0	89,140	4480	310

(a) From: Yates, K. R., and Park, U. Y., "Projections of Commercial Nuclear Capacity and Spent-Fuel Accumulation in the United States", Transaction American Nuclear Society, pp. 350-352 (June 1979).

(b) MTHM is metric tons heavy metal.

(c) Includes 4400 MTHM PW-4b existing as of 1978.

(d) Assumes 40.8 kg/MT waste for space disposal and a cermet waste form loading of 58.7 percent.

(e) Computed by multiplying 5890 MTHM by 0.0408 MT/MTHM and dividing by 0.587.

3.2.2 Reference Hanford Defense HLW Mix

As described in the last year's study,[3-2] the Hanford site, located near Richland, Washington, has been producing plutonium and other special nuclear materials since 1944. Detailed information was presented in last year's final report on the Hanford HLW mix.[3-2] For the purpose of this year's study, Rockwell Hanford was visited to discuss the possibility of additional inert removal from the Hanford waste, and to obtain updated information on radionuclide concentrations and on the radionuclide removal process currently planned. It was the conclusion of the Rockwell Hanford personnel that the chemistry suggested in last year's BCL study[3-2] was still considered feasible and appropriate for the study reported here. No new chemical treatments were suggested.

Updated radionuclide removal runsheets were supplied by Rockwell Hanford along with ORIGEN computer printouts of the radionuclide composition for present waste, future waste and a mixture of both. The radionuclide composition of the present waste is currently the most useful data for study purposes and is shown in Table 3-11.

The majority of the Hanford HLW, after being subjected to the radionuclide removal process, is in the form of sludge. Sludge composition varies, depending on the reprocessing method from which it was derived. There are five major sludges; these are: (1) bismuth phosphate sludge, (2) Redox sludge, (3) nickel-ferrocyanide-strontium sludge, (4) Purex sludge, and (5) zirconium sludge.

The gross composition of the first four major Hanford sludges, which are amenable to dissolution, is shown below--showing the previous and updated values:

	Last Year's Study[3-2] (1978-1979), MT	Current Study (1979-1980), MT
Total Mass of Inerts (Excluding ZrO_2 sludge):	15,082	14,488
Total Mass of Fission Products:	56	7
Total Mass of Thorium Oxide:	15	15
Total Mass of Uranium Oxide:	908	908
	16,061	15,418

Mass estimates for zirconia sludge, which is not amenable to typical dissolution processes, are also presented for previous and updated and values:

	(1978-1979), MT	(1979-1980), MT
Total Mass of Zirconia Sludge:	318	412
Total Mass of Waste after Radionuclide Removal:	16,379	15,830

TABLE 3-11. DEFENSE WASTE MIX (HANFORD, WCF = 25)
RADIONUCLIDE INVENTORY

Nuclide	Payload(a) Nuclide Mass, kg	Nuclide	Payload(a) Nuclide Mass, kg	Nuclide	Payload(a) Nuclide Mass, kg
C-14	4.37E-03	U-232	8.50E-09	Te-125m	3.40E-08
N-14	1.05E-05	U-233	1.30E-03	Te-125	2.34E-04
Co-59	7.02E-05	U-234	3.19E-03	Sn-126	2.97E-02
Co-60	1.95E-05	U-235	1.83E-01	Sb-126m	1.08E-11
Ni-59	4.05E-01	U-236	1.48E-06	Sb-126	1.01E-08
Ni-60	2.52E-04	U-237	2.34E-13	Te-126	4.12E-06
Ni-63	5.15E-02	U-238	2.79E+01	I-129	3.56E+00
Cu-63	8.39E-03	Np-237	1.86E+00	Xe-129	2.89E-06
Zr-93	2.32E-02	Np-239	6.42E-09	Cs-134	5.71E-09
Nb-93m	1.34E-07	Pu-238	2.98E-04	Ba-134	4.90E-06
Nb-93	8.00E-08	Pu-239	4.30E+00	Cs-135	2.67E+00
Sn-121m	8.07E-07	Pu-240	2.94E-01	Ba-135	1.23E-05
Sb-121	1.61E-07	Pu-241	8.07E-03	Cs-137	1.96E+00
Sb-125	7.69E-10	Pu-242	6.38E-03	Ba-137m	2.97E-07
Te-125m	1.88E-11	Am-241	1.61E-01	Ba-137	1.15E+00
Te-125	1.29E-07	Am-242m	2.43E-04	Ce-144	7.02E-16
He-4	1.43E-04	Am-242	2.92E-09	Nd-144	3.84E-08
Pb-207	4.87E-11	Am-243	7.72E-03	Pm-147	6.73E-05
Pb-208	6.38E-07	Cm-242	5.85E-07	Sm-147	1.33E-02
Pb-209	2.06E-12	Cm-243	1.75E-06	Sm-151	5.61E-01
Pb-210	8.88E-12	Cm-244	1.00E-04	Eu-151	9.70E-02
Pb-212	6.52E-11	H-3	4.65E-06	Sm-152	4.55E-05
Bi-209	3.77E-08	Se-79	1.45E-01	Eu-152	2.92E-05
Bi-212	6.21E-12	Br-79	3.09E-05	Gd-152	1.78E-05
Bi-213	4.97E-13	Sr-90	3.36E+00	Ed-154	2.62E-03
Ra-224	5.68E-10	Y-90	8.74E-04	Gd-154	3.60E-03
Ra-225	2.38E-10	Zr-90	2.15E+00	Ed-155	3.45E-07
Ra-226	3.88E-09	Zr-93	3.33E+01	Gd-155	7.26E-04
Ra-228	7.47E-08	Nb-93m	1.92E-04	Inerts	2.09E+03
Ac-225	1.61E-10	Nb-93	1.15E-04	Total	2.20E+03
Ac-227	2.40E-10	Tc-99	2.21E+01		
Ac-228	7.79E-12	Ru-99	1.44E-03		
Th-228	2.77E-10	Ru-106	2.82E-13		
Th-229	1.09E-07	Pd-106	2.76E-07		
Th-230	1.15E-07	Pd-107	1.48E+00		
Th-231	7.39E-13	Ag-107	2.92E-06		
Th-232	4.57E-01	Cd-113m	1.03E-04		
Th-234	4.00E-10	Cd-113	1.74E-07		
Pa-231	1.40E-06	In-113	1.74E-04		
Pa-233	6.42E-08	Sn-121m	2.91E-05		
Pa-234m	5.43E-12	Sb-121	5.82E-06		
Pa-234	1.88E-12	Sb-125	1.39E-06		

Note: (a) For 5500 kg cermet payload.

Based on laboratory tests, it may be possible to dissolve the first four sludges in molten caustic. If such a dissolution is feasible on the industrial scale, Hanford estimates that 99 percent of the inert material could be removed. Also, since uranium and thorium could be recycled as reactor fuels, it may be possible to remove 95 to 98 percent of those elements.

The total mass of Hanford waste to be carried to space, assuming the chemistry described above, is given in Table 3-12 for both previous and updated mass estimates. Overall, the mass of Hanford waste to be carried to space is nearly the same using updated information rather than last year's estimates. The reference waste concentration factor (WCF) has also changed to 25.5 (from 27.2) because of the updated information, as shown in Table 3-12.

TABLE 3-12. REFERENCE DEFENSE WASTE MIX INVENTORY (HANFORD HLW) FOR SPACE DISPOSAL

Component	Last Year's Study (1978-1979)[3-2]	Current Reference(a) (1979-1980)
	Metric Tons	
Inert Material	154	145
Fission Product Oxides	66	7.2
Thorium (ThO_2)	0.3-0.8	0.3-0.8
Uranium (UO_2)	21-52	21-51
Isolated Products from Salt Cake and Liquor	3-14	4
Zirconium Sludge	0-318	0-412
Total	244.3-604.8	177.5-620
Waste Concentraction Factor[b]	27.2	25.5

(a) Assumes same chemistry as last year's study (Reference 3-2)
(b) Based upon total masses of Hanford Waste of 16,379 and 15,830, respectively (from radionuclide removal process).

3.3 Containment Requirements Definition

The space disposal option, being conceptual, introduces many unique and unforeseen situations. An example is the need to define containment requirements and/or allowable limits for the waste payload configurations considered for use during the various mission phases (see Section 2.5). Current federal regulations cover little beyond transportation aspects. Additional information that must be developed from follow-on studies includes the handling, storage, transportation, and final disposition requirements for both commercial and defense HLW. This section outlines and completes, as much as possible, the requirements for containment of the high-level waste form during each phase of the space disposal mission.

3.3.1 Bases

The bases for defining the containment requirements are set forth here as (1) containment philosophy, (2) data application (the relationship between requirements and working limits, and the preliminary nature of these requirements), and (3) direction of future development. A glossary of terms is included to clearly establish their meaning in the context of the requirements that follow.

3.3.1.1 Containment Philosophy

The ideal goal for containment of high-level waste material would be to (1) provide an absolute barrier between the waste and the environment, and (2) minimize the radiation exposure to humans under all normal and accident conditions. Various government regulations have been developed and applied to current terrestrial transportation activities involving radioactive materials, including irradiated nuclear fuel. As yet, no specific regulations apply specifically to handling, storing, transporting, etc., high-level waste. Consequently, the containment requirements developed in this study are based on extending existing regulations; they cannot be considered final at this time. These containment requirements, whether or not covered by existing regulation, are applied first to meet current regulations and, second, to minimize human exposure to as low as reasonably achievable (ALARA).

Containment requirements are presented in three independent categories: (1) specific parameters indicative of the response of various containment systems; (2) specific systems for containing the waste (waste form, containment vessels, etc.), and (3) various mission phases during which specific levels of containment are required. Table 3-13 lists the components of these categories. The three levels containment requirements can be used to define any aspect of containment.

TABLE 3-13. SPECIFIC COMPONENTS OF CONTAINMENT REQUIREMENTS

Parameters	Components	Mission Phases
• Thermal • Mechanical • Chemical • Nuclear	• Waste Form • Primary Container • Radiation Shield • Impact Absorber • Ablation Shield • Shipping Cask	• Fabrication/Assembly • Terrestrial Transport • Launch Site Handling • Launch to Earth Orbit • Orbit Transfer to Destination

3.3.1.2 Data Application

Because of the general nature of the requirements, reference to specific designs and materials is limited to those previously identified as candidate or alternative bases for the space disposal option (see Section 2-1, Figure 2-1). Consequently, technical data is used minimally. Appendix C includes the known information that meets the containment requirements for the reference concepts. These requirements are intended to be used in various mission phase environment scenarios.

3.3.1.3 Future Developments

In this study, the requirements have been developed only to the extent needed to define preliminary concepts for space disposal of high-level waste. In follow-on study efforts, as the concepts are translated into preliminary designs, containment requirements will likely include future interaction with the Nuclear Regulatory Commission and other authorities to ensure acceptability of these requirements.

3.3.1.4 Definition of Terms

The following terms are defined in the context of the containment requirements as used in this section:

Ablation Shield - a layer of protective carbon/carbon material attached to the outside surface of the payload reentry vehicle. It is designed to reduce the heating effects during inadvertant atmospheric reentry.

Accident Conditions - as contrasted to normal conditions, are low in probability and high in severity. The corresponding philosophy for

the containment barrier is to survive accidents with low consequences rather than remain in an operable state.

ALARA - less than maximum allowable and as low as reasonably achievable. Federal regulations require this principle to be used in most nuclear technology license applications.

Barrier - any medium or mechanism by which either release of encapsulated radioactive waste material is retarded significantly or human access is restricted. Examples of barriers are: waste form, primary container, and isolation.

Cladding - a metal or ceramic covering of another material, used to improve certain properties, such as resistance to chemical interaction, and hazardous material containment.

Containment - a condition in which a hazardous material is isolated from the environment to an acceptable degree.

Criticality - a measure of the capability of sustaining a nuclear chain reaction in a package containing fissile materials.

Decomposition - any significant change in physical or chemical properties resulting in a reduction in mechanical strength, etc.

DOT - Department of Transportation; regarding handling of nuclear materials, Title 49 of the Code of Federal Regulations, Parts 173.389-173.399.

Fabrication - that stage of the waste treatment process in which the waste form is fabricated to its proper shape and placed within the primary container.

Fracture Toughness - the measure of a material's ability to absorb energy during plastic deformation; resistance to fracture.

High-Level Waste - the waste product resulting from the first separation step of Purex fuel reprocessing operations.

Impact Absorber - that portion of a nuclear waste payload RV intended to be a sacrificial energy absorber while reducing impact forces transmitted to the payload.

Launch Site - the location on Earth's surface from which the space disposal missions are launched.

Material Interaction - the behavior of materials in contact with each other where a significant change in physical or chemical properties result.

Normal Conditions - conditions that result from normal handling and transportation operations. No irreversible effects shall result to a containment barrier.

NPPF - Nuclear Payload Preparation Facility; that launch site facility providing interim storage, and remote handling operations for the waste payload from the time of receipt at the launch site until launch operations begin.

NRC - Nuclear Regulatory Commission; regarding transportation of nuclear materials, Title 10 of the Code of Federal Regulations, Part 71.

Primary Container - the shell or vessel, adjacent to the high-level waste form, that provides containment throughout all mission phases.

Radiation Shield - that component of the payload package which is intended to reduce the nuclear radiation environment to acceptable levels.

Reentry Vehicle (RV) - that component of the payload package intended to protect the payload contents during an unplanned on-pad or ascent failure or reentry into the Earth's atmosphere.

Rem - Roentgen Equivalent Man, a unit of radiation dose, which takes into account the relative biological effectiveness of radiation energy deposition.

Shipping Package - an enclosure and its systems licensed to transport radioactive materials (including high-level waste).

Storage - placement of high-level waste packages in temporary isolation as an intermediate step toward permanent isolation.

Uprated Space Shuttle - reference launch vehicle for space disposal option.

3.3.2 Parameters

Containment requirements will ultimately take the form of specific limits for key parameters. For the space disposal option, the significant parameters can be grouped into four major categories: (1) thermal; (2) mechanical; (3) chemical; and (4) nuclear. Within each category, many specific parameters can be included as containment requirements. Only the major parameters are included here. In addition, items that should eventually be described as criteria are not mentioned specifically, but rather, are understood. Examples of these criteria involve: waste package integrity; waste isolation requirements; societal constraints; and safeguards. The containment requirements given here are specific limits for use in delineating the objectives of the criteria.

As discussed earlier, containment requirement parameters are but one dimension of a threefold approach to containment. These parameters must be applied to specific forms of containment, during specific mission phases.

Once this step is accomplished, technical data may be substituted to obtain working requirements (see Appendix C).

3.3.2.1 Thermal

Thermal requirements consider only limiting conditions which, irrespective of critical parameters in other areas, serve as upper bounds to determine permissible designs and response. In interrelations with other major parameters, a single parameter is considered as the limiting requirement and, through its dependence upon other parameters, in effect produces corresponding limits. Thus parameters such as melting temperature will be independent limits, while yield strength will be a function of temperature.

The limiting thermal conditions for all forms of containment and mission phases should require that the containment barrier must not be altered in physical or chemical phase during operations that are not remote from the human environment. They must be defined in terms of probabilities. For the waste form, this implies a limit at the fabrication temperature; for metallic containment forms, this implies a creep limit. These limits are usually applied to normal conditions. For accident conditions, the temperature limit will be below the melting point for containment. (See Table 3-14.)

TABLE 3-14. THERMAL REQUIREMENTS FOR CONTAINMENT OF HIGH-LEVEL WASTE, SPACE DISPOSAL OPTION

	MISSION PHASE				
COMPONENT	FABRICATION/ ASSEMBLY	TERRESTRIAL TRANSPORT	LAUNCH SITE HANDLING	LAUNCH TO EARTH ORBIT	ORBIT TRANSFER TO DESTINATION
WASTE FORM	FABRICATION/ MELT TEMP.*	FABRICATION/ MELT TEMP.	FABRICATION/ MELT TEMP.	FABRICATION/ MELT TEMP.	FABRICATION/ MELT TEMP.
PRIMARY CONTAINER	CREEP/MELT TEMP.	CREEP/MELT TEMP.	CREEP/MELT TEMP.	CREEP/MELT TEMP.	CREEP/MELT TEMP.
FLIGHT RADIATION SHIELD	CREEP/MELT TEMP.	CREEP/MELT TEMP.	CREEP/MELT TEMP.	CREEP/MELT TEMP.	—
IMPACT ABSORBER	—	—	CREEP/MELT TEMP.	CREEP/MELT TEMP.	—
ABLATION SHIELD	—	—	CREEP/— TEMP.	CREEP/— TEMP.	—
SHIPPING CASK	—	DOT, NRC REG.	—	—	—

*NOTE: THE NORMAL LIMIT IS GIVEN FIRST; THE ACCIDENT LIMIT IS GIVEN SECOND.

C-2

3.3.2.2 Mechanical Strength

For all normal mission phases, and containment barriers, the mechanical strength must maintain stress and strain limits within normal yield limits (standard 0.2% offset). For accident conditions, stress/strain limits must not exceed ultimate strength requirements. Mechanical strength limits are assumed to be dependent on temperature and loading condition. In addition, it is assumed that all containment barriers must also have sufficient fracture toughness, fatigue endurance, and buckling stability to withstand normal and accident conditions. (See Table 3-15.) For accidents associated with reentry, mechanical integrity is not a feasible requirement. Rather, a limit on the amount dispersed will be imposed.

TABLE 3-15. MECHANICAL REQUIREMENTS FOR CONTAINMENT OF HIGH-LEVEL WASTE, SPACE DISPOSAL OPTION

	MISSION PHASE				
COMPONENT	FABRICATION/ ASSEMBLY	TERRESTRIAL TRANSPORT	LAUNCH SITE HANDLING	LAUNCH TO EARTH ORBIT	ORBIT TRANSFER TO DESTINATION
WASTE FORM	YIELD/ ULTIMATE*	YIELD/ ULTIMATE	YIELD/ ULTIMATE	YIELD/ ULTIMATE	YIELD/— LOW DISPERSION
PRIMARY CONTAINER	YIELD/ ULTIMATE	DOT, NRC REG.	YIELD/ ULTIMATE	YIELD/ ULTIMATE	YIELD/—
FLIGHT RADIATION SHIELD	YIELD/ ULTIMATE	YIELD/ ULTIMATE	YIELD/ ULTIMATE	YIELD/ ULTIMATE	—
IMPACT ABSORBER	—	—	YIELD/—	YIELD/—	—
ABLATION SHIELD	—	—	YIELD/ ULTIMATE	YIELD/ ULTIMATE	—
SHIPPING CASK	—	DOT, NRC REG.	—	—	—

*NOTE: THE NORMAL LIMIT IS GIVEN FIRST; THE ACCIDENT LIMIT IS GIVEN SECOND.

3.3.2.3 Chemical

Containment materials shall be compatible with adjacent media to the extent that no significant detrimental chemical reactions occur. For conditions not covered by existing federal regulations, specific limits will be applied to the various containment barriers and mission phases. (See Table 3-16.)

TABLE 3-16. CHEMICAL REQUIREMENTS FOR CONTAINMENT OF HIGH-LEVEL WASTE, SPACE DISPOSAL OPTION

	MISSION PHASE				
COMPONENT	FABRICATION/ ASSEMBLY	TERRESTRIAL TRANSPORT	LAUNCH SITE HANDLING	LAUNCH TO EARTH ORBIT	ORBIT TRANSFER TO DESTINATION
WASTE FORM	TBD	TBD	TBD	TBD	TBD
PRIMARY CONTAINER	SIMILAR TO DOT, NRC REG.	DOT, NRC REG.	SIMILAR TO DOT, NRC REG.	SIMILAR TO DOT, NRC REG.	TBD
FLIGHT RADIATION SHIELD	SIMILAR TO DOT NRC REG.	SIMILAR TO DOT, NRC REG.	SIMILAR TO DOT, NRC REG.	SIMILAR TO DOT, NRC REG.	—
IMPACT ABSORBER	—	—	SIMILAR TO DOT, NRC REG.	SIMILAR TO DOT, NRC REG.	—
ABLATION SHIELD	—	—	SIMILAR TO DOT, NRC REG.	SIMILAR TO DOT, NRC REG.	—
SHIPPING CASK	—	DOT, NRC REG.	—	—	—

3.3.2.4 Nuclear

The major nuclear requirements for the space disposal option include limits on dispersion, criticality, and radiation exposure.

The acceptable amount of radioactive material that may be released should be a function of the severity and frequency of the loading condition, keeping in mind ALARA criteria. Allowable releases are expected to range from near-zero, for normal conditions, to minimal values for extremely severe accidents. Values for certain mission phases already exist (see Section 3.3.4).

All waste form configurations (normal and accident) must remain subcritical. Transportation licensing regulations have interpreted this requirement to mean that K-effective (mean value plus three standard deviations) calculated using accepted techniques, to be less than 0.95. The capability of the waste form to remain subcritical shall not depend upon active, external measures.

Radiation exposure shall be controlled to limit the dose to ALARA levels. The established dose rate limits will be a function of exposure probability and design constraints. Limits exist for certain mission phases and waste packages. (See Table 3-17.)

TABLE 3-17. NUCLEAR REQUIREMENTS FOR CONTAINMENT OF HIGH-LEVEL WASTE, SPACE DISPOSAL OPTION

COMPONENT	MISSION PHASE				
	FABRICATION/ ASSEMBLY	TERRESTRIAL TRANSPORT	LAUNCH SITE HANDLING	LAUNCH TO EARTH ORBIT	ORBIT TRANSFER TO DESTINATION
WASTE FORM	SUB-CRITICAL (K_{eff}<0.95)	SUB-CRITICAL (K_{eff}<0.95)	SUB-CRITICAL (K_{eff}<0.95)	SUB-CRITICAL (K_{eff}<0.95)	SUB-CRITICAL (K_{eff}<0.95)
PRIMARY CONTAINER	NUCLIDE RELEASE: TBD	NUCLIDE RELEASE: DOT, NRC REG.	NUCLIDE RELEASE: TBD	NUCLIDE RELEASE: TBD	NUCLIDE RELEASE: TBD RADIATION DOSE: TBD
FLIGHT RADIATION SHIELD	2.0 R/HR @ 1 M.	2.0 R/HR @ 1 M.	2.0 R/HR @ 1 M.	2.0 R/HR @ 1 M.	–
IMPACT ABSORBER	–	–	TBD	TBD	–
ABLATION SHIELD	–	–	TBD	TBD	–
SHIPPING CASK	–	DOT, NRC REG.	–	–	–

3.3.3 Containment Components

Containment components (referred to as "configurations" in Section 2.5) constitute the barrier between the payload and the external environment. Depending on the mission phase, the containment barrier may be a single item (e.g., waste primary container) or multiple items (e.g., primary container, radiation shield, impact absorber, etc.). Consequently, a particular component may not be a part of containment in all mission phases. If it is not a part of the containment barrier, then the specific limits for containment do not apply.

3.3.3.1 Waste Form

The principal containment barrier for the space disposal option is the primary container. The waste form is required to minimize the possibility of nuclide release, not contain it. To meet these requirements, the waste form will still have limits for thermal, mechanical, chemical, and nuclear parameters.

For the waste form, the maximum temperature limit for normal conditions is the fabrication temperature; for accident conditions the limit is the

melting temperature. Mechanical limits, when applicable for containment, are yield (normal) and ultimate strengths or low dispersion (accident). Chemical limits are to be determined (TBD), and nuclear limits require a subcritical condition at all times.

3.3.3.2 Primary Container

The primary container, designed to enclose the waste form throughout all mission phases beyond fabrication, is also the primary containment boundary. Depending on the mission phase, it may be the only containment barrier, or it may be one in a series with other external boundaries.

The thermal limit for normal conditions is the creep limit (e.g., ASME Pressure Vessel Code, Section III, Division 1).[3-10] For accident conditions, the melting temperature is the required limit. Mechanical limits are yield (normal) and ultimate strengths or low dispersion (accident). Chemical limits are covered by existing federal regulations.[3-11] Nuclear dispersion limits are to be determined for conditions not regulated.

3.3.3.3 Radiation Shield

The radiation shield for flight is designed to function during all mission phases through transfer to the final destination. Although the radiation shield must meet containment requirements primarily for radiation exposure, it will be supplemented with auxiliary shielding materials as needed during various mission phases. For mission phases requiring such shielding, limits for other types of requirements are necessary. For mechanical strength requirements, yield (normal) and ultimate (accident) limits apply. Thermal limits are creep (normal) and melting (accident). Chemical requirements will be similar to those in existing federal regulations.

Radiation exposure limits been assumed for conditions not covered by existing regulations. Conservative limits (such as those for transportation) have not been selected due to the sensitivity of the overall system design (payload/shield mass ratio)to the dose limits. Rather, the limits chosen reflect the fact that the waste payload will be comparatively isolated from the general public throughout most of its lifetime.

3.3.3.4 Reentry Vehicle

The reentry vehicle, primarily the impact absorber and ablation shield, have similar containment requirement limits. For thermal requirements, the creep (normal) and melt temperature (accident) apply. For mechanical strength, yield (normal) and ultimate (accident) limits exist. Chemical and nuclear limits are minor factors, but largely remain to be determined. Exceptions to these limits are that the impact absorber is designed to absorb

mechanical energy during accidents and the ablation shield is designed to reduce heating effects during possible reentry phases.

3.3.3.5 Shipping Cask

During Earth transport, the high-level waste package will be enclosed within a shipping cask. Current federal regulations [10 CFR 71[3-12], 49 CFR 173[3-13]] define the requirements for this component, which is expected to be similar to conventional designs.

3.3.4 Mission Phases

As described previously, the containment requirements are also a function of mission phases, and, more specifically, the conditions within each phase. The definition of mission phase as used for containment requirements is chronological, with no clear-cut boundaries between phases. Consequently, the requirements cannot be considered to be absolute standards, but rather, are to be applied to each phase in an overall manner.

3.3.4.1 Fabrication/Assembly

This phase begins with the insertion of the waste form into the primary container, and ends with the beginning of transport of the flight-shielded primary container out of the fabrication facility. During this phase, auxiliary cooling and additional shielding may be required. The primary container is the principal containment barrier during this phase.

3.3.4.2 Terrestrial Transport

This phase begins at the time of loading of the waste container and shield into the shipping cask and ends with the unloading at the Nuclear Payload Preparation Facility (NPPF). Throughout this phase, active auxiliary cooling will be required to maintain thermal limits. At both ends of the phase, additional shielding may be required. The requirements are defined for irradiated nuclear materials in existing regulations. They are expected to be similar to regulations governing transport of processed waste. While in the shipping cask, the cask vessel will be the principal containment barrier during transport.

3.3.4.3 Launch Site Handling

This phase, similar to the initial one, begins with the arrival of the shipping cask at the NPPF and ends with the completion of transfer into

the launch vehicle. Auxiliary cooling, and possibly shielding, will be required during this phase. The principal containment barrier remains the primary container. During this phase, the primary container will be installed in the Reentry Vehicle. The RV would then play a major protection role, if an accident were to occur.

3.3.4.4 Launch to Earth Orbit

This phase begins with the loading of the waste payload into the launch vehicle, and ends after Earth orbit has been achieved. Auxiliary cooling may be required for most of this phase, with containment relying principally on the primary container. Accident conditions that might occur during this phase are among the most severe. The requirements during this phase allow for no release; namely no melting, no ultimate failure of the waste form, container, or radiation shield will be allowed.

3.3.4.5 Orbit Transfer to Destination

This mission phase commences with the removal of the waste payload (primary container) from the RV, and concludes with arrival at the final destination. For the purpose of these requirements, this phase is not open-ended. However, it is expected that conditions are steady at the conclusion of this phase. No auxiliary cooling is required; some auxiliary shielding may be required at the beginning of this phase. Containment requirements for this phase (and the long term) are expected to be less restrictive than those for near-term phases involving greater chances of public exposure. The primary container and the waste form provide the ultimate containment barrier for the waste.

3.4 Container, Shield, and Cooling Requirements Definition

The objective of this part of the Phase III study is to define basic concepts for the primary container and radiation shield, over a range of payload masses for both commercial (PW-4b) and defense (Hanford) waste mixes. The Phase II study was limited to defense waste mixes in a calcine waste form.[3-2] Phase III has a reference concept waste form defined as the ORNL cermet (see Section 3.1) and considers disposal of commercial as well as defense waste.

The commercial and defense waste forms and mixes are described in Sections 3.1 and 3.2. The reference commercial (PW-4b) and Hanford defense wastes were evaluated for waste masses ranging from an RTG-type payload [approximately 1/3 the diameter of the 5.5 metric ton (MT) payload] up to a heavy lift launch vehicle (HLLV) capability (defined by a waste payload diameter upper limit of 3 meters due to ground transport constraints). Analyses were performed for three single spherical payloads with diameters determined by the waste mass range defined above. At the time the analyses were conducted the reference waste form mass was 5.5 MT; the reference was changed to 5 MT after continuing analyses by NASA/MSFC.

A primary container wall was assumed to enclose the cermet waste form. A radiation shield surrounding the container consists of depleted uranium with an inner and outer cladding of stainless steel. The shielding thickness was determined as a function of payload waste form mass using standard shielding codes. For space flight, the shielded package is enclosed by a spherical honeycomb steel impact absorber and a thermal protection layer of insulation and ablation material. This analysis extends to, but does not including, the impact absorber. NASA's Marshall Space Flight Center performed the payload analysis for shells outside the radiation shield.

The analyses reported here covers shielding requirements, thermal characteristics (temperature profiles and auxiliary cooling requirements) in deep space and earth environments, payload mass characteristics, and parametric dose rate as a function of distance from source and intervening wall thickness.

The requirements (see Section 3.3) for each component of the reference payload concept were determined before the results presented in this section were evaluated. These evaluations can be used to further refine the space disposal payload concepts into working designs in future efforts.

3.4.1 Container Mass

The proper thickness of the waste primary container can be determined by structural analysis of the container's response to various normal and accident environments. The container wall design is not believed to be a significant parameter for shielding or thermal analyses. Structural analysis of all components of the package should be included in follow-on efforts. To begin

the shielding and thermal analyses, however, a representative thickness of 1.27 cm (0.5 in.) was assumed over the entire range of payload waste masses. Furthermore, in view of results presented in the Phase I study effort[3-1], the container material was assumed to be stainless steel. Analysis described in Section 4.3 indicated the need for a higher service temperature material for the container; however, the results of that analysis were not available until the end of this study--see Section 4.3.4. The resulting stainless steel container mass components are presented after shielding mass requirements have been determined (see Section 3.4.3).

3.4.2 Shielding Analysis

The shielding analysis consisted of determining the thickness of uranium required to reduce the gamma and neutron radiation dose rates to within the designated limits. This procedure began with development of a shielding source term for commercial and Hanford waste mixes using the ORIGEN code.[3-8] This code predicts the generation of fission products and the transmutation of isotopes as a result of neutron reactions and radioactive decay. The input nuclide quantities were taken from Tables 3-6 and 3-11. The resulting gamma photon spectrums for 10-year-old commercial (PW-4b) and 20-year-old Hanford high-level waste are shown in Table 3-18.

TABLE 3-18. COMMERCIAL (PW-4b, 10-YEAR DECAY) AND HANFORD (WCF = 25, 20-YEAR DECAY) HIGH-LEVEL WASTE MIX PHOTON SPECTRUM

Mean Energy, MEV	Activity, Photons/sec-MT*	
	PW-4b	Hanford (WCF = 25)
0.30	2.75 E15	5.29 E13
0.63	6.58 E16	3.36 E14
1.10	2.04 E15	2.86 E12
1.55	1.53 E14	4.09 E11
1.99	5.05 E11	1.23 E10
2.38	7.04 E08	9.18 E03
2.75	3.28 E08	4.27 E03
3.25	2.04 E08	2.65 E03
3.70	1.31 E08	1.71 E03
4.22	8.26 E07	1.08 E03
4.70	3.90 E07	5.09 E02
5.25	2.46 E07	3.20 E02
Neutron Source (neutrons/ sec-MT)	5.37 E09	1.61 E05
Decay Heat (kW/MT)*	19.3	0.23

*Note: MT = metric ton of waste and additives in cermet waste form.

The neutron production, also determined by ORIGEN, is negligible for Hanford waste; it was included in shielding calculations of the commercial waste mix. The neutron source term was input to the shielding code by assuming a U^{235} fission spectrum. Both commercial and Hanford shielding results were computed using the ANISN[3-14] code. In addition to gamma and neutron source terms, the waste decay heat is also predicted by ORIGEN. These values (see Table 3-18) are input to the thermal analysis.

As stated above, the shield design was assumed to consist of depleted uranium, enclosed by 0.64 cm (0.25 in) thick inner and outer layer of stainless steel cladding. Since ANISN is a one-dimensional code, the geometry was input in terms of radii for material boundaries. The shield model consisted of the known waste dimension (for each of three payload sizes: 204, 5,500 and 99,300 kg waste form mass), the stainless steel container wall, shield cladding thickness, and uranium thickness. Due to the proportionality of the results, the required uranium thickness for a given dose rate was determined by interpolating the data from the ANISN calculation. The results of these analyses are presented in Table 3-19 and in Figure 3-1.

The shielding analyses show several interesting characteristics of shield design, particularly for commercial waste, since the neutron dose component is more significant. First, the phenomena of self-shielding of gamma rays is significant. The package materials, even the waste form itself, are effective gamma shielding materials. Consequently, only the gamma radiation from the outer region of the waste requires shielding; the central portions are shielded by the outer package materials themselves. A measure of the effectiveness of self-shielding is demonstrated by the fact that as the waste radius increases, the surface gamma dose rate approaches a constant value. Thus, for waste sources in which the neutron dose is negligible (i.e., Hanford waste), the surface dose rate is nearly constant over the range of waste masses considered. (Note that the dose rates in Table 3-19 and Figure 3-1 are taken at 1 meter from the surface, and the dose rate at a distance increases in proportion to the projected area of the source.)

TABLE 3-19. SUMMARY OF SPACE DISPOSAL SHIELDING REQUIREMENTS FOR COMMERCIAL (PW-4b) AND HANFORD (WCF = 25) WASTE

Type of Waste	Dose Rate rem/hour(a)	Payload Waste Form Mass, kg: 204 $\gamma\left(\frac{rem}{hr}\right)^{(b)}$	204 $n\left(\frac{rem}{hr}\right)^{(c)}$	204 $U_t(cm)^{(d)}$	5500 $\gamma\left(\frac{rem}{hr}\right)^{(b)}$	5500 $n\left(\frac{rem}{hr}\right)^{(c)}$	5500 $U_t(cm)^{(d)}$	99,300 $\gamma\left(\frac{rem}{hr}\right)^{(b)}$	99,300 $n\left(\frac{rem}{hr}\right)^{(c)}$	99,300 $U_t(cm)^{(d)}$
PW-4b	0.5	0.22	0.28	5.6	0.01	0.49	8.4	(e)	0.50	10.9
PW-4b	1.0	0.61	0.39	4.8	0.09	0.91	7.2	0.02	0.98	9.6
PW-4b	2.0	1.51	0.49	4.1	0.46	1.54	6.0	0.08	1.92	8.2
Hanford	0.5	0.5	--	1.86	0.5	--	2.81	0.5	--	3.41
Hanford	1.0	1.0	--	1.51	1.0	--	2.44	1.0	--	3.03
Hanford	2.0	2.0	--	1.18	2.0	--	2.06	2.0	--	2.67

Notes: (a) Dose rate at 1 meter from surface of shield.
(b) Gamma radiation component.
(c) Neutron radiation component.
(d) Calculated uranium thicknesses, U_t, include consideration of the shielding available due to 2.54 cm steel (shield liner and waste container).
(e) Less than 0.005.

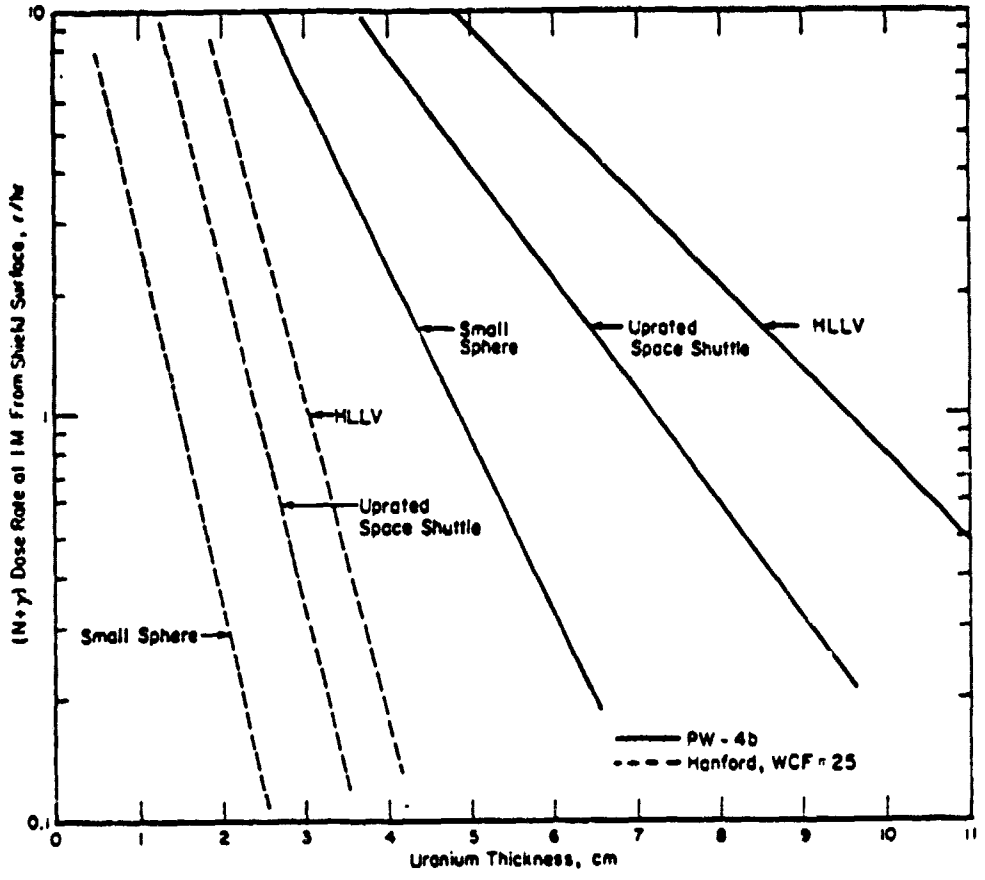

FIGURE 3-1. DOSE RATE AS A FUNCTION OF URANIUM SHIELD THICKNESS

Second, the neutrons emitted by the waste are highly energetic or "fast" neutrons. Effective self-shielding of fast neutrons does not occur in the waste material. Thus, the neutron dose rate at the surface of a waste payload increases as the radius increases. For the defense waste, the neutron radiation is sufficiently low that the thickness of the uranium required for shielding is controlled by the gamma source term. However, for commercial high-level waste, the neutron radiation is much greater. For the small (204 kg cermet) payload, the uranium required for neutron shielding is 25 percent of the total required to meet the dose rate limit of 2 rem/hr at 1 m. For the 5500 kg cermet payload, the uranium thickness needed for attenuating neutrons is significantly greater than that required just for gamma rays. For the large (99,300 kg cermet) payload the uranium needed for neutron shielding dominates the shielding thickness requirements (see Table 3-19).

In this design, uranium is used as a shield material for both neutron and gamma radiation although other materials are better suited for neutron shielding. To more efficiently shield the neutrons, it is necessary to moderate or deenergize the neutrons to lower (thermal) energy where they may be efficiently captured by the nuclei of many elements. Low-atomic-number elements are effective neutron moderators. Hydrogen, in the form of water or plastics, is the most commonly employed moderator. Metal hydrides have also

been used as moderators. The disadvantages of hydrogenous materials are that they have poor high temperature characteristics and tend to evaporate, dissociate, or decompose at the temperature of the waste package. Other light elements used as moderators include carbon (as graphite) and beryllium (either the metal or oxide). The moderator would need to be placed as a layer several centimeters thick around the outside of the waste and be surrounded by a thin layer of an efficient neutron-absorbing material such as cadmium or gadolinium or a thick layer of a less efficient absorber such as steel. However, since a massive gamma shield will be required, it could also absorb thermal neutrons.

The difficulty in employing a separate neutron shield in the waste package is that the additional materials, particularly the nonmetals, present thermal and structural design problems. If it proves effective to do so, it is probable that an efficient neutron shield can be designed for a specific size and type of waste utilizing materials incorporated into the waste matrix or gamma shield or utilizing external materials such as the auxiliary coolant in the shield or the graphite on the outside of the reentry vehicle. However, for the present study, it is not practical to consider a special neutron shield design, since it may only be beneficial for the very large commercial waste (PW-4b) packages, which have been shown unfeasible because of thermal considerations (see Section 3.4.4).

The significant production of neutrons in commercial high-level waste offers the potential of neutron activation of materials with which the neutrons may interact. Neutron activation is the term applied to the process of a free neutron being absorbed in the nucleus of an atom and transmuting that atom to an isotope of the original element with an additional unit of atomic mass. If the isotope is radioactive, as is often the case, then neutron activation is a source of additional radioactivity. An examination of the potential for neutron activation of reusable components of the waste payload such as the gamma shield or reentry vehicle shows that no significant levels of radioactivity will be produced.

3.4.3 Payload Mass

The mass of the waste, primary container, and radiation shield as a function of waste mass and dose rate is presented in Table 3-20 and graphically in Figure 3-2.

TABLE 3-20. WASTE FORM, CONTAINER AND SHIELD MASS CHARACTERISTICS (KG) FOR COMMERCIAL (PW-4b) AND HANFORD (WCF = 25) WASTE

Payload Size	Dose Rate At 1m, rem/hr	Waste Form[a]	Primary Container[b]	Commercial (PW-4b) Uranium Shield[c]	Commercial (PW-4b) Total For Shielded Waste	Hanford WCF = 25 Uranium Shield[c]	Hanford WCF = 25 Total For Shielded Waste
Small Sphere	0.5	204	50	840	1,094	277	531
	1.0	204	50	705	959	232	486
	2.0	204	50	593	847	192	446
Uprated Space Shuttle	0.5	5,500	430	8,870	14,600	2,963	8,692
	1.0	5,500	430	7,360	13,290	2,396	8,325
	2.0	5,500	430	6,100	12,030	2,270	8,199
Heavy Lift Launch Vehicle	0.5	99,300	2,920	68,600	170,820	22,548	124,770
	1.0	99,300	2,920	60,300	162,520	20,324	122,540
	2.0	99,300	2,920	51,500	153,720	18,228	120,450

Notes: (a) Cermet, density of 6.7 g/cc.
(b) 1.27 cm, stainless steel.
(c) Mass includes 0.64 cm inner and outer stainless steel cladding.

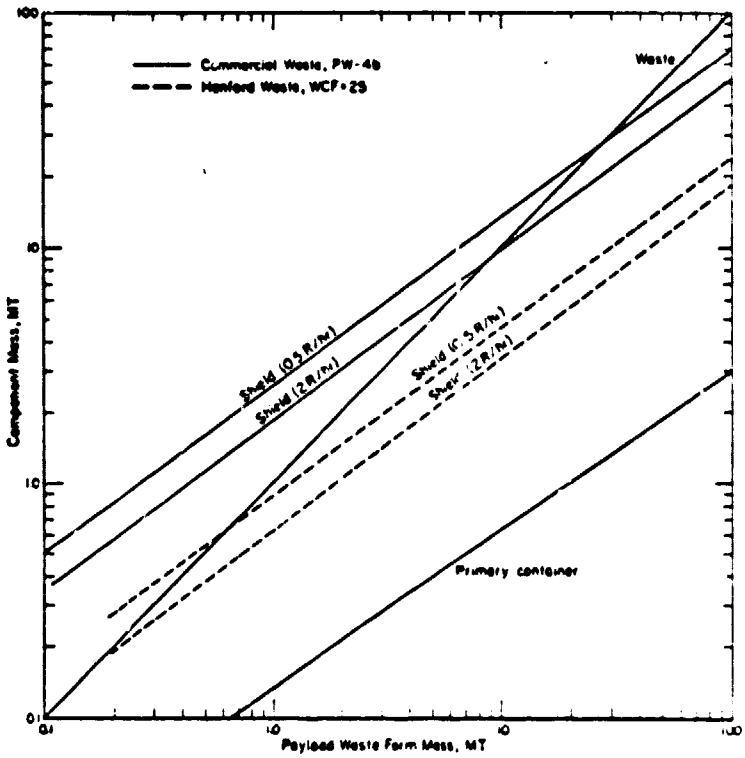

FIGURE 3-2. CONTAINER AND SHIELD MASS AS A FUNCTION OF PAYLOAD WASTE FORM MASS FOR COMMERCIAL (PW-4b) AND HANFORD (WCF=25) HIGH-LEVEL WASTE

3.4.4 Thermal Analysis

In addition to shielding requirements, temperature limits are important considerations in establishing conceptual payload designs. For example, design trade-offs are necessary to compromise the conflicting goals of minimizing waste volume (by concentration) and minimizing dose rate and thermal requirements. The purpose of this study is to provide data that can be used to assess the importance of various parameters, and thereby evaluate trade-offs in designs.

For the space disposal option, in addition to the thermal requirements stated in Section 3.3, a design constraint is that the final destination thermal equilibrium condition (by passive cooling) results in acceptable temperatures. Although this is not the most severe thermal condition for the waste package, the design philosophy must meet this criterion while relying on auxiliary cooling only for more severe, short-term conditions. Consequently, the deep space environment was chosen as the design basis condition for the unshielded primary container.

The thermal model used to describe the waste and primary container in deep space is defined in Appendix E. This model assumed spherical geometry, no gap between the waste and container wall, radiation heat transfer to a blackbody at a temperature of 3 K, uniform internal decay heat generation, and neglected solar input. Property data used in the thermal calculations are shown in Table 3-21.

TABLE 3-21. COMMERCIAL AND HANFORD HIGH-LEVEL WASTE HEAT TRANSFER INPUT PROPERTY DATA

				Reentry Vehicle		
	Waste Form[a]	Primary Container	Radiation Shield	Insulation	Ablation	Impact Absorber
Material	ORNL cermet	304 SS	Depleted uranium	Min-K	FWPF carbon/carbon	Steel honeycomb
Specific Heat, W-hr/kg-C	0.163[b]	0.13	0.03	0.21	0.17	0.13
Conductivity, W/m-C	14.0[c]	16.2	24.2	0.052	70.6	16.2
Density, g/cc	6.7	7.8	18.7	0.32	1.9	0.78[d]
Surface Emissivity	--	0.95	--	--	0.95	--

Notes: (a) From Tables 3-2 and 3-3.
(b) Specific heat for Hanford waste form is 0.233 W-hr/kg-C.
(c) Conductivity for Hanford waste form is 20.0 W/m-C.
(d) Bulk density for honeycomb.

The temperatures of interest are the maximum temperature of the waste and the temperature of the container wall. For Hanford waste, the primary container temperature will be essentially the same as at the waste surface. The results of the thermal analysis are tabulated for the three waste form mass values in Table 3-22 and also given in Figure 3-3.

TABLE 3-22. PAYLOAD WASTE AND CONTAINER TEMPERATURES FOR HANFORD AND COMMERCIAL HIGH-LEVEL WASTE, UNSHIELDED CONTAINER IN SPACE (T_∞ = 3 K)

		Temperature, C[a]					
		Commercial, (PW-4b)			Defense, Hanford (WCF = 25)		
Waste Mass, kg	Waste Radius, m	Waste Center	Waste Surface	Container	Waste Center	Waste Surface	Container
204	0.19	437	379	373	-64.5	-64.0	-64.0
5,500	0.58	1076	554	536	5.0	0.6	0.6
99,300	1.53	4357	780	732	104.0	74.0	74.0
9500[b]	0.70	514	335	329	--	--	--

Notes: (a) Temperature limits for waste and container wall are 1200 and 427 C, respectively (see Appendix C)
(b) Modified PW-4b Waste Form

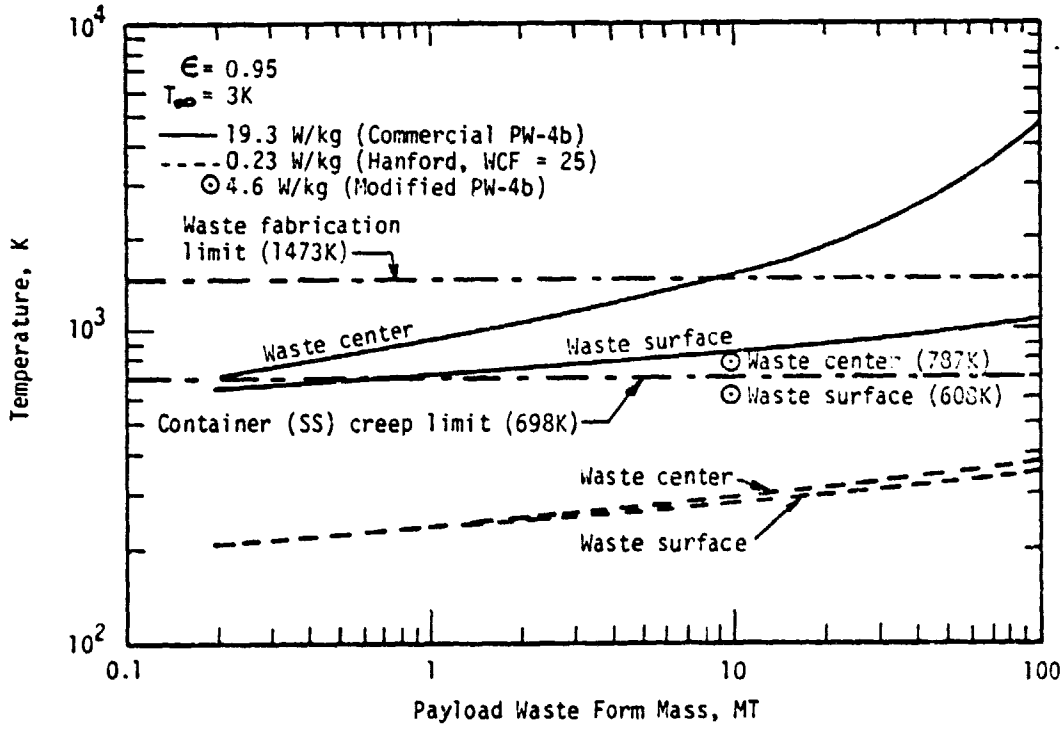

FIGURE 3-3. TEMPERATURE AS A FUNCTION OF PAYLOAD WASTE FORM MASS FOR VARIOUS LOCATIONS, WITHOUT RADIATION SHIELD, SPACE ENVIRONMENT

Results indicate that no thermal problems exist for any waste payloads analyzed for the Hanford waste (concentrations up to WCF=25). For commercial (PW-4b) waste payloads with masses greater than about 8 MT, the waste temperature exceeds the normal limit (waste fabrication temperature). For the container wall, the conservative temperature limit established is exceeded for commercial waste masses exceeding 700 kg. However, to achieve acceptable temperatures,there are several design approaches, such as: (1) decreasing payload heat output; (2) increasing waste conductivity; and (3) changing waste form or container material to permit higher limits. An attractive option is the removal of the "hottest" nuclides, thereby decreasing the heat output. This is believed to be the best option, and is discussed in Appendix F. For example, if 90 percent of the strontium and cesium nuclides (and their daughters) were removed, the decay heat load would decrease to about one-quarter its original value. (These radionuclides could be adequately handled by terrestrial disposal). Calculations for a 9.5 MT Modified PW-4b waste payload (see Appendix F) yield maximum waste center and surface temperatures of 514 and 335 C, respectively, for the deep space equilibrium condition. Both of these values are within the present thermal limits for a stainless steel container (see Figure 3-3).

3.4.5 Auxiliary Cooling Analysis

A design based on passive cooling in a space environment will require active cooling to meet the same limits in an earth environment. This is because of the large radiation heat loss created by the low temperatures in space and the insulating effect of protection systems. The following analysis compares cooling requirements to meet waste form or container thermal limits while in an earth environment. The analysis is performed for the same range of waste masses used in the thermal analysis (Section 3.4.4). Analytical methods are shown in Appendix G for the waste payload consisting of waste form, primary container, radiation shield, and reentry package. Since NASA/MSFC had not completed the reentry vehicle design at the time of this writing, it was assumed that the design would be similar to that used in the Phase II effort.[3-2] Therefore, the heat transfer characteristics of the reentry vehicle are included in Appendix G. Neglecting changes in thermal properties due to temperature, the minimum cooling requirements as a function of waste mass and temperature difference are presented in Table 3-23 and Figure 3-4. Results are also included for the 9.5 MT case with 90 percent removal of the Sr and Cs nuclides (Modified PW-4b). Since the larger commercial waste form masses (99,300 kg) do not meet the passive cooling criterion for space environment, they are excluded from auxiliary cooling analysis. The Hanford waste decay heat is low enough that temperatures are within limits without auxiliary cooling (see Table 3-24).

TABLE 3-23. MINIMUM AUXILIARY COOLING REQUIREMENTS (Q_{AC}) VS. MAXIMUM WASTE TEMPERATURE DIFFERENCE (ΔT) FROM NORMAL LIMIT FOR HIGH-LEVEL WASTE IN EARTH ENVIRONMENT (T_∞ = 21 C) WITH REENTRY VEHICLE[a]

Temperature Specification	Waste Mass, kg					
	204		5500		9500[b]	
	ΔT(C)	Q_{AC}(kW)	ΔT(C)	Q_{AC}(kW)	ΔT(C)	Q_{AC}(kW)
T_{Waste} = 1200 C	0[c]	0.59	0[c]	93	0[c]	17.1
$T_{Container}$ = 427 C	716	2.72	255	98	594	33.1
T_{Waste} = 600 C	600[c]	2.38	600	104	600	33.2
T_{Waste} = 900 C	300[c]	1.49	300	99	300	25.2

Notes: (a) Commercial Waste (PW-4b); auxiliary cooling is not required for Hanford (WCF = 25) waste mix under these conditions. ΔT = 1200 (assumed waste limit, normal conditions) - T_{Waste}. Heat generation rates for the payload sizes given are 3.94, 106 and 44 KW, respectively.

(b) Payload size for HLLV, 90 percent cesium and strontium removed from PW-4b (Modified PW-4b).

(c) Container temperature exceeds normal limit (427 C, stainless steel).

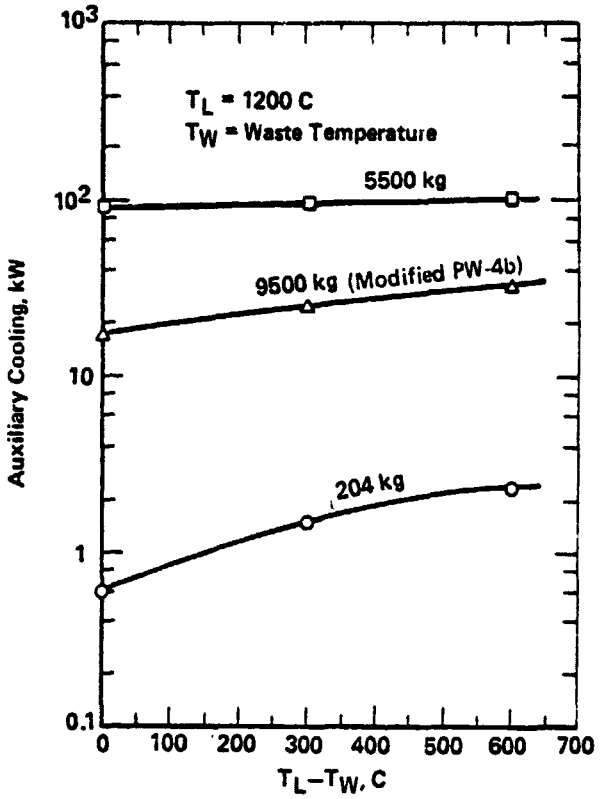

FIGURE 3-4. MINIMUM AUXILIARY COOLING REQUIREMENTS VS. MAXIMUM WASTE TEMPERATURE DIFFERENCE (T_L-T_W) FROM NORMAL LIMIT, COMMERCIAL WASTE PW-4b), EARTH ENVIRONMENT (T_∞ = 21 C), WITH REENTRY VEHICLE

TABLE 3-24. PAYLOAD WASTE TEMPERATURES FOR HANFORD (WCF = 25) HIGH-LEVEL WASTE, WITH SHIELD AND REENTRY VEHICLE, EARTH ENVIRONMENT (T_∞ = 21 C)

Waste Mass, kg	Temperature, C	
	Center	Surface
204	38.6	38.1
5,500	89.4	89.1
99,300	256	227

The cooling requirements are based on the assumption that direct cooling of the primary container is possible. If the radiation shield is to be cooled, the values in Table 3-23 and Figure 3-4 will be higher. The auxiliary cooling required is in the range of 15 - 69 percent of the heat generated for the 204 kg waste form mass, 88 - 98 percent for the 5500 kg waste form mass, and 39 -75 percent for the 9500 kg (using the Modified PW-4b) waste form mass, depending on the temperature margin desired.

After auxiliary cooling is removed, the temperatures throughout the package will rise. For commercial waste, the waste and container temperatures will eventually reach and surpass their respective limits for even the lower masses (204 kg). As the temperature rises, the amount of heat transferred through the shield and reentry vehicle increases, resulting in an asymptotic approach to equilibrium, i.e., the rate of temperature increase is not constant, but diminishes with time. The instantaneous heatup rates (C/hr) as a function of temperature margin (difference between normal operating temperature and temperature limit) and waste mass are shown in Table 3-25 and Figure 3-5. A comparison between the "instantaneous" heatup time (i.e., initial temperature difference divided by the corresponding rate of

TABLE 3-25. RATE OF TEMPERATURE INCREASE ($\dot{T}$) VS MAXIMUM WASTE TEMPERATURE DIFFERENCE (ΔT) FROM NORMAL LIMIT, COMMERCIAL WASTE (PW-4b), EARTH ENVIRONMENT, (T_∞ = 21C) WITH REENTRY VEHICLE

Design Condition	WASTE MASS, kg[a] 204 ΔT(C)	204 $\dot{T}$(C/hr)	5500 ΔT(C)	5500 $\dot{T}$(C/hr)	9500[b] ΔT(C)	9500[b] $\dot{T}$(C/hr)
$T_{Container}$ = 427 C	716	82	255	109	594	21
T_{Waste} = 600 C	600	72	600	116	600	21
T_{Waste} = 900 C	300	45	300	110	300	16
T_{Waste} = 1200 C	0	18	0	103	0	11

NOTES: (a) C_p = 0.163 W-hr/kg-C
(b) Modified PW-4b waste (90% Cs & Sr removed).

temperature increase, see Figure 3-5) and a realistic time (accounting for variation of heatup rate with time) is shown in Table 3-26. Results indicate that, for a given waste concentration, the larger the waste mass, the shorter the heatup time. If extended heatup times are required it will be necessary to increase the temperature margin, that is, reduce the normal operating temperature, by increasing the auxiliary cooling.

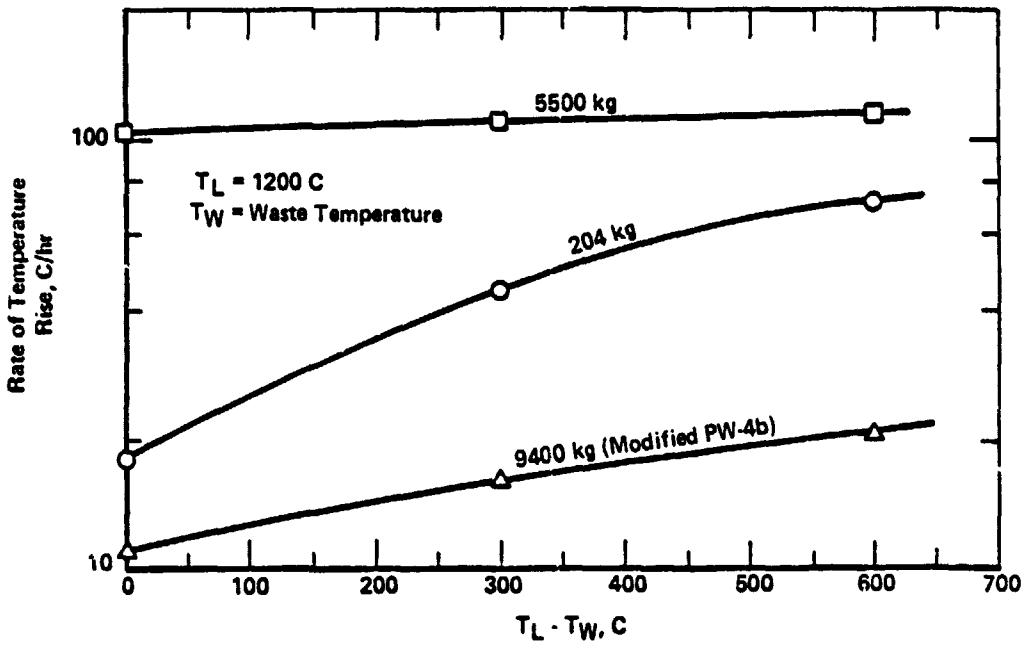

FIGURE 3-5. RATE OF TEMPERATURE INCREASE VS. MAXIMUM WASTE TEMPERATURE DIFFERENCE (T_L-T_W) FROM NORMAL LIMIT, COMMERCIAL WASTE (PW-4b), EARTH ENVIRONMENT (T_∞ = 21 C), WITH REENTRY VEHICLE

TABLE 3-26. TIME REQUIRED FOR COMMERCIAL WASTE (PW-4b) PAYLOADS TO REACH LIMIT TEMPERATURE (1200 C) STARTING WITH A 600 C MARGIN

Waste Mass, kg	Initial Rate, hours	Integrated Rate, hours
204	8.3	15.4
5,500	5.2	5.4
9,500 (a)	28.6	38

Note: (a) HLLV Payload, Modified PW-4b.

3.4.6 Parametric Analysis of Dose Rate as a Function of Shielding Thickness and Distance

During orbital handling operation of the waste payload, especially after the shield is removed, the crew and other vital components will be exposed to radiation from the waste package. To assess the potential radiation dose to personnel and equipment during this phase of the operation, the dose rate as a function of distance and thickness of intervening material was determined as a function of payload waste mass. For this study, various

thicknesses of aluminum were chosen. The ANISN[3-14] code was used with the various waste masses to determine the neutron and gamma dose rate for different thicknesses of aluminum. The results are shown in Figures 3-6, 3-7, and 3-8. Figures 3-6 and 3-7 show the dose rates for unshielded containers as a function of distance for commercial and Hanford waste, respectively. The curves in Figure 3-8 apply to both commercial and Hanford waste packages with the radiation shield, since they have been sized to a total dose rate of 2.0 rem/hr at 1 meter from the surface. For commercial waste (PW-4b), the 99,300 kg waste mass was not analyzed for dose-vs-distance behavior because of its unsuitability on a thermal basis. The curves in these three figures can be extrapolated linearly on log-log paper for distances greater than about 10 meters, since beyond this point the dose rate is inversely proportional to the distance squared. Because of the resultant proportionality of results, a family of curves was not necessary to display the shielding effects of aluminum. Due to the peaked spectrum of both commercial and Hanford waste in the same energy range, the variation of the curves with aluminum thickness reduces to a single proportionality factor (for each thickness) as:

$$F = e^{-mx} \quad ,$$

where,

F = Dose rate factor
m = Linear attenuation coefficient (cm^{-1})
x = Material thickness, cm.

For aluminum, m = 0.12 cm^{-1}, corresponding to the 2 MEV range.

To illustrate the effect of distance, for the 5500 kg commercial waste mass payload, without radiation shield, a distance of about 1000 meters is required to reduce the dose rate to 2 rem/hr. If 2.5 cm of aluminum shielding were intervening, a distance of 860 meters would be required. By contrast, a bare container of 5500 kg Hanford waste (WCF = 25) would produce a dose rate of 2 rem/hr at a distance of only 12 meters from the surface. It should be noted that because of the self-shielding effect of the waste form, waste payloads containing an outer shell of defense waste form and in inner sphere of commercial waste could improve safety and reduce shielding and cooling requirements. Another approach would be to mix the two wastes together.

3.4.7 Conclusions

This parametric evaluation of the nuclear and thermal effects of various sizes of commercial and defense high-level waste is intended to demonstrate those combinations of design parameters that are feasible for the space disposal option. Overall, there do not appear to be any shielding or steady-state thermal limitations to even the larger payloads of Hanford waste. In fact, none of the defense waste mass payloads examined required auxiliary cooling in near-earth environments.

Commercial waste (PW-4b), as produced in the manner described in Section 3.2, can be adequately shielded for all waste masses studied.

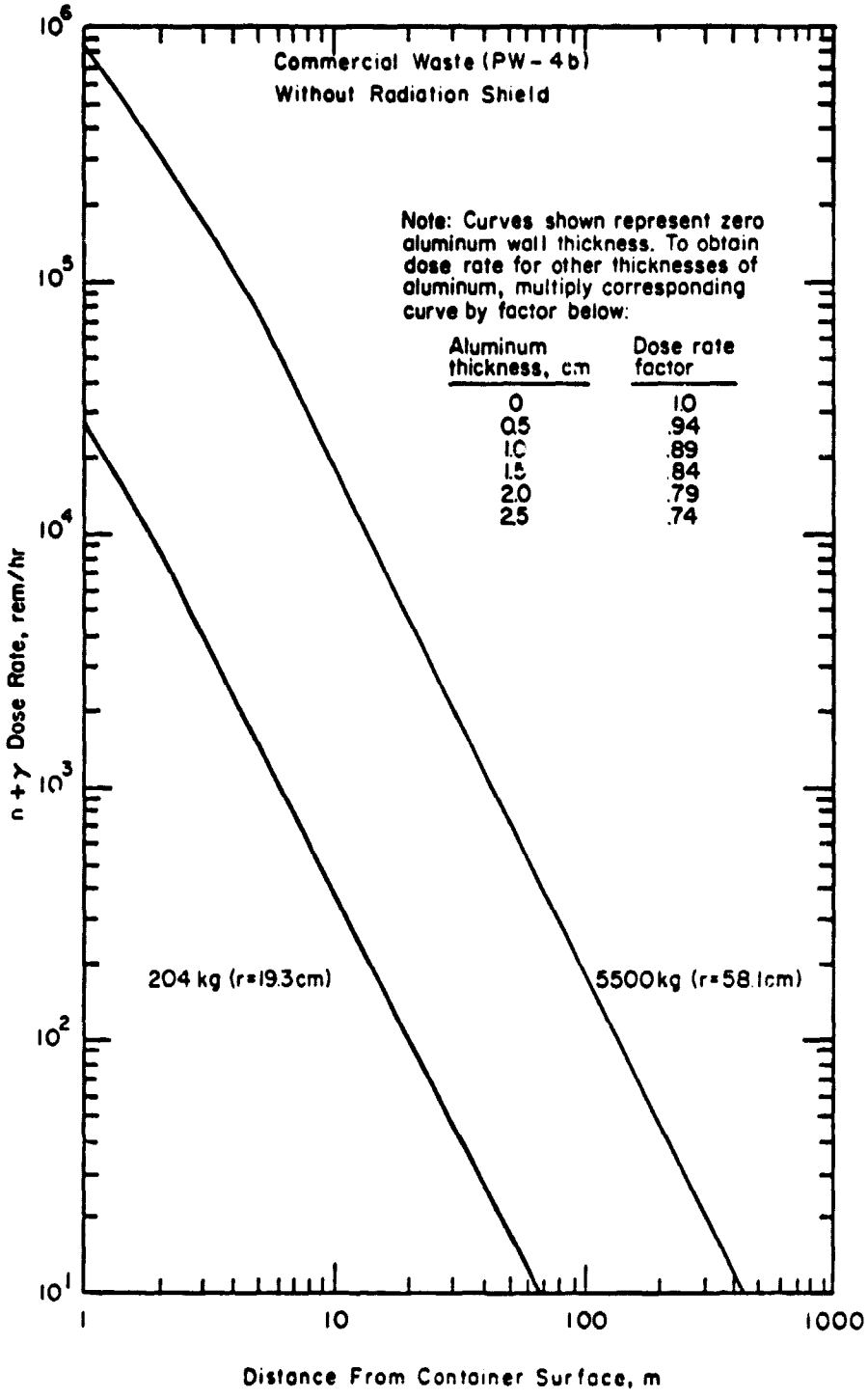

FIGURE 3-6. DOSE RATE AS A FUNCTION OF DISTANCE FROM PAYLOAD WITHOUT FLIGHT RADIATION SHIELD, COMMERCIAL WASTE (PW-4b)

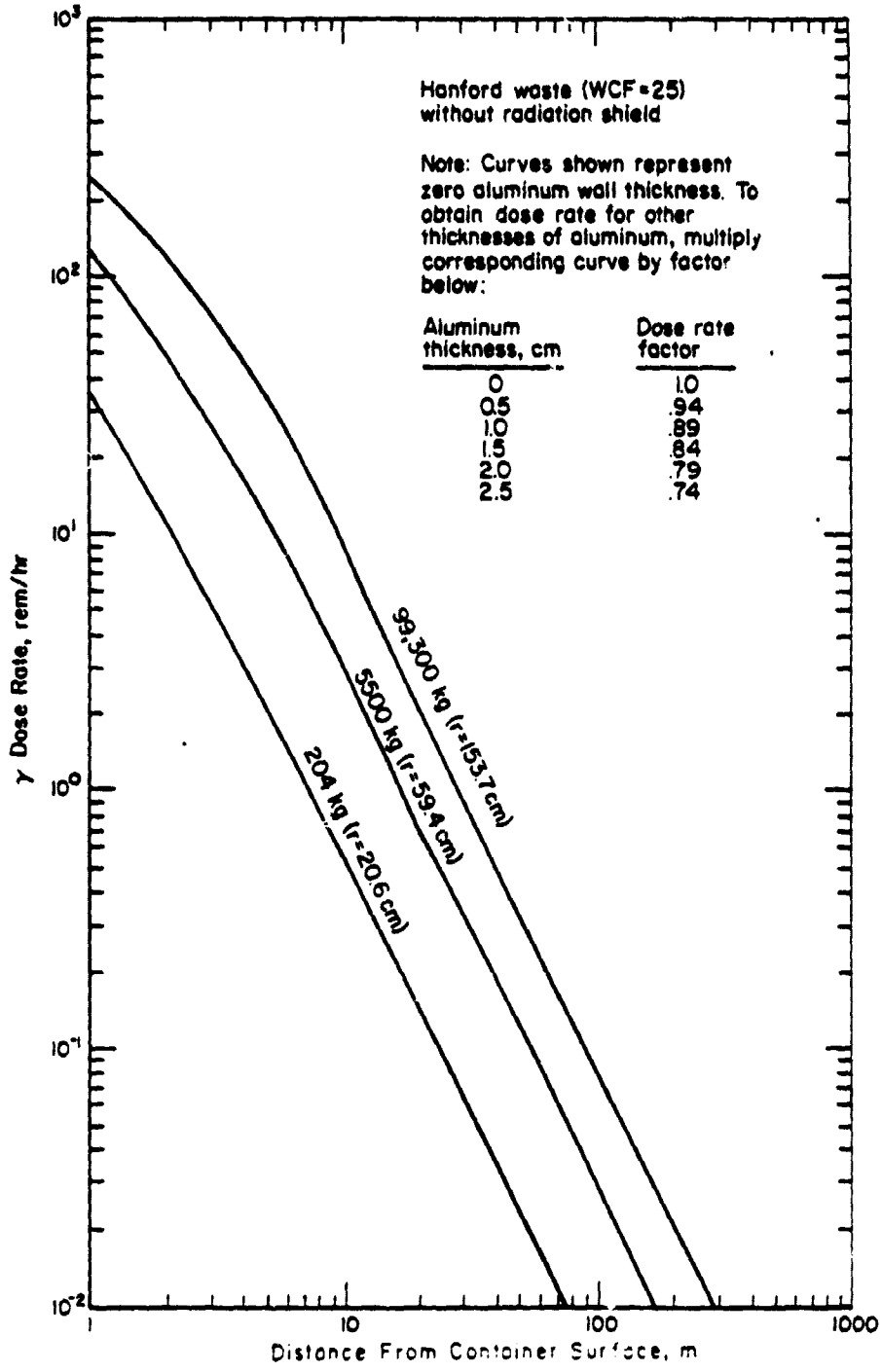

FIGURE 3-7. DOSE RATE AS A FUNCTION OF DISTANCE FROM PAYLOAD WITHOUT RADIATION SHIELD, HANFORD WASTE (WCF = 25)

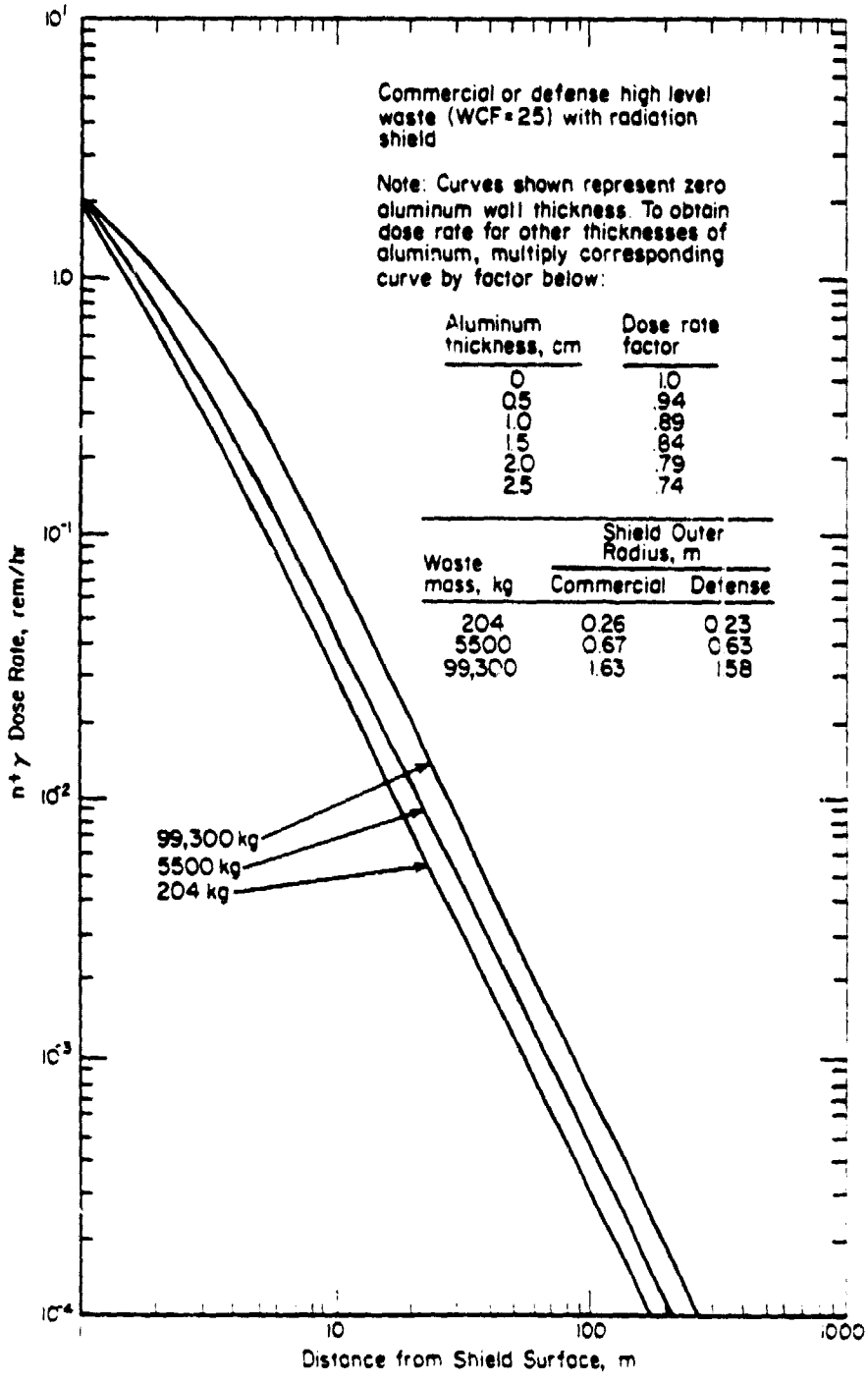

FIGURE 3-8. DOSE RATE AS A FUNCTION OF DISTANCE FROM SHIELD SURFACE, COMMERCIAL OR HANFORD (WCF = 25) HIGH LEVEL WASTE WITH RADIATION SHIELD

However, constraints in allowable temperatures in the waste and reference container material severely limit the waste mass per payload. Assuming that certain nuclides can be removed from the PW-4b mix, it has been shown that a 9500 kg waste mass can meet thermal requirements, with a minimum amount of auxiliary cooling required.

3.5 Waste Processing and Payload Fabrication System

Current regulations[3-15] prohibit the shipment of greater than 20 curies of plutonium in any form other than a solid. In effect, this regulation requires that, for other than small quantities, the liquid high-level wastes produced at a fuel reprocessing plant must be converted to a solid form prior to shipment from the site of origin. As a result, high-level waste treatment and packaging facilities are generally considered to be a part of, or adjacent to, the fuel reprocessing plant or waste storage facilities.

For high-level waste from commercial power reactor fuel, the regulations[3-16] allow storage of the waste as a liquid for a maximum of 5 years and require solidification and shipment of the wastes to a repository in a maximum of 10 years after generation. Generally, the plans for waste disposal are based on wastes which have been out of the reactor 10 years, as this allows a maximum time for fission product decay and results in a reduced heat generation rate.

The high-level liquid waste produced in a commercial reprocessing plant is planned to be stored in large tanks in the form of nitric acid solutions. For wastes planned for space disposal, the separation process should produce a nitrate solution with a minimum of diluents, as described in Section 3.1 and referred to as PW-4b. The storage tanks will be located near the reprocessing facility and positioned below grade level to utilize the earth for part of the shielding necessary to reduce to an acceptable level the radiation emanating from the wastes.[3-17] The storage tanks will have submerged cooling coils to extract heat from the liquid waste to achieve acceptable temperatures in the waste. The extracted heat will be dissipated to the environment, probably by air-cooling towers.

To initiate the treatment process, the liquid waste will be pumped from the storage tank into remotely operated closed chemical processing equipment located in a shielded cell facility. The treatment facilities for producing the waste form for space disposal will be very similar to facilities in use for reprocessing defense[3-18] and commercial[3-15] spent fuel and should be considered state-of-the-art technology. However, the specific processes employed for waste solidification and packaging have only been demonstrated in laboratory or pilot-plant-scale systems and have not been utilized in full-scale production facilities.

All processes, from modifying the waste composition through solidification, packaging, decontamination, and inspection will be conducted in the waste treatment facilities. For the present disposal concept, there is incentive to separate the majority of the strontium and cesium from the waste to remove the major heat generation sources. The solvent extraction and ion exchange processes, used for removal of these elements from defense wastes, provide a basis for this process.[3-16] The formation of the cermet from the liquid waste is carried out by coprecipitation of the waste and metal additives from an urea solution, calcination of the precipitate, and reduction of the metal phase by steps which have been demonstrated on a laboratory scale.[3-19] The fabrication of the cermet waste form has been demonstrated

at ORNL on a laboratory scale utilizing conventional powder metallurgy techniques. However, fabrication of the cermet into large shapes, as required by the present disposal concept, is beyond the present state of the art and will require a significant development program.

In the conceptual studies, the waste form is considered to be in the configuration of a large monolithic sphere. A monolithic waste form is not a requirement, but, if a large configuration is composed of an assembly of smaller pieces, the interfaces between pieces must not significantly hinder the heat flow through the assembly. The fabrication of large shapes by powder metallurgy techniques for waste disposal practices has some precedent. The capability to fabricate and hermetically seal a thick-walled corundum canister 0.5 m diameter and 2.5 m long by hot isostatic pressing of Al_2O_3 powder has been demonstrated in Sweden.(3-20) Future studies of cermet fabrication may show that configurations other than spherical are warranted for consideration.

The packaging of the waste is the final step in the waste package assembly. The spherical container concept is unique and will require development. If processes for the fabrication of large shapes by powder metallurgy are developed, they could be utilized for fabricating the container, which could be a shell of the cermet metal phase, free of radioactive products, formed around the waste form. This would be highly desirable for the transfer of heat from the waste through a continuous conductor. If the container is fabricated by the assembly and welding of sections of shells around the waste form, great care must be taken to assure good heat conduction through the waste-form-container interface.

After closure, the surface of the container must be decontaminated prior to removal from the facility. Techniques used for decontaminating large packages include wire brushing and washing, chemical etching, and electropolishing. Criteria for the allowable surface contamination have not been established; for packages for terrestrial disposal, the proposed contamination levels are in the order of 200 disintegrations per minute (dpm) for alpha emitters and 2,000 dpm for beta-gamma emitters.

Prior to leaving the facility, the package must be thoroughly inspected to verify that the packaging is free of leaks and defects, and that the package is properly identified by appropriate labeling.

All of the above steps in the treatment and packaging will be conducted in a shielded cell facility for which there is a large amount of experience to base the design and operation. The cell walls will be concrete several feet thick. All operations will be conducted remotely. Operations will be viewed with video cameras and possibly through a few shielded windows placed in the walls. The planning for maintenance of the equipment will be a dominant influence in the facility design. Although different approaches have proven effective, generally there are no plans for entry into the facility after it has begun operation, although some designs use a shielded crane cab for equipment removal. Some high-maintenance items, such as drive motors, may be located in an equipment gallery on one side of the facility with drive shafts penetrating the cell walls. Entrance to the gallery may be allowed

after removal of high-radiation sources adjacent to the area. All process equipment is designed to be remotely disconnected from the system and removed from the facility for replacement or repair.

The facility will be designed and operated to assure acceptably low radiation exposures to the work force and to the public during both normal and postulated off-normal and accident conditions. The facility cells will be sealed and ventilated with a filtered system. The bottom of each cell will have a stainless steel liner to catch spills and allow flushing and draining. The facility will be divided into a series of cells to act as barriers to the spread of contamination within the facility.

Once the waste is assembled into a massive form, it will be necessary to provide cooling to assure the waste form temperatures remain acceptable. Storage of the packaged waste may be required for periods up to 5 years. Storage will require a separate facility, in which protection of the packages from earthquakes, tornadoes, floods, civil disturbances, and sabotage is provided. The storage facility must assure adequate cooling of the packages and secondary containment for any failed packages. Adjacent to the storage facility, a facility should be located for placement of each waste package in a flight-weight radiation shield and preparation of the shielded package for transport in a shipping cask to the space launching site.

3.6 References

3-1. Pardue, W. M. et. al., "Preliminary Evaluation of the Space Disposal of Nuclear Waste," 8-3239(100), Battelle Memorial Institute, Columbus, Ohio (August 1977).

3-2. Edgecombe, D. S., Rice, E. E., Miller, N. E., Conlon, R. J., and Yates, K. R., "Evaluation of the Space Disposal of Defense Nuclear Waste--Phase II," Battelle's Columbus Laboratories, Columbus, Ohio (January 1979).

3-3. Aaron, W. S., et. al., "Progress on the Cermet Approach to Nuclear Waste Management," Transactions of American Nuclear Society, Volume 33, p 413 (November 1979).

3-4. Metal Statistics 1978, Fairchild Publications, New York, N.Y. (1978).

3-5. Bureau of Mines, Bulletin 667 (1975).

3-6. Solomito, E., and Stockton, J., "Modification of the Point-Kernel Code QAD-P5A," ORNL-4181, Oak Ridge National Laboratory, Oak Ridge, Tennessee (July 1968).

3-7. Mendel, J. E., et al., "Annual Report on the Characteristics of High-Level Waste Glass," BWNL-2252, Battelle Northwest Laboratories, Richland, Washington (June 1977).

3-8. Bell, M. J., "ORIGEN--The ORNL Isotope Generation and Depletion Code," ORNL-4628, Oak Ridge National Laboratory, Oak Ridge, Tenn. (May 1973).

3-9. Yates, K. R., and Park, U. Y., "Nuclear Capacity Projections and Spent Fuel Accumulations," Power Engineering, Vol. 83, No. 12 (December 1979).

3-10. ASME Boiler and Pressure Vessel Code, Section III, Division 1, Nuclear Power Plant Components, American Society of Mechanical Engineers, New York (1974).

3-11. "Packaging Radioactive Materials for Transport," Title 10, Part 71.31, Code of Federal Regulations, U.S. Nuclear Regulatory Commission, Government Printing Office, Washington, D.C. (November 1978).

3-12. "Packaging Radioactive Materials for Transport," Title 10, Part 71., Code of Federal Regulations, U.S. Nuclear Regulatory Commission, Government Printing Office, Washington, D.C. (November 1978).

3-13. "Requirements for Transportation of Radioactive Materials," Title 49, Parts 171-177, Code of Federal Regulations, U.S. Department of Transportation, Government Printing Office, Washington, D.C. (December 1979).

3-14. Soltesz, R. G., "Revised WANL ANISN Program User's Manual," WANL-TMI-1967, Westinghouse Astronuclear Laboratory, Pittsburgh, Pa. (April 1969).

3-15. "Packaging Radioactive Materials for Transport," Title 10, Part 71.42, Code of Federal Regulations, U.S. Regulatory Commission, Government Printing Office, Washington, D.C. (November 1978).

3-16. "Licensing of Production and Utilization Facilities," Title 10, Part 50, Appendix F, Code of Federal Regulations, U.S. Nuclear Regulatory Commission, U.S. Government Printing Office, Washington, D.C. (March 1979).

3-17. "Barnwell Nuclear Fuel Plant, Safety Analysis Report," Vol. 1, Docket-50332-1 (November 1968).

3-18. "Alternatives for Long-Term Management of Defense High-level Radioactive Waste," ERDA 77-44 (September 1977).

3-19. Aaron, W. S., Quinby, T. E., and Kobisk, E. H., "Cermet High-level Waste Forms," ORNL/TM-6404, Oak Ridge National Laboratory, Oak Ridge, Tennessee (June 1978).

3-20. Larker, Hans, "The Direct Disposal of Spent Nuclear Fuel in Alumina Containers," ASEA Central Research and Development Department, Vasteras, Sweden (August 1978).

4.0 SAFETY ASSESSMENT

Safety is probably the most important factor in the development of viable concepts for the space disposal of nuclear wastes. Therefore, the safety analysis has been given appropriate emphasis in this Phase III study effort. The major objective of this Phase III Safety Assessment was to define the major accident environments and study the response of the reference commercial nuclear waste payload to these accident environments, and to predict the degree of containment that might be expected. The response analysis was limited in this report to the fire and reentry environs. Payload response to the blast wave, shrapnel, and impact needs to be accomplished in follow-on studies. Information generated by this assessment was supplied to the Health Effects Assessment Task (see Section 5.0).

Section 4.1 briefly describes the literature review that was performed early in the study. The significant findings were supplied to other task activities (see Sections 2.5, 3.1, 3.3, 4.2, 4.3, and 7.5). Emphasis was placed upon the review of the safety and testing aspects that relate to space nuclear payloads, e.g., Radioisotope Thermal Generators (RTG). NASA/MSFC's parallel review was related to aspects of the RTG design.

Section 4.2 describes the major accident environments for the Uprated Space Shuttle and heavy lift launch vehicle (HLLV). The accident environments described include fireball, RP-1 residual fire, blast, and shrapnel. Some of the data generated for the Uprated Space Shuttle vehicle may have application toward the Space Shuttle accident environment definition. These investigations indicate that considerably more work is necessary in attempting to confidently predict the shrapnel environments that might be expected from exploding propellant tanks.

Section 4.3 describes the preliminary analysis dealing with the nuclear waste payload response to a few of the accident environments described in Section 4.2, as well as atmospheric reentry. Section 4.3.1 describes the modifications made to the BCL Reentry Thermal Analysis Code (RETAC) for this analysis. Section 4.3.2 presents the results of the fire and reentry thermal response of the payload in different protection configurations. Section 4.3.3 outlines the expected release scenarios used to estimate world population dose (see Section 5.3.) Section 4.3.4 recommends certain design changes to improve the reference concept.

A brief assessment of the safety implications of employing a HLLV for nuclear waste disposal in space is given in Section 4.4. The assessment indicates that using the HLLV as a booster for the space disposal mission provides a significant improvement in safety and viability.

References for this Safety Assessment are given in Section 4.5.

4.1 Safety Study Review

The objective of the BCL safety study review was to incorporate appropriate concepts, approaches and testing procedures for the RTG, General Purpose Heat Source (GPHS), and previous nuclear waste disposal studies into the current space option safety considerations and program plans. (NASA/MSFC also conducted an independent review of previous studies; their emphasis was to relate the "RTG" design and materials choices to the space option conceptual designs.) Appropriate information available from the BCL safety review was provided to other study activities: waste form definition (Section 3.1); payload containment requirement definition (Section 3.3); system safety design requirements (Section 2.5); accident environment definition and response (Sections 4.2 and 4.3); and the test planning activity (Section 7.5). The specific activity areas during the review were as follows:

- Review safety and testing aspects of space nuclear payloads
- Include results in the overall concept definition and test planning requirements
- Evaluate latest documents defining accident environments
- Provide information related to RTG safety requirements to the containment requirements definition.

The documentation reviewed during the study has been placed into four major categories to allow for appropriate discussion. These are:

(1) RTG Related Reports

(2) GPHS Related Reports

(3) Nuclear Waste Disposal in Space Reports (1971-1974)

(4) Accident Environment Definition and Payload Response Reports

The significant findings or items of apparent importance to the space option, contained in the reports in the four categories, are briefly discussed below. Various aspects of the RTG and GPHS Programs have been used in this space disposal option study, as a result of this brief review.

4.1.1 RTG Related Reports

A few of the safety reports from past RTG programs were briefly reviewed.(4-1 through 4-5) Only the safety aspects were evaluated and only items that are of interest to this program are discussed in the following paragraphs.

In the RTG safety analyses of the 60's only accident occurrence probabilities were examined. For significant environments, e.g., explosive overpressure, a nominal value was usually determined by consensus. Test programs were conducted simulating the selected environments, so that results of the tests constituted a demonstration of meeting or not meeting the safety requirements. In the later safety analyses emphasis was placed on estimating total probabilities associated with a given consequence, e.g., exposure of a specified number of people at a specified lung burden. Included were considerations of accident occurrence probabilities, environment and response variability, and uncertainties in source term magnitudes, meteorology and population density. Requirements now exist for parametric evaluation: the relevant question is not "will a particular configuration withstand a certain overpressure?" but "at what overpressure does it fail"? Also "what is the uncertainty in this result and what is the observed failure distribution among a number of identical, simulated configurations?" Analyses must now consider the variability or uncertainty in input quantities since these affect the estimates of the accident environments and payload response.

The Viking safety report[4-3] provides useful information regarding the safety analysis procedure, the type of tests performed, and the results of those tests. The safety procedure was described as having four basic elements: (1) identification of failure modes; (2) definition of accident environments; (3) prediction of the payload response; and (4) the analysis of the conditional fuel release probability. Figure 4-1, taken from the Viking safety report, provides a summary of the safety evaluation logic sequence. Also, it is useful to state that the safety analysis reports (SARS) for RTG's usually consist of: (1) a reference design document; (2) an accident model environment; (3) models to identify source terms; and (4) a risk assessment. The types of tests that were performed for the Viking RTG system are listed below:

- Vibration
- Graphite Oxidation
- Blast Overpressure
- Fragment Impact
- Liquid Propellant Fire
- Solid Propellant Fire
- Impact on Granite
- Drop Tests
- Reentry Heating (Plasma Tunnel)
- Heat Transfer Measurements
- Force and Moments Measurements

In summary, the Viking RTG fuel sample was tested and a few of the results of these tests are given below:

- Survived a blast overpressure of 550 N/cm^2 (800 psi)
- Fragments are no serious threat--assumes attenuation by RTG satellite support structure
- The liquid propellent fireball is no problem
- Survived impacts ranging from 23 to 107 m/s

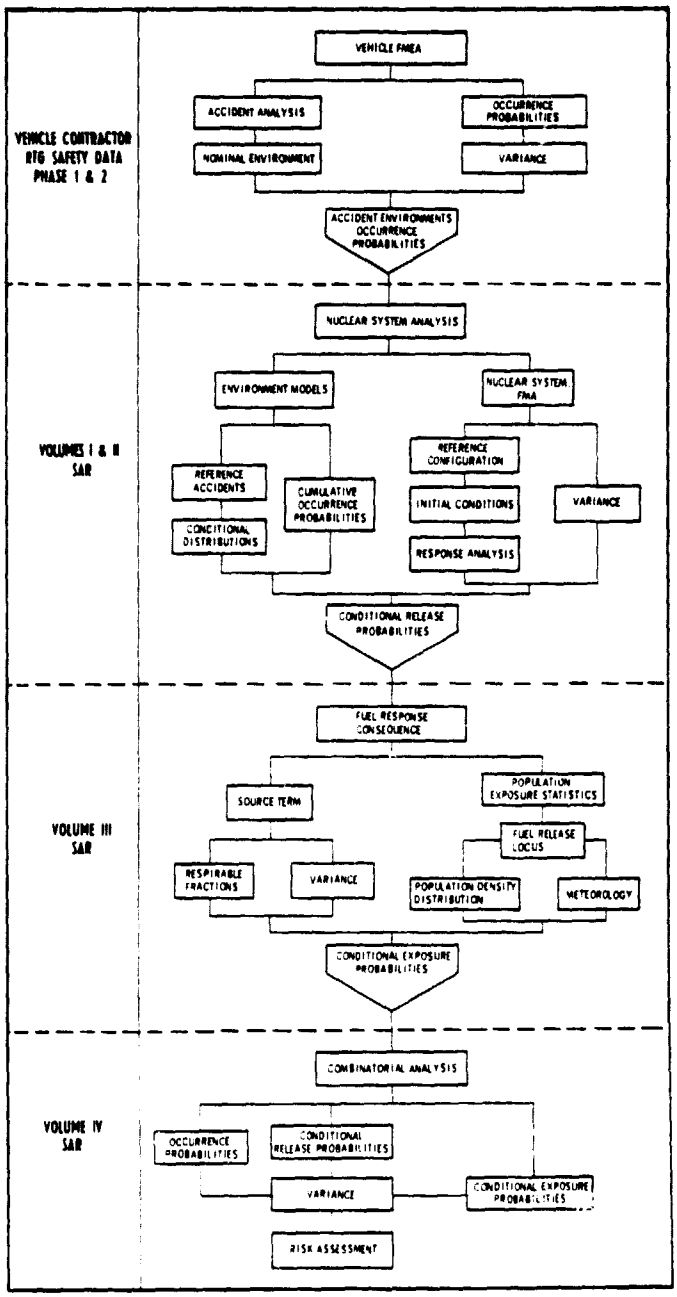

Source: Reference 4-3.

FIGURE 4-1. SAFETY EVALUATION LOGIC SEQUENCE

- The solid propellent fire (at 2870 K for 10 min) had the potential for breaking open a fuel capsule.
- Post-reentry impact contributed most to the likely release situations.

The Viking safety report called for more in-depth methods of predicting the dynamic structural response to blast, fragment and impact, as well as, better definition of probability distributions for environment magnitudes for a given accident. It goes on to state that the assignment of a single representative environment of an accident may be misleading, in that risks may be misjudged.

In addition to the RTG safety reports,(4-1 through 4-5), three other documents of importance were reviewed.(4-6, 4-7 and 4-8) Reference 4-6, "Uses of Radioactive (Nuclear) Materials by the United States of America for Space Power Generation", a working paper submitted by the U.S.A. to the United Nations Committee on the Peaceful Uses of Outer Space, contains an excellent overview of the missions previously flown and the safety philosophy that has been employed over the years. Table 4-1 summarizes the space nuclear power systems launched by the U.S.A. from 1961 to 1977.(4-6) Table 4-2 summarizes the location of all the ^{238}Pu launched into space by the U.S.A. during the same period.(4-6) Two items should be noted here for comparison with the space disposal option: (1) The Viking power source and others (see Table 4-2) employed a PuO_2-Mo cermet as the fuel form; and (2) the amount of total Curies contemplated in one payload of PW-4b is an order of magnitude larger than the total Curies launched into space through 1977 by the U.S.A. (see Table 4-2). References 4-7 and 4-8, "The Safety Specification for the Plutonium-238 Developmental Heat Sources, NRA-3", and "Safety Heat Source Design Specification for Space Applications", contained in Appendix A of the Overall Safety Manual, were reviewed and used in the preparation of the Containment Requirements Definition for the space disposal option (see Section 3.3) and the space option Safety Requirements developed in Section 2.5.

TABLE 4-2. DISPOSITION OF NUCLEAR SPACE MATERIAL THROUGH NOVEMBER 1977 BY THE U.S.A.

Disposition	Quantity ^{238}Pu, Curies (%)
Deep Space	580,000 (43)
Orbit	379,200 (28)
Lunar Surface	222,500 (17)
Mars Surface	84,000 (6)
Pacific Ocean	44,500 (3)
Recovered	34,400 (2)
Atmosphere	17,000 (1)
Total	1,361,600 (100)

Source: Reference 4-6.

TABLE 4-1. SUMMARY OF SPACE NUCLEAR POWER SYSTEMS LAUNCHED BY U.S.A. (1961-1977)[a]

Flight Number	System[b]	Mission	Launch Date	Launch Site[c]	^{238}Pu Fuel	Curies	Disposition
1	SNAP 3	Transit 4-A	6/61	ETR	Metal	1,800	In > 500 Year Orbit
2	SNAP 3	Transit 4-B	11/61	ETR	Metal	1,800	In > 1,000 Year Orbit
3	SNAP 9A	Transit 4-BN-1	9/63	WTR	Metal	17,000	In > 1,000 Year Orbit
4	SNAP 9A	Transit 5-BN-2	12/63	WTR	Metal	17,000	In > 1,000 Year Orbit
5	SNAP 9A	Transit 5-BN-3	4/64	WTR	Metal	17,000	Aborted Downrange, Burned Up on Reentry
6	SNAP 19	Nimbus B-1	5/68	WTR	Microspheres	34,400	Aborted at Launch, Recovered From Ocean
7	SNAP 19	Nimbus III	4/69	WTR	Microspheres	37,600	In ~3,000 Year Orbit
8	SNAP 27	Apollo-12	11/69	KSC/ETR	Microspheres	44,500	Lunar Surface
9	SNAP 27	Apollo-13	4/70	KSC/ETR	Microspheres	44,500	Aborted after TLI.[d] Deep Ocean Burial-South Pacific
10	SNAP 27	Apollo-14	1/71	KSC/ETR	Microspheres	44,500	Lunar Surface
11	SNAP 27	Apollo-15	7/71	KSC/ETR	Microspheres	44,500	Lunar Surface
12	SNAP 27	Apollo-16	4/72	KSC/ETR	Microspheres	44,500	Lunar Surface
13	RTG	Pioneer F (10)	3/72	CKAFS/ETR	Cermet	80,000	Jupiter/Deep Space
14	RTG	Transit	9/72	VAFB/WTR	Cermet	24,000	In < 1,000 Year Orbit
15	SNAP 27	Apollo-17	12/72	KSC/ETR	Microspheres	44,500	Lunar Surface
16	RTG	Pioneer G (11)	4/73	CKAFS/ETR	Cermet	80,000	Jupiter/Deep Space
17		LES 8/9	3/76	CKAFS/ETR	Oxide spheres	280,000	In > 4,000 Year Orbit
18		Viking-1	8/75	CKAFS/ETR	Cermet	42,000	Mars Surface
19		Viking-2	9/75	CKAFS/ETR	Cermet	42,000	Mars Surface
20		MJS-1 (Voyager)	8/77	CKAFS/ETR	Oxide spheres	210,000	Jupiter/Saturn/Deep Space
21		MJS-2 (Voyager)	9/77	CKAFS/ETR	Oxide spheres	210,000	Jupiter/Saturn/Deep Space

Notes:
(a) Source: Reference 4-6.
(b) All systems launched were radioisotope power systems except SNAP 10A (SNAPSHOT), a reactor power system. It was launched 4/65 at WTR with 4.5 kg of ^{235}U fully enriched. It is currently in a > 1,000 year orbit.
(c) ETR = Eastern Test Range, Florida; WTR = Western Test Range, California; KSC = Kennedy Space Center, Florida; and CKAFS = Cape Kennedy Air Force Station.
(d) Trans-lunar ingection.

As a result of the review of various RTG safety studies, appropriate data and information were made available to the space disposal option study, and in particular, to Sections 2.5, 3.3, and 7.5.

4.1.2 GPHS Related Reports

For most space and terrestrial applications of radioisotope-fueled heat sources, the heat source and the conversion systems to produce electrical power were designed for a specific mission or series of missions. To change the total electrical power output within these power systems required additional integral numbers of complete conversion systems, which often resulted in mass and volume penalties. As design evolved, considerable time and money were spent on the development and qualification of each different heat source (see Table 4-1). The rationale developing the General Purpose Heat Source (GPHS) was that time, money, systems mass and volume can be saved if a modular heat source can be developed and qualified to meet the needs of existing and future systems. The development has been guided by safety testing; with less emphasis on analytical approaches.

The current GPHS Program is being managed by Los Alamos Scientific Laboratory (LASL); LASL is also responsible for the fuel development, system design, and some testing. Battelle's Columbus Laboratory (BCL) developed the plan for aerothermal testing and is performing the aerothermal analysis and developing the helium vent. Oak Ridge National Laboratory (ORNL) is developing the fuel cladding, and Mound producing the primary containment shell (Ir cup). NASA/Ames Research Center (ARC) is performing the reentry testing. The Applied Physics Laboratory (APL) and NUS Corporation are involved in safety studies.(4-9, 4-10, and 4-11)

One GPHS design feature identified that has not been quantitatively evaluated for the nuclear waste disposal mission is the helium vents to relieve He pressure buildup. Apparently the production of He from alpha emitters has not been considered significant in the previously studied high-level waste disposal in space. It may very well be an important consideration for actinide payloads. Battelle's Columbus Laboratories has been developing the He vents for the GPHS.

To meet the projected needs of the various dynamic and static conversion systems and guide the GPHS development, GPHS design requirements have been developed(4-12). The primary static system considered was the Selenide Isotope Generator (SIG) being developed by Teledyne Energy Systems (TES) for the 1983 NASA International Solar-Polar Mission. This mission will be a dual Jupiter swingby by two spacecraft launched simultaneously on the Space Transportation System (Space Shuttle, etc.) to an eliptical polar orbit around the Sun. This mission is also scheduled to be the first use of the GPHS. The dynamic systems that have been considered are: the Brayton Isotope Power System (BIPS) being developed by AiResearch; the Rankine Cycle Turbine Isotope Power System (RIPS) being developed by Sundstrand; a Stirling Cycle Isotope Power System (SIPS) being developed by

General Electric (GE) and Philips Laboratories; and a free piston Stirling engine being developed by Mechanical Technology Incorporated (MTI).

Except for the SIPS, all missions applications and accident conditions considered have assumed space launch. The preliminary accident environments for the GPHS, defined by Reference 4-7, include consideration of blast overpressure, fragments, solid propellent fire, impact, and reentry (including ablation and thermal stress). Of the five mentioned, the first four must be considered as occurring in sequence.(4-12) In the GPHS design, no credit is given to the presence of auxillary equipment for protection. During reentry, no more than one-half the minimum thickness of the reentry member is allowed to ablate.(4-7)

The GPHS is being designed so that any cladding (comparable to the space option container) deformation due to impact is insufficient to breach it. Currently, platinum (Pt-3008) and iridium (Ir) are the leading candidates for the cladding (referred to as clad in GPHS documents). Iridium loses some ductility (embrittles) below about 1000 C and does not deform well without the increased possibility of cracking. This means that if Ir is to be used, one must be concerned not only with holding down the operating and the peak reentry temperatures, but also must design the modules so that the clad temperature is about 1000 C or higher at impact. Pt-3008 does not seem to suffer this impact embrittlement at low temperature but does have a much lower operating and reentry range than Ir.(4-12)

The AVCO fine-weave, pierced fabric (FWPF) 3-D carbon/carbon composite material serves as reentry and impact protection. LASL has been testing the impact of the GPHS AVCO material and cladding to velocities of about 60 m/s at temperatures around 1000 C.(4-13)

The safety goal for the GPHS is to have a safety index for all viable accident conditions of less than 10^{-6} Ci. The safety index is defined as the probability of PuO_2 release times the amount of respirable particles released, measured in Curies.(4-12) This could be the approach that should also be taken for the space option of nuclear waste disposal.

Progress Reports prepared monthly by LASL (from June 1977 through August 1979) for the GPHS program, have also been briefly reviewed.(4-13) Details of the materials testing, design testing, and the other activities of the program are presented. No discussion of these details is given here; the reader is referred to these documents for further information.

As a result of this review of GPHS safety documents appropriate information was supplied to other study activities. It was recommended to NASA/MSFC that the GPHS carbon/carbon AVCO fine-weave, pierced fabric reentry and impact material be used for the reentry vehicle. Also, it was recommended for use as a thermal protection material on the outside of the primary container (see Section 4.3.4). The safety index approach used for the GPHS/RTG should be considered for use in payload response studies for the space option. The concept of sequential safety testing in the GPHS and RTG programs have been applied to the safety requirements for the space option, as provided in

Section 2.5 of this report. It is recommended that for actinide waste payloads (to be considered in the near future), the need for helium vents be evaluated.

4.1.3 Nuclear Waste Disposal in Space Reports (1971-1974)

The safety related work performed prior to 1974 for the nuclear waste disposal in space option was briefly reviewed(4-14 through 4-26) to evaluate any procedures, conceptual designs, or safety requirements that could prove useful or interesting for the current space option studies. The bulk of the work was part of the NASA/Lewis Research Center (LeRC) study activity. Only items that are believed to be of potential interest to the current study of the space disposal option are presented in the following paragraphs.

Three studies(4-14, 4-15, and 4-16) performed, apparently independently of the NASA/LeRC activity, were briefly reviewed. In 1971 The Aerospace Corporation studied a space system for nuclear waste disposal. Interesting safety related aspects of that study were: (1) the removal of ^{90}Sr and ^{137}Cs from the waste mix to reduce heating problems; (2) the use of dedicated space launch facilities for unmanned launches (their concept did not adequately shield the waste); (3) the use of a payload ejection system (from the Space Shuttle Cargo bay--on-orbit, they recommended blowing off the cargo bay doors prior to ejection to help protect the payload's reentry system); and (4) initial disposal flights should be conducted with "fractional sized" payloads to increase safety and confidence in the early phases of a disposal program. The MIT project(4-15) presented a "bullet type" payload, discussed the safety implications of its reentry, and also provided some insights into the selection of a space disposal region. The Boeing study(4-16) presented a spherical waste packaging concept, different than that studied by others. The concept included (1) a 1.2 m diameter waste form, (2) a 2.5 cm lead radiation shield, and (3) a 0.83 m thick flotation material with a density of about 0.15 g/cc. The implication here is that payload flotation, a minimum ballistic coefficient (mass/area--the lower the value the lower the terminal velocity), impact protection, and fragment protection characteristics should perhaps be integrated into one shell.

Four documents related to impact tests of large spheres (conducted at Sandia), prepared by Richard Puthoff, NASA/LeRC, were reviewed.(4-17 through 4-20) The most significant findings were, in a 322 m/s (1055 ft/s) impact into concrete of a 508 kg (1119 lb) simulated reactor core sphere, no leaks or cracks were discovered, the concrete block was totally destroyed, and the sphere was deformed (diameter increase about 21 percent).(4-19) A soil impact test of a 2-foot-diameter mock-up model of a reactor containment vessel system is described in Reference 4-20. The test was conducted at the Aerial Cable Facility, Sandia Laboratories, Albuquerque, New Mexico. The model had a mass of 400 kg (880 pounds). It impacted soil at 367 m/s (810 ft/s) and buried itself into the soil 4.6 m (15 feet--measured to the bottom of the sphere). The following observations were made from the results of this test: (1) no leaks were detected nor were cracks observed on the model; (2) a crater 1.5 m (5 ft) in diameter by 1.5 m (5 ft) deep resulted at impact; (3) containment vessel deformation was not nearly as severe as experienced in

tests conducted on concrete blocks; (4) failure will more likely occur from local penetrations of rocks in the soil; and (5) some local deformations due to rocks in the soil occurred on the containment vessel wall. The maximum depth of these deformations was 0.91 cm (0.36 in), measured by a depth gage from the edge of the indentation.

Westinghouse adapted a multidimensional transient heat transfer analysis computer program (ESATA - Executive Subroutines for Afterheat Temperature Analysis) to analyze the temperature and pressure response of a radioactive nuclear waste disposal container following impact on the Earth for NASA/LeRC.(4-23) The ESATA program included consideration of component melting, LiH dissociation (part of neutron shield in Lewis concept), the transport property variation, pressure response and container creep stress buildup. This program was tailored to analyze both undeformed and deformed waste disposal containers with varying degrees of ground burial. The actinide waste disposal container design that was considered consisted of concentric spherical layers of tungsten shielding, LiH shielding and a stainless steel container. Twenty-one cases were analyzed for postimpact periods of up to 23 days. Variations were considered in: the nuclear waste material power level, ranging from 1.5 to 30 kW; radii of materials; degree of deformation; degree of burial; and soil properties. Constant power levels were assumed during the transient and the initial internal pressure 17.2 N/cm^2 (25 psi) was based on helium release from alpha emitters. Initial temperatures reflected the heat generation during reentry. No provision for venting was allowed. Typical results of these analyses included: (1) the integrity of the waste containers was maintained for the partial burial of both undeformed and deformed containers during the transit; (2) complete burial of waste containers with more than 5 kW of radioactive waste material resulted in creep stress rupture failures occurring 4 to 12 days after impact; (3) at the time of rupture, container temperatures were in the range of 1120 to 1170 C (2500 to 2600 R) and the internal pressure was about 80 N/cm^2 (130 psi); (4) hydrogen release from LiH dissociation was the primary cause of the pressure increase; and (5) the resultant temperature response of the container was sensitive to soil properties but not depth of burial, other than partial burial.

Physics International Company performed two fragment studies: one analytical, one experimental.(4-24 and 4-25) To simulate high velocity fragments from propellant tank explosions, aluminum rods, 2-inches, 4-inches, and 6-inches long, all with a 0.315-inch diameter, were impacted into a simulated containment vessel at 1500 m/s. The velocity at which penetration occurred for the 1.59 cm (5/8 in) thick stainless steel sphere was on the order of 1350 m/s (4400 ft/s) for the 4-and 6-inch aluminum rods. It was 1585 m/s (5200 ft/s) for the 2-inch rods. The impact vulnerability of a nuclear waste containment vessel was studied using the PISCES 2DL computer code developed by Physics International Company.(4-24) The calculations included: (1) a verification calculation of a 2-ft-diam hollow sphere impacted by a steel block at 122 m/s (400 ft/s); (2) impact studies of a containment configuration against both hard and soft surfaces at velocities from 119 m/s (392 ft/s) to 322 m/s (1055 ft/s); and (3) rocket casing debris impacts into a containment configuration at 1500 m/s (5000 ft/s). With one possible exception, the results showed that the integrity of the Lewis nuclear waste containment vessel was good. The possible exception is the impact into a

notched concrete-steel block at 322 m/s (1055 ft/s). This condition caused the most severe damage to the vessel; a more detailed analysis is still required. In general, the analytical results of the projectile impact prediction showed that light, high-speed projectiles pose no threat to the containment vessel, but larger, slower, and stronger projectiles may cause appreciable damage. They concluded that the effects of impact by these types of projectiles should be studied further.

The work of the NASA/Lewis Research Center was formally documented in BNWL 1900; Volume 4 by A. M. Platt and K.J. Schneider.(4-26) Some of the noteworthy findings in this document have been employed in the current study and some others should be investigated further in the space option study. The document includes some things of interest to the current study: (1) recommended the removal of ^{244}Cm to reduce the heat load in the payload; (2) noted that depleted uranium may not be satisfactory at high temperature--they "baselined" tungsten for the gamma shield; and (3) considered neutron-absorbing materials (poisons) for their "baseline" actinide waste mix to reduce the problem of criticality. The current space option safety requirements (see Sections 2.5 and 3.3) have considered the "safety criteria" that were developed by T. Dobry (DOE), et al., and documented in Reference 4-26.

In summary, various works resulting from the LeRC study of nuclear waste disposal in space are considered valuable in the current study. It is recommended that, prior to any new work in related areas, critical in-depth reviews be conducted of past works to establish what results and computer codes (especially the Westinghouse ESATA and Physics International PISCES 2DL codes) are appropriate for future efforts. The conclusion that the larger and slower fragments (shrapnel) pose a greater potential for payload damage than the smaller high-speed fragments (see Reference 4-24) coupled with the results of Section 4.2.4 imply that more work is needed. It is recommended that experimental work be conducted to determine the fragment velocity and size distributions for exploding propellant tanks. The Rocket Propulsion Laboratory located at Edwards AFB represents an ideal location for such experiments.

4.1.4 Accident Environment Definition and Payload Response Reports

Many documents pertaining to accident environment definition and payload response were obtained(4-27 through 4-68), and were used to develop the material in Sections 4.2, 4.3, 4.4 and 7.5 of this report. The nature of the detailed material does not warrant discussion in this section; the reader should refer to the other sections of this report for related discussions.

4.2 Accident Environment Definition

The System Safety Design Requirements for the reference space disposal concept (see Section 2.5), that have been developed as a part of this study, call for the survivability of the nuclear waste payload in low-probability launch pad accidents. Before the survivability (payload response) can be assessed, the worst-case credible accident environments must be defined. Although not done in this study, it is recommended that future efforts establish probability distribution for accident environments such that total risk estimates are realistic. This section describes the first analysis of the major accident environments for the Uprated Space Shuttle[4-69] and the heavy lift launch vehicle (HLLV) [4-70]. Much of the accident environment data generated here are applied to: the preliminary accident response analysis (see Section 4.3); the HLLV safety assessment (see Section 4.4); and the System Safety Design Requirements contained in the Concept Definition Document for Nuclear Waste Disposal in Space (also see Section 2.5). The accident environments predicted in this section are associated with events that relate to on- or near-pad catastrophic launch vehicle failures. The categories of environments analyzed are:

- Liquid Propellant Fireball
- Liquid Propellant Residual Fire
- Blast Wave Overpressure
- Fragment or Shrapnel

The RV response to the Uprated Space Shuttle fireball, and residual fire and the atmospheric reentry of the RV and the primary container have been analyzed and are discussed in Section 4.3. Because of the limited scope of this study payload response to blast overpressure, fragment impact, and payload ground surface and ocean impact were not conducted. Future studies should analyze these events.

4.2.1 Liquid Propellant Fireball Environment

Should the fully loaded, liquid hydrogen/liquid oxygen/RP-1, Uprated Space Shuttle or HLLV explode on the launch pad, the nuclear waste payload could be exposed to a severe short-term thermal environment. This section describes the basic model used and the results of calculations dealing with this thermal environment for the Uprated Space Shuttle and HLLV. The basic fireball model is that of Bader.[4-27] The results presented provide estimates of fireball temperature and radiant heat flux as a function of time after the explosion.

4.2.1.1 Fireball Model and Assumptions

The Liquid-Propellant Rocket Abort Fire Model, developed by Bader[4-27] was used to calculate the thermal environment of the fireball

resulting from an on-pad booster vehicle explosion. The general assumptions of the model used here are as follows:

- The rate of liquid propellant addition to the fireball is constant.
- Air entrainment into the fireball has been modeled, but is currently ignored, providing the worst case condition. Its inclusion would lead to lower temperatures and radiant heat fluxes.
- Complete burnup of the liquid propellants is assumed, thus providing a worst case condition.
- The fireball is an isothermal, homogeneous body which is spherical at all times. The isothermal, homogenous characteristic is based on the high degree of turbulence existing during the fireball formation.
- The fireball radiates as a blackbody with an emissivity of 1.0.
- The time until the fireball lifts off the ground and the time when all the liquid propellant is consumed are identical.
- Chemical equilibrium exists within the fireball.

Figure 4-2 is a schematic defining the assumed fireball features and fireball development with time. The explosion begins at time t = 0. All propellant is assumed to be consumed by $t = t_{liftoff}$. The features of the modeled fireball stem and possible residual fire are also shown.

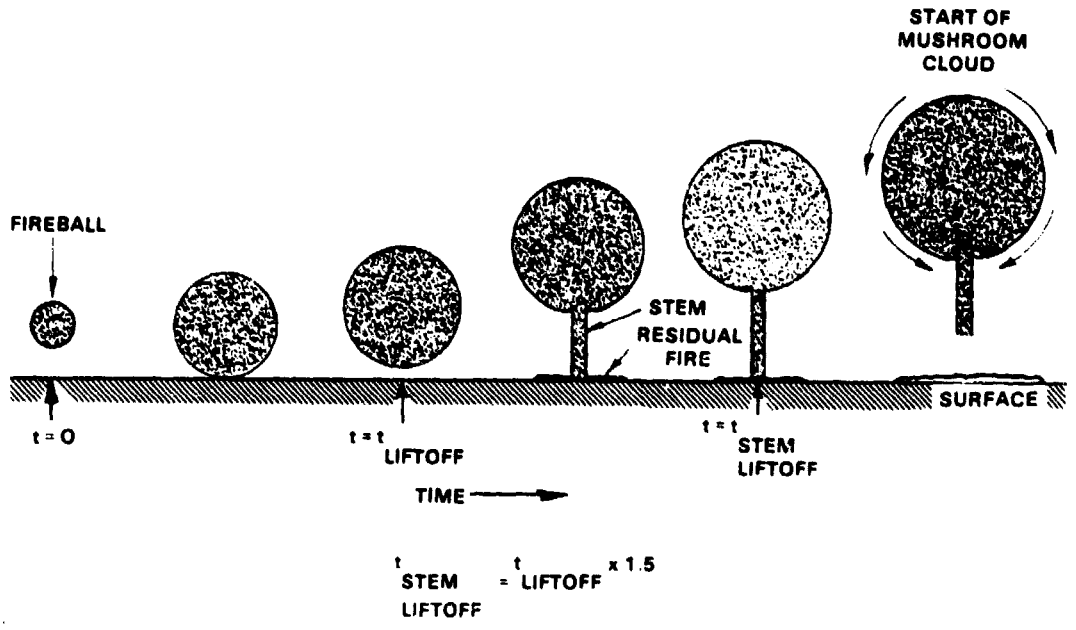

FIGURE 4-2. MODELED FIREBALL DEVELOPMENT

4.2.1.2 Thermochemical Analysis

The thermochemical analysis described in the Phase II Final Technical Report[4-71] for hydrogen and oxygen was modified to include RP-1 (assumed Uprated Space Shuttle and HLLV booster fuel) and nitrogen (added for air entrainment). For the combustion of hydrogen and hydrocarbons in air, the ten species that need to be considered are; H_2O, H_2, O_2, OH, O, H, CO_2, CO, NO, N_2. The chemical reactions are assumed to occur at constant pressure (free volume combustion). Ten species partial pressures and an equilibrium temperature are the unknowns. Therefore, eleven equations are needed to solve for eleven unknowns. Relationships involving mass, energy and state conditions provide the basis for the calculation.

Three elemental mole ratios (A, B, and C) and the relationship for the sum of partial pressures (assumed equal to 1 atmosphere) for the H/O/C/N thermodynamic system are defined as follows:

$$A = \frac{n^g_O}{n^g_H} = \frac{P_{H_2O} + 2P_{O_2} + P_{OH} + P_O + 2P_{CO_2} + P_{CO} + P_{NO}}{2P_{H_2O} + 2P_{H_2} + P_{OH} + P_H} \qquad (1)$$

$$B = \frac{n^g_C}{n^g_H} = \frac{P_{CO_2} + P_{CO}}{2P_{H_2O} + 2P_{H_2} + P_{OH} + P_H} \quad (2)$$

$$C = \frac{n^g_N}{n^g_H} = \frac{P_{NO} + 2P_{N_2}}{2P_{H_2O} + 2P_{H_2} + P_{OH} + P_H} \quad (3)$$

$$1 = P_{H_2O} + P_{H_2} + P_{O_2} + P_{OH} + P_O + P_H + P_{CO_2} + P_{CO} + P_{NO} + P_{N_2} \quad (4)$$

Six more relationships relating temperature (equilibrium constants) and partial pressures, given the equilibrium chemical condition, can be written as follows:

$$H_2 + 1/2O_2 \rightleftharpoons H_2O \qquad K_p(T)^{H_2O} = \frac{P_{H_2O}}{P_{H_2} P_{O_2}^{1/2}} \quad (5)$$

$$2H \rightleftharpoons H_2 \qquad K_p(T)^{H_2} = \frac{P_{H_2}}{P_H^2} \quad (6)$$

$$2O \rightleftharpoons O_2 \qquad K_p(T)^{O_2} = \frac{P_{O_2}}{P_O^2} \quad (7)$$

$$H + O \rightleftharpoons OH \qquad K_p(T)^{OH} = \frac{P_{OH}}{P_O P_H} \quad (8)$$

$$CO + 1/2O_2 \rightleftharpoons CO_2 \qquad K_p(T)^{CO_2} = \frac{P_{CO_2}}{P_{O_2}^{1/2} P_{CO}} \quad (9)$$

$$1/2N_2 + 1/2O_2 \rightleftharpoons NO \qquad K_p(T)^{NO} = \frac{P_{NO}}{P_{N_2}^{1/2} P_{O_2}^{1/2}} \quad (10)$$

Finally, the heat of reactants must equal the heat of products to satisfy the equilibrium requirements; thus, we can write:

$$0 = h_{reactants} - h_{products} \qquad (11)$$

The solution to the above set of eleven equations and eleven unknowns is obtained by the following procedure. For a given value of T and P_{O_2}, the value of P_{H_2} can be calculated by employing data in Table 4-3 which determines the equilibrium constants. Once values of P_{H_2} and P_{O_2} have been determined, the partial pressures of the eight other species can be calculated by using Equations 5 through 10. This calculation is performed for various values of P_{O_2} until Equation 4 is satisfied. Once this is accomplished, then the heat of products can be calculated for the given value of T. A computer program was developed with BCL resources to accomplish this tedious procedure. Table 4-4 presents the important input parameters to the model, for the Space Shuttle, the Uprated Space Shuttle, and the HLLV. Data for the Space Shuttle were taken from Reference 4-71. Data for the Uprated Space Shuttle and HLLV were derived from References 4-69 and 4-70. Heats of reactants, as shown in the Table 4-4, were calculated using data in Reference 4-73. Figures 4-3, 4-4, and 4-5 provide the results of these calculations for each of the three vehicles. The fireball equilibrium temperatures for the three vehicles are then determined from Equation 11, resulting in:

Vehicle	Fireball Equilibrium Temperature, K
Space Shuttle	2991
Uprated Space Shuttle	3057
HLLV	3058

TABLE 4-3. EQUILIBRIUM CONSTANT DATA FOR HYDROGEN/OXYGEN/CARBON/ NITROGEN THERMODYNAMIC SYSTEM

T,K	$Log_{10}K_p^{H2}$	$Log_{10}K_p^{H2O}$	$Log_{10}K_p^{O2}$	$Log_{10}K_p^{OH}$	$Log_{10}K_p^{CO2}$	$Log_{10}K_p^{NO}$
2000	5.5810	3.5405	6.3554	5.7389	2.8819	-1.7017
2100	5.0162	3.2277	5.7202	5.1744	2.5366	-1.5891
2200	4.5021	2.9428	5.1423	4.6696	2.2233	-1.4868
2300	4.0317	2.6830	4.6143	4.2079	1.9378	-1.3933
2400	3.6004	2.4441	4.1300	3.7842	1.6766	-1.3078
2500	3.2027	2.2246	3.6842	3.3939	1.4367	-1.2291
2600	2.8354	2.0217	3.2725	3.0331	1.2157	-1.1565
2700	2.4946	1.8341	2.8910	2.6986	1.0115	-1.0893
2800	2.1781	1.6594	2.5367	2.3876	0.8221	-1.0270
2900	1.8830	1.4969	2.2066	2.0978	0.6462	-0.9690
3000	1.6069	1.3455	1.8984	1.8269	0.4823	-0.9150
3100	1.3488	1.2033	1.6100	1.5733	0.3293	-0.8645
3200	1.1066	1.0701	1.3395	1.3352	0.1861	-0.8172
3300	0.8787	0.9451	1.0853	1.1113	0.0518	-0.7728

Source: Reference 4-72.

Tables 4-5, 4-6 and 4-7 provide the heat of products data and species compositions as a function of temperature for the three cases anaylzed here.

TABLE 4-4. EQUILIBRIUM MODEL INPUT PARAMETERS

Parameters	Space Shuttle	Uprated Space Shuttle	Heavy Lift Launch Vehicle
Hydrogen, kg	102,500	102,500	341,000
Oxygen, kg	609,600	1,413,034	4,812,105
RP-1(a), kg	--	277,046	987,895
A	0.3747	0.8685	0.8890
B	0.0000	0.1942	0.2082
C	0.0000	0.0000	0.0000
$h_{reactants}$, kcal/kg	213	194	194

Note: (a) RP-1 assumed to be $C_{12}H_{24}$.

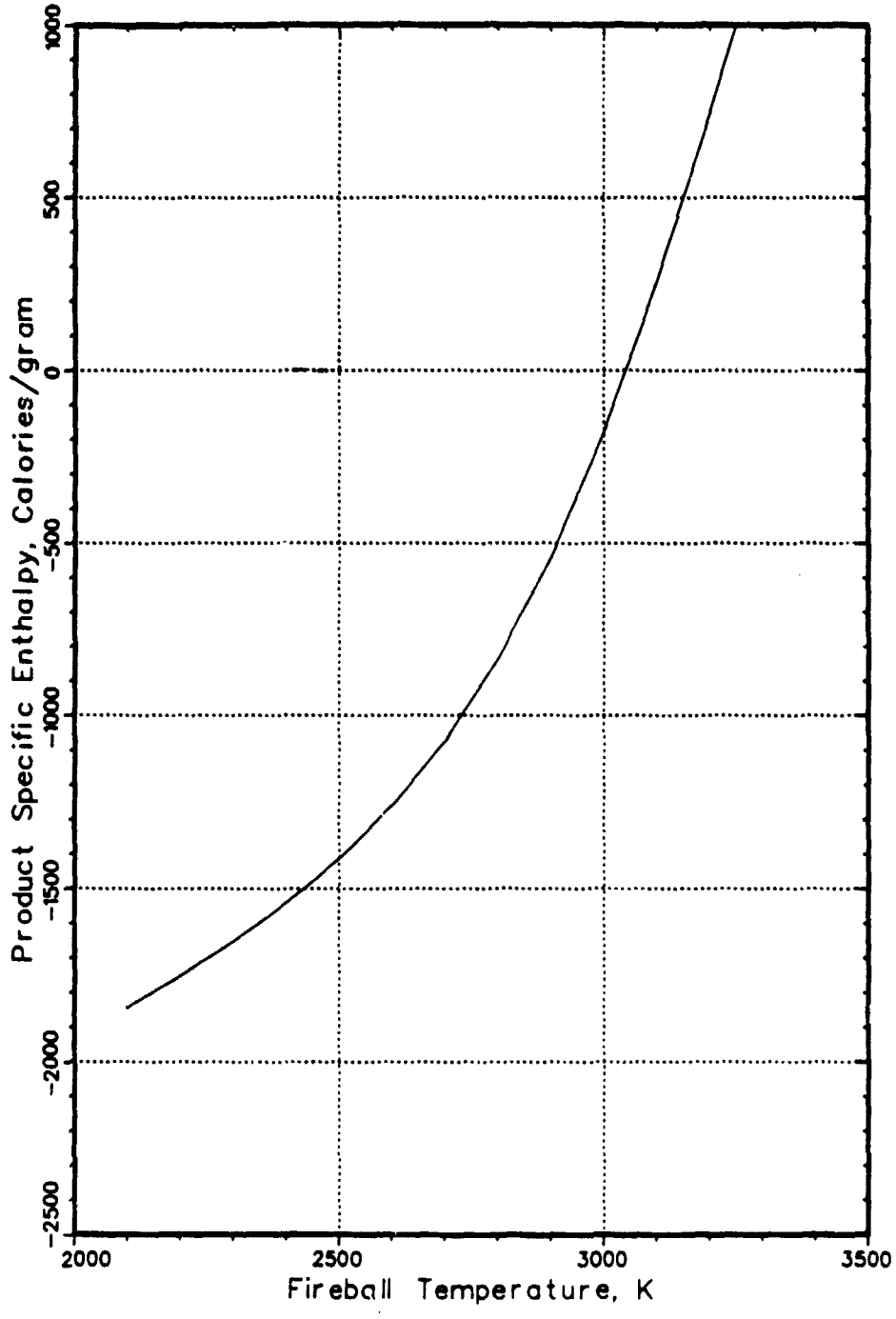

FIGURE 4-3. HYDROGEN/OXYGEN FIREBALL ENTHALPY AS A FUNCTION OF TEMPERATURE FOR SPACE SHUTTLE

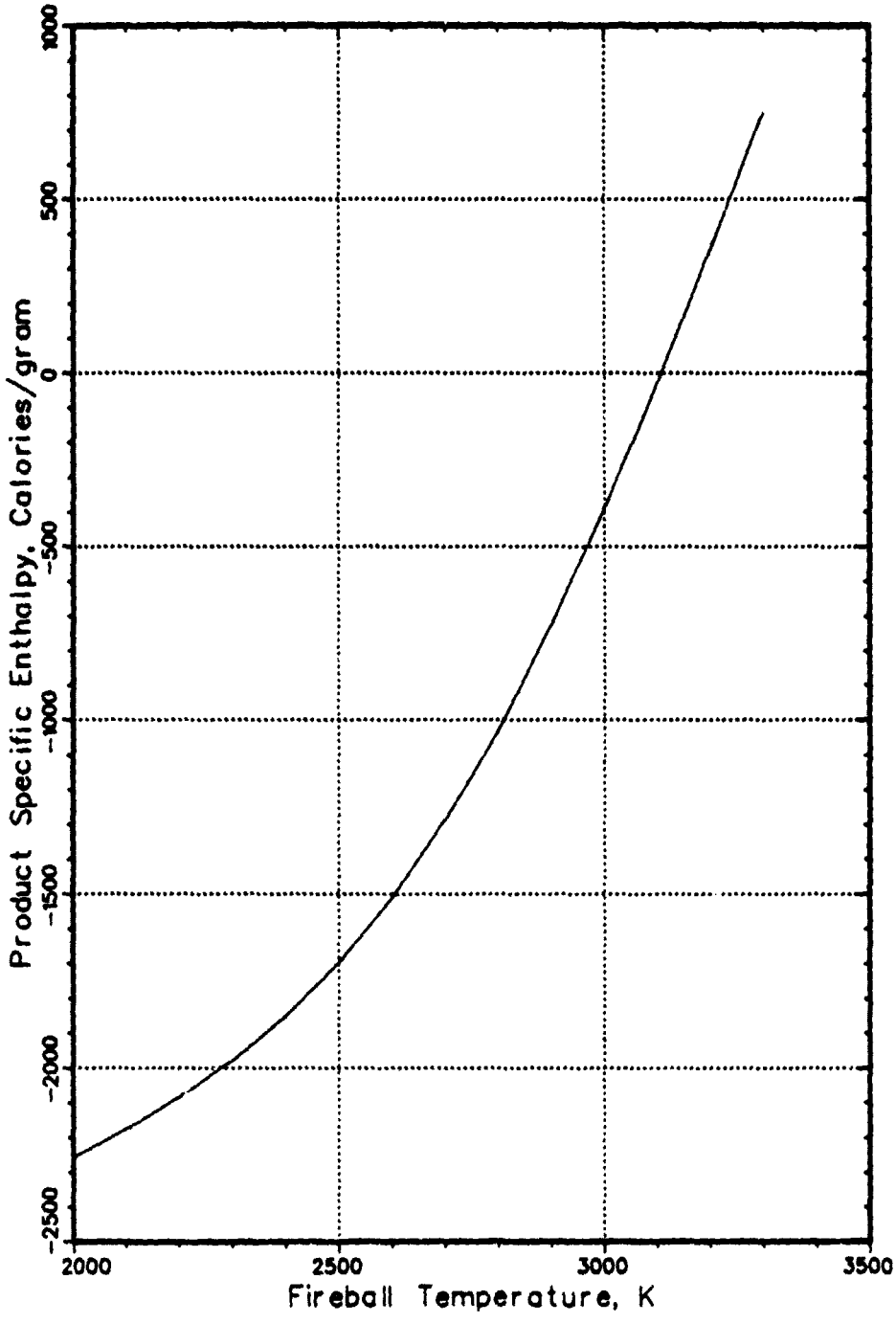

FIGURE 4-4. HYDROGEN/OXYGEN/RP-1 FIREBALL ENTHALPY AS A FUNCTION OF TEMPERATURE FOR UPRATED SPACE SHUTTLE

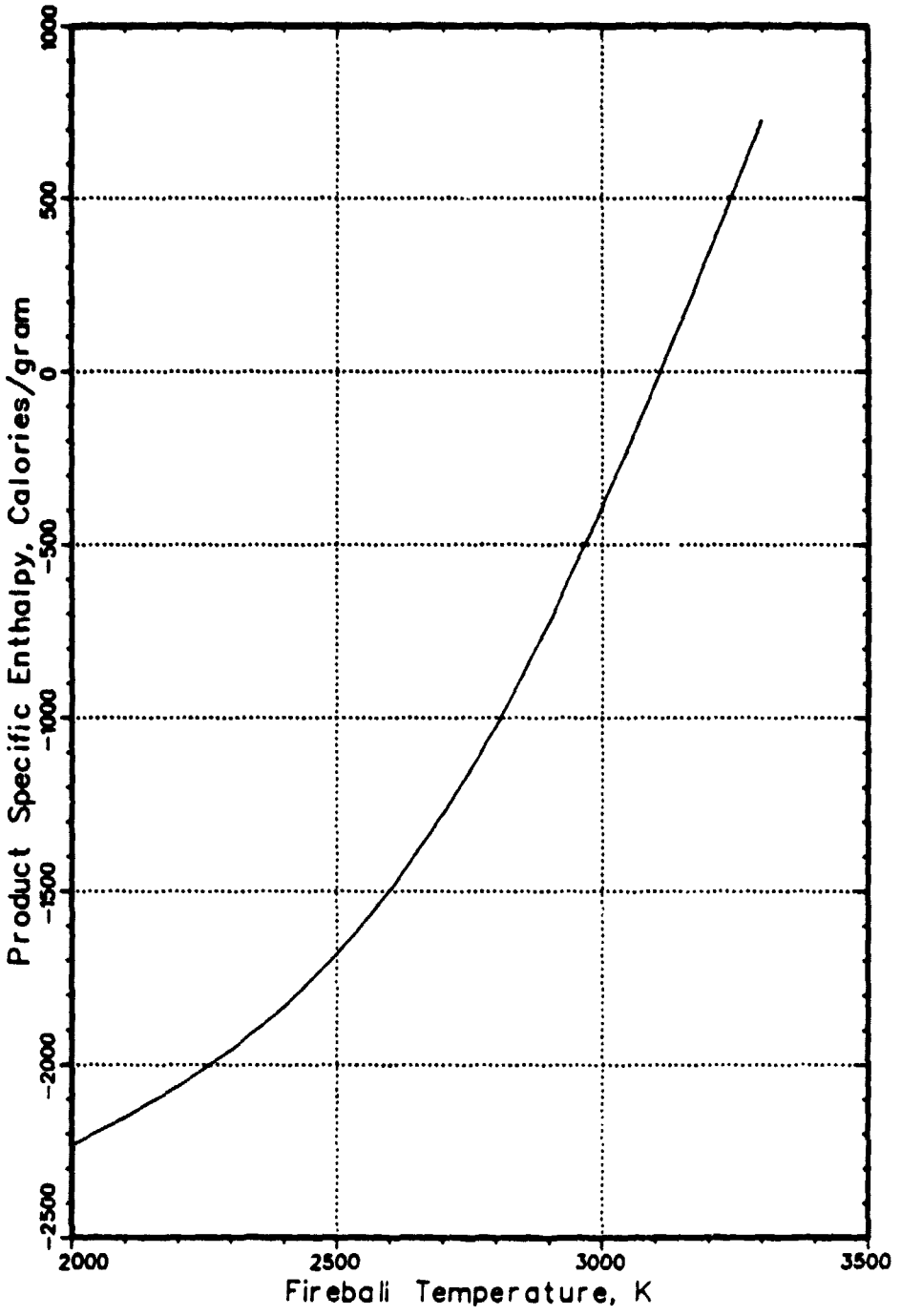

FIGURE 4-5. HYDROGEN/OXYGEN/RP-1 FIREBALL ENTHALPY AS A FUNCTION OF TEMPERATURE FOR HEAVY LIFT LAUNCH VEHICLE

TABLE 4-5. HEAT OF PRODUCTS AND COMPOSITION DATA AS A FUNCTION OF TEMPERATURE FOR SPACE SHUTTLE HYDROGEN/OXYGEN FIREBALL

T, K	h_p, cal/g*	P_O	P_H	P_{OH}	P_{O_2}	P_{H_2}	P_{H_2O}
		Atmospheres					
2100	-1844	2.45 E-6	1.55 E-3	5.67 E-4	3.14 E-6	2.50 E-1	7.48 E-1
2200	-1752	9.17 E-6	2.80 E-3	1.20 E-3	1.17 E-5	2.49 E-1	7.47 E-1
2300	-1553	3.06 E-5	4.81 E-3	2.38 E-3	3.86 E-5	2.49 E-1	7.44 E-1
2400	-1342	9.25 E-5	7.83 E-3	4.14 E-3	1.16 E-4	2.48 E-1	7.40 E-1
2500	-1414	2.55 E-4	1.24 E-2	7.45 E-3	3.14 E-4	2.46 E-1	7.33 E-1
2600	-1261	6.46 E-4	1.89 E-2	1.32 E-2	7.80 E-4	2.46 E-1	7.21 E-1
2700	-1073	1.51 E-3	2.80 E-2	2.11 E-2	1.76 E-3	2.45 E-1	7.03 E-1
2800	-834.5	3.24 E-3	4.04 E-2	3.19 E-2	3.61 E-3	2.46 E-1	6.75 E-1
2900	-540.6	6.42 E-3	5.70 E-2	4.59 E-2	6.63 E-3	2.49 E-1	6.36 E-1
3000	-178.0	1.17 E-2	7.90 E-2	6.22 E-2	1.09 E-2	2.52 E-1	5.84 E-1
3100	251.9	1.99 E-2	1.07 E-1	7.99 E-2	1.61 E-2	2.57 E-1	5.20 E-1
3200	739.6	3.15 E-2	1.42 E-1	9.70 E-2	2.16 E-2	2.59 E-1	4.48 E-1

*Note: Based upon reactant average molecular weight of 14.006 g.

TABLE 4-6. HEAT OF PRODUCTS AND COMPOSITION DATA AS A FUNCTION OF TEMPERATURE FOR UPRATED SPACE SHUTTLE HYDROGEN/OXYGEN/RP-1 FIREBALL

T, K	h_p, cal/g*	P_O	P_H	P_{OH}	P_{O_2}	P_{H_2}	P_{H_2O}	P_{CO_2}	P_{CO}
		Atmospheres							
2000	-2258	2.21 E-4	3.30 E-5	4.50 E-3	1.10 E-1	5.51 E-4	6.36 E-1	2.47 E-1	9.77 E-4
2100	-2176	4.57 E-4	1.04 E-4	7.13 E-3	1.10 E-1	1.13 E-3	6.33 E-1	2.46 E-1	2.16 E-3
2200	-2084	8.86 E-4	2.67 E-4	1.08 E-2	1.09 E-1	2.17 E-3	6.29 E-1	2.43 E-1	4.40 E-3
2300	-1977	1.62 E-3	6.05 E-4	1.58 E-2	1.08 E-1	3.93 E-3	6.23 E-1	2.39 E-1	8.37 E-3
2400	-1851	2.82 E-3	1.30 E-3	2.23 E-2	1.07 E-1	6.75 E-3	6.14 E-1	2.31 E-1	1.49 E-2
2500	-1698	4.68 E-3	2.63 E-3	3.05 E-2	1.06 E-1	1.10 E-2	6.01 E-1	2.20 E-1	2.47 E-2
2600	-1512	7.47 E-3	5.01 E-3	4.04 E-2	1.04 E-1	1.72 E-2	5.83 E-1	2.04 E-1	3.84 E-2
2700	-1288	1.15 E-2	9.04 E-3	5.20 E-2	1.03 E-1	2.56 E-2	5.60 E-1	1.84 E-1	5.56 E-2
2800	-1034	1.72 E-2	1.55 E-2	6.52 E-2	1.02 E-1	3.63 E-2	5.29 E-1	1.60 E-1	7.55 E-2
2900	-725.6	2.49 E-2	2.54 E-2	7.94 E-2	9.99 E-2	4.95 E-2	4.91 E-1	1.34 E-1	9.59 E-2
3000	-391.6	3.51 E-2	3.99 E-2	9.40 E-2	9.73 E-2	6.44 E-2	4.45 E-1	1.09 E-1	1.15 E-1
3100	-28.86	4.79 E-2	6.01 E-2	1.08 E-1	9.35 E-2	8.05 E-2	3.93 E-1	8.56 E-2	1.31 E-1
3200	355.9	6.35 E-2	8.69 E-2	1.19 E-1	8.81 E-2	9.66 E-2	3.37 E-1	6.53 E-2	1.43 E-1
3300	751.8	8.14 E-2	1.21 E-1	1.28 E-1	8.06 E-2	1.11 E-1	2.78 E-1	4.84 E-2	1.51 E-1

*Note: Based upon reactant average molecular weight of 18.547 g.

TABLE 4-7. HEAT OF PRODUCTS AND COMPOSITION DATA AS A FUNCTION OF TEMPERATURE FOR HLLV HYDROGEN/OXYGEN/RP-1 FIREBALL

T, K	h_p, cal/g*	P_O	P_H	P_{OH}	P_{O_2}	P_{H_2}	P_{H_2O}	P_{CO_2}	P_{CO}
		Atmospheres							
2000	-2234	2.22 E-4	3.75 E-5	4.47 E-3	1.12 E-1	5.35 E-4	6.72 E-1	2.59 E-1	1.12 E-3
2100	-2153	4.61 E-4	1.03 E-4	7.03 E-3	1.11 E-1	1.10 E-3	6.70 E-1	2.58 E-1	2.04 E-3
2200	-2063	8.93 E-4	2.58 E-4	1.09 E-2	1.11 E-1	2.11 E-3	6.66 E-1	2.55 E-1	4.09 E-3
2300	-1953	1.63 E-3	5.96 E-4	1.57 E-2	1.10 E-1	3.82 E-3	6.60 E-1	2.51 E-1	8.72 E-3
2400	-1804	2.83 E-3	1.28 E-3	2.21 E-2	1.09 E-1	6.56 E-3	6.01 E-1	2.42 E-1	1.55 E-2
2500	-1682	4.71 E-3	2.59 E-3	3.02 E-2	1.07 E-1	1.07 E-2	5.88 E-1	2.30 E-1	2.07 E-2
2600	-1479	7.52 E-3	4.94 E-3	4.01 E-2	1.06 E-1	1.67 E-2	5.71 E-1	2.14 E-1	4.00 E-2
2700	-1274	1.16 E-2	8.92 E-3	5.16 E-2	1.04 E-1	2.48 E-2	5.48 E-1	1.93 E-1	5.01 E-2
2800	-1027	1.73 E-2	1.53 E-2	6.49 E-2	1.03 E-1	3.54 E-2	5.18 E-1	1.68 E-1	7.09 E-2
2900	-722.3	2.50 E-2	2.51 E-2	7.87 E-2	1.01 E-1	4.82 E-2	4.80 E-1	1.41 E-1	1.00 E-1
3000	-393.4	3.52 E-2	3.94 E-2	9.31 E-2	9.81 E-2	6.23 E-2	4.36 E-1	1.15 E-1	1.21 E-1
3100	-36.03	4.80 E-2	5.94 E-2	1.07 E-1	9.40 E-2	7.87 E-2	3.85 E-1	9.01 E-2	1.38 E-1
3200	339.6	6.35 E-2	8.60 E-2	1.18 E-1	8.81 E-2	9.46 E-2	3.30 E-1	6.87 E-2	1.51 E-1
3300	727.7	8.12 E-2	1.20 E-1	1.26 E-1	8.03 E-2	1.09 E-1	2.73 E-1	5.09 E-2	1.59 E-1

*Note: Based upon reactant average molecular weight of 18.8/15 g.

4.2.1.3 Calculations Employing Bader Model

As indicated in Reference 4-27, the temperature relationship with time needs to be determined for two time periods:

(1) $0 < t \leq t_{\text{fireball liftoff}}$,
(2) $t_{\text{fireball liftoff}} < t \leq t_{\text{stem liftoff}}$.

While heat is still being added to the fireball ($0 < t \leq t_{\text{fireball liftoff}}$), the change in internal enthalpy is equal to the rate change of chemical heat energy, less radiation losses (see Equation 12). After all the fuel is consumed, the change in internal enthalpy is due to radiation losses only (see Equation 13).

$$R \cdot h_r - \varepsilon\sigma A T^4 = \frac{d(Wh_p)}{dt} \tag{12}$$

$$-\varepsilon\sigma A T^4 = (W = Wb)\,\frac{(dh_p)}{dt} \tag{13}$$

where:

- R = Constant rate of fuel addition
- ε = Emissivity
- σ = Stephen-Boltzman Constant
- A = Surface Area of Fireball
- T = Temperature
- W = Weight of Fireball (W_b = Total Weight of Liquid Propellants)
- t = Time
- h_r = Enthalpy/Unit Mass of Reactants
- h_p = Enthalpy/Unit Mass of Products

Appendix H provides a more in-depth discussion of the model used here. From Appendix H, the following equations for dT/dt were developed:

$$\frac{dT}{dt} = \left[h_r - h_p - \frac{\varepsilon\sigma 4\pi}{R}\left(\frac{3R\mathcal{R}}{4\pi P}\right)^{2/3} t^{2/3}\, T^{14/3}\right]\left[\frac{1}{t}\right]\left[\frac{1}{\frac{dh}{dT}}\right] \tag{14}$$

$$\frac{dT}{dt} = \left[-\frac{\varepsilon\sigma 4\pi}{W_b}\left(\frac{2R\mathcal{R}}{4\pi P}\right)^{2/3}\right]\left[T^{14/3}\right]\left[t\right]\left[\frac{1}{\frac{dh}{dT}}\right] \tag{15}$$

where:

- $\mathcal{R}$ = Gas Constant
- P = Pressure

The BCL computer code, previously mentioned, was used to integrate these equations by employing the 4th order Runge-Kutta-Gill Method. The resulting relationships between temperature and time, as well as heat flux and time, are provided in Figures 4-6, 4-7, and 4-8, respectively. These figures indicate that the extreme thermal environment is expected to last less than 15 seconds for all three vehicles. During actual conditions, air entrainment would be expected to lower the temperature and heat flux values. A residual fire is assumed to occur and this is discussed in the next section.

The predicted fireball diameters are a function of time, as given in Figure 4-9. The maximum predicted fireball diameters for the three vehicles agree fairly well with experimental data, as represented by relationships given in Reference 4-32. See Appendix H for further details.

4.2.2 Liquid Propellant Residual Fire Environment

Residual fires that may occur after catastrophic launch vehicle failures can be categorized into three major types: (1) burning liquid propellent fuel; (2) burning solid propellent; and (3) burning materials or pad related systems. The solid propellent fire was analyzed in last year's study[4-71] for the standard Space Shuttle vehicle. The third type is currently beyond the scope of this study and is expected not to be as important as the first two. The liquid propellent residual fire is a focus of this year's study effort.

4.2.2.1 Residual Fire Model and Assumptions

Liquid propellent residual fires have been observed with the catastrophic failures of Atlas launch vehicles (which utilize RP-1 as a fuel).[4-27] Reference 4-32 indicates that residual fires are mostly expected to occur when high-boiling-point liquid fuels are present (e.g., RP-1). Also, Reference 4-32 indicates that residual fires involving RP-1 for the Atlas have been observed to last up to or exceeding one hour. Modeling residual fires for the vehicles considered here (Uprated Space Shuttle and HLLV), which employ RP-1 as a fuel, can be a very difficult and complex task. Four major questions need to be addressed:

(1) How does one predict how much RP-1 is consumed in the initial fireball and how much becomes available for the residual fire?

(2) What is the limit on the spread or thickness of the RP-1 fuel pool on the ground?

(3) What is the burning rate of the RP-1 pool?

(4) What is the radiant heat flux that an object (payload) could see if it were in or near the residual fire?

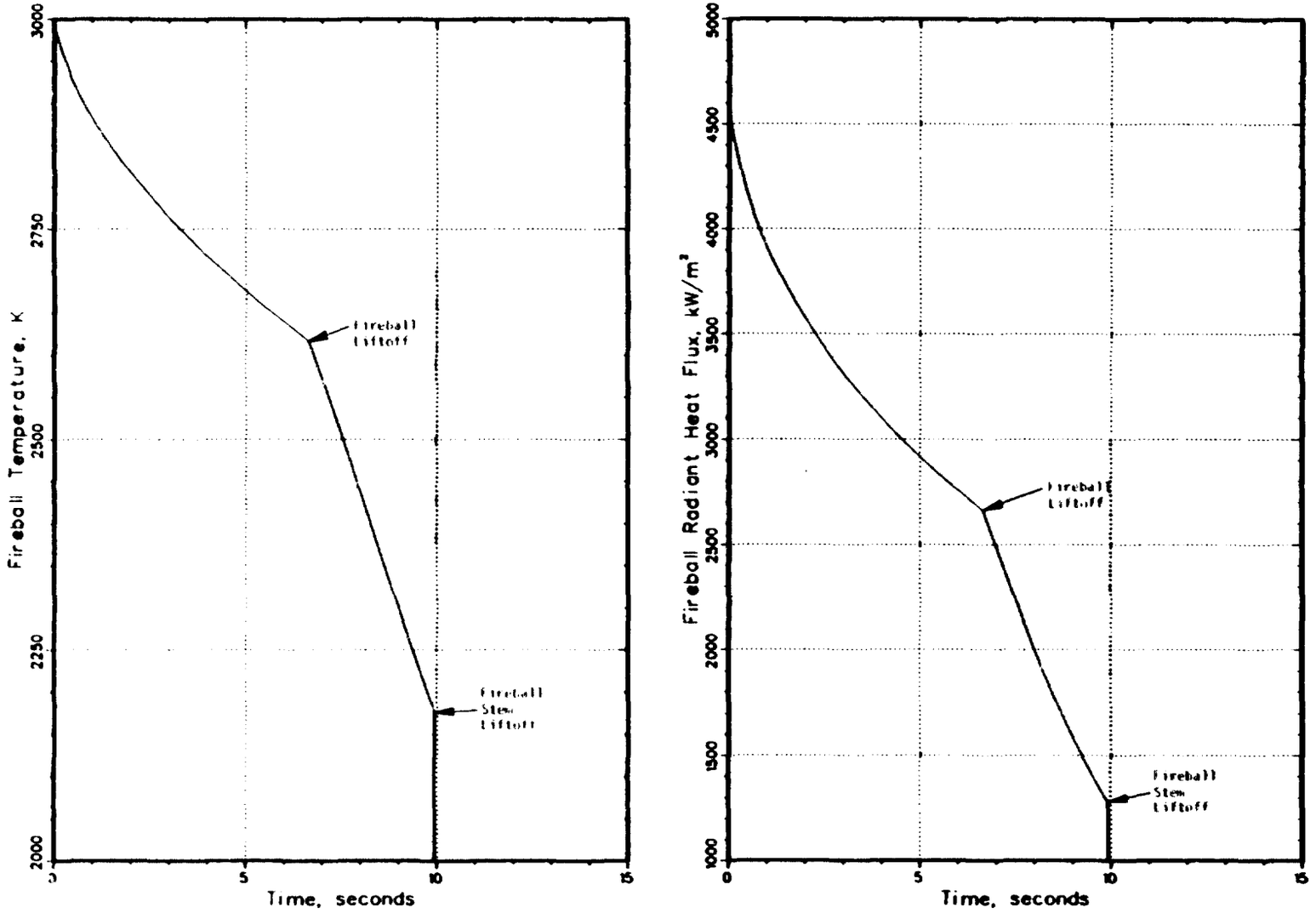

FIGURE 4-6. TEMPERATURE AND RADIANT HEAT FLUX AS A FUNCTION OF TIME FOR THE SPACE SHUTTLE HYDROGEN/OXYGEN FIREBALL ENVIRONMENT

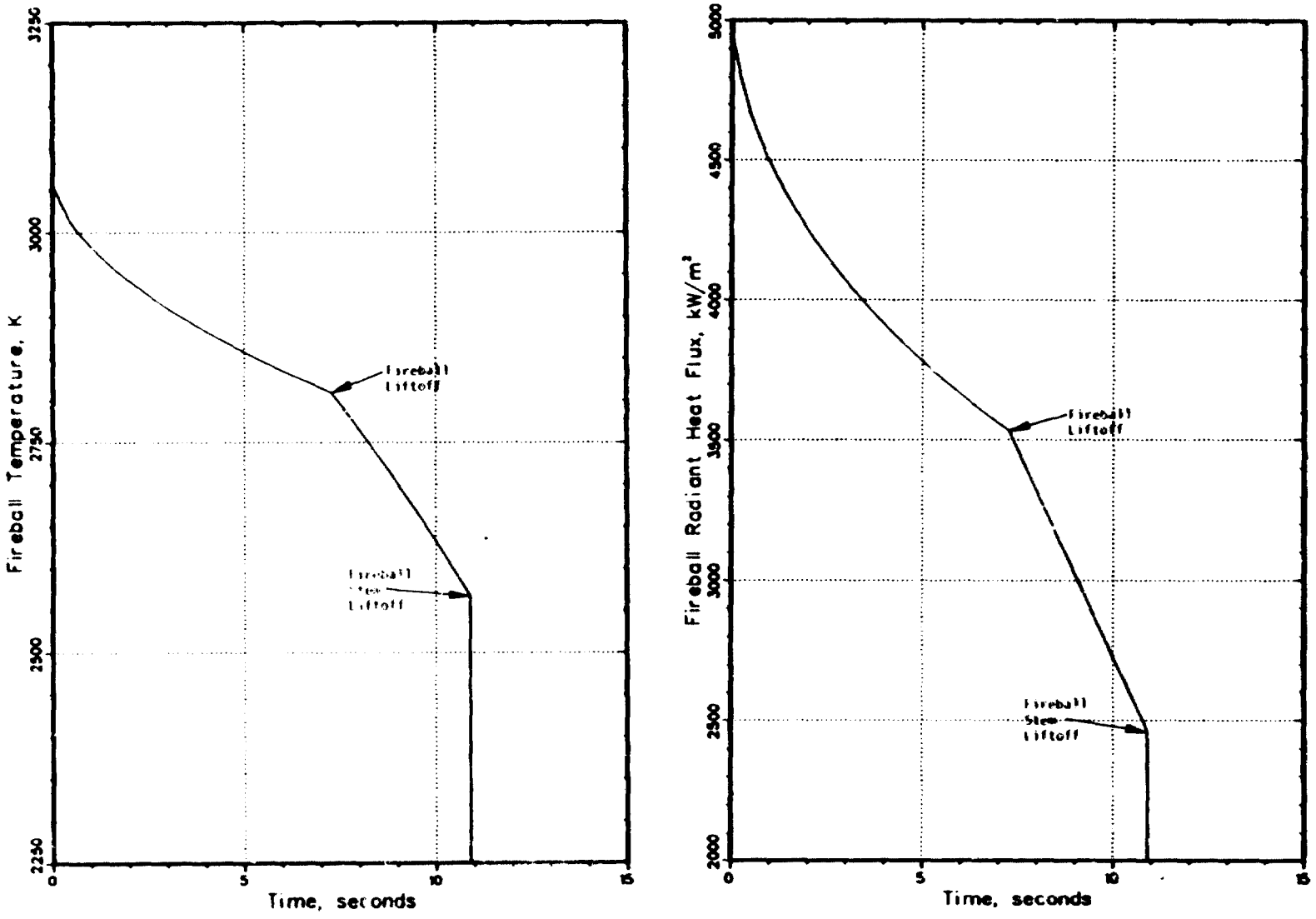

FIGURE 4-7. TEMPERATURE AND RADIANT HEAT FLUX AS A FUNCTION OF TIME FOR UPRATED SPACE SHUTTLE HYDROGEN/OXYGEN/RP-1 FIREBALL ENVIRONMENT

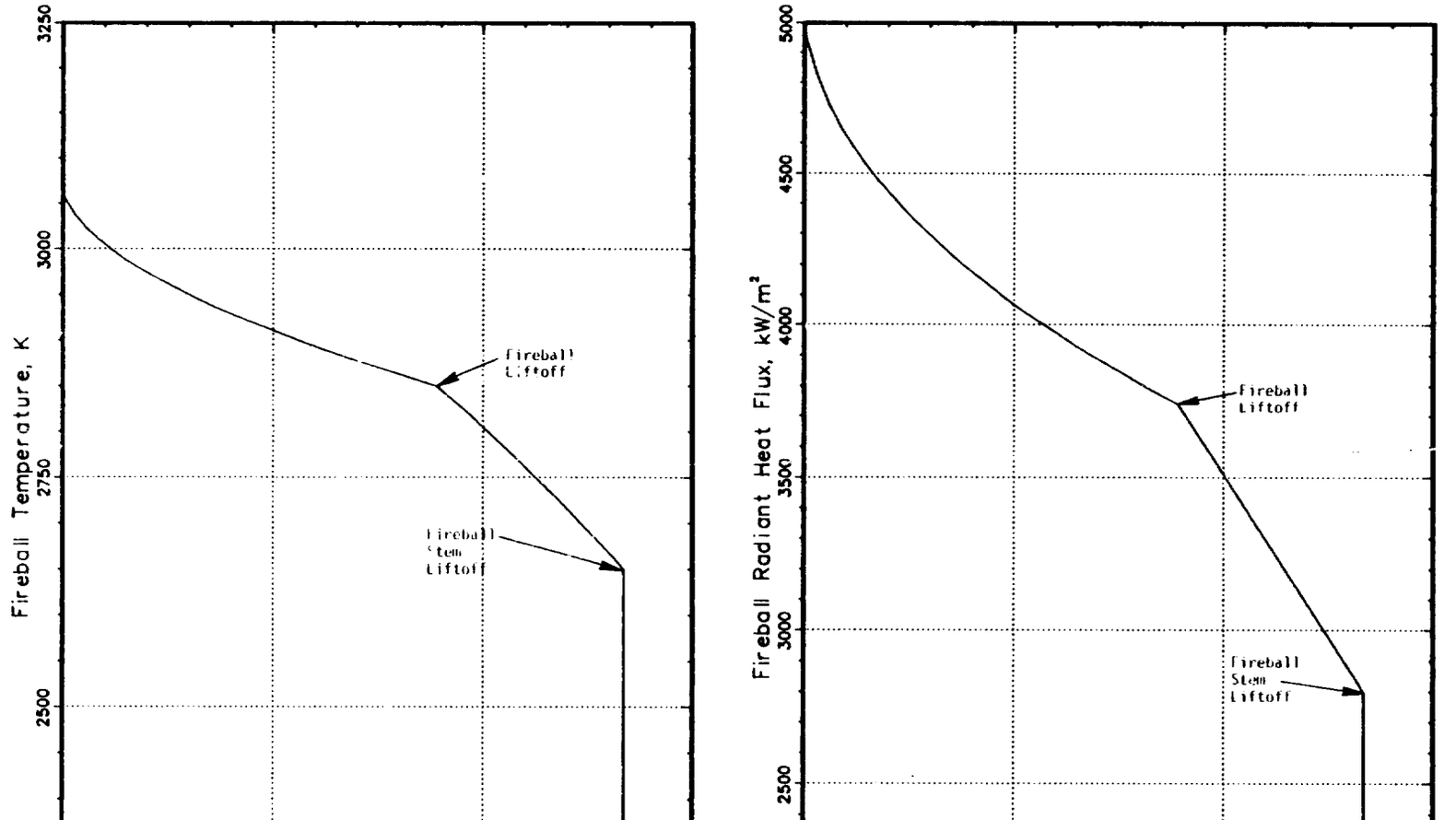

FIGURE 4-8. TEMPERATURE AND RADIANT HEAT FLUX AS A FUNCTION OF TIME FOR HLLV HYDROGEN/OXYGEN/RP-1 FIREBALL ENVIRONMENT

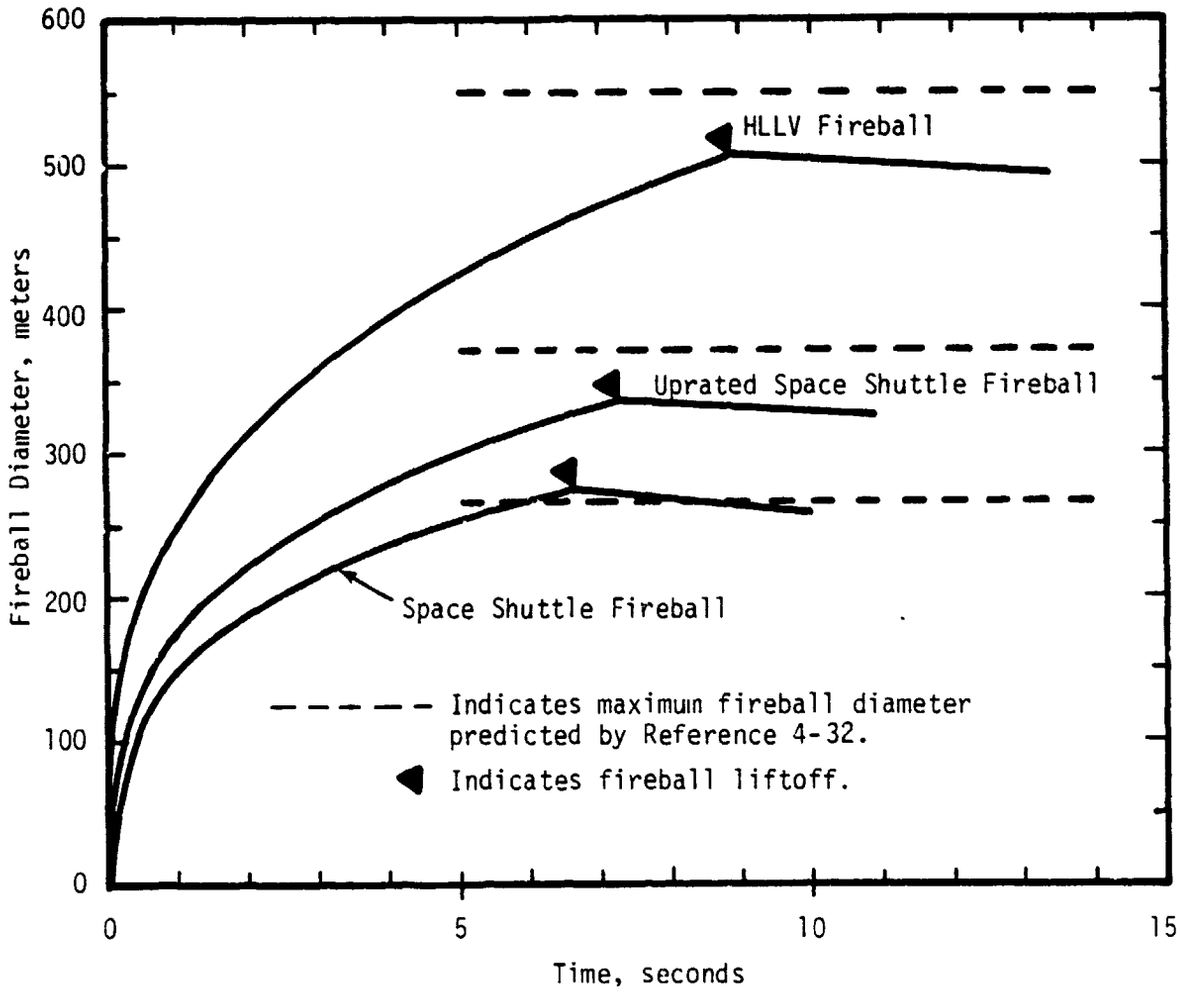

FIGURE 4-9. FIREBALL DIAMETER AS A FUNCTION OF TIME FOR THE SPACE SHUTTLE, UPRATED SPACE SHUTTLE, AND HLLV

To perform detailed modeling of all the physical phenomena expected to play roles in establishing the answers to the above questions is beyond the scope of the current study. The approach assumed here, while simplistic, allows one to evaluate the parameters that can be controlled by design (e.g., pool diameter).

An assumption that all of the RP-1 is involved in the residual fire would lead to the worst-case situation. The approach taken here is to parameterize the amount of RP-1 in the fire (from 0 to 100 percent) and the pool size. (The previous section assumed that all of the RP-1 would be included in the "fireball",---also a conservative approach from the fireball standpoint). The depth of liquid fuel in the pool, while in part is determined by the amount of fuel present, also is dependent upon the characteristics of the depressions or dykes present around the launch pad. The approach taken here is to parameterize the diameter of a cylindrically shaped dyke at the pad. This assumption also implies that the heat flux will remain constant with time. The burn rate of RP-1 has been calculated (see below) ignoring the effect of wind. The radiant heat flux has been calculated by assuming black body radiation and a temperature of 1366 K (2000 F) for the RP-1 fire.

4.2.2.2. Burn Rate

The burn rate for RP-1 was calculated by using the approach given in Reference 4-74. The burn rate of single component liquid fuels in large pools is given as:

$$V_\infty \text{ (cm/min)} = 0.0076 \frac{\Delta H_c}{\Delta H_{VAP} + \int_{Ta}^{Tb} C_p dT}$$

where: ΔH_c = Net Heat of Combustion (Lower Value)
ΔH_{VAP} = Heat of Vaporization at Normal Boiling Point, T_b
C_p = Heat Capacity

The results shown in Reference 4-74 indicate that the burn rate (V_∞) becomes constant for pool diameters greater than about 1.5 meters. The integrated heat capacity in the denominator of the above equation determines the temperature dependence of the burning rate, normally about 1/2 percent per degree centigrade variation of the initial liquid temperature, T_a. Data from References 4-75 and 4-76 were used to evaluate the above equation. A burn rate of 0.439 cm/min was calculated for RP-1. Burn rates for various other fuels are given below for comparison:

Fuel	V_∞ (cm/min)(4-74)
Benzene	0.600
Hexane	0.730
Butane	0.790
Hydrogen	1.400

4.2.2.3 Parametric Results

The liquid propellent residual fire environment was parameterized by assuming a radiant heat flux of 198 kW/m^2, corresponding to a temperature of 1366 K (2000 F), and a burn rate of 0.439 cm/min for RP-1. Figure 4-10 provides the estimated burn time, in minutes, for various RP-1 pool depths, in cm. To have a fire last over 1 hour, assuming no wind, the RP-1 pool depth would have to be greater than about 26 cm. Figures 4-11 and 4-12 provide estimates of burn time as functions of the fraction of RP-1 in the residual fire and the diameter of a cylindrical dyke wall for both the Uprated Space Shuttle and the HLLV. Figure 4-11 indicates, for residual fires lasting less than 1 hour, that the dyked area of equal depth should be greater than 1,260 m^2 for the Uprated Space Shuttle. Figure 4-12 indicates, for residual fires lasting less than 1 hour, that the dyked area of equal depth should be greater than 4,540 m^2 for the HLLV.

Because of the nature of possible residual fires, and because of the pad safety designs that would likely be employed, the following liquid propellent residual fire environment is recommended for use in payload response studies (see Section 4.3):

- Fire Duration of 3600 seconds
- Constant Heat Flux of 198 kW/m^2

It is worth noting that this environment is much less severe than the solid propellent residual fires that have been predicted for the Space Shuttle.[4-71] Figures 4-13, 4-14, and 4-15 provide the recommended combined fireball (see Section 4.2.1) and residual fire environments for the Space Shuttle (including the split motor solid propellant fire), the Uprated Space Shuttle, and the heavy lift launch vehicle (HLLV) which were used in the payload response analysis in Section 4.3.2.

4.2.3 Blast Wave Overpressure Environment

This section presents data for side-on and reflected overpressures and side-on and reflected impulses produced by explosions of the propellant tanks of interest here. The data generated were <u>not</u> used in the limited payload response analysis, but should be used in future efforts. Propellent tanks can explode as a result of various on-pad or ascent accidents or malfunctions and can be destructed deliberately by linear-shaped distruct charges, should flight controllers determine that an off-course vehicle would endanger the local population or ground features. Depending upon the event, varying degrees of explosive yield can result. The explosive yield is defined as percentage of TNT equivalent. For example, if a given liquid propellent tank explosion would produce a 100 percent yield, that means that the total mass of propellents would produce the same effect as the same mass of TNT. Reference 4-45 suggests that the following explosive yields be considered for the Space Shuttle External Tank (ET) blast hazard analysis:

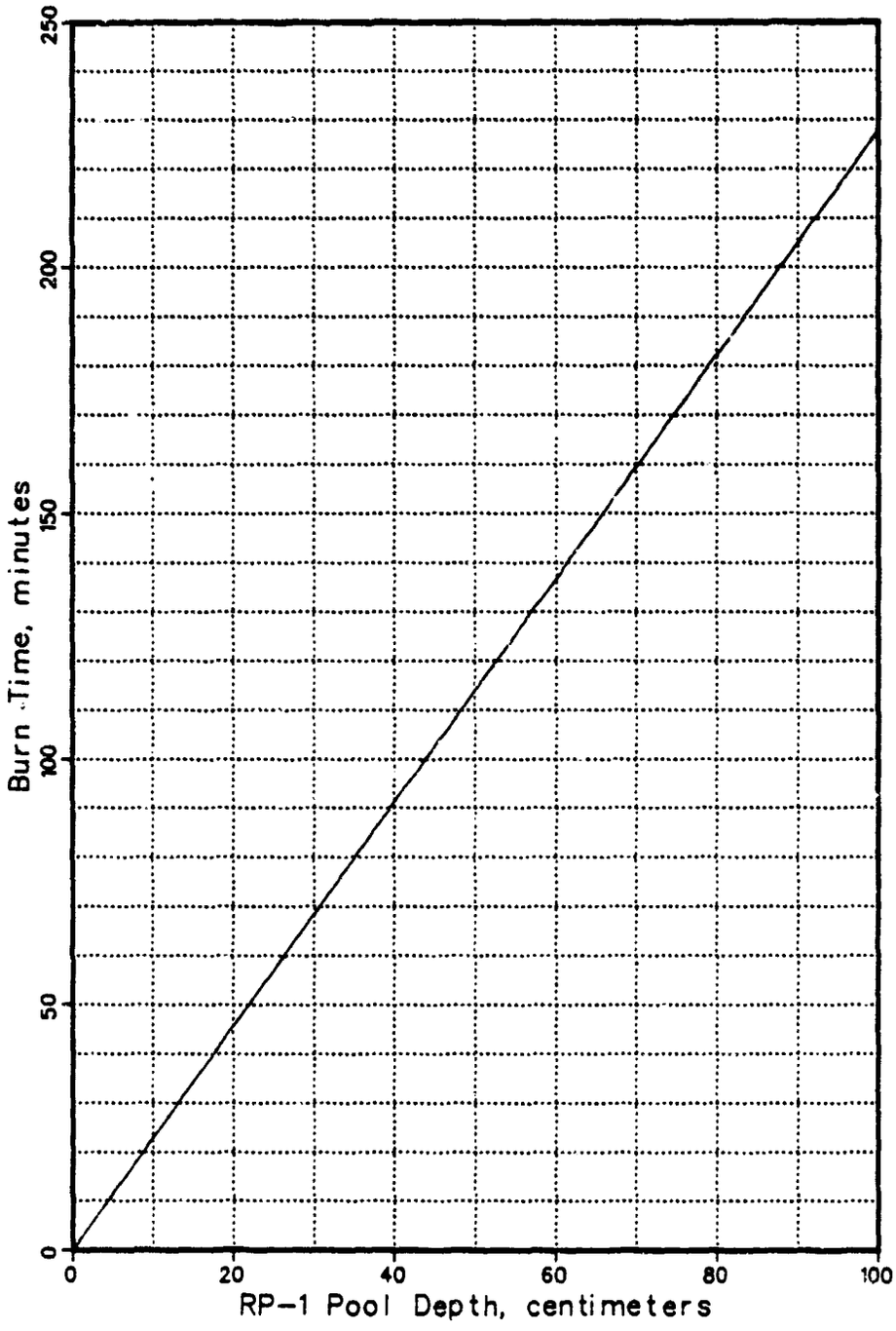

FIGURE 4-10. BURN TIME AS A FUNCTION OF RP-1 POOL DEPTH

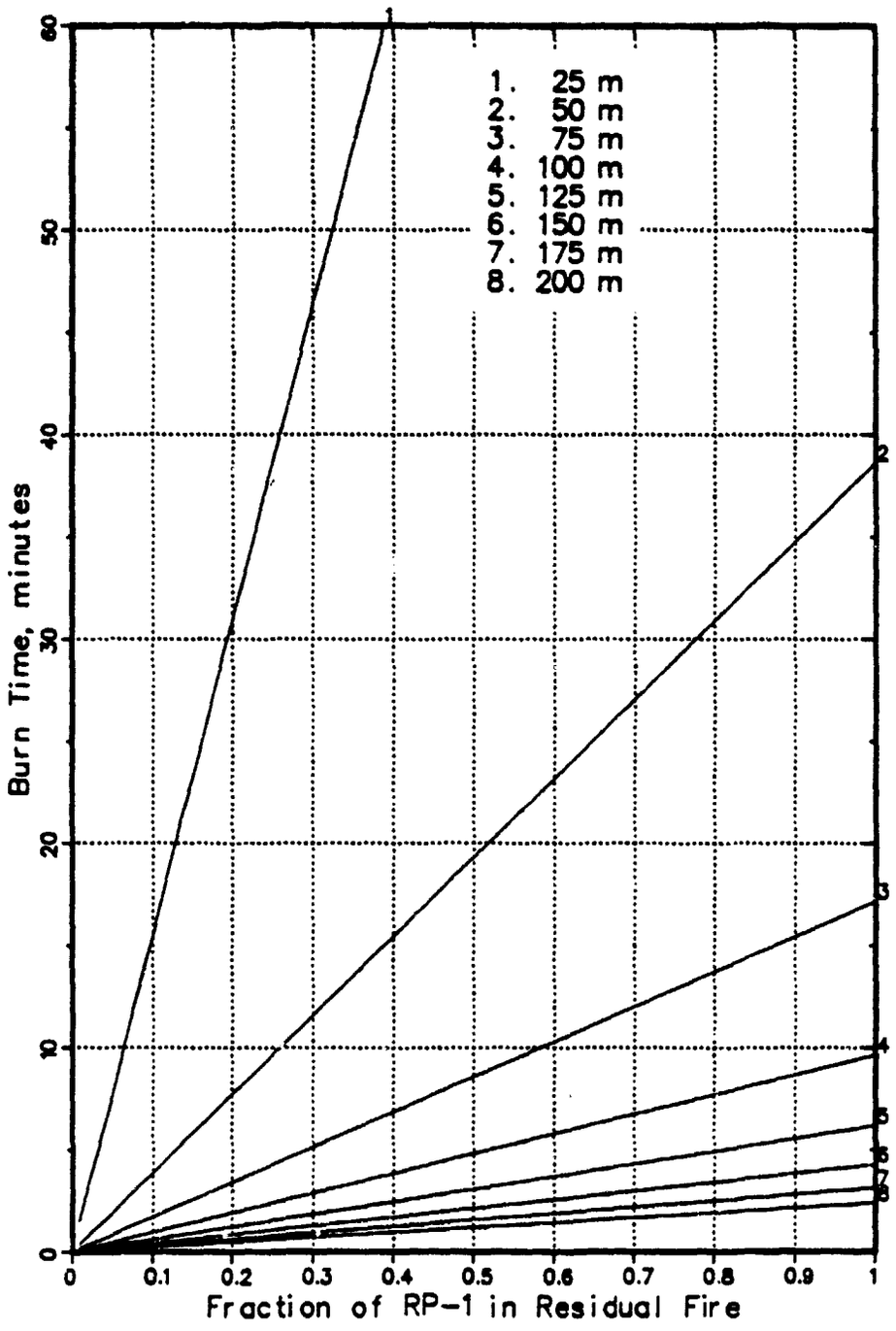

FIGURE 4-11. BURN TIME AS A FUNCTION OF RESIDUAL RP-1 FRACTION FOR THE UPRATED SPACE SHUTTLE AT VARIOUS POOL DIAMETERS

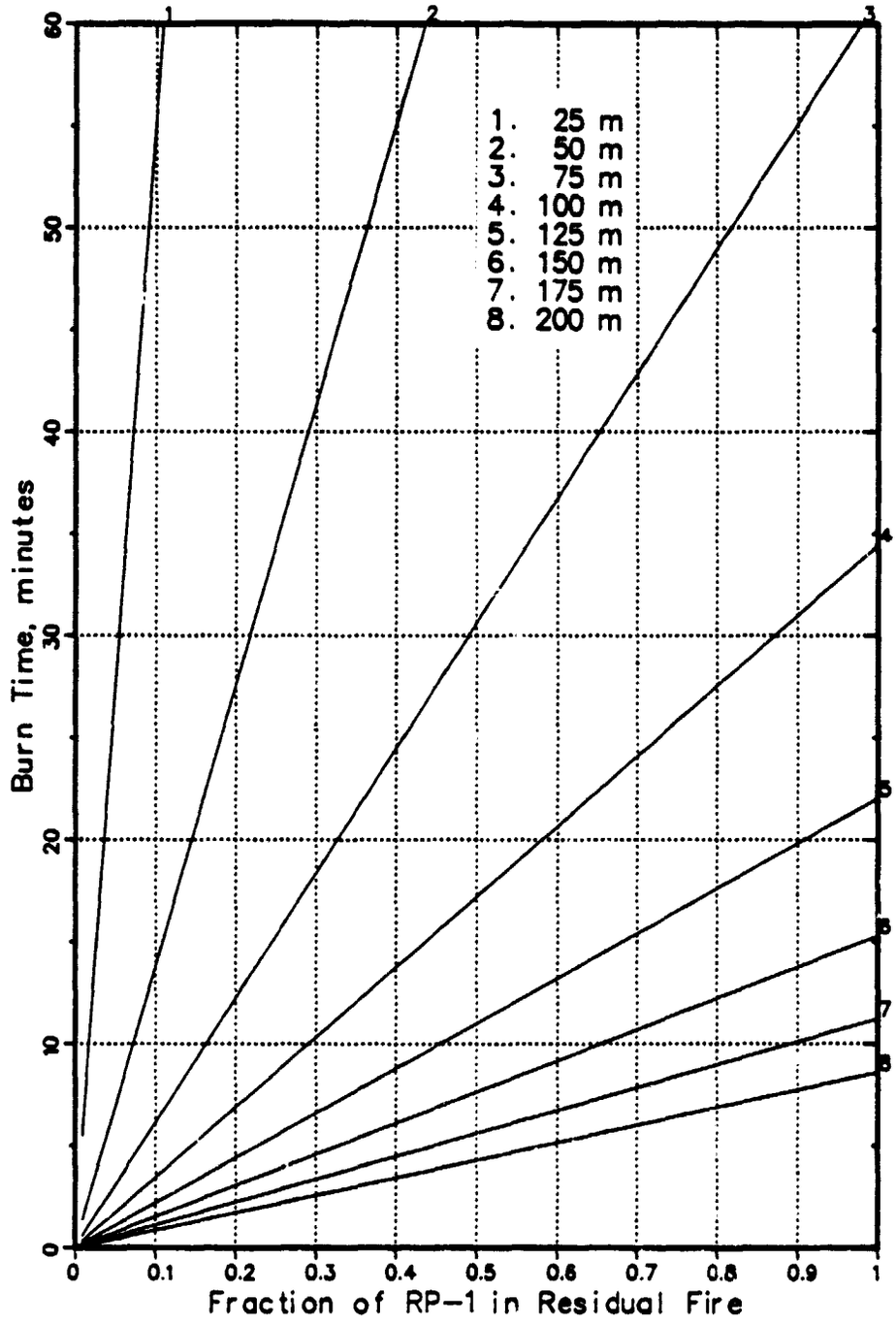

FIGURE 4-12. BURN TIME AS A FUNCTION OF RESIDUAL RP-1 FRACTION FOR THE HLLV AT VARIOUS POOL DIAMETERS

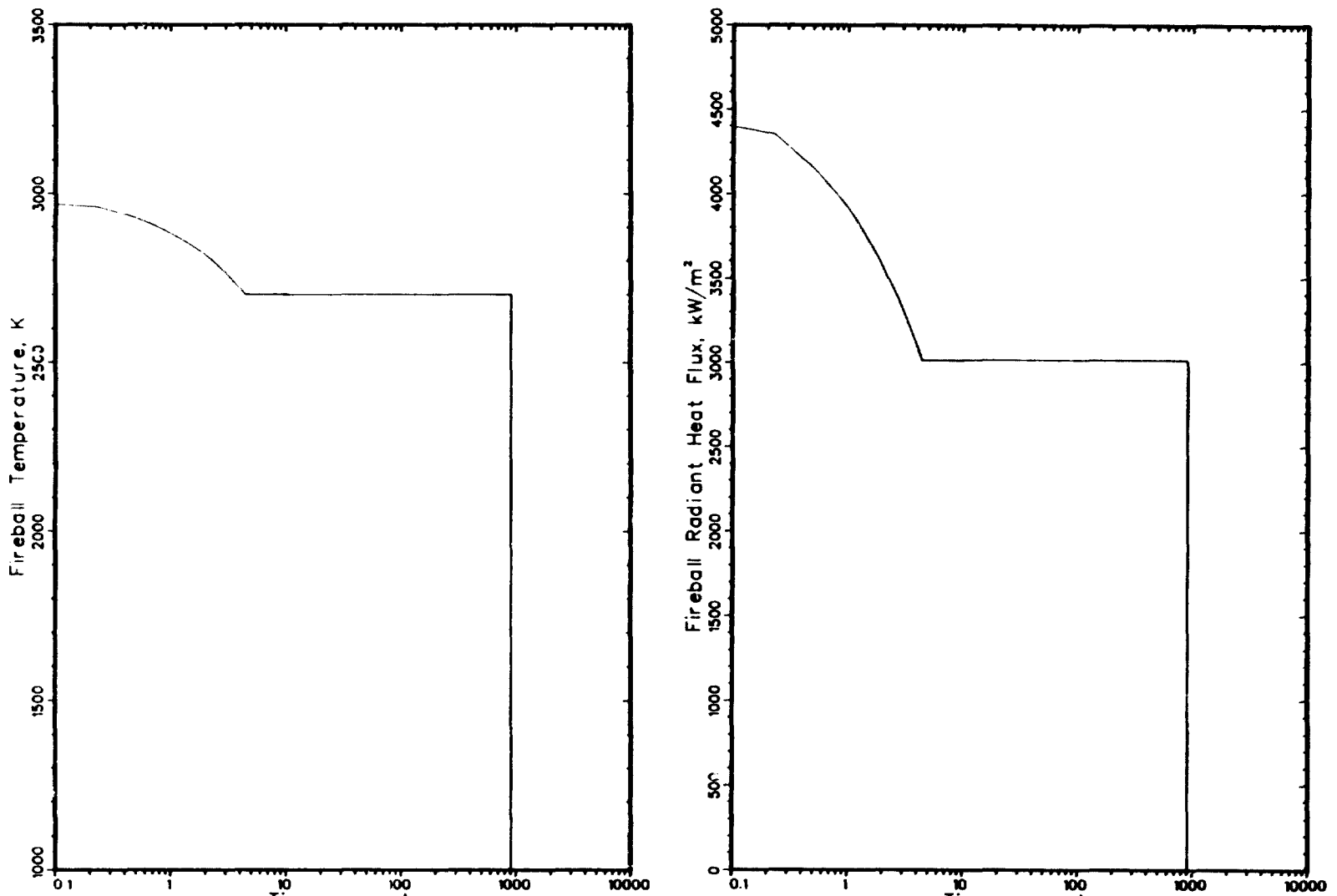

FIGURE 4-13. TEMPERATURE AND RADIANT HEAT FLUX AS A FUNCTION OF TIME FOR SPACE SHUTTLE HYDROGEN/OXYGEN FIREBALL AND SPLIT MOTOR SOLID PROPELLANT RESIDUAL FIRE ENVIRONMENTS

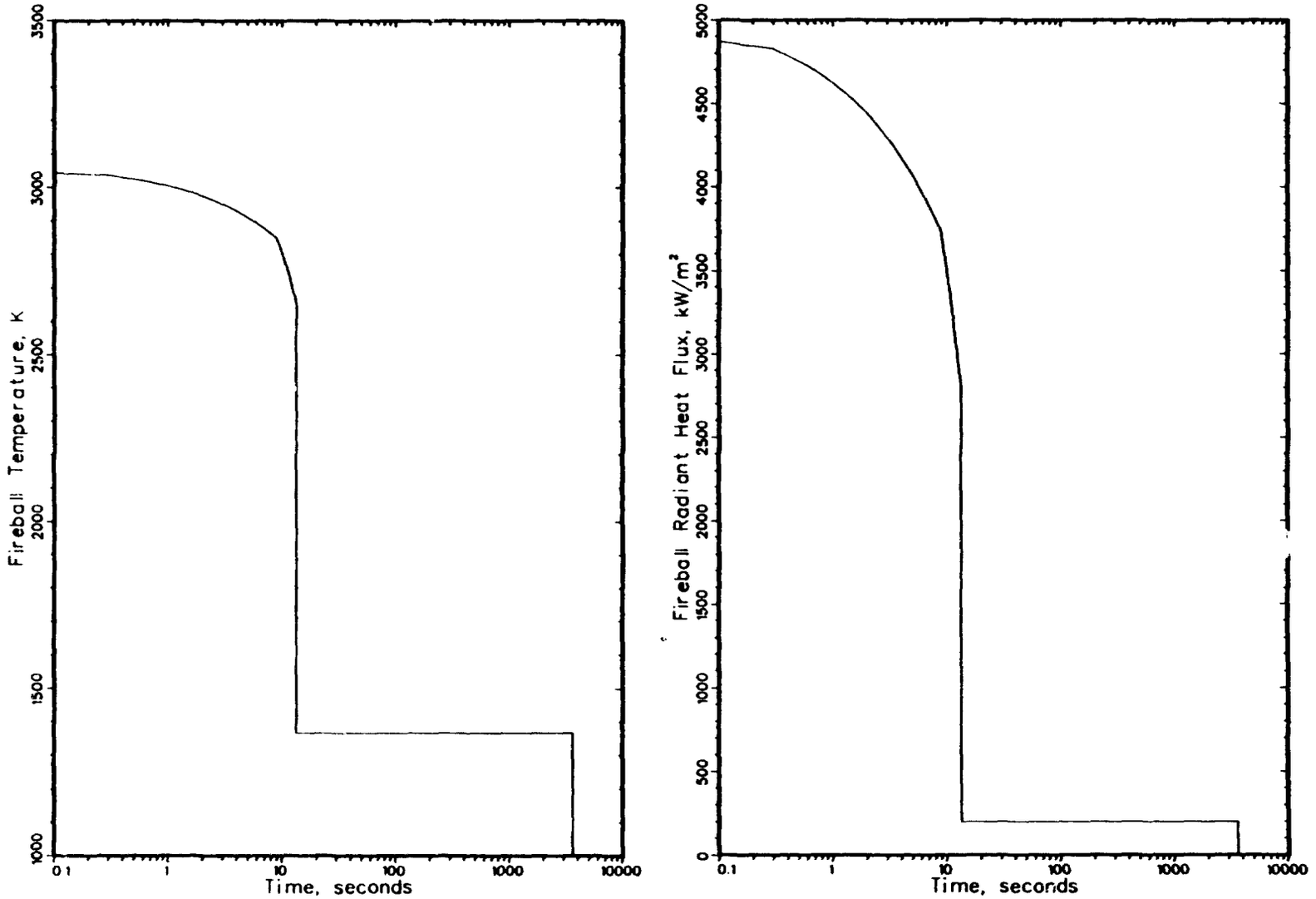

FIGURE 4-14. TEMPERATURE AND RADIANT HEAT FLUX AS A FUNCTION OF TIME FOR UPRATED SPACE SHUTTLE HYDROGEN/OXYGEN/RP-1 FIREBALL AND RP-1 RESIDUAL FIRE ENVIRONMENTS

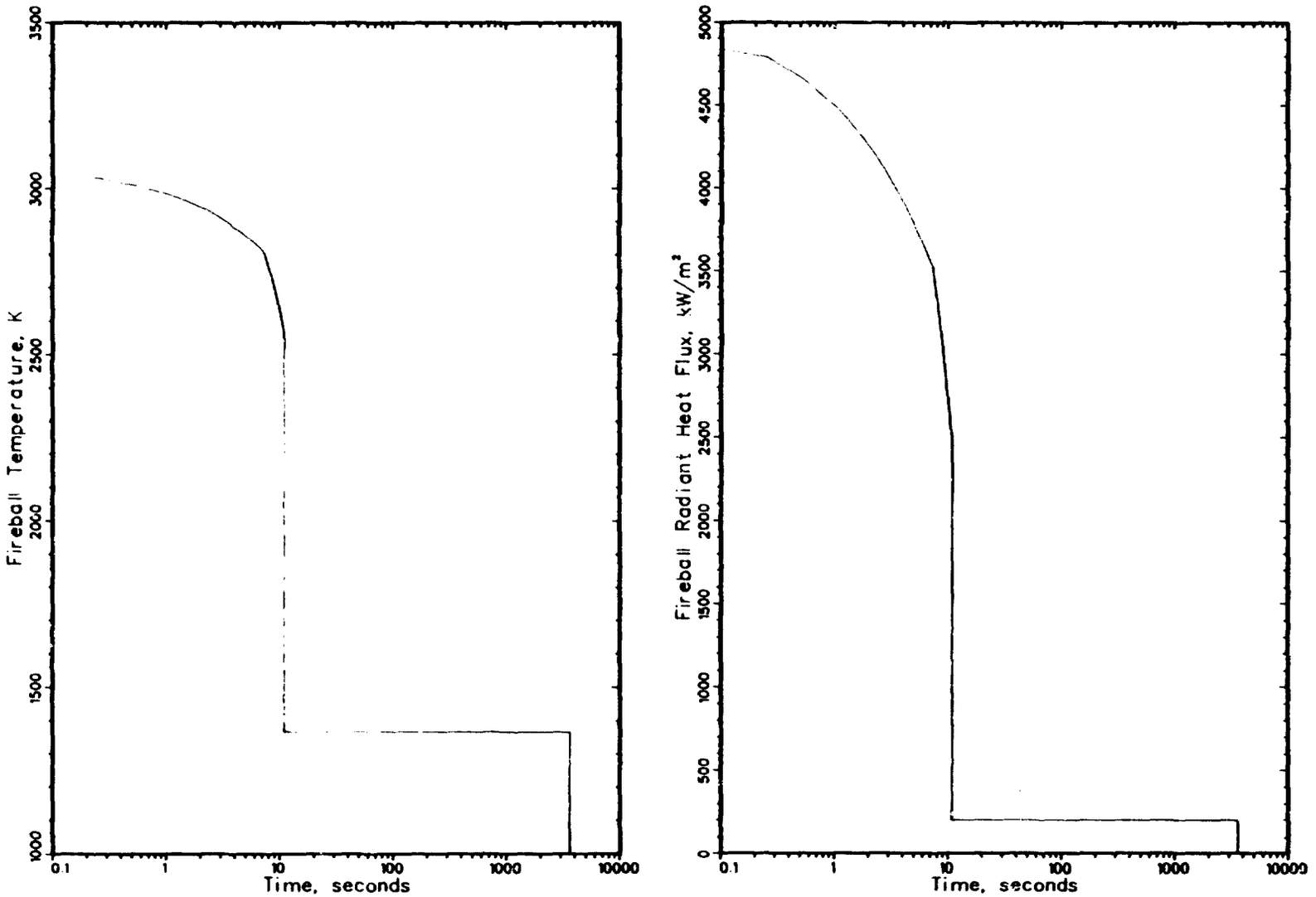

FIGURE 4-15. TEMPERATURE AND RADIANT HEAT FLUX AS A FUNCTION OF TIME FOR HLLV HYDROGEN/OXYGEN/RP-1 FIREBALL AND RP-1 RESIDUAL FIRE ENVIRONMENTS

Explosion Event	Percent Explosive Yield
Destruct	1
On-pad, no destruct	20
Fallback 30 m	50
High velocity impacts:	
350 m/s	100
550 m/s	160

Most recently, NASA/MSFC has recommended that a 10 percent yield be assumed for a failure of the Shuttle ET intertank structure during ascent.(4-44) Also recommended was that the resulting blast overpressure from an on-pad catastrophic failure, although at a higher estimated yield, would produce similar overpressures as the 10 percent yield during accent.(4-44)

Explosions of the propellent tanks are expected to produce mechanical environments that pose a hazard to payloads. For the nuclear waste mission, a shock blast wave could damage the reentry vehicle (RV) such that it might not survive the ensuing fire environment (see Sections 4.2.1 and 4.2.2). Also, and probably more importantly, the blast wave will create moving fragments which could cause a breach of the nuclear waste containment (see Section 4.2.4 for discussion of the predicted fragment environments).

Previous studies of explosion hazards for launch vehicles, carrying radioactive material, have assumed the center of explosion (COE), for a given failure, to be at the point of first potential mixing of the liquid fuel and liquid oxidizer. Last year's study(4-71) assumed the COE for the standard Space Shuttle case was taken to be the center of the ET intertank structure between the liquid hydrogen and liquid oxygen tanks. The distance from the COE to the nuclear waste payload surface was previously calculated to be 21.6 m (70.8 ft). This distance was used for all of the Phase II calculations. Recent analysis indicates that the explosion center for the ET could be in different locations. Also, the position of the payload in the cargo bay can change with varying payload packaging assumptions. Due to these facts, a parametric approach is given here for all the vehicles of interest.

Procedures outlined in "Workbook for Predicting Pressure Wave and Fragment Effects of Exploding Propellent Tanks and Gas Storage Vessels", Reference 4-39, were used to calculate the overpressure and impulse data. Propellant types and quantities used in the calculations are given below in Table 4-8.

TABLE 4-8. INPUT DATA FOR BLAST WAVE ENVIRONMENT PREDICTIONS

Vehicle/Tank	Propellent Type	Quantity, kg
Uprated Space Shuttle/ET	Oxygen/Hydrogen	712,100
Uprated Space Shuttle/LRB	Oxygen/RP-1	540,240
HLLV Booster	Oxygen/Hydrogen/RP-1	3,669,900
OTV	Oxygen/Hydrogen	20,431

Overpressure and impulse curves for the confined by ground surface (CBGS) case were used (Figures 2-12, 2-13, 2-16, and 2-17 of Reference 4-39). Figures 4-16 through 4-23 provide the results of the parameteric analysis for the four propellent tanks listed in Table 4-8. Side-on and reflected overpressures and impulses are predicted as a function of percent explosive yield (0.1 to 160) and distance (15, 20, 30, 50, and 100 m) from the COE to the point of interest. The break or bend that occurs in some of the curves is due to a discontinuity problem in the procedure outlined in Reference 4-39. Table 4-9 provides a summary of the data presented in the figures. Data are given for 1 and 10 percent yields with a COE assumed to be 20 m distant. These are the reference cases chosen for the safety design requirements (see Section 2.5 and Reference 4-77) and future payload response analysis work. NASA/MSFC has predicted side-on overpressures from 230 to 1380 N/cm^2 (4-44) for the Space Shuttle ET. The value of 230 N/cm^2 agrees well with the 250 N/cm^2 value in Table 4-9; however, different COE's and percent yields were assumed. It is believed that the 10 percent yield case for liquid propellent tanks should be used until further research indicates a suitable and justified solution to the problem.

TABLE 4-9. TYPICAL BLAST WAVE ENVIRONMENT VALUES(a)

	Propellant Tank Configurations							
	OTV		LRB		ET		HLLV	
Characteristic	1%[b]	10%[b]	1%	10%	1%	10%	1%	10%
Side-On Over-Pressure, N/cm^2	6.3	23	50	180	51	250	150	410
Reflected Over-Pressure, N/cm^2	16	82	220	1350	230	1700	1130	3050
Side-On Impulse, N-s/cm^2	0.0[illegible]	0.21	0.35	1.5	0.45	2.0	1.2	4.6
Reflected Impulse, N-s/cm^2	0.12	0.73	1.5	11	1.9	15	8.7	35

Notes: (a) All data for distance of 20 m.
(b) Percent yield, TNT equivalent.

4.2.4 Fragment Environment

This section presents data on the fragment (or shrapnel) environment produced by exploding propellant tanks of interest here. The data generated

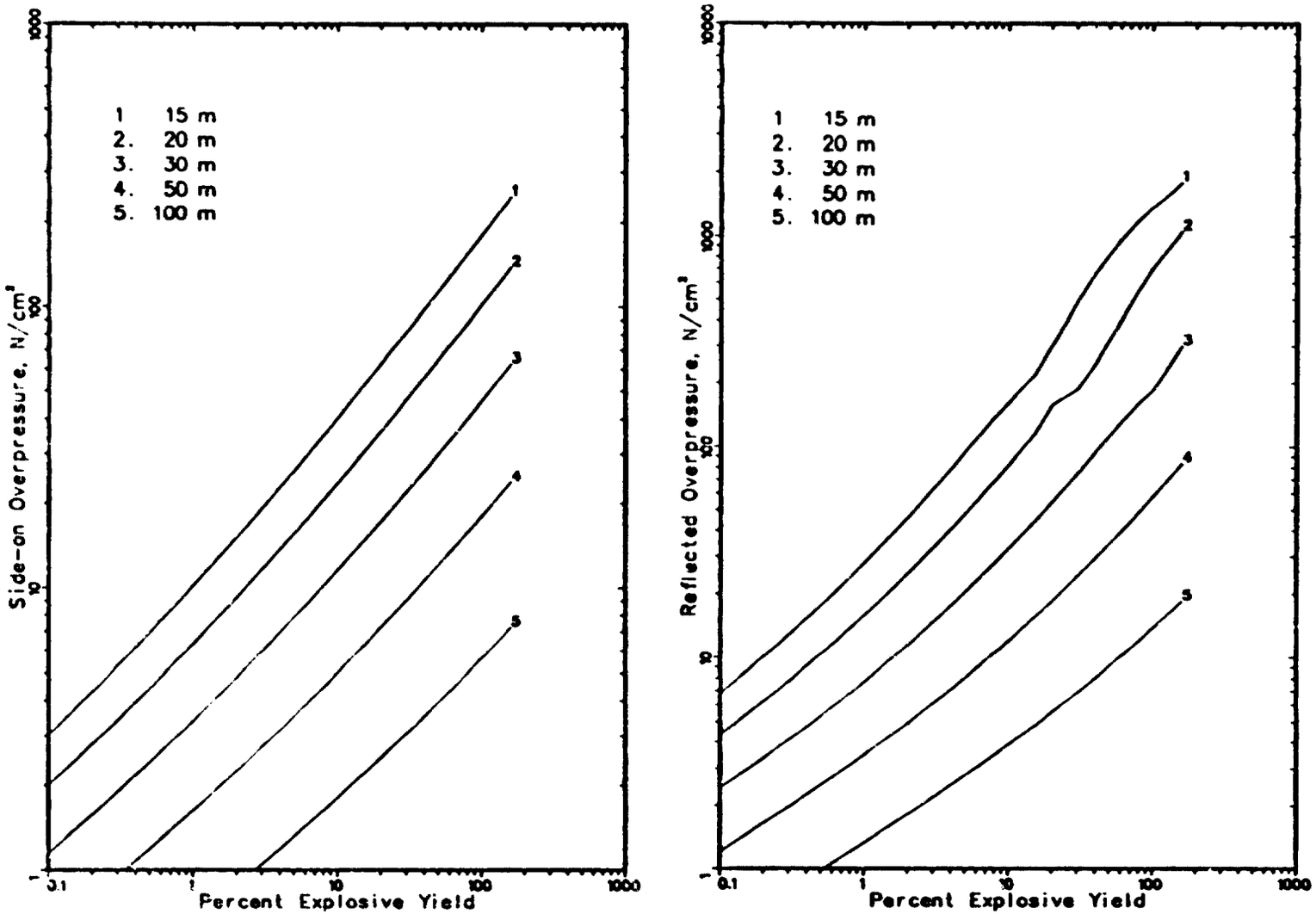

FIGURE 4-16. SIDE-ON AND REFLECTED OVERPRESSURE AS A FUNCTION OF PERCENT YIELD AND DISTANCE FROM EXPLOSION OF THE LOX/LH_2 BASED ORBIT TRANSFER VEHICLE

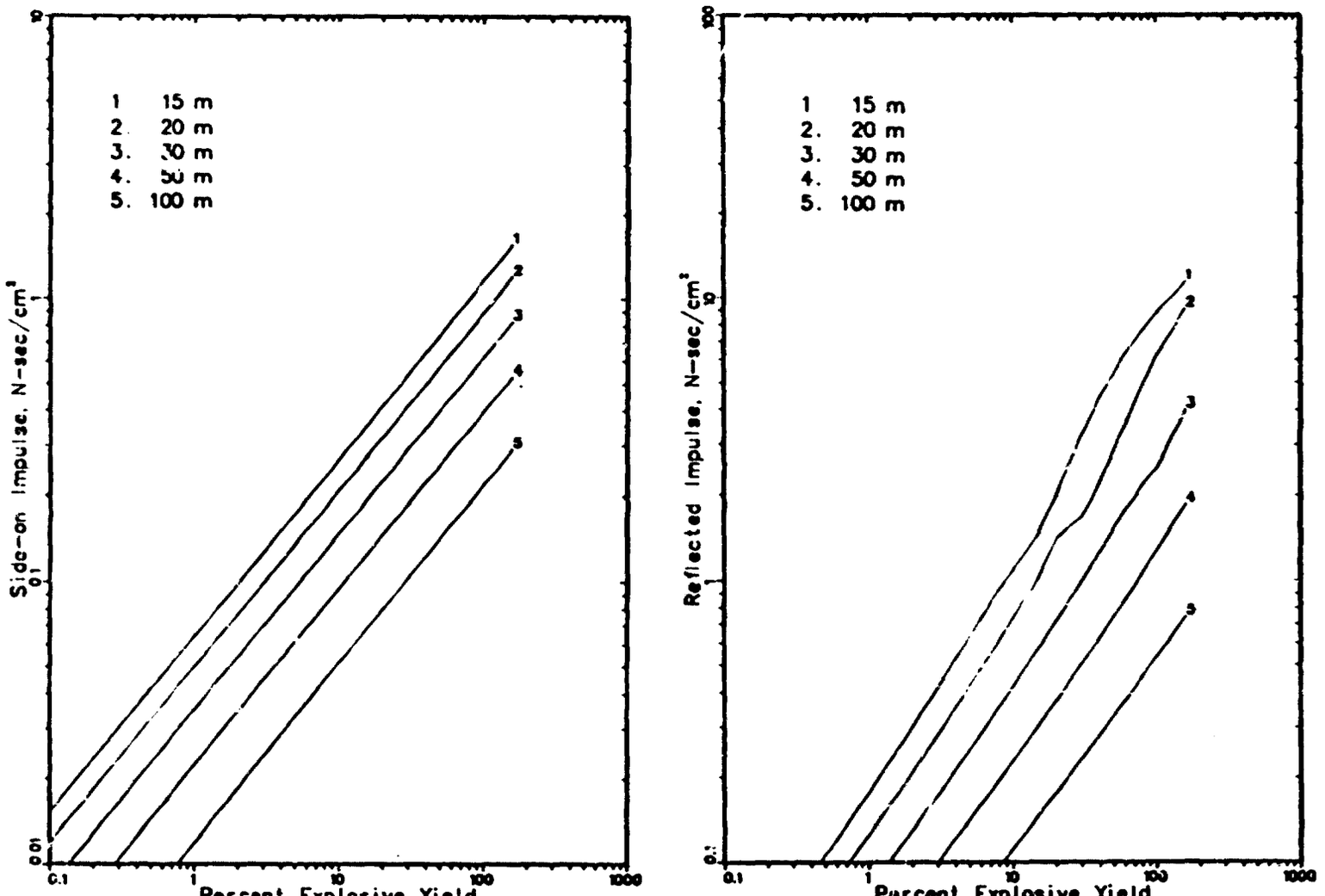

FIGURE 4-17. SIDE-ON AND REFLECTED IMPULSE AS A FUNCTION OF PERCENT YIELD AND DISTANCE FROM EXPLOSION OF THE LOX/LH_2 BASED ORBIT TRANSFER VEHICLE

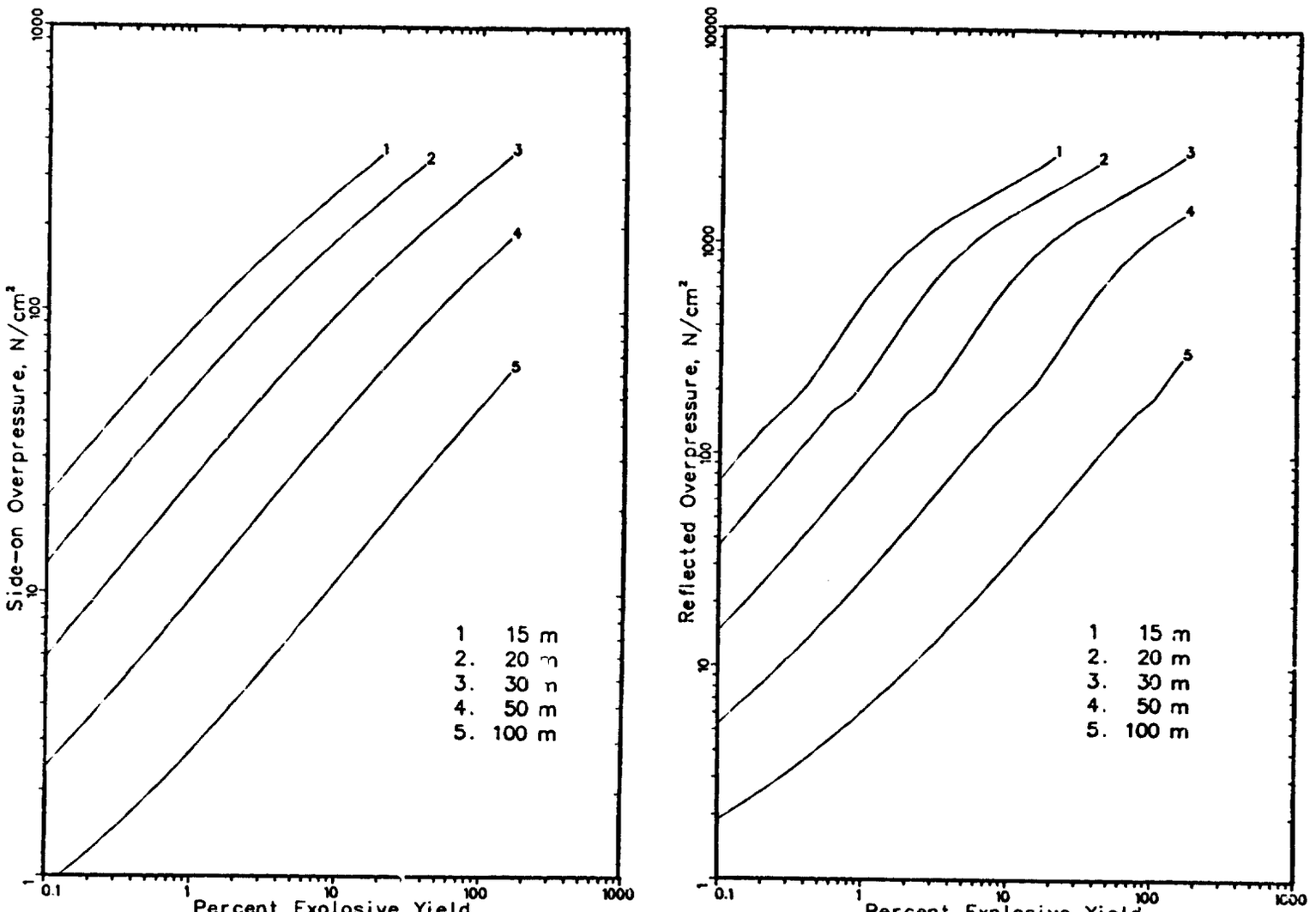

FIGURE 4-18. SIDE-ON AND REFLECTED OVERPRESSURE AS A FUNCTION OF PERCENT YIELD AND DISTANCE FROM EXPLOSION OF A SINGLE LOX/RP-1 BASED LIQUID ROCKET BOOSTER (UPRATED SPACE SHUTTLE)

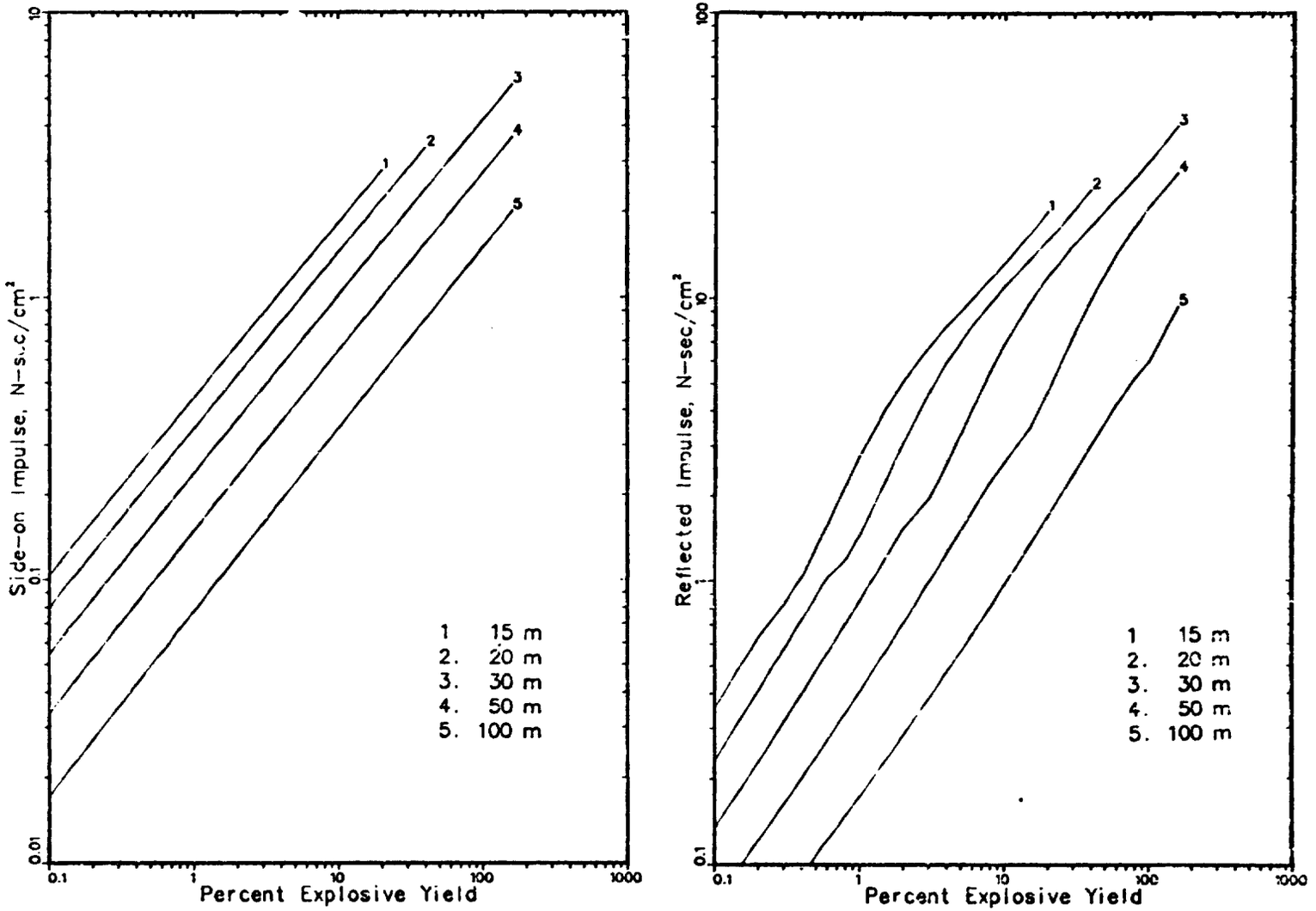

FIGURE 4-19. SIDE-ON AND REFLECTED IMPULSE AS A FUNCTION OF YIELD AND DISTANCE FROM EXPLOSION OF A SINGLE LOX/RP-1 BASED LIQUID ROCKET BOOSTER (UPRATED SPACE SHUTTLE)

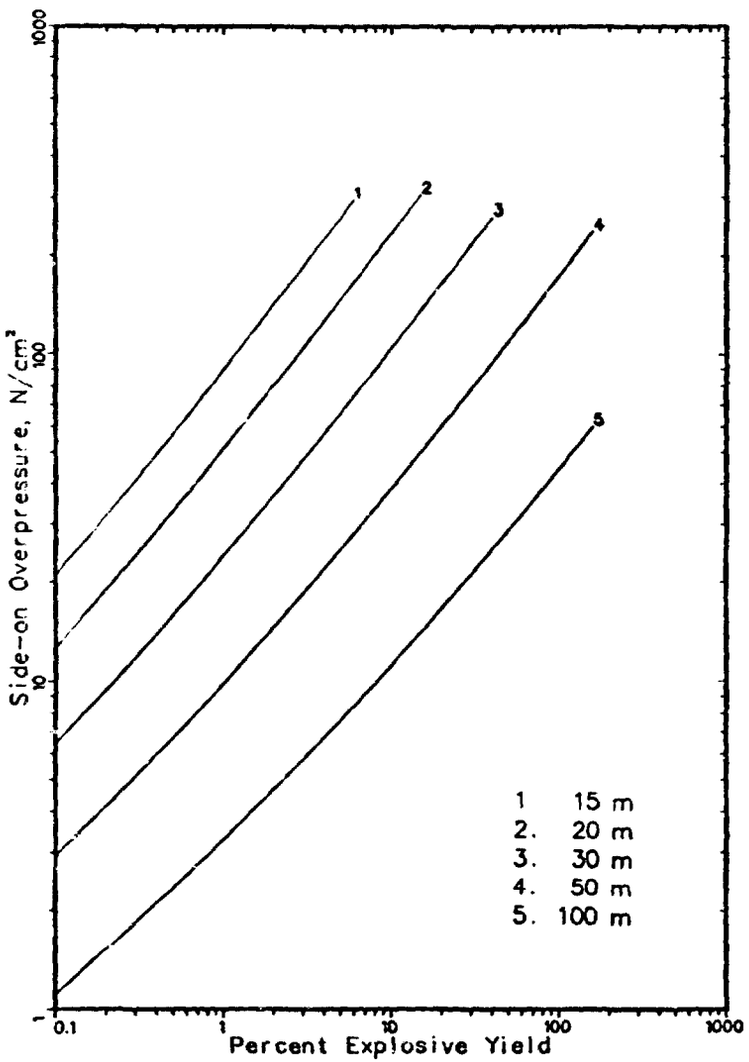

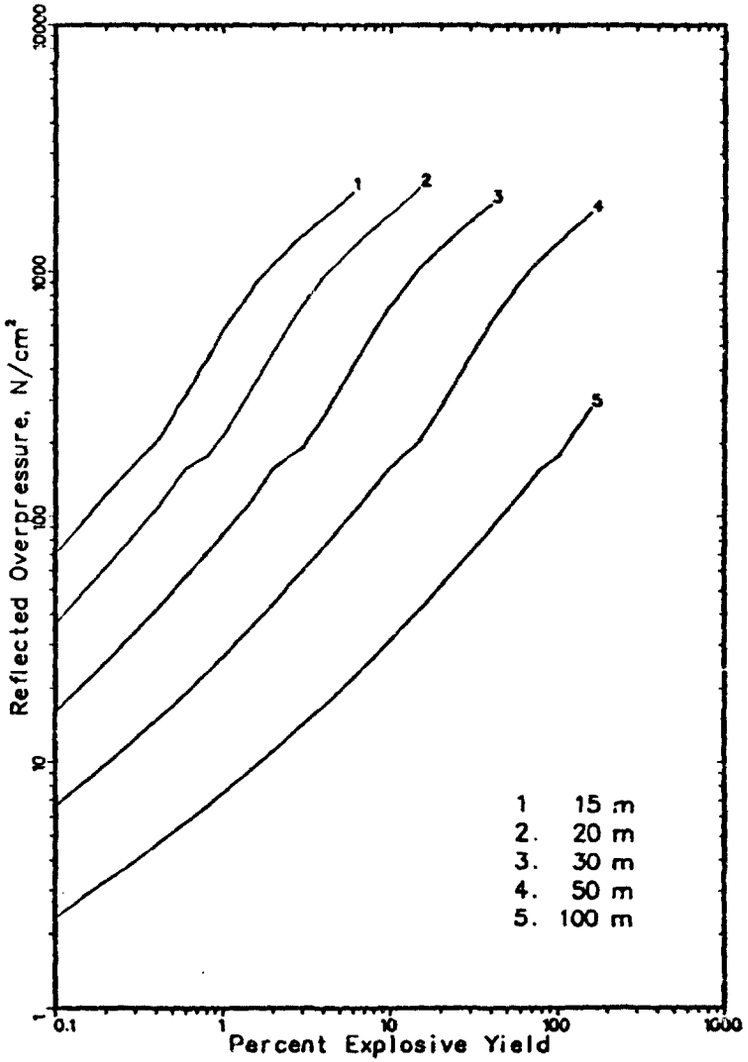

FIGURE 4-20. SIDE-ON AND REFLECTED OVERPRESSURE AS A FUNCTION OF PERCENT YIELD AND DISTANCE FROM EXPLOSION OF THE LOX/LH_2 BASED SPACE SHUTTLE EXTERNAL TANK

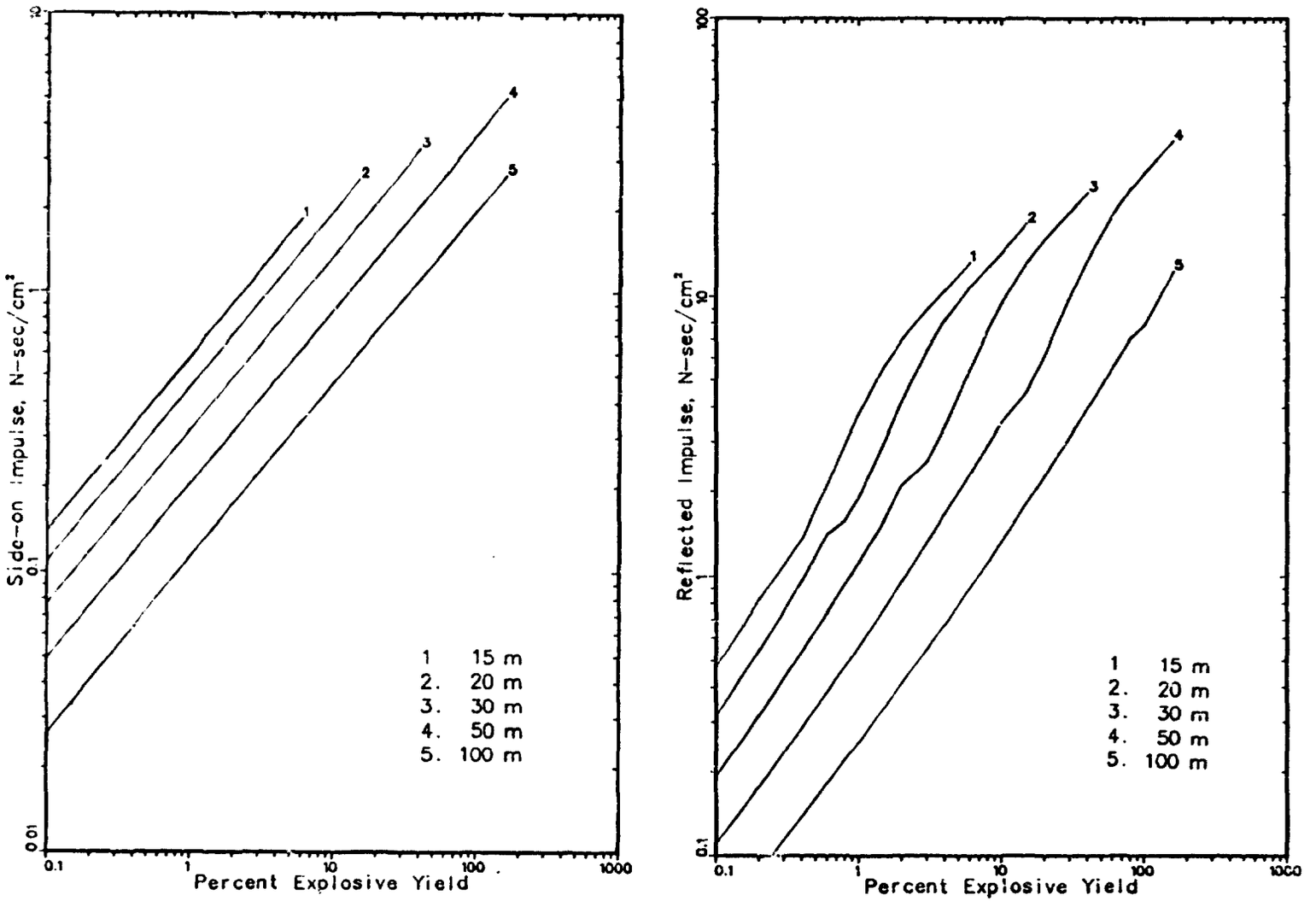

FIGURE 4-21. SIDE-ON AND REFLECTED IMPULSE AS A FUNCTION OF PERCENT YIELD AND DISTANCE FROM EXPLOSION OF THE LOX/LH_2 BASED SPACE SHUTTLE EXTERNAL TANK

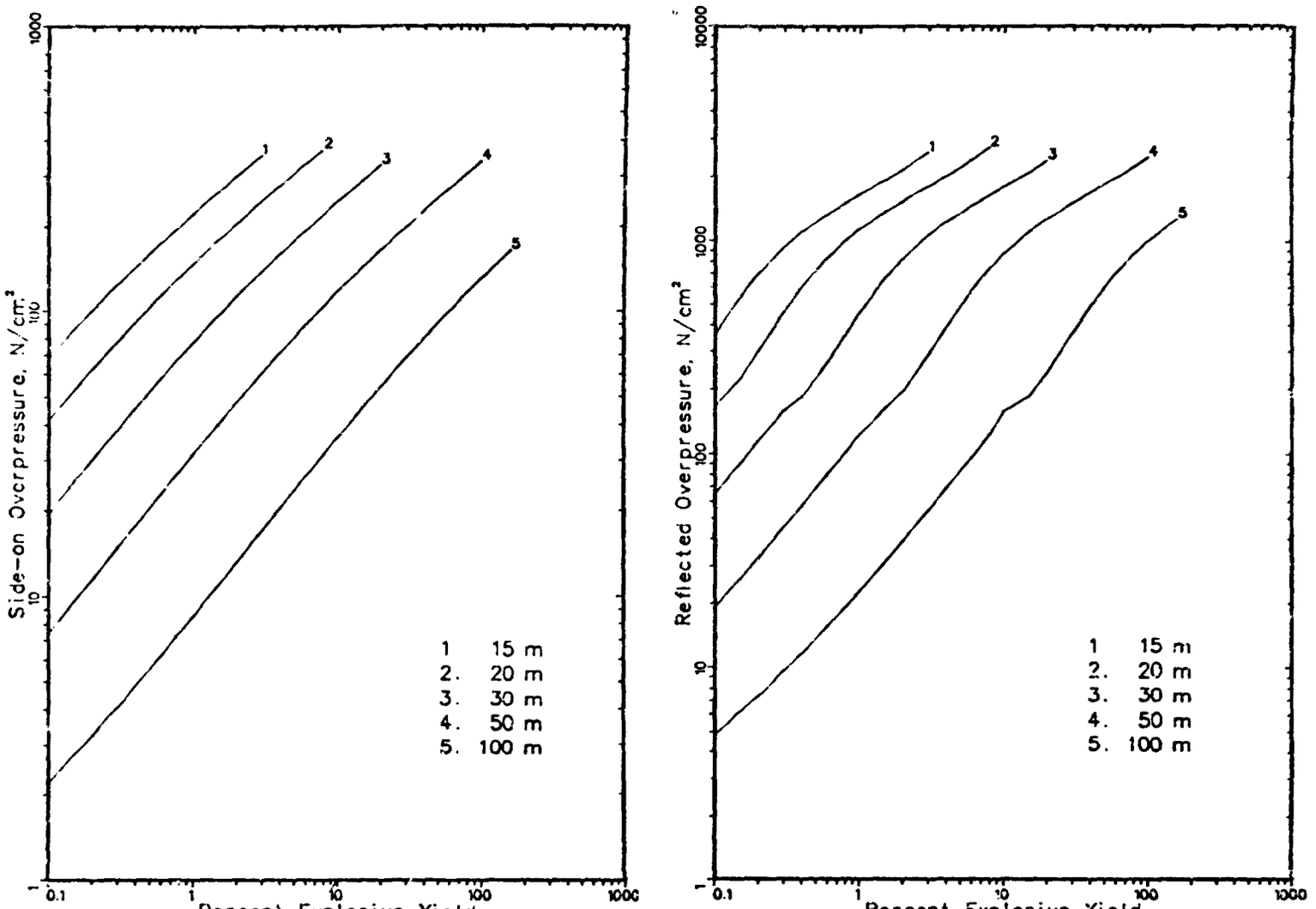

FIGURE 4-22. SIDE-ON AND REFLECTED OVERPRESSURE AS A FUNCTION OF PERCENT YIELD AND DISTANCE FROM EXPLOSION OF THE LOX/RP-1 BASED HEAVY LIFT LAUNCH VEHICLE

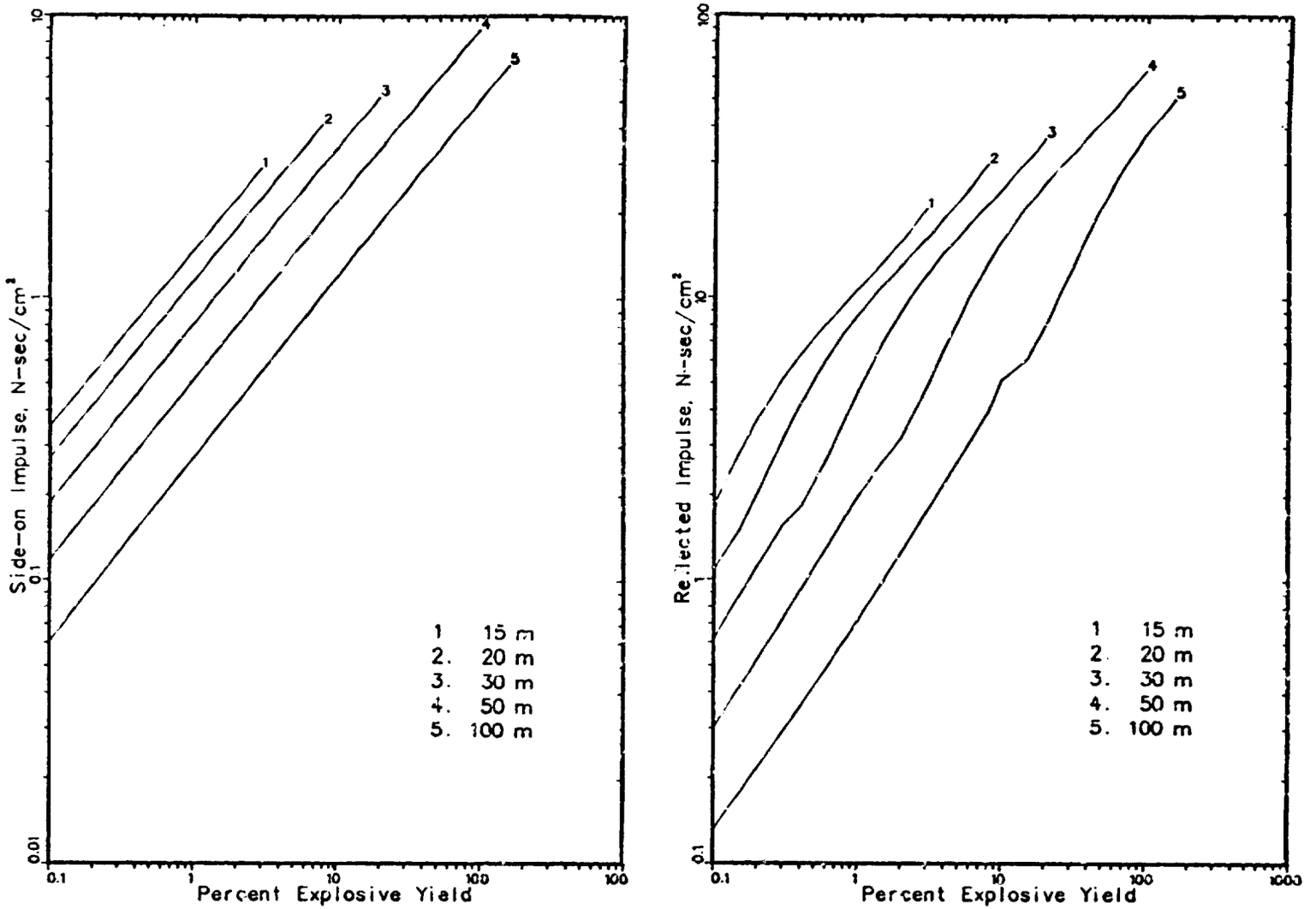

FIGURE 4-23. SIDE-ON AND REFLECTED IMPULSE AS A FUNCTION OF PERCENT YIELD AND DISTANCE FROM EXPLOSION OF THE LOX/RP-1 BASED HEAVY LIFT LAUNCH VEHICLE

were not used in the limited payload response analysis, but could be used in future studies. Considerable refinement of the fragment environment is still required before credible predictions can be made.

Prediction of the fragment environment at the payload position in the cargo bay resulting from the explosion of propellants in a rocket booster is an extremely complex problem. The fragments of primary interest, but perhaps not exclusively, are believed to originate from the propellant tankage and associated components. The primary logic in this selection is, that being closest to the explosion, these fragments will be accelerated to higher velocities (and thus present a greater hazard to the payload) than fragments derived from structures and components more remote from the explosion. A second pragmatic reason is that the available data largely represent tankage fragments.

A liquid propellent explosion follows some prior failure (e.g., bulkhead rupture or gross tank failure, such as occurs in a vehicle on-pad fall back). Before an explosion can occur, some mixing of the propellants must take place. It is generally assumed that the yield of the explosion, as calculated from the blast wave measured at an appreciable distance from the explosion, increases to some maximum as the time between initial failure (start of mixing) and ignition/explosion increases. With the increase in time before ignition, more of the propellents are mixed and can thus contribute to the explosive energy release.

The observed explosive yields tend to be relatively small. They are expressed as the ratio of the mass of TNT that would produce the observed blast wave to the total mass of propellents in the involved tanks, in tests, and derived from observations of actual failures. A still smaller fraction of the total available propellent quantity is involved in producing the observed explosion. (The "yield" is most affected by the energy released in the explosion, and the energy of explosion of liquid propellants can be significantly greater than the energy of explosion of the reference TNT.)

Considering that prior damage must have occurred to the propellent tanks, that some time must have passed between the initial failure and the explosion to permit mixing of the propellenets, and that typically only a small fraction of the total propellent contributes to the explosion, one might logically ask the following questions:

- What is the condition and position of the propellent tanks (relative to the payload) at the time of the explosion?
- Where does the actual explosion take place?
- Where is the propellant that is not participating in the explosion?

The answers to these questions, which are not known for any general case, or for the most part, even in tests actually conducted, can have profound influences both on the generation of fragments from the tankage, and

on the fragment environment resulting at the payload. The tanks may be displaced from their position in the intact vehicle. The explosion may take place near the zone of initial propellent contact, within a propellent tank after a period of initial mixing, or at some other location, perhaps even outside the original tank envelope. Unreacted propellent between the explosion center and the tank wall may absorb a significant fraction of the energy of the explosion and greatly reduce the amplitude of the blast wave at the tank wall. Also, if a cell of mixing propellant explodes at the wall surface, one would expect a very high energy blast wave at the tank wall.

In contemplating the fragment environment at the payload location, we can ask an additional question:

- What is the contribution of any structure between the propellent tanks and the payload (e.g., the Shuttle Orbiter structure) in stopping fragments from the tank or in contributing additional fragments?

Considering these problems, one is driven to empirical relationships derived from tests, such as Project Pyro[4-36]. Even here, significant problems remain. Instrumentation was external to the explosion and typically at considerable distances. Thus, the "instrumental" data tell little about the details at the explosion site. Data on fragment velocities and sizes were obtained in ways that probably lead to overrepresentation of large fragments and intermediate velocities. The direction of initial fragment motion was not recorded. Finally, the data, probably reflecting the multiplicity of different situations occurring during the tests, do not appear to fit any well-defined pattern. Thus, they are difficult to interpret in terms of predicting a specified event.

In the following sections, predictions of the fragment environment are made. To make these predictions it has been necessary to ignore the details discussed above and assume that the available empirical data can, in fact, be applied to the current problem. Some results are not particularly satisfying, and can be defended only on empirical grounds.

4.2.4.1 Fragment Mean Velocity

NASA CR 134906 [4-39] analyzed the data from Project Pyro and concluded that the mean fragment velocity from an explosion of LO_2/LH_2 propellent tankage could be represented as:

$$\bar{u} = 73.96\ Y^{0.4296}$$

where, $\bar{u}$ is the mean fragment velocity, and Y is the explosive yield expressed as the ratio of equivalent TNT mass to total propellent mass, in percent. The data failed to support any statistically significant effect of the absolute size of the explosive event.

Figure 4-24 shows the relationship and the data quoted to support the correlation.[4-39] The correlation is identified as applying to LO_2/LH_2 propellents in the confined by missile (CBM) tests. In these tests, the failure leading to explosion was caused by cutting through the bulkheads separating the two propellent tanks. The correlation seems to provide an approximate upper limit for both LO_2/LH_2 and LO_2/RP-1 propellants in the CBM and confined by ground surface (CBGS) tests (the CBGS tests were tank drop tests), and is thereby adopted as the prediction for fragment mean velocities from all launch vehicle failures resulting in propellent explosions.

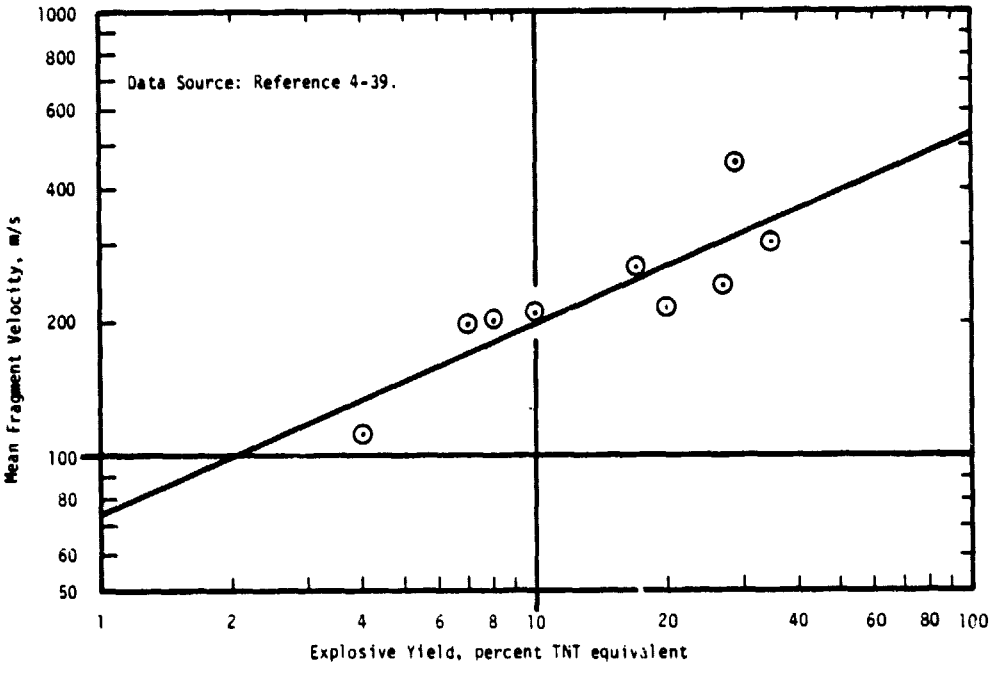

FIGURE 4-24. MEAN FRAGMENT VELOCITY AS A FUNCTION OF PERCENT EXPLOSIVE YIELD

4.2.4.2 Fragment Velocity Distribution

NASA CR 134538[4-38], on the basis of data pooled from a number of tests, suggests using a log-normal distribution of fragment velocities. The log-normal distribution is a very poor fit to the CBM data for both LO_2/LH_2 and LO_2/RP-1 propellants. It is a fair fit for the CBGS data. Appendix I discusses the difference between the normal and log-normal distribution for the present problem.

Figure 4-25 plots the data on (normal) probability paper. Ignoring the problem presented by the low velocity tails, the normal distribution is a good fit to the CBM data. If one assumes that the curvature of the CBGS plots

reflect the behavior of the low velocity tail, then a line parallel to the CBM data through the high velocity points does not seem unreasonable. Thus, the prediction method chosen for the fragment velocity distributions is a normal distribution (with the low velocity tail ignored) with a standard deviation of 145 m/s. The mean velocity is chosen from Figure 4-24.

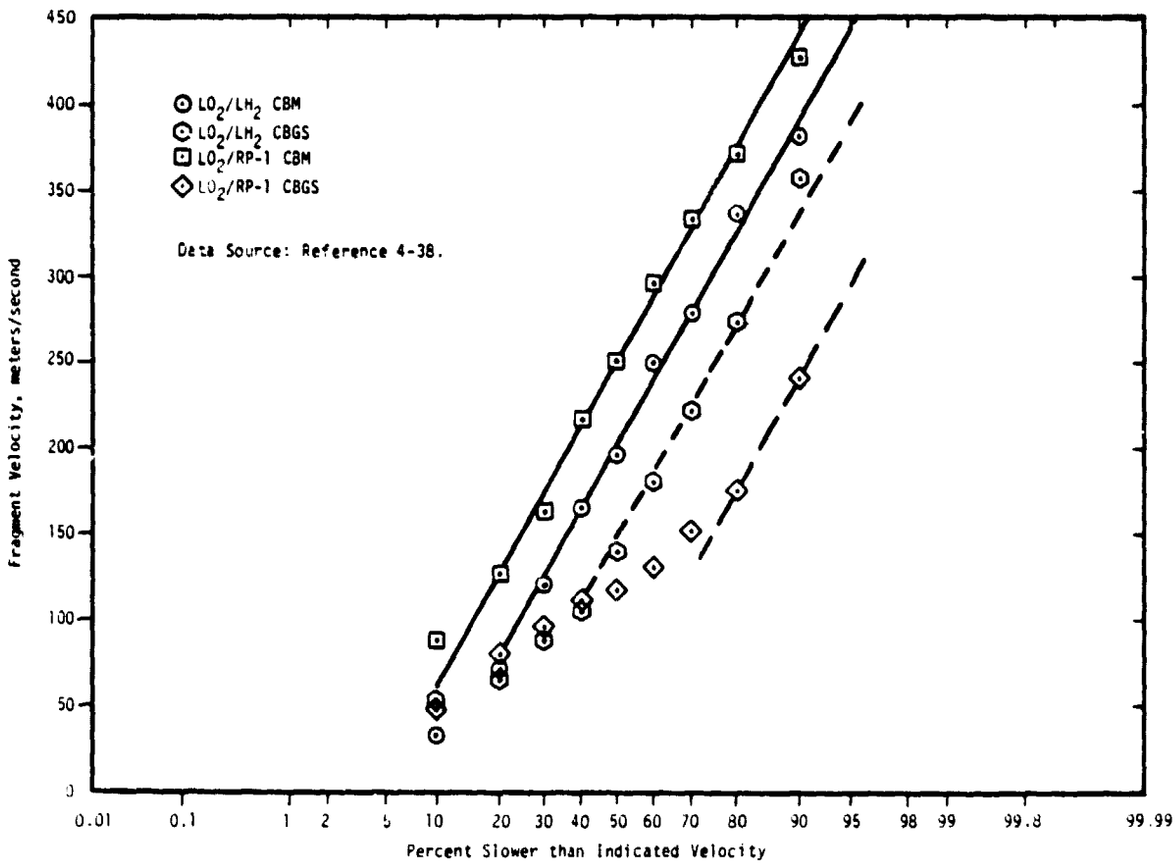

FIGURE 4-25. FRAGMENT VELOCITY DISTRIBUTIONS FOR CBM AND CBGS FOR LOX/LH_2 AND LOX/RP-1

4.2.4.3 Fragment Size

Data on fragment masses and projected areas are presented in NASA CR 134538[4-38] for eight "events", of which five appear to be relevant to the launch vehicle explosion problem. The fragment mass data does not suggest any correlation. However, the fragment projected areas seem to suggest a very simple correlation.

Figure 4-26 is a plot of the fragment projected area distributions from the five events. This plot suggests that, at least as a reasonable upper bound, the mean fragment projected area and area distribution are independent of event parameters (yield and quantity of propellent involved). The mean projected area is 0.3 m^2 and the distribution is log-normal with a standard deviation of 5.3. Although this selected combination has no dependence on yield, it seems logical that it should exist and some selected data sets do suggest such a dependence.

It is suggested that the fragment mass be calculated by assuming the fragments to be sections of tank skin and multiplying the fragment area by the areal density of the tank skins.

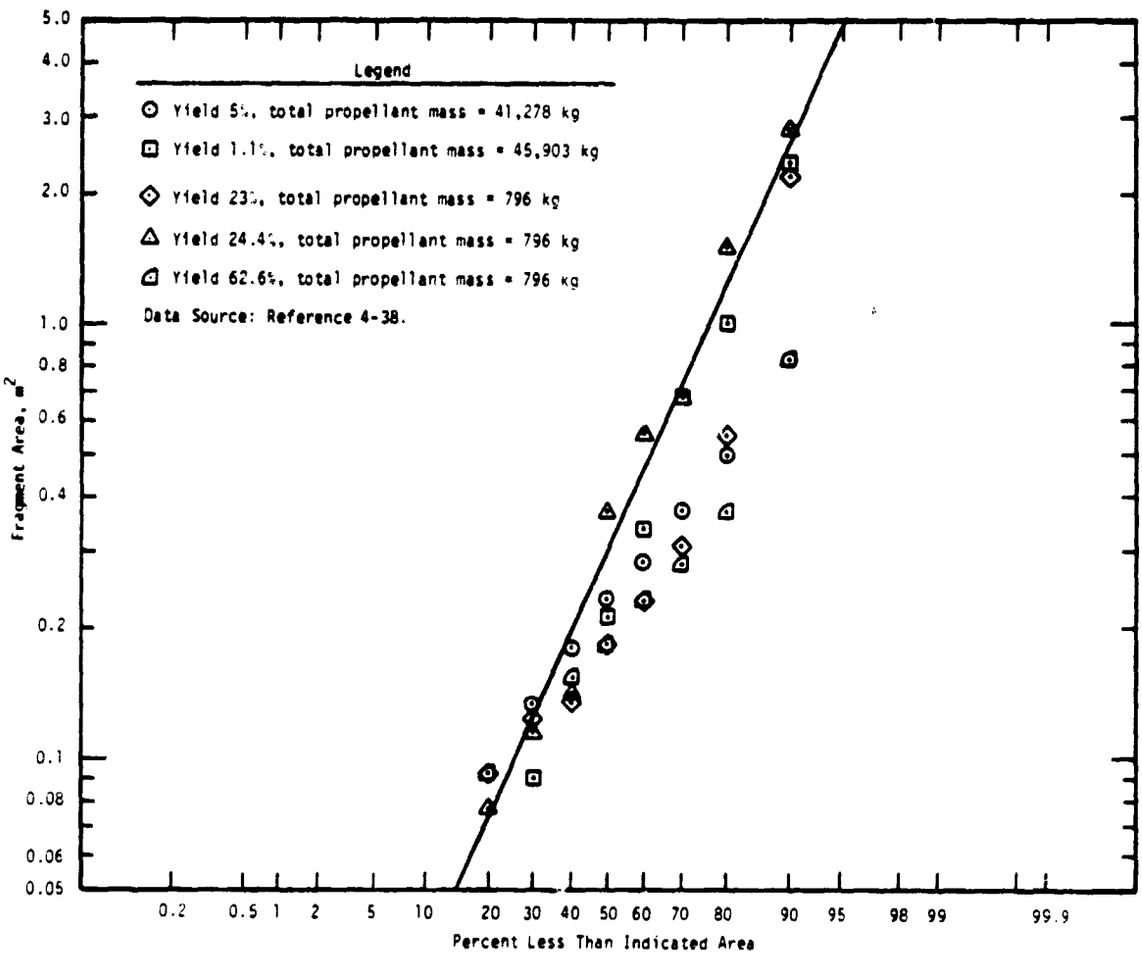

FIGURE 4-26. FRAGMENT SIZE DISTRIBUTION

4.2.4.4 Fragment Flux

No published data provide information on the initial directions of the fragments generated by propellent tank explosions. Two methods of calculating the flux are possible. First, one could assume that the fragments are driven radially outward from the "center of explosion" (COE--if such a center exists), leading to a spherical distribution of fragments. Second, one could assume that the fragments are driven radially outward from the tank centerline, leading to a cylindrical distribution of fragments.

The second case is known to be a good approximation for fragments produced by a cased, cylindrical high-explosive charge. For the launch vehicle, one can envision such a distribution if fragmentation is caused by a blast or detonation wave propagating longitudinally through the propellant tank.

The spherical geometry would seem to be a reasonable approach if there were nothing (except air) between the COE and the fragmenting tank wall, but, in fact, this space is apt to be filled with propellent. Also, the concept of a COE does not seem particularly appropriate for the typically low yield propellent explosions found in practice. Consequently, the cylindrical geometry is assumed.

Figure 4-27 illustrates the geometry. The fragment flux (fragments/m^2) at the target area is given as:

$$\Psi = \frac{1}{\bar{A}} \times \frac{D_T}{2S}$$

where $\bar{A}$ is the mean fragment area ($0.3 m^2$), D_T is the tank diameter and S is the separation of the payload from the tank centerline.

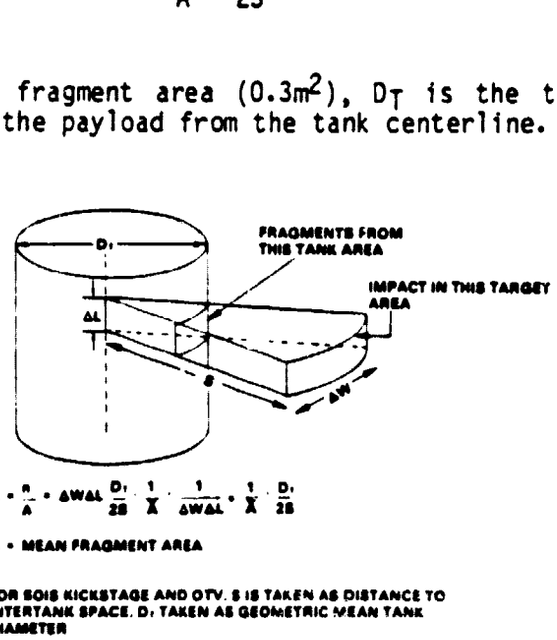

FIGURE 4-27. FRAGMENT FLUX RELATIONSHIP

Figure 4-28 presents the results of calculation of the fragment flux for explosion of the Space Shuttle External Tank (ET), the Liquid Rocket Boosters (LRB) of the Uprated Space Shuttle, the booster of the Heavy Lift Launch Vehicle (HLLV), the Orbital Transfer Vehicle (OTV), and the Solar Orbit Insertion Stage (SOIS). To apply the fragment flux model to the OTV and SOIS, where the payload is mounted on the vehicle centerline, and where multiple propellent tanks are used, S has been taken as the distance to the intertank space, and D_T was taken as the geometric mean tank diameter.

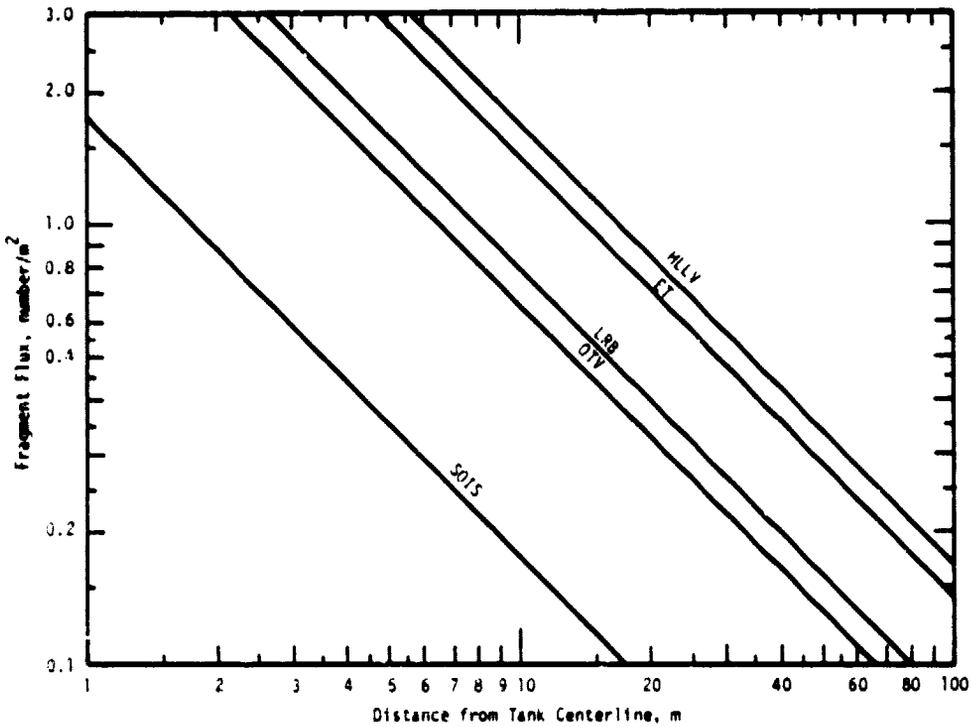

FIGURE 4-28. FRAGMENT FLUX AS A FUNCTION OF DISTANCE FROM TANK CENTERLINE FOR VARIOUS PROPELLANT TANKS OF INTEREST

4.2.4.5 Concluding Remarks

The preceding sections provide a definition of the fragment environment, mean fragment velocity, velocity distributions, mean fragment size and size distribution, and fragment flux resulting from a launch vehicle and upper stage explosions. The prediction methods are empirical, and it is recognized that some aspects of the predictions are not in agreement with one's intuitive expectations or are not theoretically defensible. The predictions are also, in a sense incomplete, in that there are no cross correlations between fragment size and fragment velocity. This is because there are no empirical data on such a correlation. A better experimental data set is required to properly characterize the fragment environment for exploding tanks (see the discussion at the end of Section 4.1.3).

In the Phase II BCL study[4-71], predictions of the fragment environment were based on a much more restricted data set coupled with hypothesized fragment acceleration mechanisms. While providing a correlation between fragment size and fragment velocity, and fragment size and yield, the correlation predicted fragment sizes and velocities for high yield explosions (>5 percent) which were respectively much smaller and much higher than have been observed experimentally. As the mechanisms used in previous predictions do not appear defensible under critical examination, the previous predictions have been abandoned and replaced by those above which are defensible on empirical grounds until new data are available, the predictions contained here should be used for payload response analysis in followon studies.

4.3 Payload Response Analysis

There is a wide range of accident payload response analyses which need to be evaluated for the space option of waste disposal. A limited response analysis was conducted in this study (see Section 4.3.2). Future safety studies need to include a more in-depth analysis of the mechanical environmental (impact, earth surface impact, etc.). The nuclear waste payload can be subjected to several possible severe accident conditions, including an on-pad launch vehicle fire, or an inadvertent reentry following an orbital malfunction. In this section, the fire and reentry, thermal response analysis conducted during the Phase III effort for various waste payload configurations is documented. The major objectives of this effort were to determine the quantity of waste mass released due to the thermal environments along and to recommend design modifications which would prevent the predicted releases.

Heat transfer models are discussed first including a description of overall model improvements that were made during the present study. The results of the thermal response analysis including a prediction of possible release of waste material are then presented. Finally, system modifications are suggested to prevent this predicted release.

4.3.1 Aerothermal Analysis Models

Analysis of the in-depth response of a material system to various accident environments was accomplished using a Battelle developed Reentry Thermal Analysis Code (RETAC) which is described briefly in Appendix J. The basic code input variables and methodologies are discussed in this section along with the improvements to the code which were incorporated for the present effort.

4.3.1.1 Model Improvements

The model used in previous payload thermal response analyses (Phase II--Reference 4-71) produced only a first-order approximation to the true solution of material temperature histories resulting from various accident environments. Several second-order effects neglected in these early analyses were:

- Two-dimensional (i.e., 2-D) heating
- Heat of fusion effects
- Material removal during melting
- Surface temperature limitations due to melting.

The addition of a 2-D (axisymmetric) heating model provided for more accurate analysis of stable vehicle (i.e., nonspinning reentry into the

Earth's atmosphere during the supersonic portion of the trajectory). This stable case results in a greater degree of heat input near the vehicle forward stagnation region. A randomly spinning 1-D case was also examined where the heat is evenly distributed around the entire body surface. In effect, the 2-D option allowed for division of the vehicle into conical-shaped sectors starting at the stagnation point and extending completely around to the rear stagnation zone. Also, the body was further subdivided into a series of concentric rings at various radii from the waste form centerline.

Heat of fusion effects were modeled by making an appropriate increase in the specific heat of the material over a specified temperature interval as its temperature exceeded the melting point. The product of specific heat increase and temperature interval was adjusted to equal the material latent heat of fusion value. This refinement provided an energy sink for melting materials that were surrounded by other materials that had not melted.

Metallic material removal during melting was also important because it would be unrealistic to allow melted material to continue to absorb heat and remain in place beyond the point where it normally would have eroded away. In the revised code, after the melt temperature was exceeded, the surface of metallic materials was allowed to recede at a rate dependent upon the net input heat flux. Thus, the surface recession rate, $\dot{S}$, can be written as

$$\dot{S} = \dot{q}_{net}/\rho\Delta H_f \qquad (1)$$

where, H_f is the heat of fusion and ρ is the material density. The term q_{net} can be written as:

$$\dot{q}_{net} = \dot{q}_{input} - \dot{q}_{rad} - \dot{q}_{cond} \qquad (2)$$

It accounts for the reduction of the actual input heat flux, $\dot{q}_{input}$, by the ammount re-radiated by the body at the melting temperature, $\dot{q}_{rad}$, and the amount of heat conducted into the body (i.e. $\dot{q}_{cond}$).

A graphite ablation subroutine already existed for the RETAC code. This subroutine has been updated to provide an accurate representation of graphite mass loss as a function of wall temperature and pressure.

The final model improvement was to provide for a method of limiting the surface temperature of a metallic material to its melting temperature. This was accomplished through a combination of the heat of fusion addition and the melting surface improvement described above. By removing surface material that had reached the melting temperature in a manner dependent on the input heat flux and the heat of fusion, the surface temperature was forced to remain at the melting temperature. The surface temperature limitation was exemplified in another way which was not evident at first. In the previous model, the surface temperature was allowed to exceed the melt temperature and attain an equilibrium value depending on the detailed surface energy balance. This assumption overestimated the amount of surface re-radiation since $\dot{q}_{rad}$ (in

Equation 2) increases with the fourth power of surface temperature. Limiting the surface temperature implied that the net flux to the body was greater. Therefore, internal material was heated to higher temperatures.

These model improvements described above provided for the most accurate calculation to date of material response to accident environments. Any further improvements in the model would not be warranted until final designs were analyzed. In this case, perhaps some 3-D analysis would be appropriate because several geometric simplifications had to be made to conform the real 3-D design to the 2-D, spherically symmetric limits imposed in the current model.

4.3.1.2 Model Descriptions

The RETAC code provides a complex thermal response model for determining the in-depth response of a material system to an external heat flux. Furthermore, internal heat generation is provided for as a code input. The external flux variation with time can be specified on input cards (e.g., to model a fire environment) or be calculated by the codes trajectory subroutines (the aerodynamic flux due to a vehicle reentering the Earth's atmosphere). A detailed surface energy balance is included to account for re-radiation, conduction, and surface mass loss effects. The conductivity, specific heat, heat of fusion, heat generation and density of various internal and surface material components are also input to the code to model the complex response of the material components to the input and internal heat fluxes. Variations of the above material properties with temperature are also included where appropriate.

Geometric parameters are inputed into the code to define various material boundaries. This geometric definition essentially divides the body into a series of nodal regions which interact with one another as heat is transferred between the various nodes. An example of this complex nodal structure is shown in Figure 4-29. Note that for 2-dimensional (2-D) calculations the body is usually divided into five sectors defined by six input angles (θ in Figure 4-29) where θ = 0, 20, 40, 80, 120, and 180 degrees were used in the present study. The 3-D shape of each sector is produced by rotation of the 2-D representation about the θ = 0 axis (i.e., symmetry axis). For example, the conically shaped 3-D representation of sector No. 2 is shown crosshatched in Figure 4-29a.

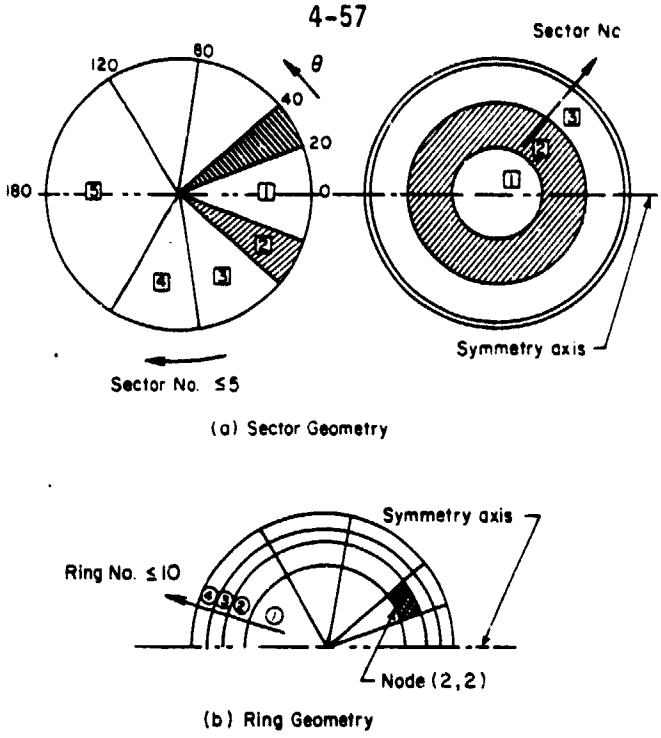

FIGURE 4-29. INTERNAL NODAL STRUCTURE USED TO MODEL THE TRANSIENT HEATING RESPONSE OF VARIOUS WASTE FORM MATERIAL CONFIGURATIONS

The spherical body is further subdivided into a series of up to 10 concentric rings (see Figure 4-29b). The various ring radii usually define spherical shell regions of the body such as the waste boundary, but several rings can also be used within a given material to better define the temperature distribution within that material. The combination of rings and sectors define various nodal regions throughout the body. The location of the (sector = 2, ring = 2) node is shown in Figure 4-29b. It is one of the 20 nodal regions shown in this figure. For 2-D calculations, up to 50 nodal regions were used with a preponderance of nodes being located in the region of highest heat flux. For 1-D calculations such as a spinning reentry or a fire environment, only one sector from 0° to 180° was used. Hence, the nodes reduced to a maximum of 10 concentric spherical shells. Regions of radiation gaps can also be conveniently defined using the ring geometry. Heat transfer across a radiation gap is incorporated in the code and material emissivity is accounted for as an input variable.

Another code input is the vehicle stability mode (i.e. randomly spinning or stable at supersonic speeds). The vehicle may also be allowed to randomly tumble at subsonic speed. For reentry cases, additional code inputs include the initial velocity, altitude and flight path angle as well as the mass to area ratio (M/A) and the initial vehicle nose radius.

The initial temperature distribution of each node (i.e., ring if the initial distribution is spherically symmetric) is an important code input. The temperature distributions used in the present accident response analyses

are shown in Figure 4-30. Note that for the 5 MT PW-4b waste form, wall temperatures are lower than that of the Modified PW-4b material for the reentry vehicle due to the increased cooling required to maintain the waste form centerline temperature below 600 C. However, for the unprotected 5 MT container, in a space environment, the opposite is true, and initial surface reentry temperatures of the Modified PW-4b are lower than the original PW-4b waste mix. Also, note that a 9.5 MT waste form has a slightly higher reentry wall temperature than a 5 MT waste payload for the same Modified PW-4b waste mix.

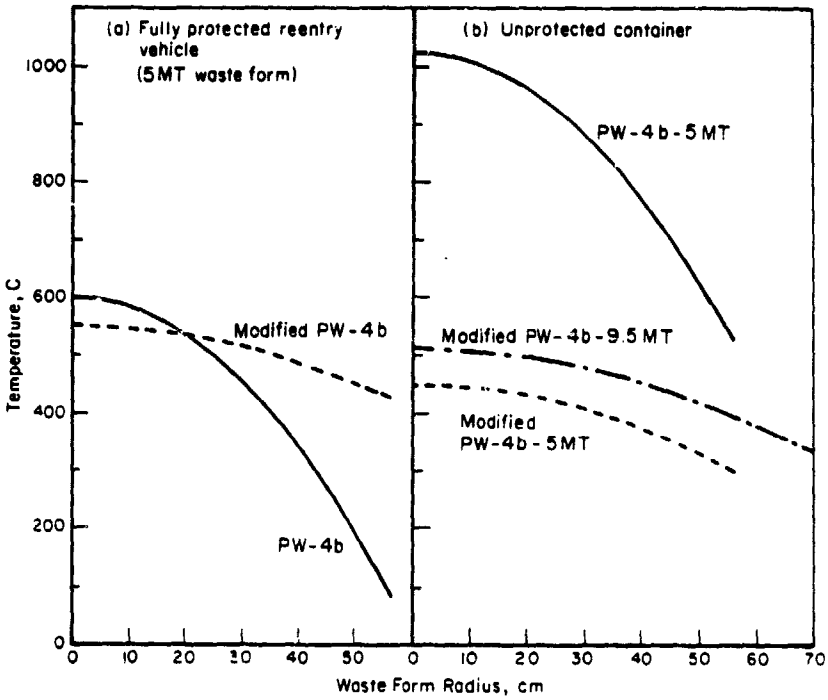

FIGURE 4-30. INITIAL WASTE FORM TEMPERATURE DISTRIBUTIONS FOR THE REENTRY VEHICLE AND THE UNPROTECTED CONTAINER

The reentry vehicle configuration (see reference concept - Section 2.4) supporting a 5 MT waste form payload is a complex material structure as shown in Figure 4-31a. It can be seen from this figure that the material configuration is not strictly 2-dimensional due to the presence of the honeycomb impact dome structure. For this reason, the in-depth thermal response of the reentry vehicle had to be modeled in a somewhat approximate manner. Two spherical, 2-D configurations utilized to model the reentry vehicle in Figure 4-31a, are shown in Figure 4-31b. The frontside (i.e., flight path direction) of the body was modeled using a spherical shell of honeycomb material of the same mass as the impact dome structure. For the backside region, the model was adjusted such that no honeycomb material was included. Ring structure for the 5 MT waste form reentry vehicle configuration is shown in Figure 4-31b. Note that 10 rings were used to model all the various material components.

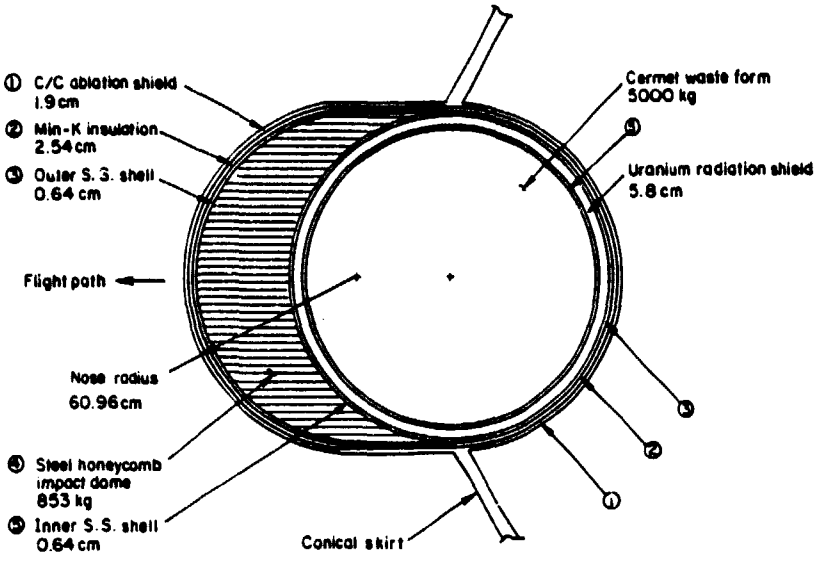

(a) Complex 3-D Reentry Vehicle (RV)

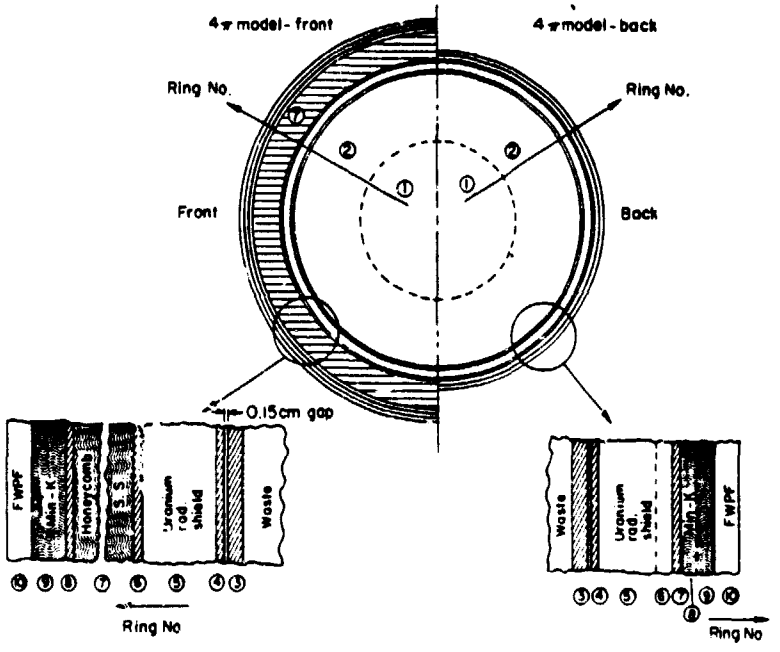

(b) Simplified 2-D Models of Complex RV

FIGURE 4-31. REENTRY VEHICLE MATERIAL DESCRIPTION AND CORRESPONDING MODELS USED IN THE PRESENT ACCIDENT RESPONSE ANALYSES

The specific ring radii for each model are given in Table 4-10. Also note, in Figure 4-31b that a 0.15 cm radiation gap was included in the thermal model. The sector model is not shown in Figure 4-31b because it varied from case to case. For reentry vehicle entry into the Earth's atmosphere, a frontside model was used and five sectors with the 4π-geometry shown in Figure 4-29 were utilized. For vehicle response to the fire environment, only one sector (i.e. 0-180°) was employed but both the frontside and backside models were employed to calculate the in-depth temperature histories of the various materials.

TABLE 4-10. RING RADII VALUES OF THE NODAL REGIONS USED IN THE REENTRY VEHICLE THERMAL RESPONSE CALCULATIONS OF A 5 MT WASTE FORM PAYLOAD CONFIGURATION

Ring Number	Frontside Model		Backside Model	
	Inner Radius, cm	Outer Radius, cm	Inner Radius, cm	Outer Radius, cm
1	0.00	25.40	0.00	25.40
2	25.40	56.26	25.40	56.26
3	56.26	57.53	56.26	57.53
4	57.68	58.32	57.68	58.32
5	58.32	64.16	58.32	63.40
6	64.16	64.80	63.40	64.16
7	64.80	81.05	64.16	64.80
8	81.05	81.69	64.80	66.07
9	81.69	84.23	66.07	67.51
10	84.23	86.13	67.51	69.24

The nodal model used to compute the thermal response of the waste form plus container is shown in Figure 4-32. Both 5000 kg and 9500 kg models are shown to scale in this figure. Eight rings were utilized with the majority of rings being located near the outer surface where the largest temperature gradients are expected to occur. Radii of the various rings are also given in Figure 4-32 and as before, no sector geometry is specified in the figure since it varied according to the particular event being examined.

Another model that was used in the present study involved the presence of a spherical shell of AVCO Fine Weave Pierced Fabric (FWPF) 3-D graphite material on the outer surface of the container shell during reentry (thermal protection). This model is shown in Figure 4-33 where nine rings were employed to better define the near-surface in-depth temperature profile. Note that 0.89 cm of FWPF graphite ablator is shown in Figure 4-33. This amount was twice the recession loss for a stable reentry of the waste form plus container plus graphite aeroshell combination. For a randomly spinning

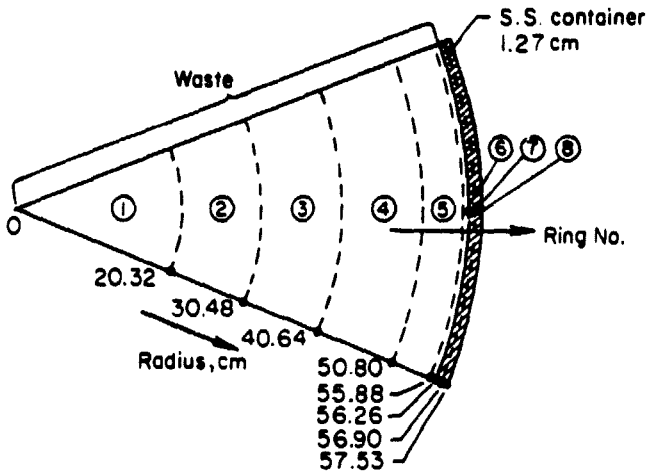

(a) 5000 kg Payload

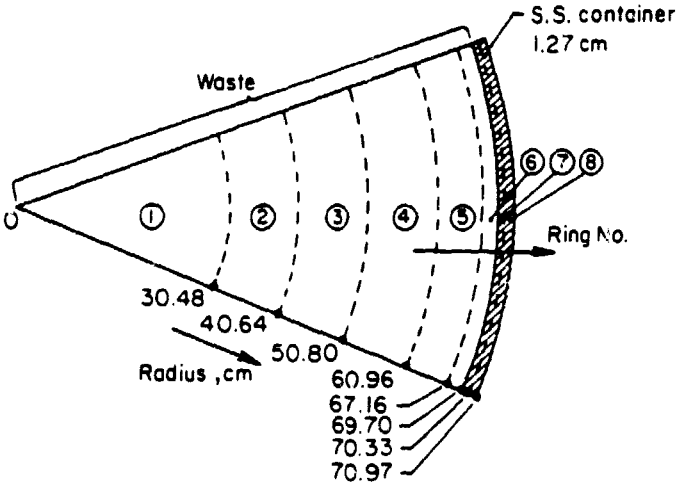

(b) 9500 kg Payload

FIGURE 4-32. NODAL MODELS USED TO COMPUTE THE THERMAL RESPONSE OF THE UNPROTECTED CONTAINER FOR THE 5 AND 9.5 MT WASTE FORM PAYLOADS

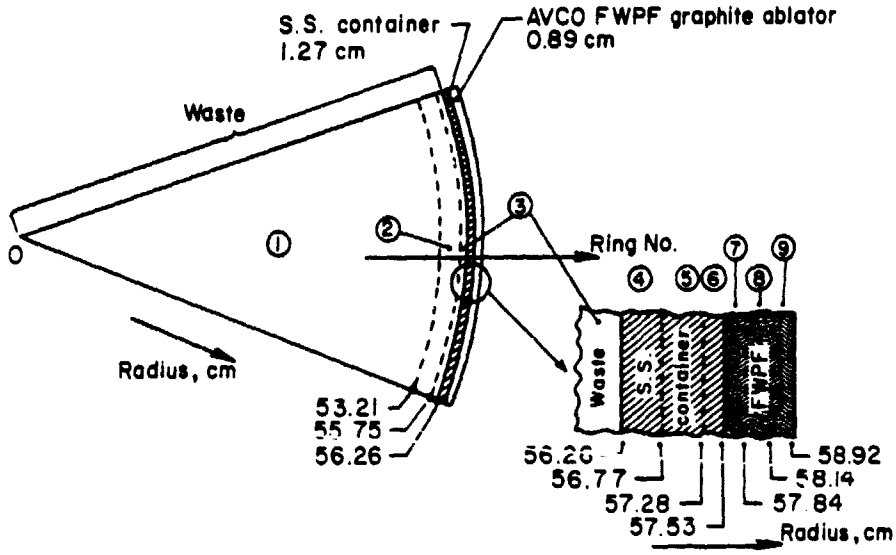

FIGURE 4-33. NODAL MODEL USED TO COMPUTE THE THERMAL RESPONSE OF A GRAPHITE PROTECTED CONTAINER FOR THE 5 MT WASTE FORM

case, less graphite was required and this reduction was also properly modeled by appropriate changes in the radii of Rings 7, 8, and 9 (see Figure 4-33).

The final nodal model used in the present accident response study was set up to represent a waste form, container, plus the uranium radiation shield configurations. This specific arrangement could result from a scenario where the ablation protection on the backside of the reentry vehicle is stripped away by flying debris. Ten rings were used in this model, as shown in Figure 4-34, with four rings being located in the uranium to accurately predict the temperature distribution. The radii of the various rings including the presence of a 0.15 cm radiation gap are also shown in Figure 4-34.

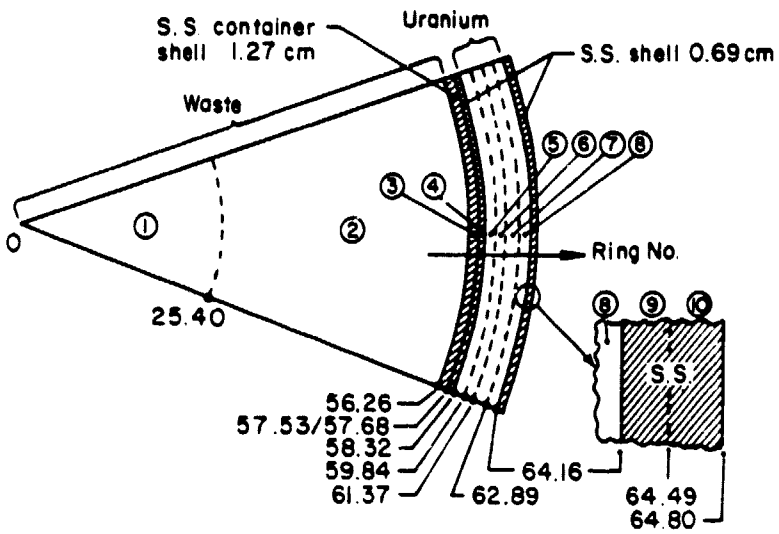

FIGURE 4-34. NODAL MODEL USED TO COMPUTE THE THERMAL RESPONSE OF A CONTAINER PLUS URANIUM RADIATION SHIELD FOR THE 5 MT WASTE FORM

4.3.2 Payload Thermal Analysis

The models described in the previous section were used to predict the response of specific configurations to the various thermal environments, including unplanned reentry into the Earth's atmosphere, as well as, an on-pad launch vehicle fire (see Figures 4-14 and 4-15).

4.3.2.1 Payload Reentry With/Without Reentry Protection

Various types of low probability malfunctions that could occur might lead to the atmospheric reentry of the loaded reentry vehicle or an unprotected nuclear waste container. The RV may reenter after an emergency ejection from the Uprated Space Shuttle cargo bay just prior to achieving orbit, or the unprotected container (having been removed and attached to the payload adapter of the OTV/SOIS configuration) may reenter after a grossly inaccurate OTV burn, coupled with other malfunctions. The aerothermal responses of these configurations were characterized by using the RETAC computer code. Material losses and resultant shape changes were calculated during reentry for various positions around the surfaces. The change in vehicle mass to area ratio (i.e., M/A) due to this mass loss was not accounted for in the trajectory calculations; however, the nose radius was updated as material recession

proceeded. Nose-blunting effects due to this recession lowered the heat flux to the nose region somewhat, since this quantity is inversely proportional to the square root of nose radius.

Both the RV and the unprotected container were assumed to reenter the Earth's atmosphere at a velocity of 7620 m/s, having a -1 degree flight path angle, at an altitude of 91.4 km. These initial conditions were chosen to standardize the reentry analysis. They represent an orbital decay type trajectory which should provide the maximum heat input to the reentry body and hence the maximum in-depth temperature rise and surface mass loss. However, other trajectory scenarios should be examined in future updated payload response studies to insure that this standard reentry assumption is the most conservative case.

The aerodynamically shaped reentry vehicle was assumed to enter in a stable mode. The material response analysis and recession predictions for this case were computed using the frontside spherical model shown in Figure 4-31b. However, the actual vehicle mass, projected area, and nose radius were used in the reentry trajectory and heat flux calculations. The unprotected spherical container was assumed to enter in a stable mode, as well as in a randomly spinning condition. For the unprotected container case, the model shown in Figure 4-32 was used to predict the thermal response characteristics. A summary of the reentry parameters used in the present analyses is given in Table 4-11. The assumed drag coefficient curves used to calculate the ballistic coefficient for the two configurations are shown in Figure 4-35.

TABLE 4-11. INPUT VARIABLES FOR REENTRY ENVIRONMENT ANALYSIS

Parameter	Payload Configuration	
	Unprotected Container	Reentry Vehicle
Mass, kg	5401	14,913
Cross Sectional Area, m^2	1.04	15.69
Mass/Area Ratio, kg/m^2	5193	950.6
Nose Radius, cm	57.53	60.96
Initial Velocity, m/s	7620	7620
Initial Altitude, km	91.4	91.4
Initial Flight Path Angle, degrees	-1	-1
Drag Curve	-- see Figure 4-35 --	

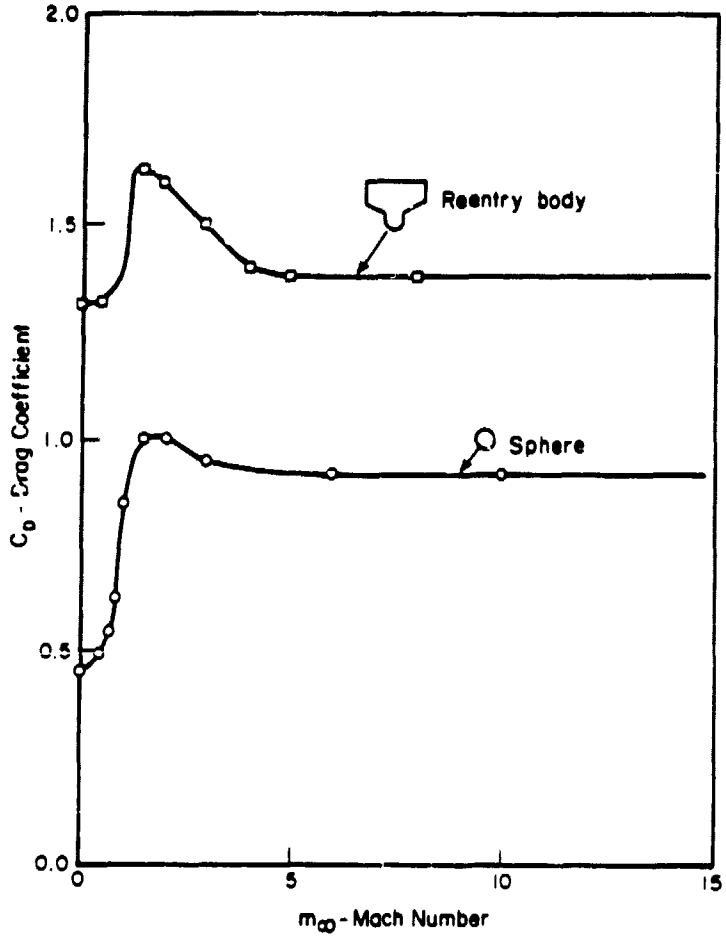

FIGURE 4-35. DRAG COEFFICIENT CURVES USED TO CALCULATE BALLISTIC COEFFICIENT AS A FUNCTION OF VEHICLE MACH NUMBER DURING REENTRY

Example results of reentry trajectory calculations for the two cases indicated in Table 4-11 are presented in Figures 4-36 and 4-37 where stagnation point heating rate, and vehicle velocity are plotted as a function of time after reentry.

For the reentry vehicle itself, the aerothermal analysis indicates that the 1-inch-thick layer of MIN-K insulation is sufficient to protect the impact dome structure, gamma-shield, and 5000 kg (5 MT) waste form from overheating during the reentry heating pulse. In-depth material temperatures as well as the surface temperature at the stagnation point for this reentry case are shown plotted in Figure 4-38. Note, that little temperature rise occurs in the internal structure of the vehicle during reentry.

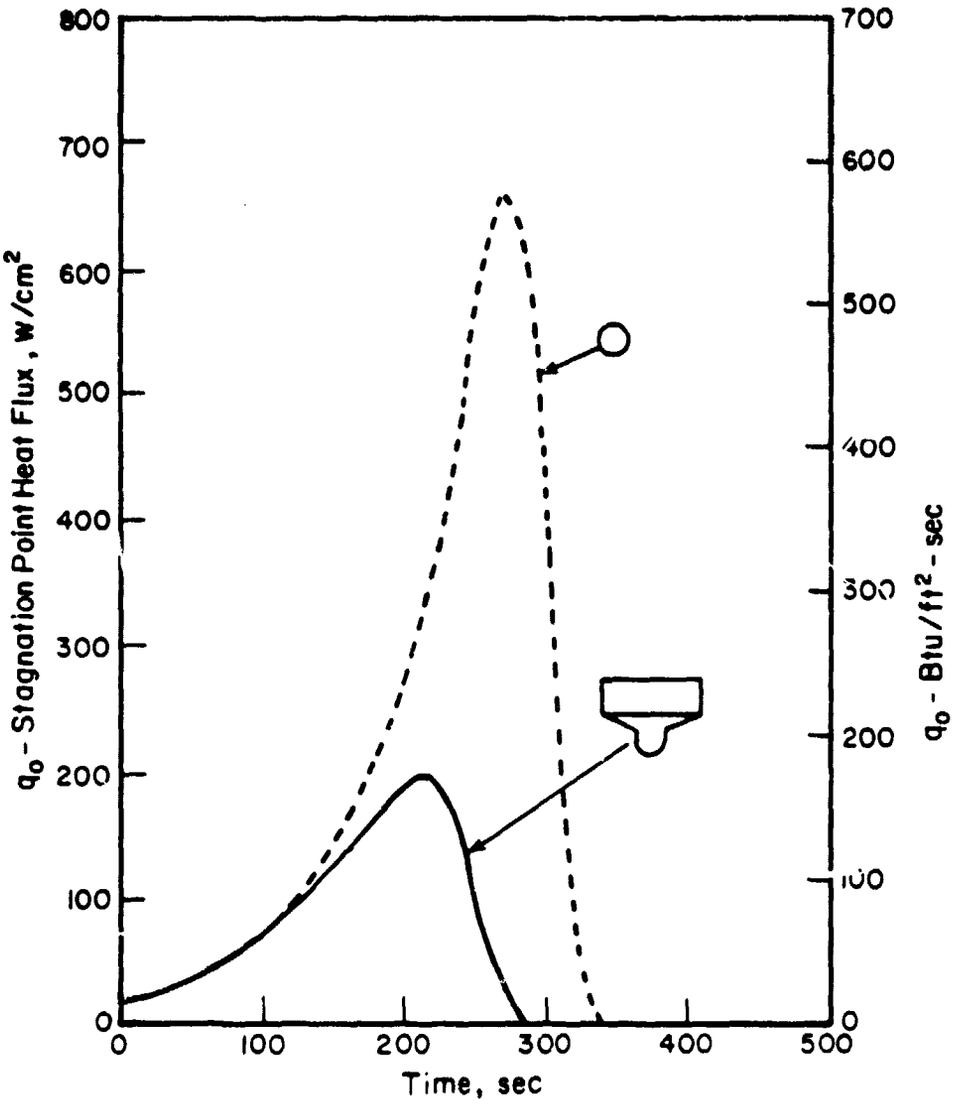

FIGURE 4-36. VEHICLE STAGNATION POINT HEAT FLUX AS A FUNCTION OF TIME FOLLOWING ENTRY OF THE TWO BASIC REENTRY CONFIGURATIONS

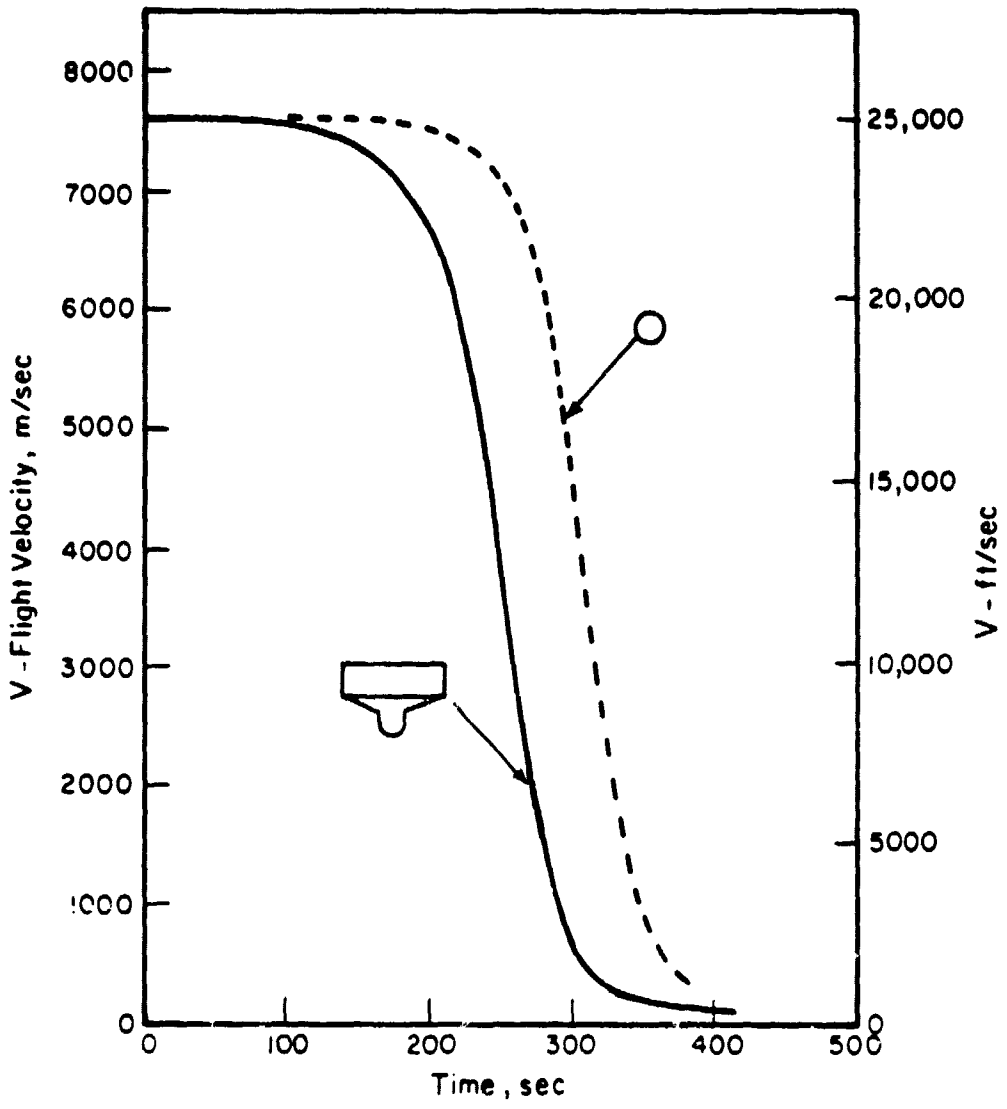

FIGURE 4-37. VELOCITY AS A FUNCTION OF REENTRY TIME FOR THE TWO BASIC VEHICLE CONFIGURATIONS

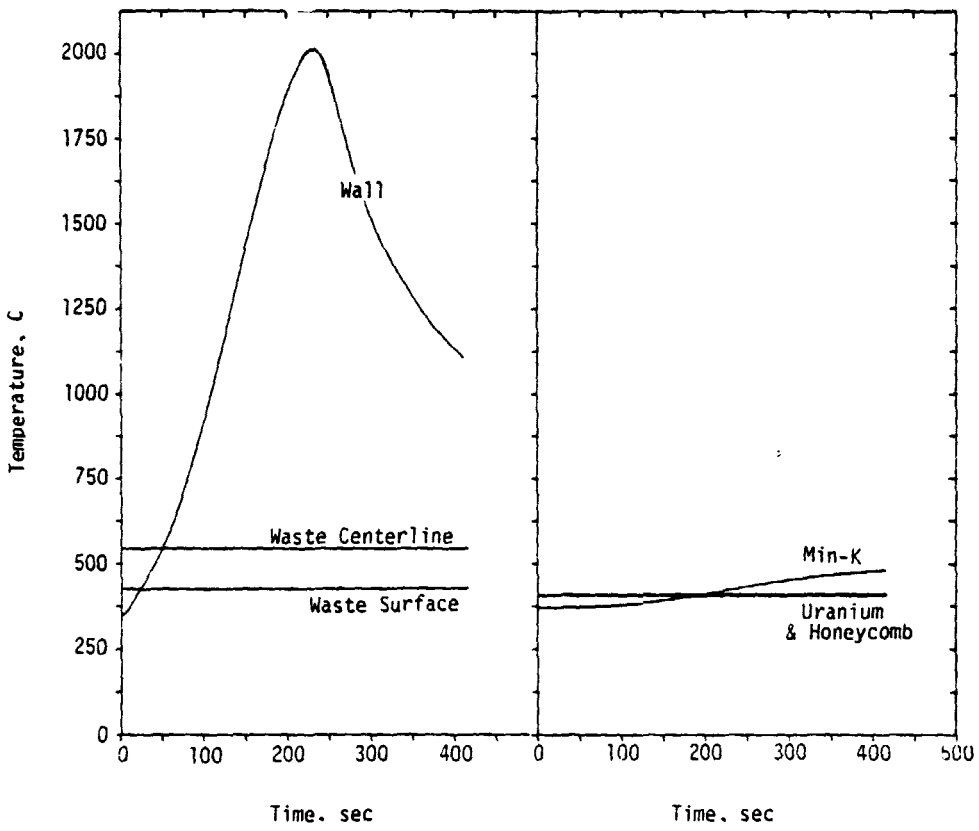

FIGURE 4-38. TEMPERATURE-TIME PLOTS FOR VARIOUS MATERIAL SURFACES AND NODAL REGIONS OF THE REENTRY VEHICLE (5000 KG PW-4b WASTE FORM PAYLOAD) DURING ATMOSPHERIC REENTRY

C-3

The impact velocity of the reentry vehicle is predicted to be 110.9 m/s. The honeycomb steel impact dome is designed to cushion the waste form package to prevent gamma-shield rupture at impact. However, heat generated within the waste form package will increase with time after impact. The material impact temperature shown in Figure 4-38 could be used as an initial condition to predict the thermal history of the reentry vehicle container after impact. This analysis was not performed in the present study, but system overheat problems would be expected to occur unless the Modified PW-4b waste mix or other "cooler" mixes are utilized.

For an unprotected 5000 kg waste form surrounded by only a 1.27 cm thick stainless steel container, the aerothermal analysis indicates that severe material recession is predicted to occur for the stable reentry mode. Calculations of this recession were performed for both stable and spinning reentry modes, as well as for two initial temperature scenarios (see Table 4-12). Initial temperatures for both the reference PW-4b and Modified PW-4b cases were examined and it was found that the resultant recession was quite sensitive to the initial material temperature values. The difference in internal heat generation, itself, was not an important factor in the calculation. Recession results for the above cases are given in Table 4-12. Note that only for the case of Modified PW-4b and a randomly spinning reentry, is a zero waste recession predicted. For all other cases, a varying amount of waste material is expected to be dispersed into the Earth's atmosphere.

TABLE 4-12. RECESSION RESULTS FOR REENTRY OF VARIOUS UNPROTECTED CONTAINER CASES

Case	Waste Mix[a]	Reentry Mode	Initial Waste Form Surface Temperature, K	Total Recession, cm	Waste Recession, cm
1	PW-4b	Staple	800	19.16	17.89
2	PW-4b	Spinning	800	1.72	0.45
3	Modified PW-4b[b]	Staple	573	14.09	12.82
4	Modified PW-4b[b]	Spinning	573	0.95	0.00

Notes: (a) Waste mix determined heating rate and initial temperature condition.
(b) Modified PW-4b assumes 90 percent removal of Cs and Sr from the PW-4b mix.

A detailed aerothermal analysis was also completed for the case of a Modified PW-4b 5000 kg waste form, including a stainless steel container plus a 4π shell of AVCO 3D Fine Weave Pierced Fabric (FWPF) ablation protection.*

*Conceptually, the AVCO FWPF could be applied to the container by winding it with carbon fiber yarn, impregnating it with carbon fiber, then properly processing it to the desired properties. The internal heat generation of the waste form might very well aid in the fabrication process.

It was found that 0.89 cm thickness of ablator was required to provide a 100 percent margin of safety for ablator burn through during a stable reentry (a GPHS design requirement). However, the results of temperature calculations shown in Figure 4-39 indicate that the stainless steel container beneath the graphite ablation member completely melted over most of the forward portion of the waste form mass (see Figure 4-40). The waste form surface itself did not melt, but a question arises as to possible release of waste material if the unsupported graphite aeroshell were to structurally fail during reentry, thus exposing the waste form directly to the reentry environment.

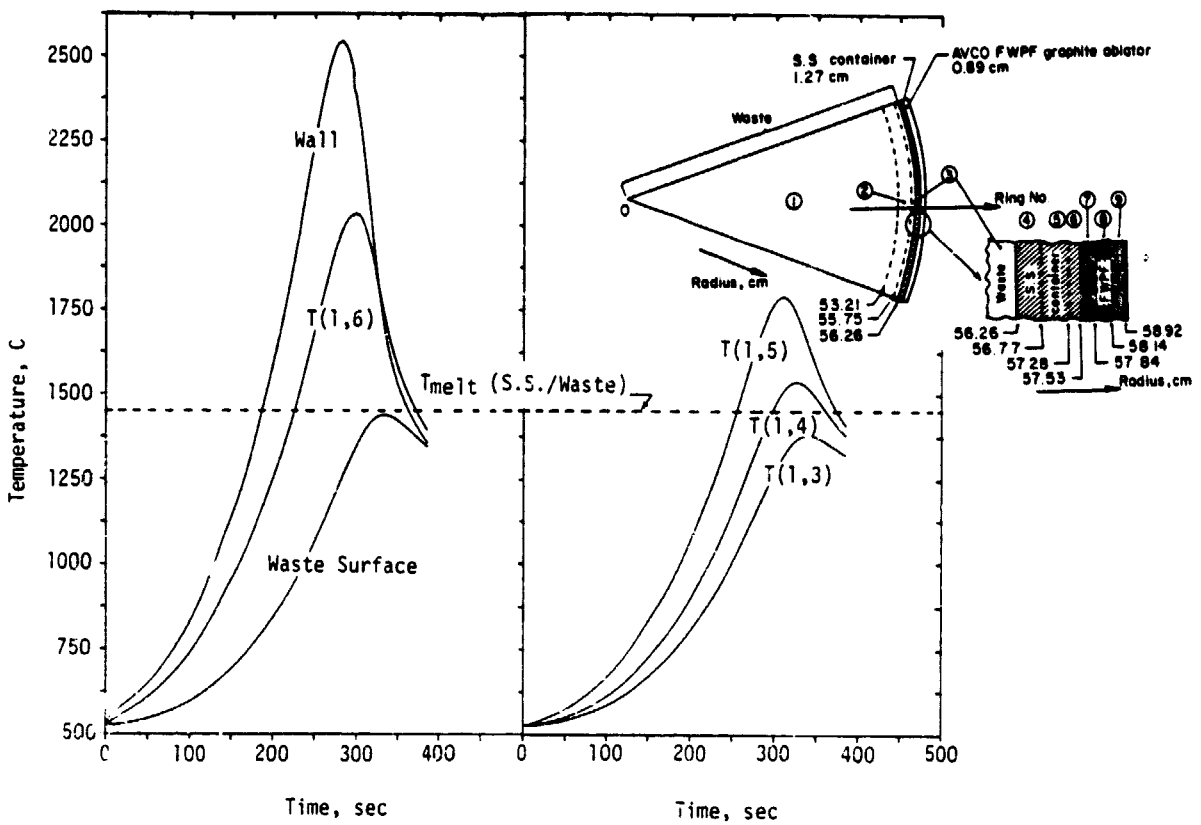

FIGURE 4-39. TEMPERATURE-TIME PLOTS FOR VARIOUS MATERIAL SURFACES AND NODAL REGIONS OF THE 5000 KG WASTE FORM IN A GRAPHITE PROTECTED AEROSHELL DURING ATMOSPHERIC REENTRY

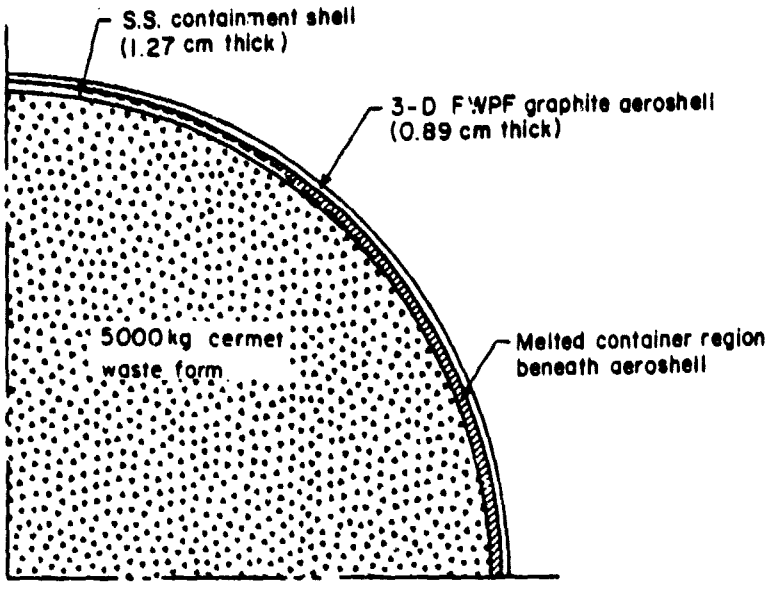

FIGURE 4-40. EXTENT OF MELTING OF THE STAINLESS STEEL CONTAINER UNDER THE GRAPHITE SHELL ABLATION MEMBER

For the spinning reentry case, only 0.25 cm of 3D-FWPF graphite ablator thickness is required for 100 percent margin of safety on recession. Also, no container material melting is predicted to occur. Therefore, the 4π graphite protection, spinning reentry case will result in no predicted release of waste to the atmosphere for the initial temperature profiles chosen (see Table 4-12).

In summary, some extra thermal protection of the waste form is required, other than the thin stainless steel container shell, to prevent severe recession of the waste form during a possible stable reentry. Furthermore, the addition of a 4π graphite ablation shell will reduce, but cannot guarantee a zero mass loss because the stainless steel container melts and may not structurally support the graphite material. Following a detailed structural analysis, it is very likely that some other type of higher melting point container material would be recommended to ensure that no waste release occurs.

Impact velocity of the unprotected container is 365 m/s which is nearly four times that of the reentry vehicle configurations. There is little impact protection offered by the stainless steel container or even an additional graphite aeroshell. The container impact on land is therefore expected to create a large crater with the high likelihood of structural damage. In any event, since no radiation protection would be available, a significant radiation hazard would exist in the impact region, unless the waste form is buried deep enough under the surface. The probability of traces of radioactivity being present in airborne material released from the crater zone should be examined, as well as the consequences of a possible breach due to melt down.

4.3.2.2 On-Pad Launch Vehicle Pad Fire Analysis

Three configurations were examined to determine the in-depth material response to an on-pad launch vehicle fire. The first two configurations embodied different orientations of the entire reentry vehicle. Both the backside and frontside model orientations given in Figure 4-31b were utilized to examine the effects of the honeycomb impact dome structure which existed only on the nose region of the reentry vehicle. The third configuration included the waste container and radiation shield only and neglected the reentry protection and impact structure (see Figure 4-34). The latter case simulates the case where a possible fragment impact event would strip away the reentry vehicle ablation shield on the backside (no impact protection exists on the backside).

Transient material response of these configurations was analyzed using the RETAC computer code. Input radiant heat flux from the fire is given in Figure 4-14. It should be noted that the total heat flux from the liquid fire is significantly less than that of the worst-case solid propellant fire, used in previous accident response analyses (Phase II study--Reference 4-71). This heat flux was assumed to be incident on the entire surface of the configuration being examined. Reradiation by the entire material surface was also included. For this reason the wall temperature approaches an equilibrium limit. In-depth temperature history calculations proceeded for 1 hour following the natural termination of the fire. This extended analysis was performed to examine the possibility that auxillary cooling could not be applied to the waste form package until 1 hour after fire burnout.

The heat of fusion of all material components was accounted for in the analysis and surface metallic material was removed as the melting temperature was reached and the heat of fusion supplied. For the cases where a graphite outer shell was present, it was assumed that no graphite material loss occurred. This is a good assumption for a fire environment because nearly all the available oxygen is removed by the combustion process. Therefore, during the fire, little graphite oxidation is expected. However, after the fire ceases, some oxidation may occur because the graphite surface is now hot and oxygen is available. An example of such a material loss event is that of a piece of charcoal after initial heating by an auxillary flame. This possibility of postfire graphite loss was not accounted for in the present analysis, since it was assumed that sufficient cooling would be supplied by the fire fighting equipment to lower the surface to below the oxidation temperature limit of approximately 1100 C.

The in-depth thermal responses of various material components of the reentry vehicle to the fire environment are shown in Figure 4-41. Temperatures for the PW-4b and Modified PW-4b 5000 kg-based reentry vehicles are given in this figure for comparison purposes to indicate the effects of inital temperature distributions and internal heat generation on the overall materials thermal response. It should be noted that loss of coolant was also assumed to accompany the explosion/fire event such that the contribution of internal heat would be included in the analysis. When the results of Figure 4-41 were compared to calculations that assume coolant loss only, it showed

that the internal heat generating term tends to dominate the external fire heat flux effect, especially for the waste form. This dominance occurs because the MIN-K insulation material is excellent for keeping the fire generated heat from penetrating very far into the reentry vehicle surface. It also retards internally generated heat from escaping. Finally, the results in Figure 4-41 indicate that the PW-4b waste mix temperature increases rapidly with time due to the increased internal heat generation. Therefore, waste payload overheat problems are likely to occur unless auxiliary cooling is somehow applied to the configuration (see Section 3.4 for discussion of temperature rise rate).

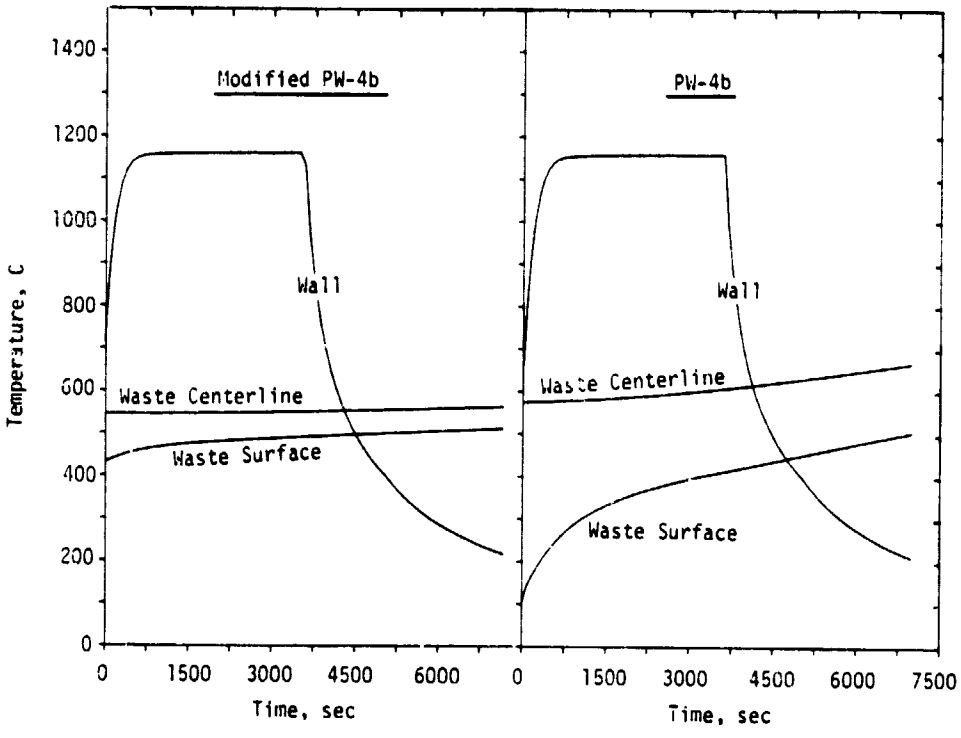

FIGURE 4-41. TEMPERATURE-TIME PLOTS FOR THE WASTE SURFACE AND WASTE CENTERLINE AS A RESULT OF A LAUNCH VEHICLE FIRE FOR BOTH PW-4b AND MODIFIED PW-4b 5000 KG WASTE FORM PAYLOADS ENCLOSED IN THE REENTRY VEHICLE CONFIGURATION

The thermal response of the reentry vehicle without impact and thermal protection systems shield (simulating the loss of TPS on the backside) to a launch pad fire environment is shown in Figures 4-42 and 4-43. In Figure 4-42 results for the waste form response are shown, and in Figure 4-43, the

uranium radiation shield component temperatures are presented. Note, that when no thermal protection is present, the fire heat flux adds considerably to the temperature rise of the waste material. In fact, within 1 hour after the fire, the waste form temperatures approach a value indicative of the case of a 6 hour coolant loss. Uranium temperature history data, shown in Figure 4-43, indicate that the outer stainless steel shell (i.e., Node 9) remains well below the melting temperature, and that the temperature drops off initially after the fire burns out. However, if the analysis were extended to include a few more hours, the uranium radiation shield temperature (i.e., Nodes 5 through 8) would increase, due to the internal heat generation.

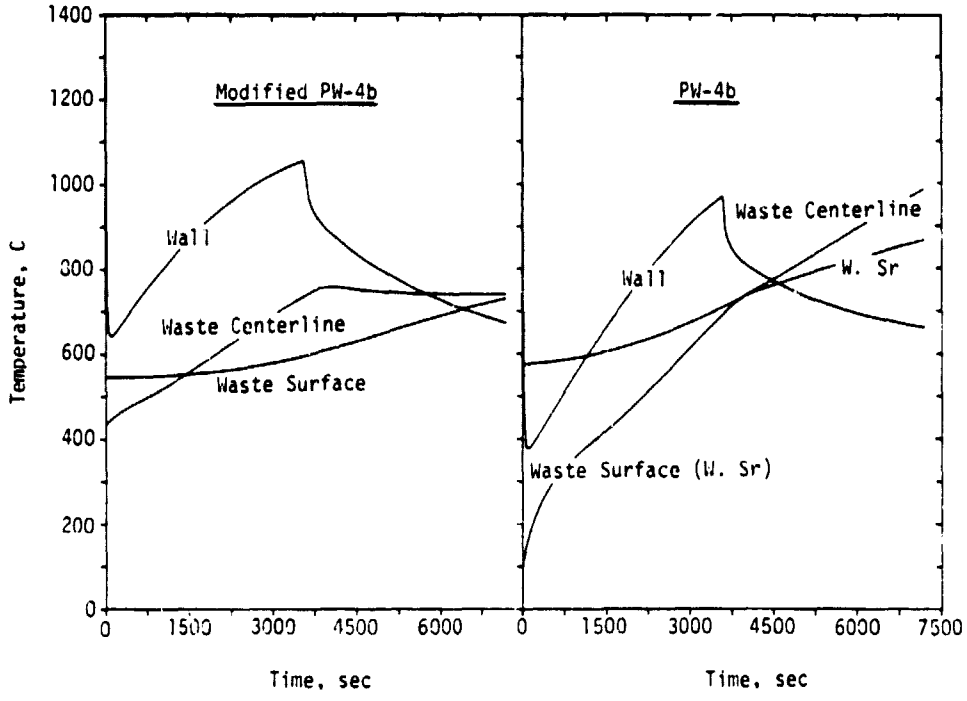

FIGURE 4-42. TEMPERATURE-TIME PLOTS FOR THE WASTE FORM AS A RESULT OF AN ON-PAD LAUNCH VEHICLE FIRE FOR PW-4b AND MODIFIED PW-4b 5000 KG WASTE FORMS SURROUNDED BY CONTAINER AND RADIATION SHIELD ONLY

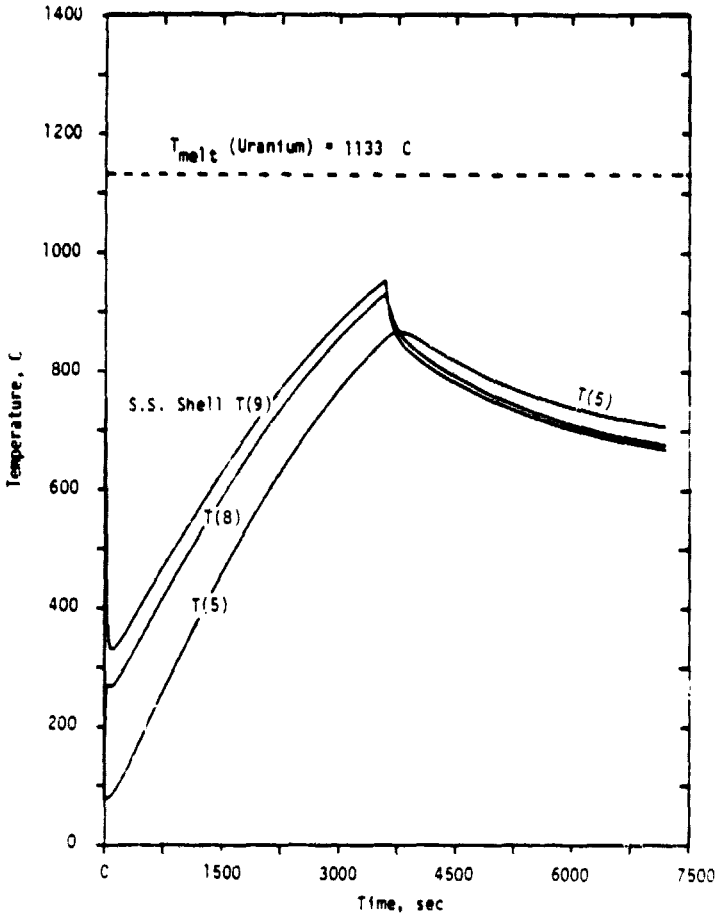

FIGURE 4-43. TEMPERATURE-TIME PLOTS FOR THE URANIUM RADIATION SHEILD SURROUNDING A 5000 KG PW-4b WASTE FORM MIX AS A RESULT OF AN ON-PAD LAUNCH VEHICLE FIRE

4.3.3 Release Predictions

For an inadvertent reentry and an on-pad launch vehicle fire, the thermal analysis given in Section 4.3.2 indicated that no waste form release is expected to occur for the fully protected reentry vehicle configuration. However, for an unprotected container, severe stagnation point recession was predicted to occur during stable-mode atmospheric reentry as discussed in Section 4.3.2.1. The resultant change in waste form shape due to recession following a stable reentry is shown in Figure 4-44. Note that severe recession occurs on the entire forward portion of the body for the stable reentry attitude. The percent mass loss accompaning this severe recession was computed using the recession radii obtained from Figure 4-44; the resultant percent of mass loss values are also shown in this figure. Note that 11.2 percent of the 5000 kg waste form mass was predicted to be released into the atmosphere for the Modified PW-4b waste form configuration. Also note, that

due to the expected higher initial temperatures, an additional 12.6 percent mass loss (23.8 percent total) was predicted to occur for the PW-4b waste payload. Much less release is predicted to occur for a randomly spinning unprotected container. Calculations for the spinning case indicate that the release amounts to 2.4 percent of the initial 5000 kg payload for the PW-4b waste form and no release for the Modified PW-4b waste form.

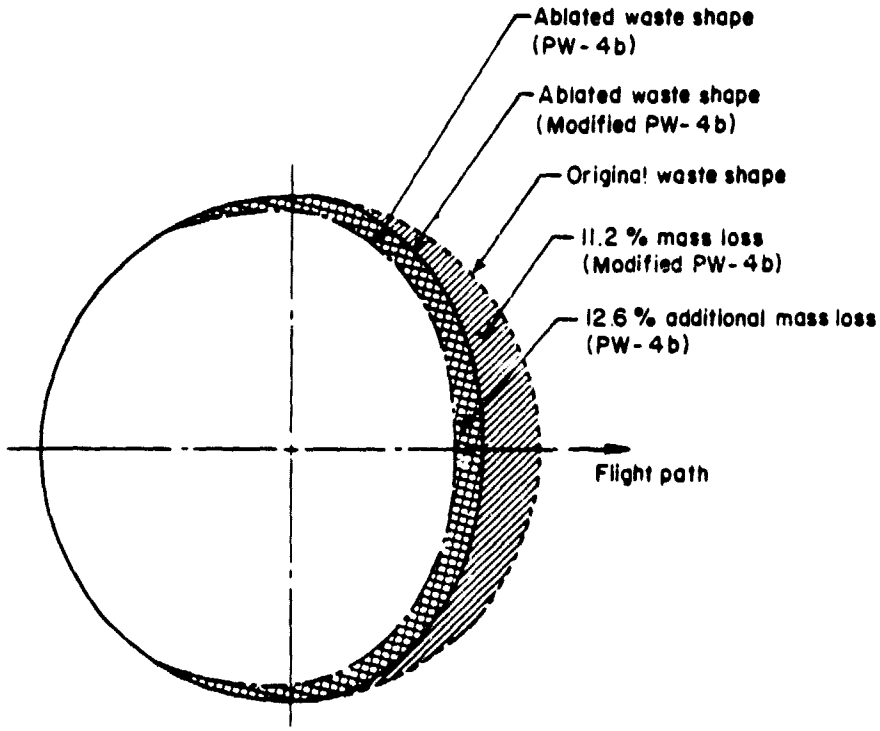

FIGURE 4-44. WASTE FORM SHAPE CHANGE FOLLOWING ATMOSPHERIC REENTRY OF AN UNPROTECTED 5000 kg WASTE MASS

Waste release results for the 9500 kg Modified PW-4b waste form plus unprotected container also show a significant mass loss of 10.6 percent for the stable mode during inadvertent reentry and no release for the spinning case. This percent release is less than the smaller 5000 kg waste form but more material is actually released due to the larger initial mass. These calculations were performed in support of the preliminary HLLV safety assessment (see Section 4.4).

A summary of mass released into the Earth's atmosphere due to the inadvertent reentry of various unprotected containers is given in Table 4-13.

TABLE 4-13. WASTE MASS RELEASE DURING UNPROTECTED WASTE FORM PLUS CONTAINER REENTRY

Reentry Mode	Mass/Area, kg/m^2	Waste Mix	Initial Waste Form Wall Temperature, K	Initial Waste Form Mass kg	Percent Released	Mass Released, kg
Stable	5193	PW-4b	800	5000	23.8	1190
Stable	5193	Modified PW-4b	573	5000	11.2	560
Spinning	5193	PW-4b	800	5000	2.4	120
Spinning	5193	Modified PW-4b	573	5000	0.0	0
Stable	6622	Modified PW-4b	608	9500	10.6	1007
Spinning	6622	Modified PW-4b	608	9500	0.0	0

Note: (a) Iron/nickel-based cermet waste form.

The large disparity in waste mass loss due to randomly spinning and stable reentry indicates that some vehicle stability analysis would prove helpful in support of a more accurate assessment of unprotected waste form release during inadvertent reentries. It is likely that a strictly stable reentry produces a conservative release prediction. Also, a randomly spinning mode is not likely to occur, but rather, spinning about some particular body axis such that an increased amount of nonuniform 3-D ablation would occur. The actual waste mass release is likely to be between the limits given in Table 4-13. It should also be noted that aerodynamic techniques to induce vehicle spinning could be utilized to reduce the amount of waste release.

Due to these large predicted releases of waste mass, the case for a 4π graphite ablation member surrounding the unprotected waste container was examined (see Figure 4-33). However, uncertainty as to the structural integrity of the stainless steel container shell, makes it impossible to predict waste form mass release at this time. It would be less than indicated in Figure 4-44 because of the protection afforded by the graphite member, but how much less, cannot be easily determined.

Finally, with regard to the the PW-4b waste form, container, and radiation shield configuration as shown in Figure 4-34, no release is predicted to occur due to an on-pad launch vehicle fire provided that cooling is initiated within approximately 1 hour after fire burnout. This time limit would be significantly extended for the Modified PW-4b waste mix, because of the reduced internal heat generation rate.

4.3.4 Recommended Design Changes

Based upon the release analysis given in the previous section, design changes can be suggested to improve the accident response of the reference

waste payload configuration. In the case of the on-pad launch vehicle fire environment, no design changes are recommended at this time, since no release is predicted. However, the Modified PW-4b cermet waste form will have a decreased probability of over heating due to loss of coolant, so, it is recommended that this waste form mix be utilized based upon this safety concern.

For an inadvertent reentry of the waste form plus container, it was found that large amounts (approximately 1 MT) of waste could be released into the Earth's atmosphere under certain conditions. Therefore, some design recommendations have been made.

Several methods available to reduce the waste mass loss are indicated by the results shown in Table 4-13. These techniques are:

- Aerodynamic devices to insure vehicle spinning during reentry
- Reduction in initial surface temperature
- Reduction in the vehicle ballistic coefficient
- Addition of a reentry protection shell to the outside wall of the sphere
- New container material

Spinning the vehicle distributes the heat and thereby reduces mass loss. Therefore, following a detailed reentry stability analysis, methods could be devised to destabilize the unprotected spherical container. For example, small protrubances and/or indentations properly placed around the vehicle to disrupt symmetry could cause rotation of the waste form about some particular body axis. This method may not eliminate mass loss, but it will dramatically reduce it.

Results given in Table 4-13 indicate that waste mass loss is approximately proportional to the initial surface temperature squared. This dependency occurs because more heat is required to raise the cooler waste material to its melting temperature. The simplest method of reducing the waste form wall temperature would be to use the Modified PW-4b waste mix which has 90 percent of the Cs and Sr removed. Smaller waste form payload sizes would also reduce surface temperature, somewhat.

Further examination of Table 4-13 shows that waste release is roughly proportional to the vehicle ballistic coefficient squared. This dependance arises because the total heat input to a reentry vehicle varies directly with its ballistic coefficent. The simplest way to reduce the ballistic coefficient is to reduce the payload mass by reducing the waste form radius, (i.e., reduce the mass to area ratio). However, a more efficient way is to make the waste form hollow and maintain the same outside radius or even increase the outside radius to maintain the same mass. (The hollow sphere concept would also be advantageous during normal operation--thermal limits.) The mass to area ratios of a solid and hollow sphere are related to their respective outside radii, R_s and R_h, by the following equation:

$$R_h = R_s \left[\frac{(M/A)_s}{(M/A)_h}\right]^{1/2} \quad (16)$$

where $(M/A)_s$ and $(M/A)_h$ are the mass to area ratios (i.e., ballistic coefficient) for the solid sphere and the hollow sphere, respectively. To maintain constant waste payload mass, the inside radius of the hollow sphere is given by:

$$R_i = (R_h^3 - R_s^3)^{1/3} \quad (17)$$

Given the initial sphere radius, Equations (16) and (17) can therefore be used to determine the dimensions of a hollow sphere of equal mass, once the desired increase in M/A is chosen. For example, to double the M/A ratio [i.e., $(M/A)_s/(M/A)_h = 1/2$] for the 5000 kg waste form the initial solid sphere radius of 56.26 cm should be increased to 79.56 cm and an inside radius of 68.79 cm should be used for the hollow sphere. This configuration is estimated to have a waste form release of only 140 kg, if the Modified PW-4b waste mix is assumed (i.e., 2.8 percent mass loss).

It is shown in the Section 4.3.3 that addition of a graphite ablation shell surrounding the container would likely produce a decrease in the waste mass release. However, quantifying the reduction is difficult because the container completely melted on the forward stagnation point region for a stable reentry mode. This container melting could possibly cause structural failure of the graphite shell, thus negating some of it's mass loss reduction capability. Again, destabilization techniques would reduce, if not eliminate, mass loss, because container melting was not predicted for a randomly spinning reentry stability mode.

Another way to improve reliability of the ablation shell concept would be to replace the stainless steel container shell with another material that has a higher melting temperature. It could also be important that this new material have thermal properties similar to those of stainless steel. This latter restriction is desirable to insure that substitution of the new material to eliminate the melting problem, would not cause some other problem to occur.

Several candidate ceramic and metallic materials that could be used to replace the stainless steel container are given in Table 4-14. Also listed in this table are the melting temperature, specific heat, conductivity, density, and product of density and specific heat for these candidate high-melting-point materials. The properties of stainless steel are also listed in Table 4-14 for comparison purposes. Many of these materials have similar properties to those of stainless steel, and could serve as the substitute container shell. Economics, manufacturing difficulty, and other factors would be instrumental in the final choice.

TABLE 4-14. CANDIDATE MATERIALS TO SUBSTITUTE FOR STAINLESS STEEL IN A HIGH MELTING POINT CONTAINER

Material	Heat Capacity-C_p at 400 C, cal/g-C	Melting Pt., C	Conductivity at 400 C, W/cm-C	Density, g/cm^3	$C_p \cdot \rho$, cal/cm^{3}C
Metals:					
SS 304	0.16	1450	0.2	7.8	1.25
Niobium	0.07	2700	0.5	8.6	0.60
Tungsten	0.04	3650	1.2	19	0.76
Zirconium	0.07	1850	0.2	6.5	0.46
Titanium	0.13	1800	0.2	5.0	0.65
Molybdenum	0.06	2800	0.12	9.9	0.59
Ceramics:					
Alumina	0.30	2000	0.10	3.6	1.08
Zirconia	0.15	2700	0.02	5.6	0.84
Silicon Carbide	0.30	2700	0.33	3.2	0.96
Beryllium Oxide	0.45	2500	0.8-1.0	2.97	1.34
Boron Nitride	0.40	3200	0.42	2.25	0.90

In summary, a series of design modifications are available to reduce and/or eliminate waste material release into the atmosphere during an inadvertent reentry of an unprotected container. The choice of the most appropriate techniques/concepts should be evaluated during the detailed systems concepts studies that are expected during 1980.

4.4 Preliminary HLLV Safety Assessment

The HLLV concept considered is a design proposed in Satellite Power System (SPS) studies. It is shown in Figure 2-13 and is described in Section 2.8.5. Principal differences between the HLLV and reference concept, as applied to the waste disposal operation are summarized in Table 2-9 (also see Section 2.8). The HLLV could reduce disposal transportation costs from $8000/kg (value for Uprated Shuttle) to $2400/kg (see Section 4.4.2 for details).

The HLLV represents a moderate step forward in vehicle design (2-stages fully reusable) from the reference Uprated Space Shuttle concept, and assumes moderate improvements in some vehicle subsystems. From a safety standpoint, use of the HLLV should not be significantly different from use of the Uprated Space Shuttle. Flight operations and payload handling techniques would be very similar, and the overall reliability of the HLLV should be comparable to that of the Uprated Space Shuttle. However, the HLLV is a much larger vehicle with greater payload capability (231,000 kg versus 45,400 kg for the Uprated Space Shuttle). Hence, the potential for more severe accident environments (e.g., much more propellents involved in the explosion and ensuing fireball) exists, as does the potential for more serious consequences of protection system failure--larger HLLV waste packages have a higher release potential.

This preliminary analysis discusses the hazard posed by the two most serious accident possibilities: on-pad or near-pad explosion and fire, and inadvertent reentry with an uprotected payload.

4.4.1 On-Pad or Near-Pad Explosion/Fire

The HLLV uses the same propellents (RP-1, hydrogen, oxygen) as does the Uprated Space Shuttle, and in approximately the same proportions. However, the HLLV requires over three times the total propellent load of the Uprated Shuttle. Thus, in the event of an on-pad or near-pad failure a larger explosion and fire environment could result. Table 4-15 compares typical on-pad accident environments of the HLLV and Uprated Space Shuttle, that have been compiled from data developed in Section 4.2.

TABLE 4-15. COMPARISON OF HLLV AND UPRATED SPACE SHUTTLE ON-PAD ACCIDENT ENVIRONMENTS

Environment[a]	Uprated Space Shuttle	HLLV
Fireball		
Initial Fireball Temperature, K	3057	3058
Time to Fireball Liftoff, s	7.27	8.90
Time to Stem Liftoff, s	10.9	13.4
Heat Flux at Stem Liftoff, kW/m^2	2470	2700
Residual Fire		
Fire Temperature, K	1366	1366
Duration, sec[b]	3600	3600
Blast Wave[c]		
Side-on Overpressure, N/cm^2	250	410
Reflected Overpressure, N/cm^2	1700	3050
Side-on Impulse, N-s/cm^2	2.0	4.6
Reflected Impulse, N-s/cm^2	15.0	35.0
Fragments		
Mean Fragment Velocity, m/s	200	250
Mean Fragment Size, m^2	0.3	0.3
Fragment Flux, number/m^2	0.8	0.9

Notes: (a) Data from work performed in Section 4.2.
(b) Proper dike design is assumed to limit residual fires to 1 hour.
(c) Assumes a distance from COE of 20 meters and a 10 percent explosive yield for both cases. In reality, the percent yield is likely to be less for the HLLV than the Uprated Space Shuttle.

The data in the table (constructed from data in Section 4.2) indicate that the accident environments for these two vehicles actually are predicted to be very similar. The blast wave environment for the HLLV is significantly higher; however, in reality this is not expected to be the case. The yield for the HLLV is expected to be lower than the yield for the Uprated Shuttle for a similar event. One can conclude, from reviewing these data, and with the assumption that the reentry vehicles are properly designed, such that adequate margin exists for surviving the on-pad accident, that there is little difference in the overall risk. On the other hand, if the reentry vehicle/protection system does fail, the amount of radioactive material released in a single incident is potentially much greater for the HLLV (28,500 kg) than for the Uprated Space Shuttle (5000 kg) case. This fact is of little concern; however, since proper design (and overall concept) can all but eliminate the probability of such a release.

4.4.2 Inadvertent Reentry

Each HLLV launch will orbit three OTV/SOIS/waste package configurations. Each waste/package contains a spherical 9,500 kg cermet waste form. Thus, failure of an OTV, following removal of the payload protection system could result in the reentry of a 9,500 kg waste mass. In the equivalent event for the Uprated Space Shuttle case, 5,000 kg of waste mass could reenter. For one event, the larger mass will result in a larger upper atmospheric release of radioactive material and would produce increased health effects. Assuming a similar unprotected waste package configurations and a nonspinning reentry mode, the reentry of the 9,500 kg HLLV waste package would result in the release of 1007 kg of waste, as compared to 560 kg for the 5,000 kg Uprated Space Shuttle package (see Section 4.3.3). This increased release for the HLLV would result in an 80 percent increase in total health effects. Therefore, the hazard potential for a single inadvertent reentry accident (assuming no-change in waste package design) is greater for the HLLV than for the Uprated Space Shuttle. However, OTV reliability would be expected to be the same in both cases, and the HLLV option requires fewer OTV flights for the total program. Thus, the probability of a failure occurring is less for the HLLV option. The net result is that overall program risk and potential health effects can be expected to be approximately the same for both options.

As noted, the above assessment assumes the HLLV option uses the same waste package design as the Uprated Space Shuttle. Under that assumption a significant savings in space Transportation cost is achieved. Each HLLV mission (HLLV + 3 OTV'S + 3 SOIS's) costs $68 million (MSFC provided) and disposes of 3 x 9500 kg or 28,500 kg of waste. Each Uprated Space Shuttle mission (Uprated Space Shuttle + 1 OTV + 1 SOIS) costs $40 million (MSFC provided) and disposes of 5000 kg of waste. Thus, for the Uprated Space Shuttle, disposal costs $8000/kg, and for the HLLV, it costs $2400/kg. The HLLV cost is less than one-third the Shuttle cost. If risk becomes a more critical issue, then some (or all) of the transportation cost savings could be sacrificed to further reduce risks. Individual HLLV waste spheres could be made smaller and the weight saved could be used to increase protective packaging/shielding. For example, in the limiting case, where the HLLV waste spheres are reduced to the point where HLLV transportation cost equals Uprated Space Shuttle cost, the HLLV spheres could be encased in a 22 cm thick steel shell. This would significantly reduce the risk associated with all types of accidents. Therefore, it may be concluded that the HLLV option holds significant potential for reducing cost and/or reducing risk.

4.5 References

4-1. "Updated Safety Analysis Presentation -- Multi-Hundred Watt RTG Program, LES 8/9 Mission," Contract No. AT (29-2)-2831, General Electric, Energy Systems Programs, Space Division, Philadelphia, Penn. (January 1974).

4-2. "Multi-Hundred Watt Radioisotope Thermoelectric Generator Program," Vol. I & II, GEMS-419, General Electric, Nuclear Programs, Space Division, Philadelphia, Penn. (March 1975).

4-3. "SNAP 19/Viking Final Safety Analysis Report," Vol. I and II, ESD-3069-15, Teledyne Isotopes, Energy Systems Divsions, Timonium, Md. (August 1974).

4-4. "TRANSIT RTG Final Safety Analysis Report Vol. II Accident Model Document," TRW (A)-11464-0492, TRW Systems Group, Redondo Beach, Calif. (March 1971).

4-5. "SNAP 19/Pioneer F Safety Analysis Report," Vol. II, INSD-2873-42-2, Teledyne Isotopes, Timonium, Md. (June 1971).

4-6. "Uses of (Nuclear) Radioactive Materials by the United States of America for Space Power Generation," A/AC .105/L.102, a working paper submitted by the United States of America to the United Nations Committee on the Peaceful Uses of Outer Space, New York, N.Y. (March, 1978).

4-7. "Safety Specification for Plutonium-238 Developmental Heat Sources, NRA-3," Division of Nuclear Research and Applications, Energy Research and Development Administration, Washington, D.C. (April 1977).

4-8. "Overall Safety Manual - Volume 1, Summary," NUS Corporation, Rockville, Maryland (June 1974).

4-9. Snow, E. C., "Project Overview--General Purpose Heat Source Project," briefing charts, Los Alamos Scientific Laboratory, at the University of California (December 1977 and June 1978).

4-10. "GPHS Fuel Characterization," Los Alamos Scientific Laboratory, Los Alamos, New Mexico (December 1977).

4-11. Schaffhauser, A. C., "Isotope Fuel Cladding Development for the General Purpose Heat Source," GPHS Review, Metals and Ceramics Division, Oak Ridge National Laboratory, Oak Ridge, Tenn. (December 19-20, 1977).

4-12. Snow, E. C., and Zocher, R. W., "General-Purpose Heat Source Development, Phase I--Design Requirements," LA-7385-SR, Los Alamos Scientific Laboratory, at the University of California (1977).

4-13. Baker, R. D., "General Purpose Heat Source Project, Space Nuclear Safety Program, and Radioisotopic Terrestrial Safety Program," Progress Reports, Los Alamos Scientific Laboratory, Los Alamos, New Mexico (June 1977 thru August 1979).

4-14. Leonard, B. P., "Space Systems for the 1980's--Volume VI: Nuclear Waste Disposal," ATR-72 (7259-01)-1, Volume VI, Aerospace Corporation, Los Angeles, California (September 1971).

4-15. McCarthy, J. F., Jr., et al., "Concepts for Space Disposal of Nuclear Waste," Massachusetts Institute of Technology, Cambridge, Mass. (Spring Term 1972).

4-16. Archer, Waine, "Space Disposal of Nuclear Waste," presentation charts, The Boeing Company, Seattle, Washington, (July 1972).

4-17. Puthoff, R. L., "High Speed Impact Tests of A Model Nuclear Reactor Containment System," NASA TM X-67856, NASA/Lewis Research Center, Cleveland, Ohio (June 1971).

4-18. Puthoff, R. L., and Dallas, T., "Preliminary Results on 400 Ft/sec Impact Tests of Two 2-Foot Diameter Containment Models for Mobile Nuclear Reactors," NASA TM X-52915, NASA/Lewis Research Center, Cleveland, Ohio (October 1970).

4-19. Puthoff, R. L.,"A 1055 Ft/Sec Impact Test of a Two Foot Diameter Model Nuclear Reactor Containment System Without Fracture," NASA TM X-68103, NASA/Lewis Research Center, Cleveland, Ohio (June 1972).

4-20. Puthoff, R. L., "A 810 Ft/Sec Soil Impact Test of a 2-Foot Diameter Model Nuclear Reactor Containment System," NASA TM X-68180, NASA/Lewis Research Center, Cleveland, Ohio (December 1972).

4-21. Hyland, R. E., Wohl, M. L., Thompson, R. L., and Finnegan, P. M., "Study of Extraterrestrial Disposal of Radioactive Wastes--Part II," NASA TMX-68147, NASA/Lewis Research Center, Cleveland, Ohio (October 1972).

4-22. Hyland, R. E., Wohl, M. L., and Finnegan, P. M., "Study of Extraterrestrial Disposal of Radioactive Wastes, Part III," NASA TM X-68216, NASA/Lewis Research Center, Cleveland, Ohio (April 1973).

4-23. Van Bibber, L. E., and Parker, W. G., "Analysis of Temperature and Pressure Distribution of Containers for Nuclear Waste Material Disposal in Space," NASA CR-121186, (WANL-FR-NAS3-16819-8) prepared by Astronuclear Laboratory, Westinghouse Electric Corporation, Pittsburgh, Pa. for NASA/Lewis Research Center, Cleveland, Ohio (April 1973).

4-24. Crispino, A. J., et al., "Nuclear Waste Containment Vessel Impact Study," Volume I, PIFR-444, prepared by Physics International Company, San Leandro, Calif., for NASA/Lewis Research Center, Cleveland, Ohio (June 1973).

4-25. Seifert, K., and Wilhoit, D., "Nuclear Waste Containment Vessel Impact Study," PIFR-444 Volume II--Experimental Program, prepared by Physics International Company, San Leandro, California for NASA/Lewis Research Center, Cleveland, Ohio (July 1973).

4-26. Platt, A. M., and Schneider, K. J., "High-Level Radioactive Waste Management Alternatives," BNWL-1900, Volume 4, Battelle Northwest Laboratories, Richland, Washington (May 1974).

4-27. Bader, B. E., Donaldson, A. B., and Hardee, H. C., "Liquid-Propellant Rocket Abort Fire Model." AIAA Journal of Spacecraft, Vol. 8, No. 12 (December 1971).

4-28. "Hazards of Chemical Rockets and Propellants Handbook," Vol. I, CPIA/194, Applied Physics Laboratory, The Johns Hopkins University, Silver Springs, Md. (May 1972).

4-29. Grelecki, C., "Fundamentals of Fire and Explosion Hazards Evaluation," American Institute of Chemical Engineers (AICHE), New York, N.Y. (1976).

4-30. Blake, V. E., "An Experimental Investigation of the Behavior of Beryllium Metal in Simulated Launch Pad Abort Environments," SC-DC-65-1637, prepared by TRW Systems for Sandia Corporation, Albuquerque, New Mexico (July 1965).

4-31. Seabourn, C. M., "Safety Test of an Improved Multihundred Watt FSA: Launch Abort, Solid Propellant Fire," LA-7314-MS, UC-71, Los Alamos Scientific Laboratory, Los Alamos, New Mexico (July 1978).

4-32. Gayle, J. B., and Bransford, J. W., "Size and Duration of Fireballs from Propellant Explosions," NASA-TMX-53314, NASA Marshall Space Flight Center, Huntsville, Alabama (August 1965).

4-33. Price, E. W. et al., "The Fire Environment of a Solid Rocket Propellant Burning in Air," AFWL-TR-78-34, prepared by Georgia Institute of Technology, Atlanta, Georgia, for Air Force Weapons Laboratory, Kirkland AFB, N.M. (March 1979).

4-34. Zabetakis, M. G., and Burgess, D. S., "Research on the Hazards Associated with the Production and Handling of Liquid Hydrogen," U.S. DoI and Bureau of Mines (1961).

4-35. Elwell, R. B., et al., "Project Sophy-Solid Propellant Hazards Program," AFRPL-TR-67-211, Volumes I and II, Prepared by Aerojet General Corporation for the USAF Rocket Propulsion Laboratory, Edwards AFB, Calif. (August 1967).

4-36. Willoughby, A. B., Wilton, C., and Mansfield, J., "Liquid Propellant Explosive Hazards, Final Report--December-1968," URS 652-35/AFRPL-TR-68-92, Volumes I, II and III, Prepared by URS Research Company, Burlingame, California for the USAF Rocket Propulsion Laboratory, Edwards AFB, Calif. (December 1968).

4-37. Gunther, P., and Anderson, G. R., "Statistical Analysis of Project Pyro Liquid Propellant Explosion Data," TM-69-1033-3, Bellcomm, Inc., Washington, D.C. (July 1969).

4-38. Baker, W. E., et al., "Assembly and Analysis of Fragmentation Data for Liquid Propellant Vessels," NASA CR-134538, Prepared by Southwest Research Institute, San Antonio, Texas for NASA/Lewis Research Center, Cleveland, Ohio (January 1974).

4-39. Baker, W. E., et al., "Workbook for Predicting Pressure Wave and Fragment Effects of Exploding Propellant Tanks and Gas Storage Vessels," NASA CR-134906, prepared by Southwest Research Institute, San Antonio, Texas for NASA/Lewis Research Center, Cleveland, Ohio (November 1975).

4-40. Baker, W. E., et al., "Workbook for Estimating Effects of Accidental Explosions in Propellant Ground Handling and Transport Systems," NASA CR-3023, prepared by Southwest Research Institute, San Antonio, Texas for NASA/Lewis Research Center, Cleveland, Ohio (August 1978).

4-41. Crawford, R. E., "Protection from Non-Nuclear Weapons," AFWL-TR-70-127, prepared by Mechanics Research, Inc., for USAF Weapons Laboratory, Kirkland AFB, New Mexico (February 1971).

4-42. Riehl, W. A., "Shock Wave Environment at SNAP-27 Fuel Capsule in a Saturn V Explosion," NASA-TM-53822, NASA/Marshall Space Flight Center, Huntsville, Alabama (July 1969).

4-43. Bell, J. M. "Orbital Reentry Breakup Analysis Report, P74-1 Payload System," D00604, TRW Systems Group, Redondo Beach, Calif. (November 1973).

4-44. Riehl, W. A. Presentation Charts on Shuttle Accident Environments, NASA/Marshall Space Flight Center, Huntsville, Alabama (December 1978).

4-45. "Minutes of INSRP Shuttle (STS) Data Meeting held October 26-27, 1977," U. S. Department of Energy, Washington, D.C. (November 1977).

4-46. Anderson, D., et al., "Blast Overpressure Environment for STS," EIS-TMO-035, Teledyne Energy Systems, Timonium, Md. (August 9, 1977).

4-47. Alexander, A., "Failure Analysis of Shuttle Orbiter, BIPS PCS and KIPS PCS Due to Blast Overpressure," EIS-AA-038, Teledyne Energy Systems, Timonium, Md. (September 1, 1977).

4-48. Anderson, D., "Launch Complex Accident Model, Probability Distributions and Yield Densities," EIS-DCA-027, Teledyne Energy Systems, Timonium, Md. (June 13, 1977).

4-49. Weatherwax, R. K., "Space Shuttle Failure Modes Important to the AFSATCOM II/III Mission," EIS-RKW-044, Teledyne Energy Systems, Timonium, Md. (December 14, 1976).

4-50. Weatherwax, R. K., "Orbital Injection Failure Probability Analysis," EIS-RKW-047, Teledyne Energy Systems, Timonium, Md. (February 9, 1977).

4-51. Weatherwax, R. K., "Shuttle Failure Modes and Prababilities Important to AFSATCOM II/III," EIS-RKW-045, Teledyne Energy Systems, Timonium, Md. (February 25, 1977).

4-52. Linsley, E. L., "Fragment Velocities from S-IVB Explosion," memorandum #R-AERO-AD-69-13, NASA/Marshall Space Flight Center, Huntsville, Alabama (March 1969).

4-53. Guess, T. R., and Butler, B. L., "Thermal Shock Modeling of Carbon Fiber/Carbon Matrix Composites," SLA-73-0620, Sandia Laboratories, Albuquerque, New Mexico (October 1973).

4-54. Bennett, G. L., Hagan, J. C., and Tantino, D. C., "Evaluating Aeroshell Materials for the MJS/Multi-Hundred Watt Heat Source," ANSP-M-14, ERDA/DNRA 3060-014, APL/John Hopkins University, Laurel, Md. (July 1976).

4-55. Chard, W. C., and McCall, J.,"Assessment of the Availablity and Utilization of Carbon-Base Fibers for DoD Applications," Parts I and II, Battelle's Columbus Laboratory, Columbus, Ohio (December 1977).

4-56. Simonen, F. A., Bansal, G. K., and Duckworth, W. H., "RTG Impact Member Materials: A Preliminary Technical Review," Battelle's Columbus Laboratories, Columbus, Ohio (June 1975).

4-57. Simonen, F. A., and Duckworth, W. H., "Analysis of Ceramic Materials for Impact Members in Isotopic Heat Sources," BMI-X-670, Battelle's Columbus Laboratories, Columbus, Ohio (May 1976).

4-58. Bansal, G. K., and Duckworth, W. H., "Experimental Screening of Carbon-Base Materials for Impact Members in Isotopic Heat Sources," BMI-X-673, Battelle's Columbus Laboratories, Columbus, Ohio (November 1976).

4-59. Duckworth, W. H., "Goals of RTG Impact Member Research," BMI-X-694, Battelle's Columbus Laboratories, Columbus, Ohio (May 1978).

4-60. Pursey, H. C., Volin, R. H., and Showalter, J. G., "An International Survey of Shock and Vibration Technology," Department of Defense, Naval Research Laboratory, Washington, D. C. (March 1979).

4-61. Heuberlin, S. W., et al., "Consequences of Postulated Losses of LWR Spent Fuel and Plutonium Shipping Packages at Sea," BNWL-2093 (Draft report), Battelle Northwest Laboratories, Richland, Washington (December 1976).

4-62. Gough, P. S., "Meteoroid-Bumper Interactions Program," NASA CR-72800, Space Research Institute, Montreal, Canada (November 1970).

4-63. Coleman, T. L., "Nuclear and Space Radiation Effects on Materials," NASA SP-8053, NASA/Langley Research Center, Hampton, Va. (June 1970).

4-64. West, Jr. G. S., Wright, J. J. and Euler, H. C., "Space and Planetary Environment Criteria Guidelines for Use in Space Vehicle Development," 1971 and 1977 Revisions, NASA TM X-64627 and NASA TM 78119, NASA/Marshall Space Flight Center, Huntsville, Ala. (November 1971 and 1977).

4-65. Martin, J. E., "Considerations of Environmental Protection Criteria for Radioactive Waste," U.S. Environmental Agency, Office of Radiation Programs, Washington, D. C. (February 1978).

4-66. Pardue, W. M., "Heat Source Component Development Program," Quarterly Reports, Battelle, Columbus Laboratories, Columbus, Ohio (October 1976-January 1979).

4-67. Fussell, J. B., and Burdick, G. R., Nuclear Systems Reliability Engineering and Risk Assessment, Society for Industrial and Applied Mathematics, Philadelphia, Pennsylvania (1977).

4-68. Fletcher, L. S., Aerodynamic Heating and Thermal Protection Systems, Volume 59, Progress in Astronautics and Aeronautics, American Institute for Aeronautics and Astronautics, New York, N.Y. (1978).

4-69. "Shuttle Liquid Rocket Booster Study," NASA/Marshall Space Flight Center, Huntsville, Alabama (April 1979).

4-70. Hanley, G. M., et al., "Satellite Power Systems (SPS) Concept Definition Study--Final Report (Exhibit C), Transportation Analysis," SSD79-0010-4, Volume IV, Rockwell International, Downey, California (March 1979).

4-71. Edgecombe, D. S., Rice, E. E., Miller, N. E., Yates, K. R., and Conlon, R. J., "Evaluation of the Space Disposal of Defense Nuclear Waste-Phase II," Volumes I, II, and III, Battelle's Columbus Laboratories, Columbus, Ohio (January 1979).

4-72. McBride, B. J., Heimel, S., Ehlers, J. G., and Gordon, S., "Thermodynamic Properties to 6000°K for 210 Substances Involving the First 18 Elements," NASA SP-3001, NASA/Lewis Research Center, Cleveland, Ohio (1963).

4-73. Rowe, J. R., "Properties and Performance of Liquid Rocket Propellants," Aerojet Liquid Rocket Company, Sacramento, California (May 1975).

4-74. Grumer, J., Strasser, A., Kubala, T. A., and Burgess, D. S., "Uncontrolled Diffusive Burning of Some New Liquid Propellants," Fire Research Abstracts and Reviews, Volume 3, No. 1, Washington, D.C. (January 1961).

4-75. Kreenan, J. H., and Keyes, F. G., Thermodynamic Properties of Steam, John Wiley and Sons, New York, N.Y. (1936).

4-76. "Liquid Propellant Manual," Chemical Propulsion Information Agency, Silver Spring, Md. (1966).

4-77. "Concept Definition Document for Nuclear Waste Disposal in Space (a working draft)," NASA/Marshall Space Flight Center, Huntsville, Alabama (January 1980).

5.0 HEALTH EFFECTS ASSESSMENT

The overall objective of the continuing Health Effects Assessment is to provide estimates of radiation doses and health effects from major space disposal accidents, where nuclear wastes are postulated to be released to the biosphere. An additional subobjective of this activity was to support the selection process for the nuclear waste mix composition for space disposal.

The postulated accidents previously studied[5-1] were a catastrophic on-or near-pad booster failure and an upper atmospheric payload burnup. Estimates of individual and population doses and health effects were based on the internal dose due to inhalation of radioactive aerosol for defense waste payloads. Studies conducted during this Phase III effort provide: (1) an assessment of various generalized indices for comparing the potential hazard associated with different nuclear waste mixes (Section 5.1); (2) a critical review of methods available for dealing with the resuspension problem (Section 5.2); and (3) an assessment of the upper atmospheric burnup of commercial waste payloads, by the estimation of the potential world population dose, including the consideration of inhalation of resuspended fallout particles (Section 5.3). Analysis performed in Section 5.3 was based upon the use of Modified PW-4b waste mix (see Sections 3.2, 3.4 and Appendix F).

The health effects assessment conducted in Section 5.3 is not intended to be used in comparisons with other waste disposal options or used in environmental assessments of the space option. Its sole purpose is to influence the design selection and operational alternatives, such that, a safe space disposal concept is evolved.

5.1 Hazard Index Evaluation

One of the problems associated with geologic disposal is the uncertainty associated with waste package performance over long periods of time. Furthermore, radionuclide transport from the geologic repository to man's environment is based on uncertain values of K_D, the transport coefficient. The AEGIS (Assessment of Effectiveness of Geologic Isolation Systems) Program is developing models for radionuclide transport and is experimentally attempting to determine the necessary K_D values. It is believed that space disposal of the long-term hazardous or otherwise noxious portions of high-level waste (HLW) could beneficially augment terrestrial disposal.

To assess the possible risk/benefits derived from space disposal, two hazard models were evaluated. The two models selected for study were ORIGEN[5-2] and AMRAW-A.[5-3] ORIGEN is an isotope generation and depletion code which can calculate the quantity of air or water necessary to dilute each radionuclide contained in HLW to the maximum permissible concentration (MPC) at various points in time. It does not account for geologic transport of radionuclides, their subsequent uptake in food chains, nor estimate the subsequent dose rate to individuals in the vicinity of the repository. In contrast, AMRAW-A has a source term-model similar to ORIGEN to calculate radionuclide concentrations at various points in time, a release model which simulates geologic transport, an environmental model which simulates radionuclide uptake in food chains, and can estimate the resultant dose rate to individuals in the vicinity of the repository at various points in time.

5.1.1 Analysis Based Upon ORIGEN Hazard Model

Using the PW-4b commercial HLW mix as input (see Section 3.2), several ORIGEN cases were run to determine the most "hazardous" radionuclides with respect to dilution requirements for water and air (ignoring transport, uptake, etc.). The most hazardous radionuclides, as defined in this model, are those which require the greatest quantity of air or water to be diluted to the maximum permissible concentration (MPC). Figure 5-1 presents the results of ORIGEN calculations for air dilution. Included in Figure 5-1 are curves showing the air dilution required for the total mass of radionuclides for spent fuel and for PW-4b HLW plus structural materials, cladding, and volatile fission products. Additional curves show the reduction in air dilution resulting from: (1) terrestrial disposal of PW-4b HLW, plus the other radionuclides described above; (2) space disposal 99 percent of the actinides (Am, Cm, and Np); and (3) space disposal of the PW-4b HLW fraction, where only the structural materials, cladding, and volatile fission products remain on Earth. It is worth noting (assuming the ORIGEN code) that space disposal of Tc or I contributes an insignificant reduction in air dilution requirements. It is also evident that the space disposal of 99 percent of the Am, Cm, and Np provides a lessening of the hazard only to < 10,000 years, and that after 10,000 years, actinide removal has little effect based on this simple dilution hazard model.

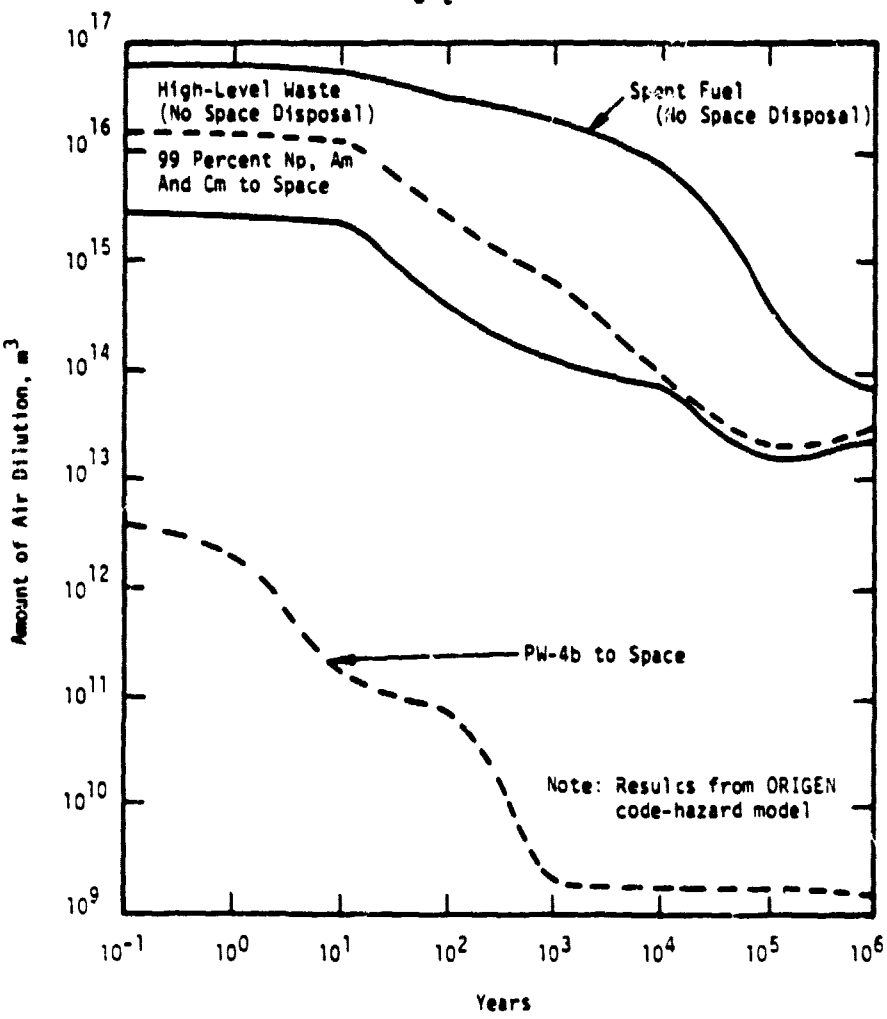

FIGURE 5-1. POTENTIAL HAZARD INDEX (AIR) AS A FUNCTION OF TIME FOR COMMERCIAL WASTE (ORIGEN CODE)

For water dilution, curves similar to those described above are shown in Figure 5-2. Again, space disposal of 99 percent of Am, Cm, and Np, only provides a slight lessening of the "hazard" up to 10,000 years. The space disposal of the entire PW-4b HLW portion to space, with terrestrial disposal of structural materials, cladding, and volatile fission products, provides a more significant lessening of the hazard throughout the time period examined. Figure 5-3 depicts the lessening of hazard if Tc or I is sent to space and the remaining PW-4b radionuclides, structural materials, cladding, and volatile fission products remain on Earth. This dilution model indicates Tc and I contribute insignificantly to the reduction in potential hazard.

The conclusions which may be made with respect to the ORIGEN hazard analysis for commercial waste are:

- The only mix which significantly lessens the hazard of terrestrial disposal is sending the entire HLW fraction to space and keeping the structural materials, cladding, and volatile fission products on Earth.

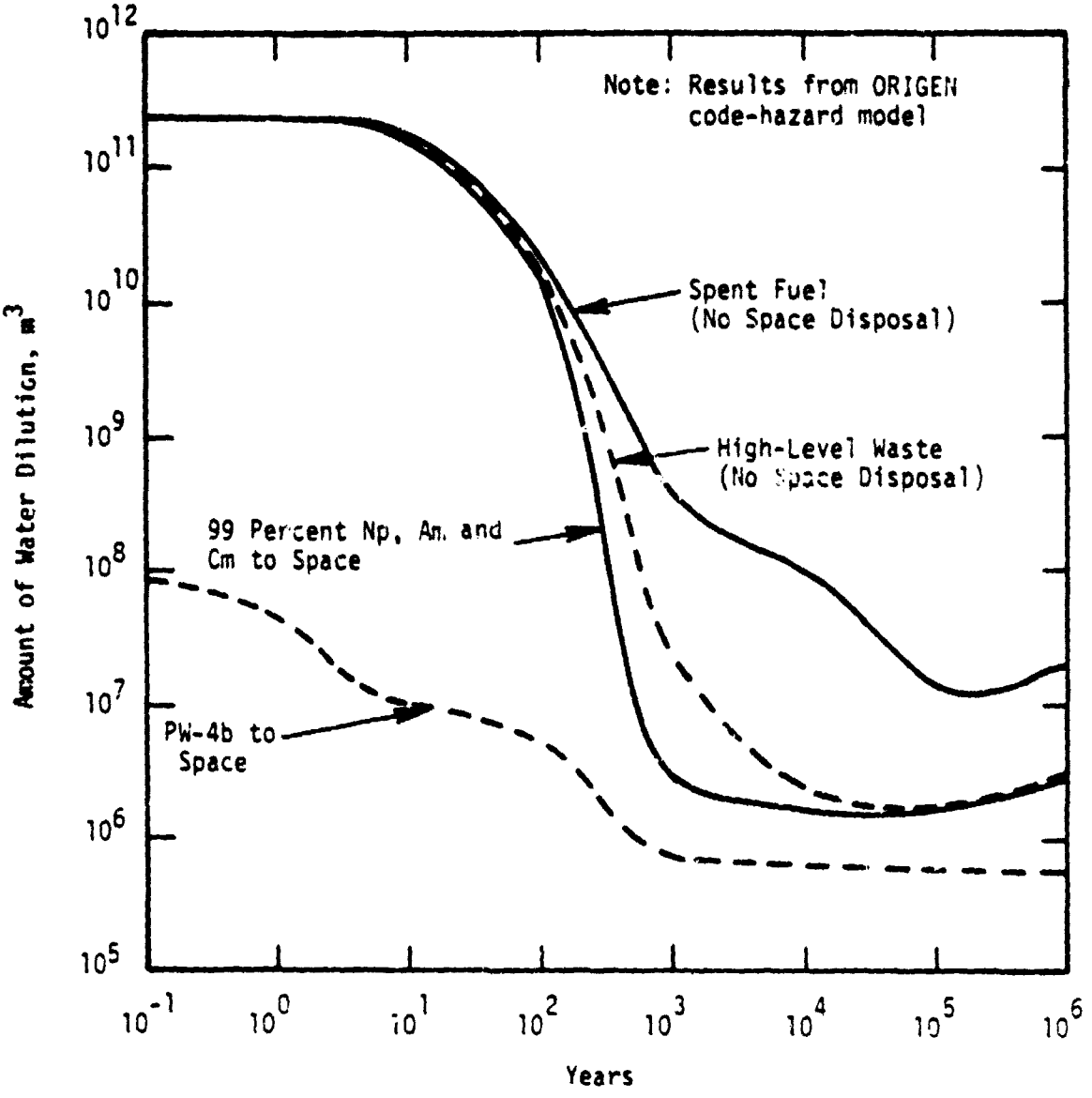

FIGURE 5-2. POTENTIAL HAZARD INDEX (WATER) AS A FUNCTION OF TIME FOR COMMERCIAL WASTE (ORIGEN CODE)

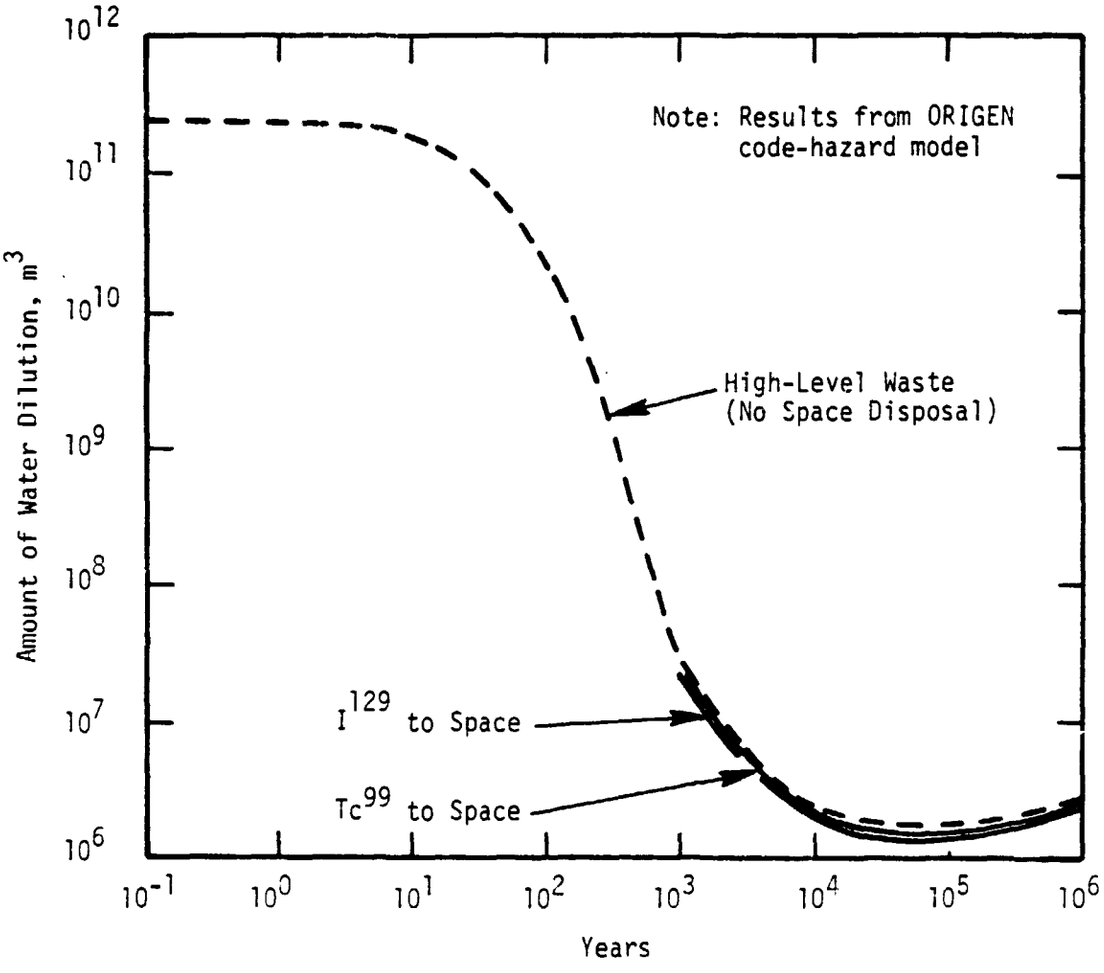

FIGURE 5-3. POTENTIAL HAZARD INDEX (WATER) AS A FUNCTION OF TIME FOR COMMERCIAL WASTE (ORIGEN CODE) WITH I AND TC TO SPACE

- "Hazard" as defined in the ORIGEN model is a naive approach which should not be taken seriously; the model is overly simplistic and does not provide a realistic evaluation of the problem.

5.1.2 Analysis Based Upon AMRAW-A Hazard Model

The AMRAW-A model, developed for the USEPA[5-3], represents an attempt to mathematically model the radioactive source term, resultant transport or release of radionuclides, their uptake in food chains, and subsequent dose rate to man in the vicinity of a repository. Even though many assumptions are required, AMRAW-A is much more realistic in defining the hazard associated with specific radionculides for terrestrial disposal.

Although time and funding constraints did not permit actual implementation of the AMRAW-A model on the BCL computer, a valuable example is provided in the AMRAW-A report itself.[5-3] The example is for HLW (with 99.5 percent of U and Pu removed for recycle) stored in bedded salt at a specific site in New Mexico. Figure 5-4 presents the results of the AMRAW-A analysis for the example described above, showing the radionuclides which contribute most significantly to the dose rate versus time. ^{90}Sr and ^{137}Cs contribute significantly to the dose rate for the first few hundred years and then decay away. Because of this relatively quick decay, engineered barriers should be able to sufficiently contain Sr and Cs, thus they are not suitable candidates for space disposal (see Appendix F). From approximately 500 years to 5000 years after HLW emplacement, ^{241}Am and ^{243}Am contribute most significantly to dose rate. Since engineered barriers cannot presently demonstrate reliable containment for periods up to 5000 years both ^{241}Am and ^{243}Am are candidates for space disposal. From approximately 5000 years to about 900,000 years, ^{99}Tc and ^{226}Ra are the major contributors to dose rate. If ^{99}Tc can be effectively removed from HLW it is obviously a candidate for space disposal. ^{226}Ra is a daughter product of ^{238}U and ^{234}U, therefore it cannot be sent to space itself. However, if uranium can be more efficiently separated at the reprocessing plant and recycled, the quantity of uranium included in the HLW will be less. This will ultimately result in a reduction in the quantity of ^{226}Ra generated. Finally, beginning at approximately 900,000 years, ^{237}Np becomes a major contributor to the dose rate and is a candidate for space disposal.

The conclusions which may be made with respect to the AMRAW-A analysis for commercial waste are:

- A potential mix for space disposal, useful in effectively reducing the hazard associated with terrestrial disposal, is the actinide fraction of HLW plus Tc.

- AMRAW-A represents a significantly more realistic assessment of the terrestrial disposal hazard and possible benefits of space disposal than ORIGEN.

- It is important to note that ^{129}I, often considered as a major problem for terrestrial disposal, does not contribute significantly to the dose rate for the time span shown.

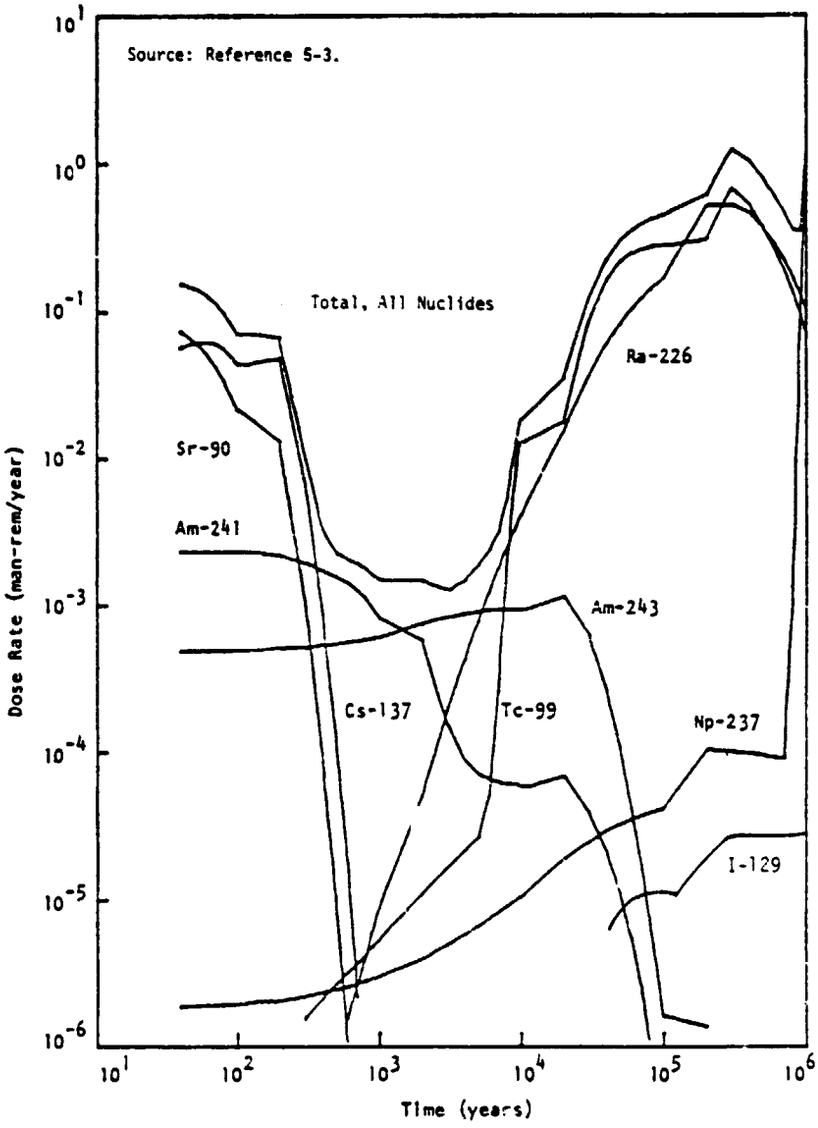

FIGURE 5-4. RESULTS FROM AMRAW-A MODEL

In summary, the continuation of this type of analysis is vital to the proper selection of the nuclide mix for space disposal. The models, like the AMRAW-A or AEGIS codes, should be applied to space disposal option. The 4-year Concept Definition and Evaluation Program Plan developed during the course of this Phase III effort (see Section 7.2) emphasizes the importance of this activity.

5.2 Resuspension Effects

Assessment of the impact on world health of the accidental reentry and possible partial burnup of a nuclear waste payload is based on a model designed to provide estimates of world population doses due to inhalation of particulate burnup debris (particles $\leq$10 μm AMAD) into the upper atmosphere. One assumption upon which the model (fully described in Reference 5-1) was based is that inhalation of fallout particles descending into surface air will account for the principal component of world population dose. Inhalation of resuspended particles was ignored as were the various modes of external exposure and the potential organ doses due to ingestion of food and water containing radioactive burnup debris.

Numerous studies (some of which are cited below) have demonstrated that radioactive particles deposited on soil or other environmental surfaces are susceptible to resuspension by wind action and/or mechanical disturbance. Measured values of the resuspension factor, the ratio of air concentration ($\mu Ci/m^3$) to soil deposition density ($\mu Ci/m^2$) generally range from 10^{-3} to 10^{-14} m^{-1}. Studies conducted in fallout fields at the Nevada Test Site and elsewhere indicate that the resuspension factor in relatively undisturbed environments decreases with time after deposition and tends to an asymptotic value of about 10^{-9} m^{-1}. Consequently, inhalation of resuspended particles could be a significant component of the world population dose due to a burnup accident. After the somewhat sustained period of fallout following an upper atmospheric burnup (6-10 years approximately), resuspension could account for the total inhalation dose.

The purpose of this section is to provide a brief review of alternative methods of dealing with the resuspension problem and a justification of the method selected to include the resuspension effect in the model used to estimate world population doses due to inhalation of burnup debris.

5.2.1 Deposition Models

Worldwide deposition of particulate burnup debris is based[5-1] on the HASL model of atmospheric transport.[5-4 and 5-5] During the fallout period, deposition exceeds resuspension. After the fallout period, it is reasonable to assume that resuspension and deposition are approximately equal, if sampled over a sufficiently large area for a sufficiently long time. Under assumed steady-state conditions, radionuclide deposition velocities could be used to estimate air concentrations and radionuclide inhalation rates.

The rate at which resuspended radioactive particles are redeposited on soil surfaces may be estimated as the product of a deposition velocity (cm/day) and concentration in air ($\mu Ci/cm^3$) to yield a deposition rate having dimensions of $\mu Ci/cm^2$-day. Given the deposition rate and the deposition velocity, it would then be a simple matter to calculate the air concentration and radionuclide inhalation rate.

Deposition velocities measured under field conditions have been reported by Van der Hoven[5-6], Sehmel, Sutter and Dana[5-7], and Healy [5-8]. Pertinent wind-tunnel measurements have been reported by Sehmel [5-7 and 5-8]. Sehmel[5-9] and Healy[5-8] both present results of models used to predict deposition velocities. Healy's results indicate that deposition velocity is proportional to air velocity and strongly dependent on atmospheric stability. Sehmel's results indicate that deposition velocity increases as a nonlinear function of air velocity, exhibits a minimum value as a function of particle size, and is not strongly dependent on atmospheric stability. The minimum deposition velocity in Sehmel's data is generally in the particle diameter range between 0.01 and 1.0 μm. For particles >1 μm, deposition velocity increases with increasing particle diameter; and for particles < 0.01 μm, deposition velocity increases with decreasing particle diameter. Both Sehmel's and Healy's results indicate a strong dependence of deposition velocity on surface roughness. Application of either Sehmel's or Healy's deposition model would require detailed measurements of wind profiles and surface roughness worldwide. These data are not presently available.

5.2.2 Resuspension Models

The resuspension of radioactive soil particles is often expressed as the ratio of air concentration ($\mu Ci/m^3$) to surface soil concentration ($\mu Ci/m^2$). Many such measurements have been made in the field at the Nevada Test Site[5-11 and 5-12] and in the vicinity of Rocky Flats, Colorado [5-13]. The measured values, most of them in the range from 10^{-5} to $10^{-11} m^{-1}$, are quite variable with respect to environmental conditions such as wind speed and direction, rainfall, mechanical disturbances, and the aerodynamic properties of soil surfaces and soil particles.

Several studies[5-14, 5-15 and 5-16] have reported that the air/soil ratio decreases with time. Anspaugh, et al.[5-17] propose the following empirical expression,

$$C_a/C_s = 10^{-4} \exp(-K\sqrt{t}) + 10^{-9}\ m^{-1}$$

where

C_a is the concentration in air ($\mu Ci/m^3$),
C_s is the concentration on surface soil ($\mu Ci/m^2$),
$k = 0.15\ days^{-1/2}$,

and t is the time after deposition, days.

Equation (1) was derived from experimental field data. It provides no fundamental understanding of the resuspension process but merely describes it according to the following constraints based upon the data: (1) the apparent half-time of decrease during the first 10 weeks should approximate a value of 5 weeks and should approximately double over the next 30 weeks; (2) the initial resuspension factor should be about $10^{-4}\ m^{-1}$; and (3) the resuspension factor 17 years after the contaminating event (close-in fallout

from a nuclear explosion) should approximate 10^{-9} m^{-1}. While Equation (1) is consistent with much of the data collected over the years at the Nevada Test Site, its applicability to other environmental circumstances has not been demonstrated. Its incorporation in the existing world population dose model was considered but rejected because it would greatly complicate the mathematical analysis, thus increasing the probability of errors and result in a program which, because of the time required, would be excessively expensive to run.

Many attempts have been made (5-18, 5-19, and 5-20) to develop mathematical models which simulate or predict resuspension. Most of these are based on wind-erosion models developed by Bagnold(5-21) and, as a function of wind speed, take the following form:

$$C_a = K(U - U_T)^3 C_s/U$$

where U is the wind speed, m/s, U_T is a threshold wind speed, m/s, and K is a site-specific constant, s^2/m^3. Others(5-22 and 5-23) have used a power-law expression as follows:

$$C_a = KU^n$$

where K and n are constants derived from the data. Sehmel and Orgill(5-22) obtained the following empirical expression from Volchok's(5-13) data fitted to Equation (3):

$$C_a = 5.26\ E\text{-}32\ U^{2.1}$$

The empirical value of about 2 for the exponent of wind speed is an indirect verification of Equation (2). Shinn and Anspaugh(5-23) found n = 2.1 for dust flux at the Nevada Test Site; but for a plowed field in Texas, the same procedure gave n = 6.4. BCL examined Sehmel's(5-10) data for calcium molybdate resuspension near Hanford, Washington, and also arrived at a value of $n \approx 2$.

An empirical fit of Mork's(5-11) data to Equation (2) gave the following expression:

$$C_a/C_s = 3.35\ E\text{-}25\ (U\text{-}5.79\ E6)^3/U$$

Mork's data were based on air concentrations and wind speeds averaged over a 24-hour period. Volchok's(5-13) data were 1-week averages and gave the following empirical expression:

$$C_a/C_s = 6.58\ E\text{-}27\ (U\text{-}2.51\ E6)^3/U$$

Due to the scatter in both sets of data, both Equations (5) and (6) are rough approximations. The fact that Equation (5) predicts ratios about 50 times larger than those predicted by Equation (6) may be insignificant or it may be due to site-specific environmental differences between the Nevada Test Site (open shrub desert) and Rocky Flats, Colorado (semiarid grassland).

The empirical value of $n \approx 2$, Equation (3), when derived for different tracers, different soils (provided the soils are undisturbed), and different climates, is an indirect confirmation of Equation (2). However, both K and U_T are functions of particle size, soil moisture, surface roughness, and perhaps the time period over which C_a and U are averaged. Attempts have been made to include particle size and other factors in theoretical treatments of resuspension, but none of the currently available theories adequately account for the variability of the data. Thus, K and U_T must be treated, for the present, as empirical constants to be derived only from site-specific data sets. Consequently, no practical benefit appears to be derived from using Equation (2) in preference to Equation (3); but to use either equation for predictive purposes, site-specific measurements are required to obtain estimates of K, U, or n.

5.2.3 Mass Loading

In the absence of data to implement either Equation (2) or Equation (3), Anspaugh[5-16] suggested that a mass loading factor of L_a = 100 micrograms of soil per cubic meter of air be used for predictive purposes. Anspaugh et al.[5-17] provide data which show that predicted air concentrations based on L_a = 100 $\mu g/m^3$ are in good agreement with measured air concentrations. Using data reported by the National Air Pollution Control Administration[5-24], Anspaugh[5-16] showed that the annual mean mass loading for 217 urban stations in the United States was 102 $\mu g/m^3$ while the comparable mean value for 30 rural stations was 38 $\mu g/m^3$. While standard deviations were not reported, the range of values for urban stations was 33 $\mu g/m^3$ at St. Petersburg, Florida, to 254 $\mu g/m^3$ at Steubenville, Ohio, in 1966; the values for rural areas ranged from 9 $\mu g/m^3$ in White Pine County, Nevada, to 79 $\mu g/m^3$ in Curry County, Oregon.

Anspaugh et al.[5-17] discuss the progress made toward development of a realistic model of the resuspension process but notes that "no such general model presently exists". Included is a discussion of the mass-loading approach and a comparison of measured air concentrations of ^{239}Pu, ^{238}U, ^{40}K, ^{232}Th, and natural uranium at various times and places. In all cases, the predicted air concentrations based on L_a= 100 $\mu g/m^3$ were larger than the measured values.

While recent work by Sehmel[5-25] indicates little experimental justification for the mass-loading approach, the empirical results reported and interpreted by Anspaugh[5-16] and Anspaugh et al.[5-17] are conducive to the conclusion that the use of L_a=100 $\mu g/m^3$ for predictive purposes is a reasonable alternative and should prove to be conservative in most cases as it is greater than the National Air Quality Standards for Particulate Matter.[5-26] It should, of course, be noted that higher than average wind velocities or mechanical disturbances, such as plowing,[5-23 and 5-27] can cause the mass-loading factor to be temporarily much higher than 100 $\mu g/m^3$.

An implicit assumption of the mass-loading approach is that the specific activity of airborne particulates is the same as that of contaminated

surface soil. For fresh deposits, this assumption may be invalid because the contaminated particles are more readily resuspended and have not had time to mix with the surface soil. In any case, the apparent specific activity of surface soil will be affected by the depth to which soil is sampled. At the Nevada Test Site, in an undisturbed area contaminated about 20 years before the study was made, the specific activity of plutonium in soil sampled to a depth of 5 cm was about 2700 dpm/g while the specific activity of plutonium in particles recovered from all stages of high-volume cascade impactors was only 890 dpm/g. The measured mass loading for the cascade impactor samples was 70 g/m^3[5-16]. In this case, predicted air concentrations based on L_a = 100 g/m^3 and the assumption that soil and airborne particles have the same specific activity would have been conservatively high by a factor of 4.33.

5.2.4 Conclusions

Finding no satisfactory model of the resuspension process and lacking an adequate data base for implementation of the empirical models currently available, we have decided to use the mass loading approximation suggested by Anspaugh[5-16] and further supported by Anspaugh et al.[5-17], as providing a reasonable basis for approximating the effect of resuspension on the estimation of world population doses resulting from the accidental reentry burnup of a nuclear waste payload. The resulting method of using L_a = 100 g/m^3, expressed as an equivalent resuspension factor, to estimate radionuclide inhalation rates is described in the following section. The equivalence of the mass loading factor and the resuspension factor is based on studies of plutonium-contaminated environments at the Nevada Test Site[5-28], where "surface soil" was defined as the top 5 cm and the bulk density of the soil was approximately 1 g/cm^3. In other words, the radioactivity per square meter was associated with approximately 50 kg of soil (5 cm x 1 $\mu g/cm^3$ x 10^4 cm^2/m^2 = 50 kg/m^2). Consequently, a mass loading factor of 100 $\mu g/m^3$ is equivalent to a resuspension factor of 100 $\mu g \cdot m^{-3}/50$ $kg \cdot m^{-2}$ = 2 E-9 m^{-1} which is just twice the lower asymptote of Equation (1).

5.3 Burnup Accident Analysis

The accidental burn up of a portion of the nuclear waste payload resulting from the atmospheric reentry of an unprotected container would produce worldwide distribution of small radioactive particles. The purpose of this section is to provide an assessment of the impact on world health, such that, proper system design changes and operational procedures are incorporated into the reference concept for nuclear waste disposal (see Sections 2.3 and 2.4). The results of this assessment are not intended to be used in comparisons with other waste disposal options or to be used in environmental assessments of the space option.

The following paragraphs provide an overview of the model description, new input data, and results of the analysis.

5.3.1 Model Description

The basic assumptions, general formulation, and mathematical development of the model used to estimate world population doses due to the accidental reentry and burnup in the upper atmosphere of a nuclear waste payload are described in Reference 5-1 and are not repeated here. However, the burnup accident assessment results for the Modified PW-4b commercial waste mix are given here, and include estimates of both fallout and resuspension dose factors. The general design of the world population dose model has not changed; but metabolic parameters for three radionuclides not occurring in the other mixes studied have been added and the population data for equal-area latitude bands have been updated to reflect the estimated world population distribution in the year 1980. The procedure for calculating the resuspension dose factors is described below.

Figure 5-5 is a diagram of the modified HASL atmospheric transport model showing the contribution of fallout (F) and of resuspension (R) to the radionuclide inhalation rate of an individual in equal-area latitude band k. In this model, A, B, and C are layers of atmosphere and S is the soil surface. A_{ir} is the amount (μCi) of radionuclide r injected into the atmosphere above 21 km in latitude band i, and f_{ik} is the fraction of burnup debris injected in band i and deposited in band k.

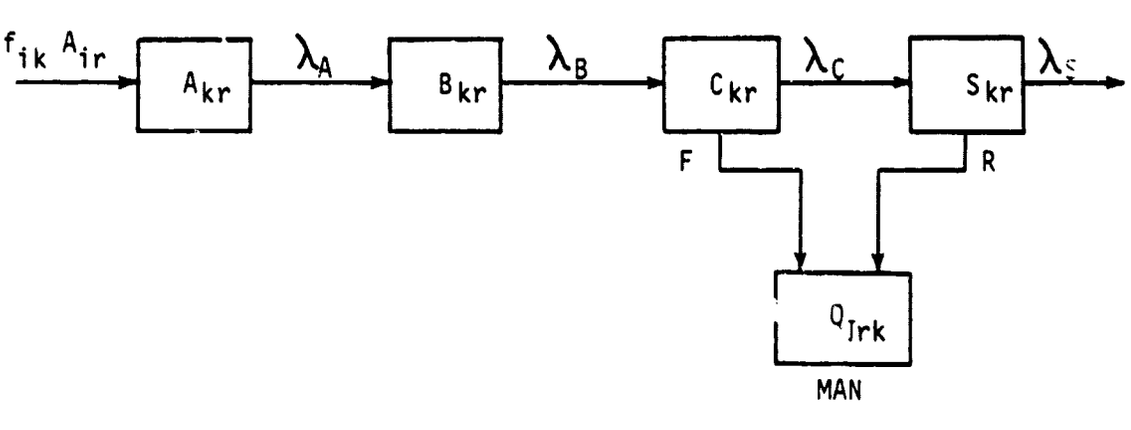

FIGURE 5-5. CONTRIBUTION OF FALLOUT (F) AND RESUSPENSION (R) TO RADIONUCLIDE (r) INHALATION RATE (Q_{Irk}) FOR AN INDIVIDUAL (I) IN EQUAL-AREA LATITUDE BAND k

The differential equations and initial values for compartments A, B, C, and D are:

$$dA_{kr}/dt = -(\lambda_A+\lambda_r)A \qquad ; A_{kr}(0) = f_{ik}A_{ir} \quad (7)$$

$$dB_{kr}/dt = (\lambda_A A_{kr} - (\lambda_B + \lambda_r)B_{kr}; B_{kr}(0) = 0 \quad (8)$$

$$dC_{kr}/dt = \lambda_B B_{kr} - (\lambda_C + \lambda_r)C_{kr} \; ; \; C_{kr}(0) = 0 \tag{9}$$

$$dS_{kr}/dt = \lambda_C C_{kr} - (\lambda_S + \lambda_r)S \; ; \; S_{kr}(0) = 0 \tag{10}$$

Solving this system of differential equations yields the following for $S_{kr}(t)$:

$$S_{kr}(t) = f_{ik} A_{ir} \lambda_A \lambda_B \lambda_C \left[\frac{\exp[-(\lambda_A+\lambda_r)t]}{(\lambda_B-\lambda_A)(\lambda_C-\lambda_A)(\lambda_S-\lambda_A)} + \frac{\exp[-(\lambda_B+\lambda_r)t]}{(\lambda_A-\lambda_B)(\lambda_C-\lambda_B)(\lambda_S-\lambda_B)} \right.$$

$$\left. \frac{\exp[-(\lambda_C+\lambda_r)t]}{(\lambda_A-\lambda_C)(\lambda_B-\lambda_C)(\lambda_S-\lambda_C)} + \frac{\exp[-(\lambda_S+\lambda_r)t]}{(\lambda_A-\lambda_S)(\lambda_B-\lambda_S)(\lambda_C-\lambda_S)} \right] \tag{11}$$

where $S_{kr}(t)$ is the amount (Ci) of radionuclide r on the surface of equal-area latitude band k at time t,

$\lambda_A = \ell n(2)/182.5$ days
$\lambda_B = \ell n(2)/304.2$ days
$\lambda_C = \ell n(2)/30.42$ days
$\lambda_S = \ell n(2)/10^4$ days (Reference 5-21)
$\lambda_r = \ell n(2)/T_r$ days

and T_r is the half-life of radionuclide r.

The radionuclide inhalation rate due to resuspension, i.e., pathway R of Figure 5-5, is

$$Q_{irk}(t) = K \, S_{kr}(t) \tag{12}$$

where $K = (20 m^3/day)(2E\text{-}9 m^{-1})/2.55E13 m^2$

20 m^3 air/day is the inhalation rate for reference man,
2E-9 m^{-1} is the resuspension factor defined in Section 5.2.4,
and 2.55E13 m^2 is the area of latitude band k, i.e., 1/20th of the Earth's surface area based on an Earth mean radius of 6371 km.

The equation for the radionuclide inhalation rate due to fallout, i.e., pathway F of Figure 5-5, is given in Appendix G of Reference 5-1. The mathematical development of equations for inhalation doses due to resuspension is parallel to that of equations for inhalation doses due to fallout as explained in Appendix G of Reference 5-1.

5.3.2 New Input Data

The quantities of radionuclides contained in 1 kg of Modified PW-4b commercial waste mix in cermet are listed in Table 5-1. Generalized dose factors represent the dose (rem) to an individual in equal-area latitude band k per microcurie (μCi) of radionuclide r falling in band k. For a given burnup case, a fraction of the waste mix, having a specified activity median aerodynamic diameter (AMAD), is injected in the upper atmosphere in latitude band i. The amount falling in band k is the product of the amount injected in band i, A_{ir}, and a distribution fraction, f_{ik}, taken from Table 6-14 of Reference 5-1.

TABLE 5-1. RADIOACTIVITY IN 1 KILOGRAM (CERMET) OF MODIFIED* PW-4b COMMERCIAL WASTE MIX

Nuclide	Activity, Ci	Nuclide	Activity, Ci
Rb-87	2.73 E-07	Eu-154	6.87 E+01
Sr-90	1.00 E+02	U-235	2.60 E-07
Y-90	1.00 E+02	U-236	3.87 E-06
Zr-93	2.64 E-02	U-238	4.69 E-06
Tc-99	2.38 E-01	Np-237	7.73 E-05
Pd-107	1.29 E-03	Pu-239	4.64 E-03
Cs-134	1.23 E+01	Pu-240	4.61 E-03
Cs-135	4.71 E-04	Pu-241	1.43 E+00
Cs-137	1.45 E+02	Am-241	6.35 E+00
Ba-137m	1.36 E+02	Am-243	9.84 E-02
Pm-147	1.41 E+03	Cm-244	4.24 E+01
Sm-151	8.00 E+00		

*Ninety percent of the original ^{90}Sr-^{90}Y and ^{137}Cs-^{137m}Ba contained in the PW-4b commercial waste mix have been removed.

Recently developed Skylab hazard model population data were used to obtain updated estimates of world population with respect to equal-area latitude bands. The results for 1980 are given in Table 5-2. The population data base includes estimates of population growth rates for various geopolitical units which permit estimation of future population size and distribution. Using 1980 population data for 70-year dose calculations may result in a slight underestimate of world health effects; but in view of the many uncertainties involved in such calculations, it does not seem worthwhile to extrapolate the population data beyond the current year.

TABLE 5-2. ESTIMATED WORLD POPULATION, 1980(a)

Equal Area Latitude Band k	Lat.(b)	Estimated Population, millions	Equal Area Latitude Band k	Lat.(b)	Estimated Population, millions
1	64-90° N	33.3	11	0-6° S	90.6
2	54-64° N	176.4	12	6-11° S	165.5
3	44-54° N	459.2	13	11-17° S	51.9
4	36-44° N	599.7	14	17-24° S	72.8
5	30-36° N	763.1	15	24-30° S	56.4
6	24-30° N	677.2	16	30-36° S	47.6
7	17-24° N	473.7	17	36-44° S	10.2
8	11-17° N	245.1	18	44-54° S	1.0
9	6-11° N	249.3	19	54-64° S	0.1
10	0-6° N	100.7	20	64-90° S	0.0

Notes: (a) Based on BCL-developed Skylab hazard model data base.
(b) Approximate boundaries.

Table 5-3 provides a listing of metabolic parameters used in the calculation of dose factors for four radionuclides found in waste mix PW-4b, which are not in the mixes previously studied. The same parameters for the other radionuclides listed in Table 5-1 are given in Table G-4 of Reference 5-1.

5.3.3 Results

Dose factors for assumed AMAD values of 0.2, 1.0, and 5.0 μm are listed in Tables 5-4, 5-5, and 5-6 for the radionuclides in Modified PW-4b commercial waste mix (Table 5-1). Each value listed is the sum of a fallout dose factor and a resuspension dose factor; the former is generally between two and three orders of magnitude larger than the latter. Based on a resuspension factor of 2E-9 m^{-1}, resuspension accounts for less than 1 percent of the organ dose due to inhalation. As the resuspension dose factor is proportional to the resuspension factor, an order of magnitude increase in the resuspension factor would be reflected by increases of less than 10 percent in the factors listed in Tables 5-4, 5-5, and 5-6.

The summation of population factors for each injection band (i = 1,2,...19) is given in Table 5-7 based on the population values in Table 5-2.

TABLE 5-3. METABOLIC PARAMETERS FOR DOSE FACTOR CALCULATIONS*

	Radionuclide	Rb-87	Y-90	Ba-137m	U-236
	Trans. Class	D	Y	W	Y
	f_j (GIT Blood	1.0	10^{-4}	1.0	10^{-4}
	T_r (days)	1.8E13	2.68	0.002	8.7E9
T_N	Total Body	45	14,000	65	100
	Bone	0	18,000	65	300
	Liver	63	0	975	0
	Kidney	0	0	8.5	15
	Thyroid	0	0	0	0
f'_{2N}	Total Body	1.0	1.0	1.0	1.0
	Bone	0	0.75	0.7	0.11
	Liver	0.07	0	0.0006	0
	Kidney	0	0	0.0001	0.11
	Thyroid	0	0	0	0
E_N	Total Body	0.09	0.89	0.59	47
	Bone	0	4.4	1.4	230
	Liver	0.09	0	0.41	0
	Kidney	0	0	0.37	47
	Thyroid	0	0	0	0
E_N (Resp. Syst.)		0.09	0.89	0.41	47
E_G (Large Intestine)		0.09	0.89	0.34	0.45

*Parameters for other radionuclides listed in Table 5-1 are given in Table G-4 of Reference 5-1.

TABLE 5-4. DOSE FACTORS (REM/μCi FOR EACH NUCLIDE) FOR AMAD OF 0.2 MICRONS

Radio-nuclide	Class	Organ									
		NP	TB	P	LM	GIT	Bone	Liver	Kidney	Total Body	Thy-roid
RB-187	D	3.931E-18	6.899E-20	7.253E-18	4.836E-17	5.825E-19	0.	2.386E-17	0.	5.914E-18	0.
SR-090	W	1.644E-15	9.142E-18	5.092E-15	1.386E-14	2.672E-17	2.019E-13	0.	0.	3.821E-15	0.
Y-090	Y	1.566E-20	3.162E-23	2.915E-21	1.033E-22	8.564E-22	3.490E-24	0.	0.	9.412E-26	0.
ZR-093	W	2.990E-17	1.669E-19	9.310E-17	2.552E-16	2.556E-18	1.201E-16	1.730E-17	2.802E-17	3.002E-18	0.
TC-099	W	1.482E-16	8.256E-19	4.636E-16	1.263E-15	1.265E-17	2.128E-19	3.155E-19	3.973E-19	8.513E-20	0.
PD-107	Y	1.540E-17	1.107E-19	4.339E-16	1.840E-14	1.324E-18	0.	2.891E-19	2.303E-18	2.853E-20	0.
CS-134	D	1.440E-17	2.527E-19	2.655E-17	1.769E-16	1.422E-18	4.011E-17	1.127E-16	3.624E-17	5.999E-17	0.
CS-135	D	2.883E-18	5.050E-20	5.313E-18	3.546E-17	4.271E-19	2.698E-17	2.500E-17	9.445E-18	6.746E-18	0.
BA-137M	W	3.042E-20	1.245E-32	1.247E-31	4.145E-38	1.211E-31	2.272E-34	2.349E-37	2.001E-37	1.368E-35	0.
CS-137	D	1.705E-17	2.992E-19	3.146E-17	2.097E-16	2.095E-18	1.076E-16	1.466E-16	5.564E-17	5.705E-17	0.
PM-147	Y	7.202E-17	4.838E-19	1.337E-15	1.137E-14	5.376E-18	3.740E-17	3.495E-18	6.601E-18	1.415E-18	0.
SM-151	Y	7.193E-17	5.136E-19	1.977E-15	7.296E-14	5.941E-18	1.352E-16	2.322E-17	2.605E-17	5.582E-18	0.
EU-154	Y	1.358E-15	9.623E-18	3.510E-14	7.660E-13	9.094E-17	1.985E-15	1.790E-16	1.021E-15	1.211E-16	0.
U-235	Y	7.959E-14	5.724E-16	2.227E-12	9.509E-11	7.718E-17	1.641E-14	0.	3.824E-15	9.943E-16	0.
U-236	Y	8.132E-14	5.848E-16	2.276E-12	9.714E-11	6.697E-17	1.641E-14	0.	3.911E-15	1.016E-15	0.
NP-237	Y	1.479E-14	6.097E-16	2.372E-12	1.013E-10	7.232E-17	2.434E-11	2.100E-12	7.307E-12	9.641E-13	0.
U-238	Y	7.446E-14	5.350E-16	2.092E-12	8.889E-11	6.399E-17	1.569E-14	0.	3.579E-15	9.295E-16	0.
PU-239	Y	8.172E-14	6.594E-16	2.556E-12	1.095E-10	7.738E-17	3.383E-12	2.052E-12	6.693E-13	1.616E-13	0.
PU-240	Y	8.164E-14	6.593E-16	2.555E-12	1.092E-10	7.736E-17	3.374E-12	2.047E-12	6.675E-13	1.611E-13	0.
AM-241	Y	8.435E-14	7.065E-16	2.743E-12	1.133E-10	8.237E-17	2.050E-12	2.151E-12	9.942E-13	1.285E-13	0.
PU-241	Y	9.231E-17	5.809E-19	2.094E-15	4.196E-14	6.826E-20	4.022E-14	1.618E-14	7.338E-15	1.539E-15	0.
AM-243	Y	8.541E-14	6.719E-16	2.614E-12	1.114E-10	8.134E-17	2.301E-12	2.142E-12	9.791E-13	1.276E-13	0.
CM-244	Y	8.589E-14	6.806E-16	2.637E-12	5.403E-11	7.765E-17	8.633E-13	3.452E-13	8.344E-14	5.852E-14	0.

Class = Translocation Class
D = Day
W = Week
Y = Year

NOTE: NP = Nasopharyngeal Region
TB = Tracheobronchial Region
P = Pulmonary Lung Region
LM = Thoracic Lymph
GIT = Large Intestine

TABLE 5-5. DOSE FACTORS (REM/μ Ci FOR EACH NUCLIDE) FOR AMAD OF 1.0 MICRONS

Radionuclide	Class	Organ									
		NP	TB	P	LM	GIT	Bone	Liver	Kidney	Total Body	Thyroid
RB-097	D	3.8[illegible]E-17	6.[illegible]E-20	4.[illegible]E-18	2.713E-17	4.56AE-18	0.	2.754E-17	0.	6.824E-18	0.
SR-090	W	1.589E-14	7.617E-14	2.451E-15	7.775E-15	1.244E-17	7.163E-13	0.	0.	4.094E-15	0.
Y-090	Y	1.517E-14	9.232E-21	1.635E-21	5.823E-23	1.421E-21	1.088E-23	0.	0.	2.935E-25	0.
ZR-093	W	2.996E-16	1.291E-19	5.223E-17	1.432E-16	3.139E-19	1.105E-16	1.592E-17	2.573E-17	2.762E-19	0.
TC-099	W	1.433E-15	6.355E-19	2.594E-16	7.083E-16	1.553E-17	2.359E-19	3.497E-19	4.404E-19	9.436E-20	0.
PD-107	Y	1.449E-16	1.255E-20	2.417E-16	1.032E-14	1.668E-18	0.	2.750E-19	2.184E-18	1.953E-20	0.
CS-134	D	1.392E-16	2.527E-19	1.430E-17	9.924E-17	2.115E-17	4.629E-17	1.321E-16	4.183E-17	6.924E-17	0.
CS-135	D	2.787E-17	5.060E-20	2.994E-18	1.989E-17	3.350E-18	3.114E-17	2.885E-17	1.090E-17	7.784E-18	0.
BA-137M	W	2.940E-29	1.048E-32	4.937E-32	2.325E-39	1.964E-31	4.503E-34	4.654E-37	3.966E-37	2.711E-35	0.
CS-137	D	1.648E-16	2.932E-19	1.765E-17	1.176E-16	1.643E-17	1.242E-16	1.692E-16	6.420E-17	6.592E-17	0.
PM-147	Y	5.962E-16	4.137E-19	7.340E-16	6.380E-15	7.343E-18	2.467E-17	2.305E-18	4.354E-18	9.330E-19	0.
SM-151	Y	6.920E-16	4.296E-19	1.103E-15	4.093E-14	7.554E-18	8.150E-17	1.402E-17	1.572E-17	3.364E-18	0.
EU-154	Y	1.313E-14	9.082E-14	1.953E-14	4.297E-13	1.165E-16	1.150E-15	1.092E-16	6.224E-16	7.385E-17	0.
U-235	Y	7.694E-13	4.744E-14	1.249E-12	5.334E-11	9.747E-17	9.867E-15	0.	2.302E-15	5.940E-16	0.
U-236	Y	7.661E-13	4.848E-14	1.277E-12	5.450E-11	8.435E-17	9.867E-15	0.	2.392E-15	6.110E-16	0.
NP-237	Y	8.195E-13	5.096E-14	1.331E-12	5.681E-11	9.185E-17	2.853E-11	2.466E-12	8.564E-12	1.129E-12	0.
U-239	Y	7.192E-23	4.472E-24	1.159E-12	4.986E-11	8.060E-17	9.438E-15	0.	2.152E-15	5.590E-16	0.
PU-238	Y	3.864E-13	5.511E-14	1.439E-12	6.141E-11	9.746E-17	2.042E-12	1.237E-12	4.039E-13	9.757E-14	0.
PU-239	Y	4.462E-13	5.610E-14	1.439E-12	6.128E-11	9.744E-17	2.036E-12	1.234E-12	4.024E-13	9.729E-14	0.
AM-241	Y	3.502E-13	5.406E-14	1.539E-12	6.353E-11	1.046E-16	1.239E-12	1.299E-12	5.943E-13	7.754E-14	0.
PU-241	Y	7.947E-16	4.882E-19	1.153E-15	2.354E-14	8.765E-20	2.460E-14	6.230E-15	4.484E-15	9.419E-16	0.
AM-243	Y	4.330E-13	5.614E-14	1.465E-12	6.247E-11	1.012E-16	1.257E-12	1.293E-12	5.911E-13	7.701E-14	0.
CM-244	Y	4.269E-13	5.713E-14	1.431E-12	3.253E-11	9.925E-17	5.262E-13	2.102E-13	5.080E-14	3.078E-14	0.

Class = Translocation Class
D = Day
W = Week
Y = Year

NOTE: NP = Nasopharyngeal Region
TB = Tracheobronchial Region
P = Pulmonary Lung Region
LM = Thoracic Lymph
GIT = Large Intestine

TABLE 5-6. DOSE FACTORS (REM/μCi FOR EACH NUCLIDE) FOR AMAD OF 5.0 MICRONS

Radionuclide	Class	Organ									
		NP	TB	P	LM	GIT	Bone	Liver	Kidney	Total Body	Thyroid
RB-087	D	1.0[illegible]E-16	6.899E-20	1.946E-18	1.297E-17	1.193E-17	0.	4.466E-17	0.	1.892E-17	0.
SR-090	W	4.218E-14	5.601E-18	1.363E-15	3.719E-15	5.563E-17	3.203E-13	0.	0.	6.863E-15	0.
Y-090	Y	4.017E-19	7.613E-23	7.921E-22	2.789E-21	2.733E-21	2.475E-23	0.	0.	6.673E-25	0.
ZR-093	W	7.690E-16	1.022E-19	2.435E-17	6.847E-17	5.313E-18	1.336E-16	1.925E-17	3.116E-17	3.339E-18	0.
TC-099	W	3.415E-15	5.054E-19	1.236E-16	3.387E-16	2.629E-17	3.626E-19	5.375E-19	6.769E-19	1.458E-19	0.
PD-107	Y	3.952E-16	8.043E-20	1.156E-16	4.935E-15	2.818E-18	0.	3.779E-19	3.005E-18	2.683E-20	0.
CS-134	D	3.696E-14	2.527E-18	7.124E-18	4.746E-17	2.912E-17	7.408E-17	2.082E-16	6.693E-17	1.108E-16	0.
CS-135	D	7.400E-17	5.060E-20	1.427E-18	9.514E-18	5.745E-18	4.982E-17	4.615E-17	1.744E-17	1.245E-17	0.
BA-137M	W	7.807E-29	9.167E-33	1.347E-32	1.112E-35	3.844E-31	9.079E-34	9.384E-37	7.996E-37	5.466E-35	0.
CS-137	D	4.377E-16	2.992E-19	8.439E-18	5.626E-17	4.289E-17	1.987E-16	2.767E-16	1.127E-16	1.053E-16	0.
PM-147	Y	1.449E-15	3.670E-19	3.536E-16	3.051E-15	1.296E-17	1.984E-17	1.854E-18	3.561E-18	7.506E-19	0.
SM-151	Y	1.839E-15	3.736E-19	5.935E-16	1.957E-14	1.278E-17	5.131E-17	8.612E-18	9.884E-18	2.118E-18	0.
EU-154	Y	3.488E-14	7.055E-18	3.330E-15	2.055E-13	1.987E-16	7.517E-16	7.140E-17	4.671E-16	4.828E-17	0.
U-235	Y	2.043E-12	4.157E-16	9.975E-13	2.551E-11	1.646E-16	6.167E-15	0.	1.439E-15	3.738E-16	0.
U-236	Y	2.087E-12	4.247E-16	6.135E-13	2.606E-11	1.425E-16	6.167E-15	0.	1.472E-15	3.819E-16	0.
NP-237	Y	2.176E-12	4.428E-16	6.355E-13	2.717E-11	1.551E-16	4.613E-11	3.977E-12	1.384E-11	1.024E-12	0.
U-239	Y	1.910E-12	3.886E-16	5.596E-13	2.385E-11	1.361E-16	5.899E-15	0.	1.345E-15	3.494E-16	0.
[illegible]-239	Y	2.354E-12	4.789E-16	6.954E-13	2.937E-11	1.646E-16	1.291E-12	7.791E-13	2.553E-13	6.179E-14	0.
PU-240	Y	2.353E-12	4.788E-16	6.891E-13	2.931E-11	1.646E-16	1.288E-12	7.772E-13	2.547E-13	6.162E-14	0.
AM-241	Y	2.523E-12	5.133E-16	7.359E-13	3.039E-11	1.767E-16	7.863E-13	8.233E-13	3.761E-13	4.934E-14	0.
PU-241	Y	2.116E-14	4.266E-18	5.531E-16	1.126E-14	1.498E-19	1.623E-14	4.187E-15	2.[illegible]61E-15	6.214E-16	0.
AM-243	Y	2.[illegible]E-12	4.874E-16	7.012E-13	2.987E-11	1.709E-16	7.976E-13	8.190E-13	3.746E-13	4.866E-14	0.
CM-244	Y	2.461E-12	4.994E-16	6.703E-13	1.553E-11	1.631E-16	5.431E-13	1.366E-13	3.302E-14	2.805E-14	0.

Class = Translocation Class
D = Day
W = Week
Y = Year

NOTE: NP = Nasopharyngeal Region
TB = Tracheobronchial Region
P = Pulmonary Lung Region
LM = Thoracic Lymph
GIT = Large Intestine

TABLE 5-7. SUMMATION OF POPULATION FACTORS FOR EACH INJECTION BAND BASED ON 1980 POPULATION

Injection Latitude Band (i)	$\sum_{1}^{20} f_{ik} P_k$	Injection Latitude Band (i)	$\sum_{1}^{20} f_{ik} P_k$
1	4.68536E+08	11	1.70878E+08
2	4.68518E+08	12	1.26086E+08
3	4.67582E+08	13	9.20265E+07
4	4.61132E+08	14	6.61382E+07
5	4.67584E+08	15	6.67407E+07
6	4.24298E+08	16	3.43820E+07
7	3.93752E+08	17	2.88125E+07
8	3.53866E+08	18	2.79405E+07
9	3.01842E+08	19	2.79405E+07
10	2.31231E+08	--	

Table 5-8 provides a world population dose summary for a 1 kg burnup (above 21 km) of Modified PW-4b waste mix in cermet form. The values given for different particle sizes (AMAD), organs, and injection bands have units of man rem/kg (cermet), and are based on the following formula for a given particle size:

$$W_{ni} = \sum_{r=1}^{r=23} \left(D_{nrk} A_{ir} \sum_{k=1}^{k=20} f_{ik} P_k \right)$$

Where,

W_{ni} is the world population dose (man-rem/kg of PW-4b in cermet) to organ n due to a 1 kg burnup of Modified PW-4b waste mix in latitude band i, (see Table 5-8).

D_{nrk} is the lifetime (70-year) radiation dose (rem) to organ n of an individual member of the population (P_k) of equal-area latitude band k per μCi of radionuclide r falling in band k, based on inhalation of radioactive particles falling through surface air and particles resuspended from soil, rem/μCi.

A_{ir} is the amount (μCi) of radionuclide r initially injected in band i, see Table 5-1.

f_{ik} is the fraction of the material (particles 0.2 to 5.0 μm AMAD) injected in latitude band i, which falls in latitude band k, see Table 6-14 of Reference 5-1.

TABLE 5-8. WORLD POPULATION DOSE SUMMARY FOR A ONE-KILOGRAM BURNUP ABOVE 21 KM OF MODIFIED PW-4b WASTE MIX IN CERMET

Injection Latitude Band	AMAD Value (μm)	World Population Doses (man-rems) Organs*									
		NP	TB	P	LN	GIT	Bone	Liver	Kidney	Total Body	Thyroid
4	0.2	2.33E+03	1.65E+01	5.92E+04	1.51E+06	9.54E+00	3.24E+04	1.32E+04	4.61E+03	1.56E+03	0.
6	↓	2.15E+03	1.52E+01	5.44E+04	1.39E+06	8.77E+00	2.98E+04	1.21E+04	4.24E+03	1.43E+03	0.
8		1.79E+03	1.26E+01	4.54E+04	1.16E+06	7.32E+00	2.49E+04	1.01E+04	3.53E+03	1.19E+03	0.
10		1.17E+03	8.26E+00	2.97E+04	7.55E+05	4.78E+00	1.63E+04	6.61E+03	2.31E+03	7.80E+02	0.
12		6.34E+02	4.50E+00	1.62E+04	4.12E+05	2.61E+00	8.86E+03	3.60E+03	1.26E+03	4.26E+02	0.
14		3.35E+02	2.36E+00	8.49E+03	2.16E+05	1.37E+00	4.65E+03	1.89E+03	6.61E+02	2.23E+02	0.
16		1.74E+02	1.23E+00	4.41E+03	1.12E+05	7.11E-01	2.42E+03	9.83E+02	3.43E+02	1.16E+02	0.
4	1.0	2.26E+04	1.38E+01	3.32E+04	9.45E+05	1.34E+01	2.48E+04	8.38E+03	2.79E+03	1.03E+03	0.
6	↓	2.09E+04	1.27E+01	3.06E+04	7.77E+05	1.23E+01	2.21E+04	7.36E+03	2.57E+03	9.48E+02	0.
8		1.73E+04	1.06E+01	2.55E+04	6.48E+05	1.02E+01	1.84E+04	6.14E+03	2.14E+03	7.90E+02	0.
10		1.13E+04	6.92E+00	1.67E+04	4.23E+05	6.70E+00	1.21E+04	4.01E+03	1.40E+03	5.16E+02	0.
12		6.17E+03	3.77E+00	9.08E+03	2.31E+05	3.65E+00	6.57E+03	2.19E+03	7.63E+02	2.82E+02	0.
14		3.24E+03	1.98E+00	4.76E+03	1.21E+05	1.92E+00	3.45E+03	1.15E+03	4.00E+02	1.48E+02	0.
16		1.68E+03	1.03E+00	2.48E+03	6.30E+04	9.96E-01	1.79E+03	5.96E+02	2.08E+02	7.68E+01	0.
4	5.0	5.31E+04	1.20E+01	1.59E+04	4.84E+05	2.48E+01	2.39E+04	5.15E+03	1.79E+03	8.27E+02	0.
6	↓	5.51E+04	1.11E+01	1.46E+04	3.72E+05	2.21E+01	2.20E+04	4.74E+03	1.65E+03	7.61E+02	0.
8		4.62E+04	9.22E+00	1.22E+04	3.10E+05	1.84E+01	1.83E+04	3.95E+03	1.37E+03	6.35E+02	0.
10		3.00E+04	6.32E+00	7.96E+03	2.03E+05	1.20E+01	1.20E+04	2.58E+03	8.98E+02	4.15E+02	0.
12		1.64E+04	3.29E+00	4.34E+03	1.10E+05	6.57E+00	6.53E+03	1.41E+03	4.89E+02	2.26E+02	0.
14		8.59E+03	1.72E+00	2.24E+03	5.79E+04	3.45E+00	3.43E+03	7.38E+02	2.57E+02	1.19E+02	0.
16		4.47E+03	9.96E-01	1.14E+03	3.01E+04	1.79E+00	1.78E+03	3.84E+02	1.33E+02	6.17E+01	0.

*Note: NP = Nasopharyngeal
TB = Tracheobronchial Region
P = Pulmonary Lung Region
LN = Thoracic Lymph
GIT = Large Intestine

P_k is the population (number of people) of band k, see Table 5-2.

$\sum_{K-1}^{K-20} f_{ik} P_k$ is the population factor for burnup injection in band i, see Table 5-7.

5.3.4 Significant Results and Conclusions

The population factors listed in Table 5-7 reflect two facts: (1) the population of the northern hemisphere is larger (see Table 5-2) than that of the southern hemisphere; and (2) the further north injection occurs, the greater the deposition in the northern hemisphere. The effect of this is shown also in Table 5-8, i.e., the further north the injection latitude, the greater the world population dose estimate. Except for the nasopharyngeal (NP) region and the gastrointestinal tract (GIT), organ dose estimates (see Table 5-8) tend to decrease with increasing particle size (AMAD). Consequently, the highest dose estimates, except for NP and GIT, are those given in the first line of Table 5-8. These values and the health effects risk factors[5-1], given in Table 5-9, coupled with the predicted releases for Modified PW-4b cermet payloads as given in Section 4.3.3, Table 4-12, are the basis for the range of possible health effects predicted in Table 5-10. The results shown in Table 5-10 confirm the recommendations given in Section 4.3.4, that thermal reentry protection should be added to the container surface, and that the stainless steel container material be replaced by a higher melting point alloy.

Using the predicted 11.2 percent Modified PW-4b payload burnup (see Table 4-12 for a 5 MT cermet waste form) and AMAD = 0.2 μm, the maximum individual lifetime doses would be about 0.043 rem to the lungs, 0.016 rem to bone and 0.0011 rem to the total body. These estimates are well below the annual dose-rate limits for individual members of the public.

The graphic display of results shown in Figure 5-6 illustrates two important points; first, the risk is proportional to the amount of Modified PW-4b in cermet form injected into the upper atmosphere and second, the upper and lower bounds of risk are strongly influenced by assumed particle size.

TABLE 5-9. HEALTH EFFECTS RISK FACTORS

Type of Risk	Predicted Incidence per 10^6 Man-Rem
Cancer deaths from:	
Total body exposure	50
Lung Exposure	5
Bone Exposure	2
Thyroid Exposure	3
Specific genetic effects to all generations from:	
Total Body Exposure	50

Source: Reference 5-1.

TABLE 5-10. RANGES OF EXPECTED HEALTH EFFECTS FOR INADVERTENT PAYLOAD REENTRY BURNUP, AS PREDICTED BY PAYLOAD BREAKUP ANALYSIS (MODIFIED PW-4b IN CERMET)

Type of Risk	Releases, kg[a] 1	1007	560	0
Cancer deaths from:				
Total Body Exposure	0.0031 - 0.078	3-79	1-44	0
Lung Exposure	0.0059 - 0.296	5-299	3-166	0
Bone Exposure	0.0036 - 0.065	3-66	2-37	0
Genetic effects from:				
Total Body Exposure	0.0031 - 0.078	3-79	1-44	0

Notes: (a) See Section 4.3.3, Table 4-12, Table 5-8, and Table 5-9.
(b) 9.5 MT Payload, stable reentry, no thermal protection.
(c) 5.0 MT Payload, stable reentry, no thermal protection.
(d) 5.0 MT Payload, spinning reentry, no thermal protection.

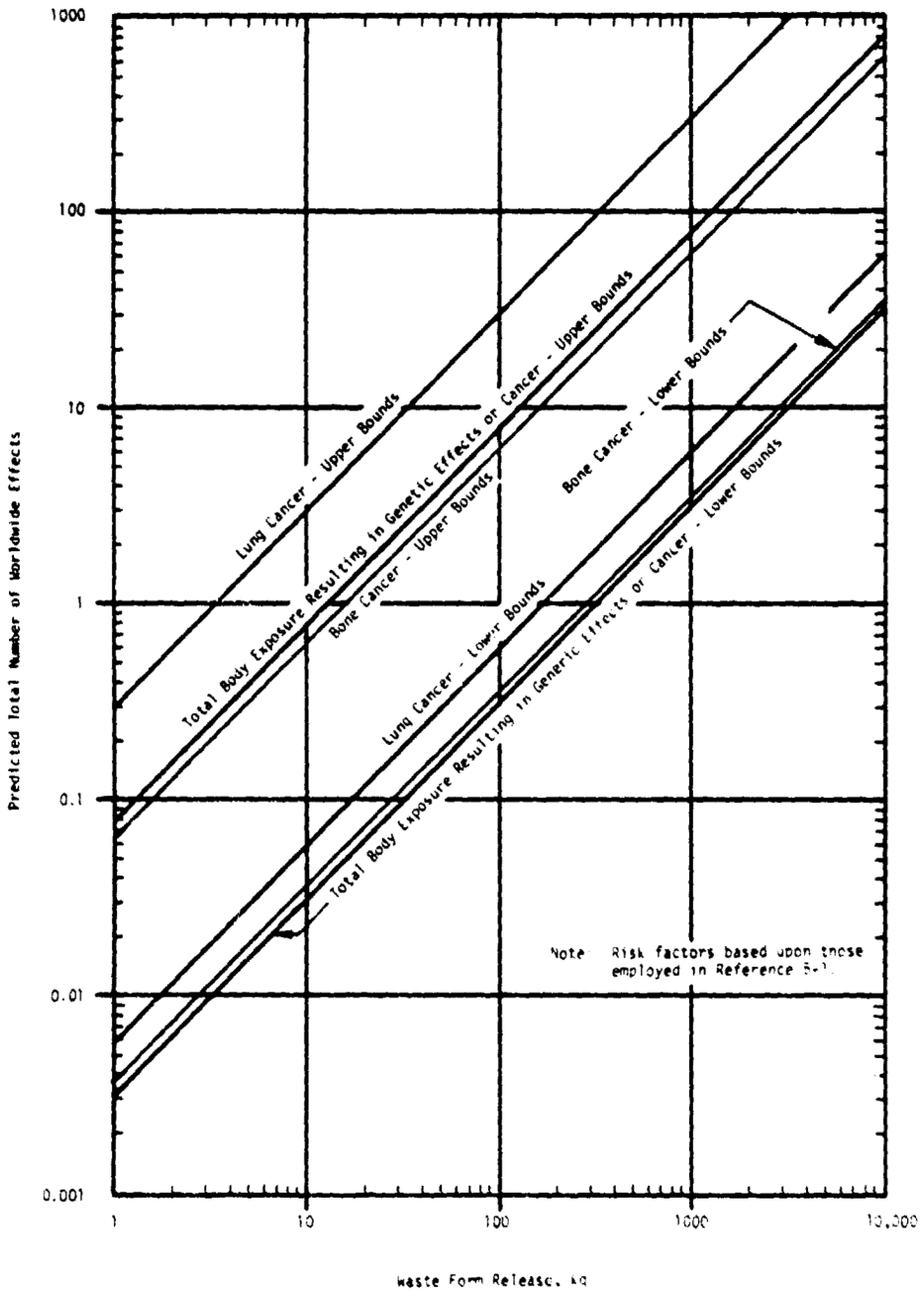

FIGURE 5-6. PREDICTED WORLDWIDE HEALTH EFFECTS AS A FUNCTION OF UPPER ATMOSPHERIC RELEASE OF MODIFIED PW-4b IN CERMET FORM

5.4 References

5-1. Edgecombe, D. S., Rice, E. E., Conlon, R. J., Miller, N. E., and Yates, K. R., "Final Technical Report on Evaluation of the Space Disposal of Defense Nuclear Waste-Phase II," Battelle's Columbus Laboratories, Columbus, Ohio (January 1979).

5-2. Bell, M. J., "ORIGEN - The ORNL Isotope Generation and Depletion Code," ORNL 4628, Oak Ridge National Laboratory, Oak Ridge, Tennessee (May 1972).

5-3. Logan, S. E., and Berbane, M. C., "Development and Application of a Risk Assessment Method for Radioactive Waste Management," EPA 520/6-78-005, The University of New Mexico, Albuquerque, N.M. (July 1978).

5-4. Krey, P. W., and Krajewski, B., "HASL Model of Atmospheric Transport," U. S. Atomic Energy Commission Report, HASL-25 (1969).

5-5. Krey, P. W., and Krajewski, B., "Comparison of Atmospheric Transport Model with Observations of Radioactive Debris," Journal Geophysics. Res. 75(15) (1970).

5-6. Van der Hoven, I., "Deposition of Particles and Gases," Chapter 5-3 in D. H. Slade, ed., "Meteorology and Atomic Energy," Atomic Energy Commission, U. S. Report TID-24190 (1968).

5-7. Sehmel, G. A., Sutter, S. L., and Dana, M. T., "Dry Deposition Processes", in "Pacific Northwest Laboratory Annual Report for 1972, Vol. II, Physical Sciences, Part 1, Atmospheric Sciences," Atomic Energy Commission, U.S. Report BNWL-1751-Pt1 (April 1973).

5-8. Healy, J. W., "A Proposed Interim Standard for Plutonium in Soils," LA-5483-MS, Los Alamos Scientific Laboratory, University of California, LA-5483-MS (1974).

5-9. Sehmel, G. A., "Particle Eddy Diffusivities and Deposition Velocities for Iso-thermal Flow and Smooth Surfaces," Aerosol Science 4:125-138 (1973).

5-10. Sehmel, G. A., "Experimental Measurements and Predictions of Particle Deposition and Resuspension Rates," Report BNWL-SA-5228 U. S. ERDA (March 1975).

5-11. Mork, H. M., "Redistribution of Plutonium in the Environs of the Nevada Test Site," Report UCLA-590 U.S. Atomic Energy Commission (August 1970).

5-12. Anspaugh, L. R., and Phelps, P. L., "Resuspension Element Status Report, VI. Results and Data Analysis" in P. B. Dunaway and M. G. White (eds.) "The Dynamics of Plutonium in Desert Environments, NAEG Progress Report, 1974," Report NVO-142 U.S. Atomic Energy Commission (July 1974).

5-13. Volchok, H. L., "Resuspension of Plutonium 239 in the Vicinity of Rocky Flats," in E. B. Fowler, R. W. Henderson, and M. F. Milligan, eds., "Proceedings of Environmental Plutonium Symposium," Report LA-4756, U.S. Atomic Energy Commission (December 1971).

5-14. Kathren, R. L., "Towards Interim Acceptable Surface Containmination Levels for Environmental Plutonium Oxide," in "Radiological Protection of the Public in a Nuclear Mass Disaster," Report CONF-680507, U.S. Atomic Energy Report (1968).

5-15. Anspaugh, L. R., Phelps, P. L., Kennedy, N. C., and Booth, H. G., "Wind-Driven Redistribution of Surface-Deposited Radioactivity," in "Environmental Behavior of Radionuclides Released in the Nuclear Industry," STI/Pub. 345, International Atomic Energy Agency (1973).

5-16. Anspaugh, L. R., "Resuspension Element Status Report, X. Use of NTIS Data to Predict Air Concentration of Plutonium," in P. B. Dunaway and M. G. White, eds., "The Dynamics of Plutonian in Desert Environments," Report NVO-142, U.S. Atomic Energy Commission (1974).

5-17. Anspaugh, L. R., Shinn, J. H., Phelphs, P. L., and Kennedy, N. C., "Resuspension and Redistribution of Plutonium in Soils," Health Phyyics 29:571-582 (1975).

5-18. Amato, A. J. "A Mathematical Analysis of the Effects of Wind on Redistribution of Surface Contamination, WASH-1187," U.S. Atomic Energy Commission (1971).

5-19 Mills, M. T. and Olson, J. A., "A Model for Suspension and Atmospheric Transport of Dust," Annual Meeting of the American Geophysical University, San Francisco, California (December 1973).

5-20. Killough, G. G. and McKay, L. R., "A Methodology for Calculating Radiation Doses from Radioactivity Released to the Environment," Report ORNL-4992, U.S. Atomic Energy Commission (1976).

5-21. Bagnold, R. A., "The Physics of Blown Sand and Desert Dunes," Methuen, New York (1960).

5-22. Sehmel, G. A. and M. M. Orgill, "Resuspension by Wind at Rocky Flats," in "Pacific Northwest Laboratory Annual Report for 1972, Vol. II Physical Sciences, Pt. 1 Atmospheric Sciences," BNWL-1751-PT1, Battelle's Pacific Northwest Laboratories, (1973).

5-23. Shinn, J. H. and Anspaugh, L. R., "Resuspension-New Results in Predicting Vertical Dust Flux," pp 207-215 in M. G. White and P. B. Dunaway, eds., "The Radioecology of Plutonium and Other Transuranics in Desert Environments," Report NVD-153, U.S. ERDA (1975).

5-24. "Air Quality Data from the National Air Surveillance Networks and Contributing State and Local Networks, 1966 Edition," Publication APTD-68-9 National Air Pollution Control Administration (1968).

5-25. Sehmel, G. A., "Radioactive Particle Resuspension Research Experiments on the Hanford Reservation," BNWL-2081, Battelle's Pacific Northwest Laboratories, Richland, Washington (1977).

5-26. U. S. Environmental Protection Agency, Federal Register 36:22384-22385 (1971).

5-27. Milham, R. C., Schubert, J. F., Watts, J. R., Boris, A. L., and Corey, J. C., "Measured Plutonium Resuspension and Resulting Dose from Agricultural Operations on an Old Field at the Savannah River Plant in the Southeastern United States," in: "Transuranium Nuclides in the Environment," IAEA-SM-199/83, STI/PUB-410, International Atomic Energy Agency, (1976).

5-28. Martin, W. E., and Bloom, S. G., "Plutonium Transport and Dose Estimation Model," in: "Transuranium Nuclides in the Environment," IAEA-SM-199/83, STI/PUP-410, International Atomic Energy Agency (1976).

6.0 LONG-TERM RISK ASSESSMENT*

The disposal of nuclear waste products in space involves some level of attendant risk due to the small but finite chance of failure occurrences during the transport and placement sequence. A broad definition of failure mechanisms includes natural catastrophic events after destination placement, such as meteoroid impact and fragmentation, in addition to the more obvious types of accidents or malfunction in the space vehicle transport system. Because of the serious potential consequences of failures, even if highly unlikely, it is imperative that quantitative risk analyses be performed in a careful and exhaustive manner. This will point the way toward risk reduction requirements as needed, provide a measure of confidence in the concept viability, and allow decision makers a risk perspective comparison of the space option with alternative disposal concepts.

Safety risk may be separated into two categories on the basis of timeline consequences and response. Short-term risk, measured in hours or days, is associated with accidents occurring prior to deep space injection. Included in this category are the sequential phases of waste payload ground handling, launch, ascent to parking orbit, orbital operations, and the early phase of the injection burn while the payload is still bound to Earth's gravitational field. Long-term risk, measured in hundreds or thousands of years, commences after the payload has attained Earth-escape conditions. For the reference concept of a solar orbit destination, this category encompasses deployment system (propulsion and control) failures which prevent the payload from achieving its stable orbit destination, and accidental explosion or other fragmentation events (meteor encounters) which break up the payload and upset the long-term orbit stability. These failures or events could result in the waste material being stray objects in planet-crossing orbits with subsequent future risk of reentry in Earth's biosphere. Some of the short-term safety problems are addressed in Sections 4.0 and 5.0 of this report. This section addresses two new aspects of the long-term problem which have been identified in previous studies of this kind (see References 6-1, 6-2 and 6-3).

A key result of earlier studies is that it may be possible to attain acceptably low levels of long-term risk only through the mechanism of retrieval and final disposal of failed payloads. Rescue mission capability is defined as the ability to send another propulsion system to rendezvous with the failed payload in orbit and to place it into the desired disposal orbit. Suppose, however, that the payload has fragmented, making rescue impossible. Section 6.1 addresses the fragmentation problem and its consequences with the objective of describing the orbital evolution characteristics of small particles in solar orbit and the probability of eventual Earth reentry of this material. Section 6.2 then takes up the more likely disposition of failure

*Note: This section was prepared by "Science Applications, Incorporated, Schaumburg, Illinois, under subcontract to Battelle's Columbus Laboratories.

wherein the payload remains intact and is subject to rescue attempts. The objective here is to provide a technology assessment of the (critical) automated rendezvous and docking phase of the rescue mission with emphasis on noncooperative or only partially cooperative rendezvous due to failure of crucial payload subsystems such as communications and attitude control.

6.1 Payload Breakup Effects

Small remnant particles on the order the 1000 microns or less are subject to various nongravitational forces in the space environment, such as solar radiation pressure and the electromagnetic field carried by the solar wind. Physical processes such as photoionization and surface erosion can induce changes in the state of material that enhance the nongravitational effects. The orbital evolutionary consequences for small particles are very different from those applying to objects influenced by gravitational forces alone. This subsection considers: (1) the initial mass-size distribution of small particles for different types of waste forms; (2) the characteristics of nongravitational forces and the orbital changes produced; and (3) the resulting mass-time distribution of material with focus on the fraction of initial mass intercepted by Earth.

6.1.1 Small Particle Mass Distribution

Although the reference waste form selected for the present study is the ORNL cermet. Other waste forms such as calcine powder have been considered in previous studies. Since the physical properties of calcine and cermet are very different, one would expect wide differences in the particle size distributions resulting from a payload breakup event. Both waste forms are treated in the analysis. This allows a broader perspective of the evolutionary effects of breakup by defining two extreme boundary conditions representing weak material (calcine) and strong material (cermet).

It may be best to present first the derived particle distributions for the two waste forms and then to discuss the conditions leading to these results. Figure 6-1 shows the cumulative mass distributions as a function of particle radius over the range 1 to 1000 microns. Note that the total mass in small-particle state may be less than or equal to the total payload mass, depending on the waste form and the fragmentation condition--this will be clarified later. For calcine, the median particle radius by mass is 6.5 microns with 20 percent of the total mass residing in particles smaller than 3.5 microns and 80 percent of the mass in particles smaller than 20 microns. The cermet distribution, by contrast, is skewed toward larger particles. The median cermet radius is 240 microns with 20 percent of the mass residing in particles smaller than 40 microns and 80 percent of the mass in particles smaller than 620 microns.

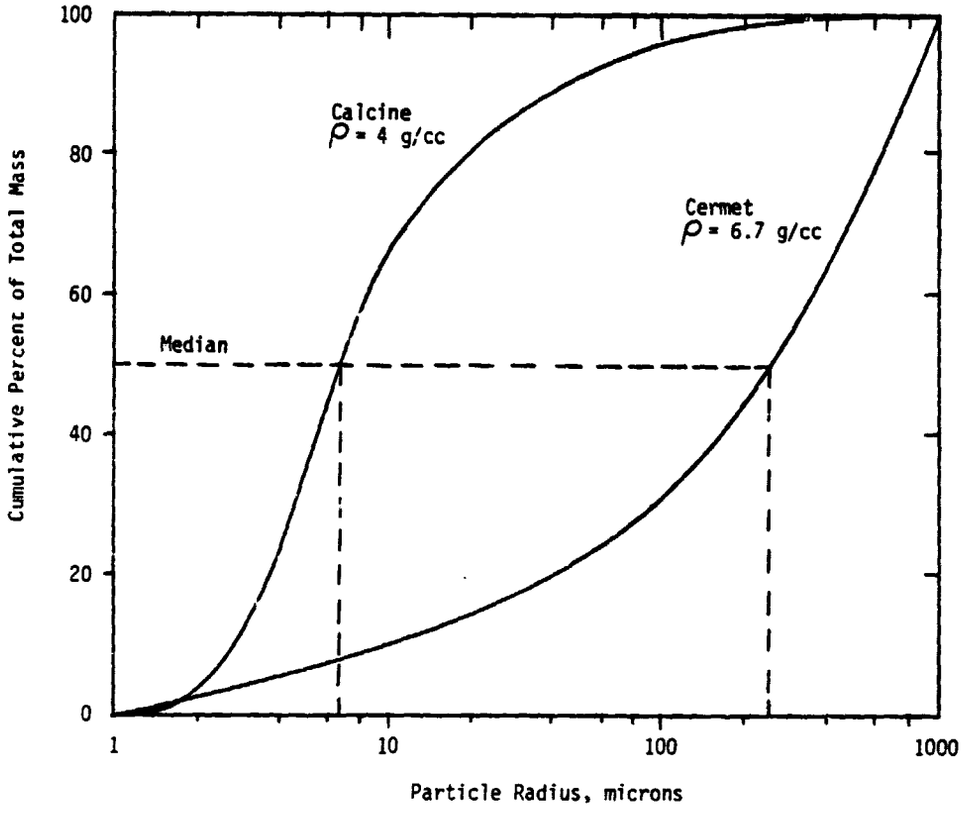

FIGURE 6-1. MASS DISTRIBUTION BY PARTICLE SIZE - CALCINE AND CERMET WASTE FORMS

6.1.1.1 Calcine Waste Form Fragmentation

A simplifying assumption is made for calcine in keeping with the desire to represent an extreme boundary on payload breakup. Namely, whether the breakup was caused by a propulsion system explosion or by a meteoroid impact, it is assumed that the container wall is completely fragmented and that the waste payload disintegrates and is totally released as a fine powder. Although the probability of fragmenting a calcine waste payload has not been evaluated quantitatively, it is estimated that this probability would be very small. The particle size distribution shown in Figure 6-1 was obtained from an earlier Battelle-Northwest data source[6-4] which reported on the physical properties of spray calcine.

6.1.1.2 Cermet Waste Form Fragmentation

The solid cermet waste form should have mechanical properties similar to an iron-nickel alloy. It is reasonable to assume that the likely payload response to a propulsion system explosion in deep space at worst, would be to deform the package with negligible or no release of waste material in small particles. An event of very low probability of occurrence (but having sufficient energy to cause cratering or fragmentation of the payload), is a high-speed impact by a meteoroid projectile.

Fujiwara[6-5] conducted a series of experiments in which high energy projectiles impacted basalt targets. It was found that the target catastrophically fragmented when the energy of the projectile relative to the target mass (E_p/M_t) exceeded 750 Joules/kg. Over a range of energy per unit mass less than this critical value only target cratering occurred. These results may be scaled to the cermet material which is approximately ten times stronger than basalt, i.e., the critical energy level for cermet is taken to be 7500 Joules/kg. Assuming a waste payload mass of 5000 kg and a typical impact velocity of 17.5 km/s, a projectile mass greater than 0.24 kg is expected to result in catastrophic fragmentation of the payload.

Another important result from the above-mentioned experiments[6-5] is the characteristics of the fragment size distribution produced in collisions. For particles less than 1 mm (1000 microns), the fraction of mass which is smaller than a given size, b, can be approximated very well by a square-root distribution.

$$M(<b)/M(<1mm) = (b/1mm)^{1/2} \qquad (1)$$

This result is apparently independent of the sizes of the target and projectile. The distribution for larger fragments is sensitive to the ratio of projectile energy to target mass, but particles larger than 1 mm are not of concern in this analysis. The cermet particle distribution graphed in Figure 6-1 is based on the above equation normalized to the size range 1 to 1000 microns.

The basalt impact experiments[6-5] also give the fragmented fraction of the target mass less than a given size as a function of the energy/mass ratio. These results can be used to find the absolute value of M(<1 mm) as a function of projectile mass. Figure 6-2 shows this characteristic for a target (payload) mass of 5000 kg and an impact velocity of 17.5 km/s; the increased strength of cermet relative to basalt has been accounted for by scaling. A cratering collision produces less than 10 kg of small particles. A 0.24 kg projectile will fragment the target but most of the fragments are large. As the projectile mass and impact energy increase beyond the critical value for fragmentation, an increasing fraction of the payload mass becomes transformed into small particles. In the limit, a 30 kg projectile causes the entire 5000 kg payload to be broken into small pieces.

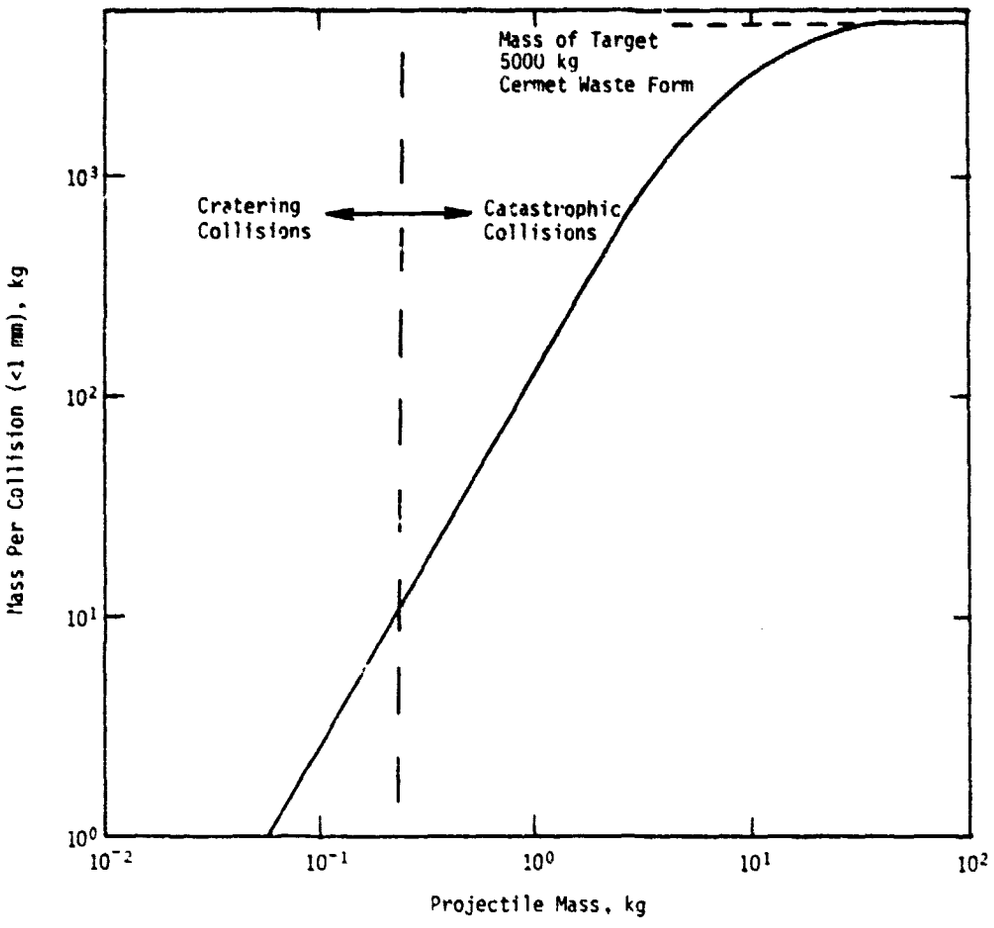

FIGURE 6-2. MASS OF SMALL PARTICLES (<1 mm) PRODUCED BY IMPACTS

The discussion so far focuses on what happens if a meteoroid collision occurs. The remaining question is what is the probability of such an occurrence. Figure 6-3 shows the cumulative flux or collision frequency for projectiles with mass greater than m. The relationship F(>m) is derived from the spatial density of interplanetary debris given by Wall[6-6] using 17.5 km/s as the impact velocity and 1.0 m^2 as the payload cross section area. The probability of a catastrophic collision is less than 5×10^{-9} per year, or 0.005 in a million years.

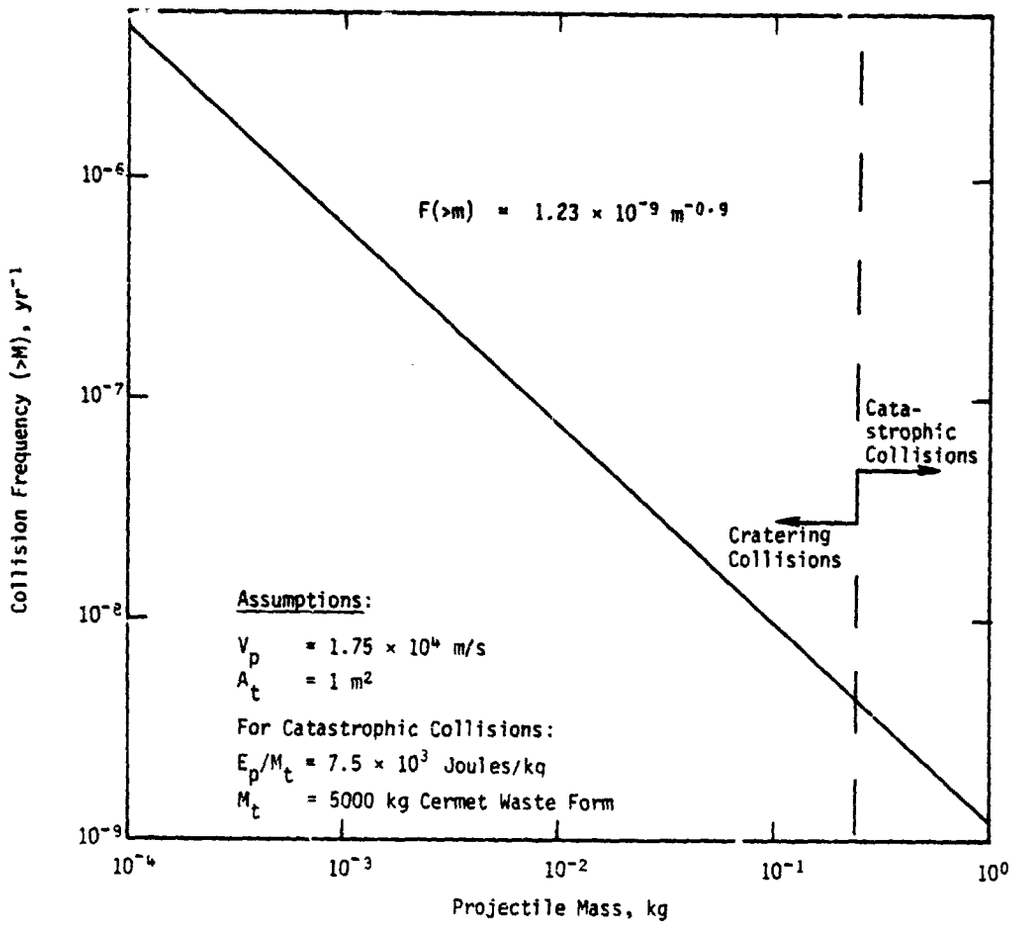

FIGURE 6-3. FREQUENCY DISTRIBUTION OF IMPACTING PROJECTILES

The production rate of particles less than 1 mm is found by integrating the product of the differential collision frequency and the mass of particles produced. This rate is found to be 1.6×10^{-6} kg/year. If all small particles immediately reencountered Earth due to nongravitational effects (which is certainly not the case), then this production rate is equivalent to a probability of only 3×10^{-10}/year that the entire waste payload returns to the Earth. Projectile masses between 1 and 100 kg account for over 90 percent of the total production. Thus, catastrophic collisions dominate and cratering collisions contribute little to the production of small particles. In any event, over a period of one million years, the probability of any significant amount of cermet waste returning to Earth is very small. Keeping this perspective in mind, the next subsection addresses the manner in which small particles, under various orbit perturbing influences, could return to Earth.

6.1.2 Physical Effects on Small Particles in Solar Orbit

Table 6-1 presents a fairly complete, qualitative description of the various perturbation sources affecting small particles, their basic characteristics, and the orbit evolutionary consequences expected. Gravitational forces act on all bodies independent of size. The perturbing effects of these forces have been described in detail in previous analyses of long-term risk, but they are noted again here because of their interaction with nongravitational force effects which are strongly dependent on particle size. In particular, the close planetary encounters which could arise as a result of the latter perturbations is one of the principal mechanisms for waste particle interception by Earth.

Nongravitational forces fall into two main categories: (1) those which are induced either directly or indirectly by solar radiation pressure; and (2) those which are induced on a charged particle moving in the electromagnetic field carried by the solar wind. The momentum carried by the photon and corpuscular flux of solar radiation and solar wind produce a radially outward force on the orbiting particle. This direct force results in orbit perturbations that are generally negligible except for particles on the order of 1 micron or less near the Sun. The indirect effect of solar radiation and wind pressure arises in two ways: (1) Poynting-Robertson drag acting on a moving particle as a result of the reradiated energy flux; and (2) Yarkovsky "drag" acting on a spinning particle as a result of asymmetric reradiation induced by thermal lag between the morning and evening hemispheres of the rotating particle. These two forces can act together or in opposite directions depending on whether the particle is spinning in a retrograde or prograde sense. Poynting-Robertson drag is generally the dominant of the two indirect forces, except for large particles spinning rapidly. The orbit evolutionary consequence is then generally an inward spiral to the sun, the speed of which depends on particle size as will be described later.

All dust particles take on some equilibrium electric potential when in the space environment. This potential is further enhanced for radioactive particles. The Lorentz force induced on charged particles moving through the interplanetary magnetic field can be a very significant perturbation source, but only on very small grains in the submicron size range. In the range 1 to 10 microns, Lorentz and Poynting-Robertson forces have comparable magnitudes although the orbital consequences of each are very different. Because of the randomly fluctuating magnetic field, the Lorentz force phenomenon is best described statistically in the sense of a scattering or diffusion process.

The final categorization in Table 6-1 refers to material changes rather than forces, although the two are not unrelated and can be strongly interactive in the case of very small particles. Surface erosion or sputtering caused by solar wind ions takes place at a rate of approximately 1 Å/year = 10^{-4} microns/year.[6-7] The eroded material will be swept out with the solar wind while the remaining material, diminished in size, will be acted upon by the nongravitational forces in a slightly stronger manner than before. Another material change is caused by vaporization of particles when very near the sun, e.g., in the final stages of a Poynting-Robertson spiral.

TABLE 6-1. SUMMARY OF PHYSICAL EFFECTS ON SMALL PARTICLES IN SOLAR ORBIT

PERTURBATION SOURCE	BASIC CHARACTERISTICS	EVOLUTIONARY CONSEQUENCES
A. GRAVITATIONAL FORCES INDEPENDENT OF PARTICLE SIZE		
1. DISTANT PLANETARY ATTRACTION	• PERVADING SMALL FORCES • VARIABLE MAGNITUDE AND DIRECTION	• LONG-TERM SECULAR CHANGE IN ORBITAL ELEMENTS
2. CLOSE PLANETARY ENCOUNTERS	• IMPULSIVE TYPE FORCE • INFREQUENT BUT MULTIPLE OCCURRENCE • BEST DESCRIBED STATISTICALLY	• SMALL-TO-LARGE ORBITAL CHANGE • PLANETARY COLLISION
B. NONGRAVITATIONAL FORCES DEPENDENT ON PARTICLE SIZE		
3. SOLAR RADIATION PRESSURE SOLAR WIND PRESSURE	• MOMENTUM CARRIED BY PHOTON FLUX AND CORPUSCULAR FLUX, THE LATTER BEING SMALL IN COMPARISON • RADIALLY OUTWARD FORCE	• EFFECTIVE REDUCTION OF SOLAR GRAVITY • GENERALLY NEGLIGIBLE EXCEPT FOR SUBMICRON PARTICLES WHERE ABRUPT ORBITAL CHANGE AND SOLAR SYSTEM ESCAPE CAN OCCUR
4. POYNTING-ROBERTSON DRAG	• INDIRECT EFFECT OF RERADIATED ENERGY FLUX (MOMENTUM LOSS) ON MOVING PARTICLE • TANGENTIALLY BACKWARD FORCE	• PARTICLE SPIRALS IN TOWARD SUN AS ORBIT SIZE AND ECCENTRICITY DECREASES • CAN BE SIGNIFICANT EFFECT FOR PARTICLES SMALLER THAN 1 mm
5. YARKOVSKY DRAG (±)	• INDIRECT EFFECT OF ASYMMETRIC RERADIATION FOR A SPINNING PARTICLE HAVING THERMAL LAG • ADDS TO POYNTING-ROBERTSON FOR RETROGRADE SPIN	• CAN SPEED UP OR SLOW DOWN SPIRAL • STRONG DEPENDENCE ON SPIN RATE, SIZE AND COMPOSITION • CAN BE SIGNIFICANT FOR PARTICLES LARGER THAN 1 mm
6. ELECTROMAGNETIC FIELD CARRIED BY SOLAR WIND	• LORENTZ FORCE INDUCED BY FLUCTUATING MAGNETIC FIELD INTERACTING WITH CHARGED PARTICLES IN MOTION • BEST DESCRIBED STATISTICALLY	• DIFFUSION OF ORBITAL ELEMENTS WITH TIME IN THE SENSE OF RANDOM WALK PROCESS • CAN BE SIGNIFICANT FOR SUBMICRON PARTICLES
C. MATERIAL CHANGES		
7. SPUTTERING	• SURFACE EROSION BY SOLAR WIND IONS AT RATE ~ 1A°/YEAR	• ERODED MATERIAL SWEPT OUT WITH SOLAR WIND • FOR REMAINING MATERIAL, THE INTERACTION WITH OTHER FORCES DUE TO SIZE REDUCTION CAN BE IMPORTANT ONLY FOR SUBMICRON PARTICLES
8. SUBLIMATION/EVAPORIZATION	• CHANGE TO MOLECULAR STATE DUE TO HIGH TEMPERATURES NEAR THE SUN	• VAPORIZED MATERIAL SWEPT OUT WITH SOLAR WIND • STRONG INTERACTION WITH OTHER FORCES FOR UNVAPORIZED SMALL PARTICLES
9. PHOTOIONIZATION	• SOLAR RADIATION IONIZATION OF VERY SMALL PARTICLES AND FREE MOLECULES AND ATOMS	• ALL FREE GAS SWEPT OUT WITH SOLAR WIND • ELECTROMAGNETIC EFFECTS ON CHARGED PARTICLES

The vaporized material will be swept out with the solar wind. Solar radiation ionization of very small particles and free molecules and atoms can also be expected to occur. All free gas will be carried away by the solar wind, and charged particles will be subject to electromagnetic effects as discussed before.

The purpose in the following quantitative analysis is to gain some measure of understanding about this plethora of small particle phenomena. Fortunately, much of the recent work in the field of planetary science dealing with the nature and dynamics of interplanetary particles has direct application to this problem (see References 6-7, 6-8, and 6-9).

6.1.2.1 Solar Radiation and Solar Wind Forces

The solar radiation pressure acting on a perfectly absorbing body at 1 A.U. distance is 4.5×10^{-2} N/cm^2, and varies inversely with the square of the distance to the sun. The solar wind pressure under average solar activity conditions is 1.7×10^{-5} N/cm^2. Each radiation and solar wind component contributes to the direct radial pressure, but the latter is more than three orders of magnitude smaller and can usually be neglected. The one exception here is particles that are much smaller than the wavelength of light ($\sim$0.5 micron). In this case the particle becomes increasingly transparent to solar radiation pressure but not to solar wind pressure.

The ratio of the radial acceleration (due to solar radiation or wind) to that of solar gravity is easily calculated and gives some insight to the magnitude of this direct perturbation force. This ratio which is independent of solar distance is listed below for several values of particle radius assuming a particle density of 4 g/cm^3.

Particle Radius, microns	Solar Radiation to Gravity Ratio (A_r/A_g)
0.01	1.0×10^{-1}
0.1	8.0×10^{-1}
1	1.5×10^{-1}
10	1.5×10^{-2}
100	1.5×10^{-3}

Since the radial acceleration acts in the opposite direction of solar gravity, the result is an effective reduction in the gravity force seen by the particle. If the particle is released in a circular orbit at distance r, then immediately the orbit becomes elliptical with perihelion at r and aphelion at $r/(1 - 2\ A_r/A_g)$. For example, a 1 micron particle released at r = 0.85 A.U. would have an orbit aphelion distance of 1.214 A.U. A 10 micron particle would be perturbed into a 0.85 x 0.876 A.U. orbit. To summarize, then, the direct effect of solar radiation pressure is an instantaneous orbit perturbation of generally small magnitude except for particle sizes in the range 0.05 to 2 microns.

6.1.2.2 Poynting-Robertson Drag

A particle moving in a circular orbit with velocity u will experience a tangentially backward acceleration as a result of the momentum loss associated with the reradiation of incident energy. Taking into account both the photon and corpuscular energy flux, the magnitude of this acceleration may be expressed as

$$A_{pr} = (u/c) \cdot A_{rp} + (u/v_w)A_{sw} \tag{2}$$

where A_{rp} and A_{sw} are the solar radiation and solar wind accelerations in the radial direction, $c = 3 \times 10^8$ m/s is the velocity of light, and $v_w = 4 \times 10^5$ m/s is the solar wind velocity. It will be noted that although A_{sw} is several orders of magnitude less than A_{rp}, the larger coefficient (u/v_w) makes up most of this deficit so that the solar wind component contributes about 16 percent of the total Poynting-Robertson acceleration (actually a drag deceleration).

The above argument holds in the more general case of an initial elliptical orbit, and one can write the differential equations that govern the change in orbit semimajor axis, a, and eccentricity, e.

$$\frac{da}{dt} = \frac{-k}{a}\left[\frac{2+3e^2}{(1-e^2)^{3/2}}\right] \tag{3}$$

$$\frac{de}{dt} = \frac{-k}{a^2}\left[\frac{5e}{2(1-e^2)^{1/2}}\right] \tag{4}$$

$$k = \frac{4.2 \times 10^{-4}}{\rho r_p} \tag{5}$$

where r_p and ρ are the particle radius and density. The constant in Equation (5) is chosen such that the units for a and t are A.U. and years, and the units for r_p and ρ are microns and g/cm^3. Examination of these equations shows that, for any initial conditions a_0 and e_0, the Poynting-Robertson drag causes the orbit to spiral in toward the Sun and become more circular as it does so. Also, small low density particles spiral in at a higher rate.

When the initial eccentricity is small ($e_0 < 0.1$), which is the case of interest here, the solution to the above equations is very well approximated by the following expressions.

$$a = a_0(1 - t/t_F)^{1/2} \quad (6)$$

$$e = e_0(a/a_0)^{5/4} \quad (7)$$

$$t_F = 595\ a_0^2\ \rho\ r_p \quad (8)$$

where t_F is the Poynting-Robertson lifetime in years. The normalized orbit decay time history is graphed in Figure 6-4, and Figure 6-5 shows the orbit decay lifetime as a function of particle radius and density for $a_0 = 0.85$ A.U. If the density is 4 g/cm^3, the lifetime of a 1 micron particle is only 1720 years but a 1000 micron particle would orbit for 1.72 million years before reaching the sun.

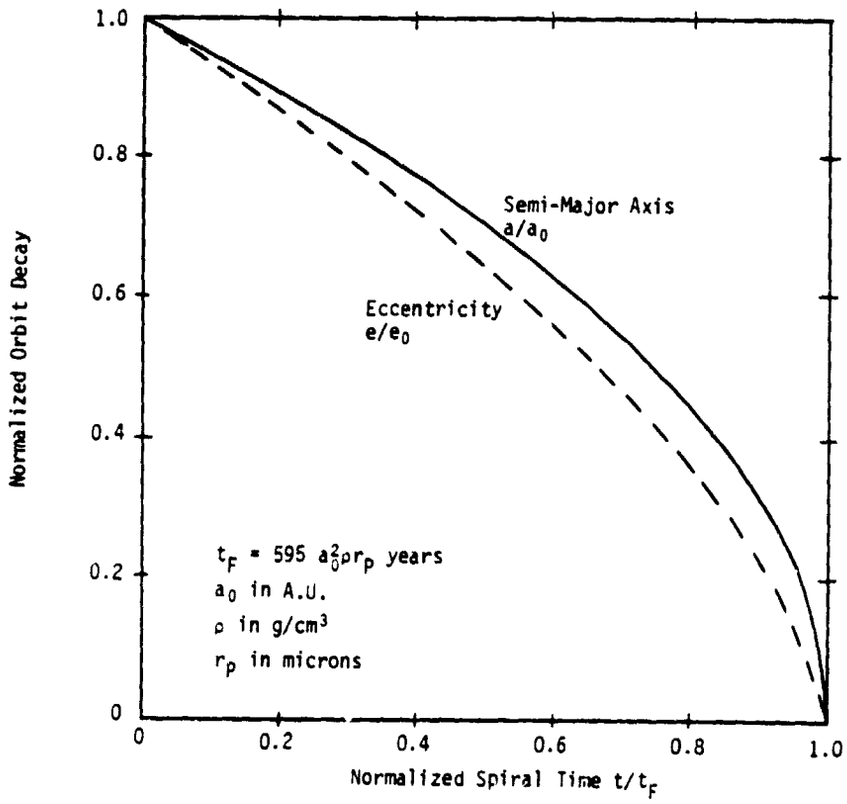

FIGURE 6-4. ORBIT DECAY UNDER POYNTING-ROBERTSON DRAG FORCE FOR NEAR-CIRCULAR INITIAL ORBITS AND $r_p > 0.5$ MICRON

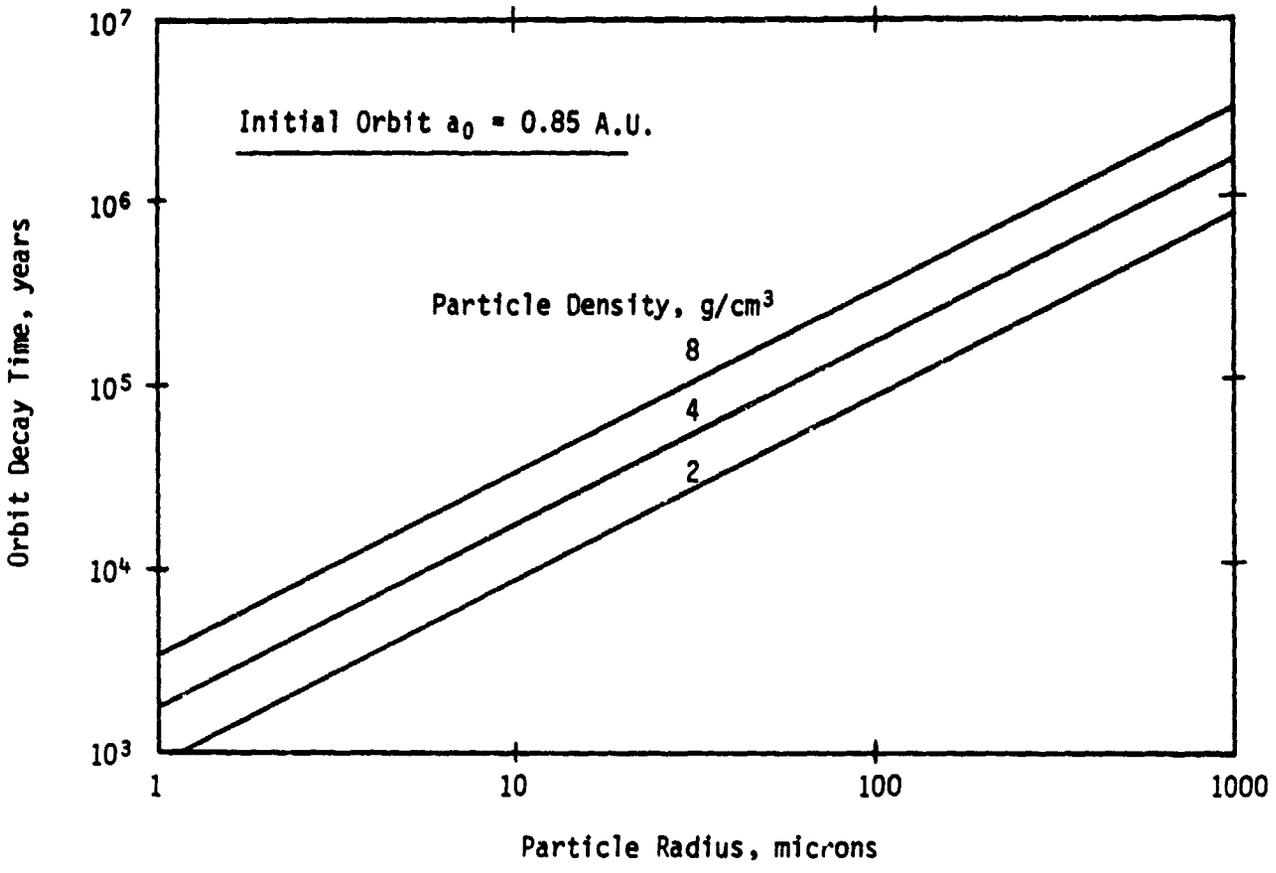

FIGURE 6-5. PARTICLE LIFETIME UNDER POYNTING-ROBERTSON DRAG

There is apparently little chance that a particle following a Poynting-Robertson spiral will actually be absorbed by the sun. As it nears the close vicinity of the sun the material state changes due to sputtering, vaporization and photoionization become significant. These effects in combination with the dramatically increased radiation pressure and electromagnetic forces should cause the material to be rapidly ejected outward within a relatively short time and should eventually escape the solar system. There exists some low probability that ejected material could be captured by Earth as it sweeps past the Earth's orbit. An upper bound on this probability can be calculated by assuming a charged particle state and a capture cross section equal to the Earth's magnetosphere (63,800 km radius). Taking into account the probability that Earth will be located in the interception region at the time of 1 A.U. crossing, the capture probability (P_c) is given by the bounded expression:

$$P_c = (5.76 \times 10^{-8}/\tan i) \leq 1.35 \times 10^{-4} \qquad (9)$$

where i is the orbit inclination of the ejected material. If i = 1° then the capture probability is only 3×10^{-6}. At i = 7°, which is the difference between the solar equator and the ecliptic planes, the capture probability is 5×10^{-7}.

A second indirect effect of solar radiation pressure was noted earlier. This is the transverse reaction force termed the Yarkovsky effect which is induced in spinning particles because of the differential reradiation from the lightside and darkside hemispheres. For particles in retrograde spin, the Yarkovsky drag force adds to the Poynting-Robertson drag; for prograde spin this force acts in the opposite direction and is therefore a "negative drag." The magnitude of the Yarkovsky force depends upon the particle size, physical composition,* rate of spin, and orbital distance. The importance of this force is best described in terms of its magnitude relative to Poynting-Robertson drag as shown in Figure 6-6 for cermet particles. Two asymptotic regimes describe the main result. The sloping lines correspond to "slow" rotating bodies and the horizontal lines to "fast" rotating bodies, where the designations slow and fast refer to the spin period as measured against the thermal penetration time; in fast rotation the thermal effect is confined to the surface layers of the particle. Although estimation of induced spin rates is beyond the scope of this study, we could at least bound the Yarkovsky effect by examining the maximum drag ratio as indicated by the dashed lines in Figure 6-6. For cermet particles, the maximum drag ratio does not exceed unity until the particle radius is larger than 1000 microns. The equivalent particle size for calcine is 100 microns. Since the actual drag ratio is likely to be much less than the maximum, the Yarkovsky effect is thought to be relatively unimportant compared to the Poynting-Robertson effect for the range of particle sizes considered here. Furthermore, one could reasonably argue that the long-term Yarkovsky force might average to near zero value due to precession of the spin axis produced by solar radiation pressure.

6.1.2.3 Lorentz Scattering

A particle in solar orbit can take on an electric charge because of the combined effects of solar wind ions and electrons, photoionization, and alpha and beta emissions in the case of radioactive material. This charge is given by the expression

$$q = (r_p\ V/300)\ \text{esu} \qquad (10)$$

where r_p is the particle radius in cm and V is the electric potential in volts. The potential of a small particle from a radioactive waste package has recently been calculated by Williams[6-10] for specific particle sizes, distances from the sun, and ages of the reprocessed waste. This calculation assumes the PW-4b reference waste mix and cermet form, and reprocessing 10 years after reactor removal.

The equilibrium potential for ordinary, nonradioactive particles lies in the range 7 to 12 volts for all particle sizes and solar distances; V increases from 7 volts at a = 0.1 A.U. to 12 volts at a = 1 A.U. and remains constant beyond 1 A.U. Radioactive particles have a higher equilibrium potential, especially at large values of r_p and a, but this decreases with time

* Thermal conductivity and specific heat

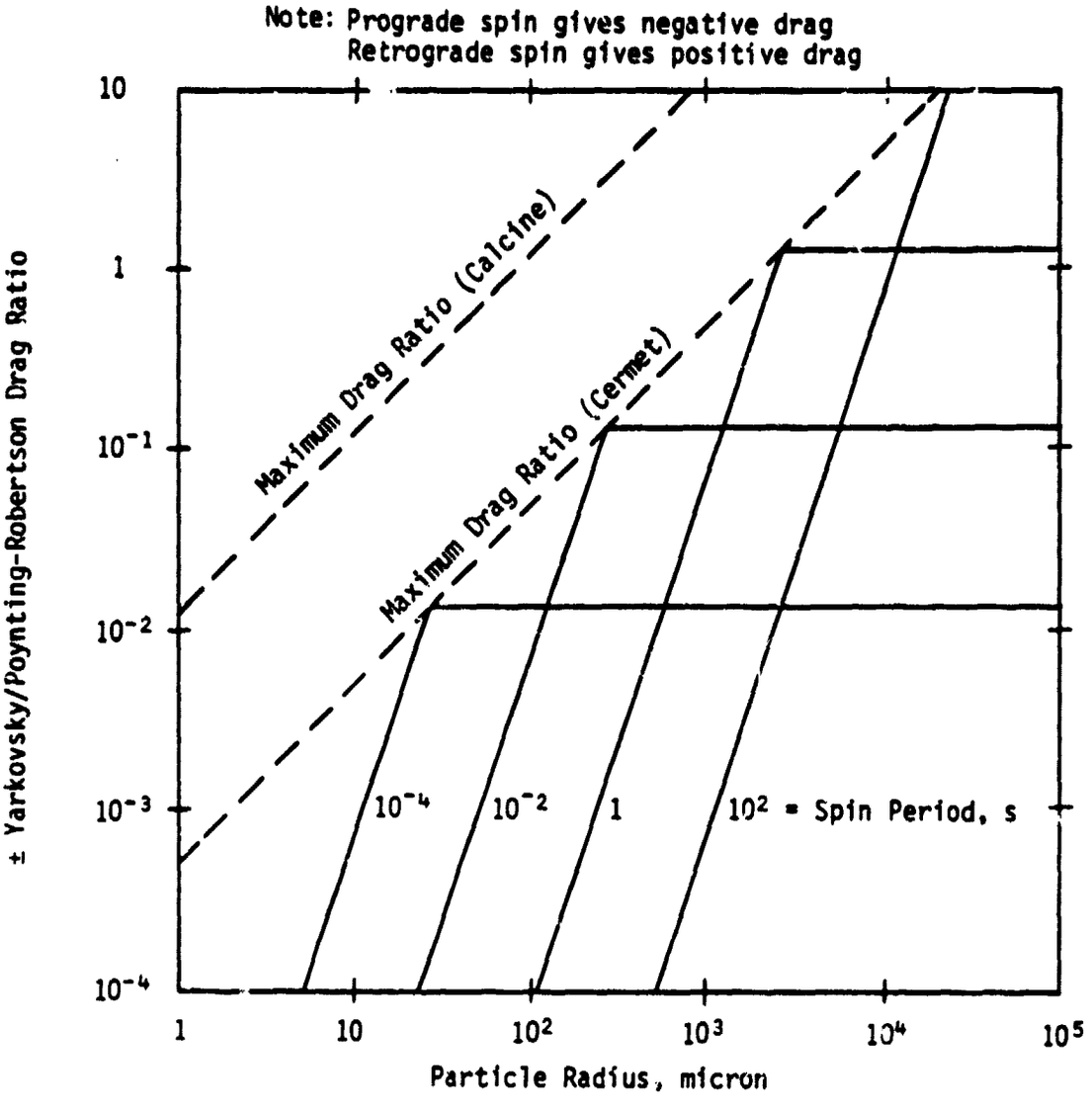

FIGURE 6-6. COMPARISON OF YARKOVSKY AND POYNTING-ROBERTSON DRAG FORCES AT 0.85 A.U. SOLAR DISTANCE

as the emission activity diminishes and eventually reaches the free space potential. For example, at t = 0, a 1 micron particle would take on potentials of 12, 14 and 32 volts, respectively, if placed at distances of 1, 2 and 5 A.U. The initial potential values of a 10 micron particle at these distances are 19, 48 and 350 volts.

Figure 6-7 is a graphical restatement of Williams' data for cermet particles orbiting the Sun at the nominal storage orbit distance of 0.85 A.U. The equilibrium potential as a function of time can be represented by the empirical equation

$$V(t) = 11 \text{ volts} + V_{ro} \exp(-t/30 \text{ years}) \quad (11)$$

where 11 volts is the potential without radioactivity and V_{ro} is the additional potential with radioactivity at t = 0. The decay constant of 30 years

corresponds to the half-lives of ^{137}Cs and ^{90}Sr fission products, which are the primary sources of the radioactive emissions that cause a higher equilibrium potential. It should be noted that the Modified PW-4b waste mix (90 percent removal of ^{137}Cs and ^{90}Sr) would only hasten the time (<100 years) for decay to the free space potential of 11 volts.

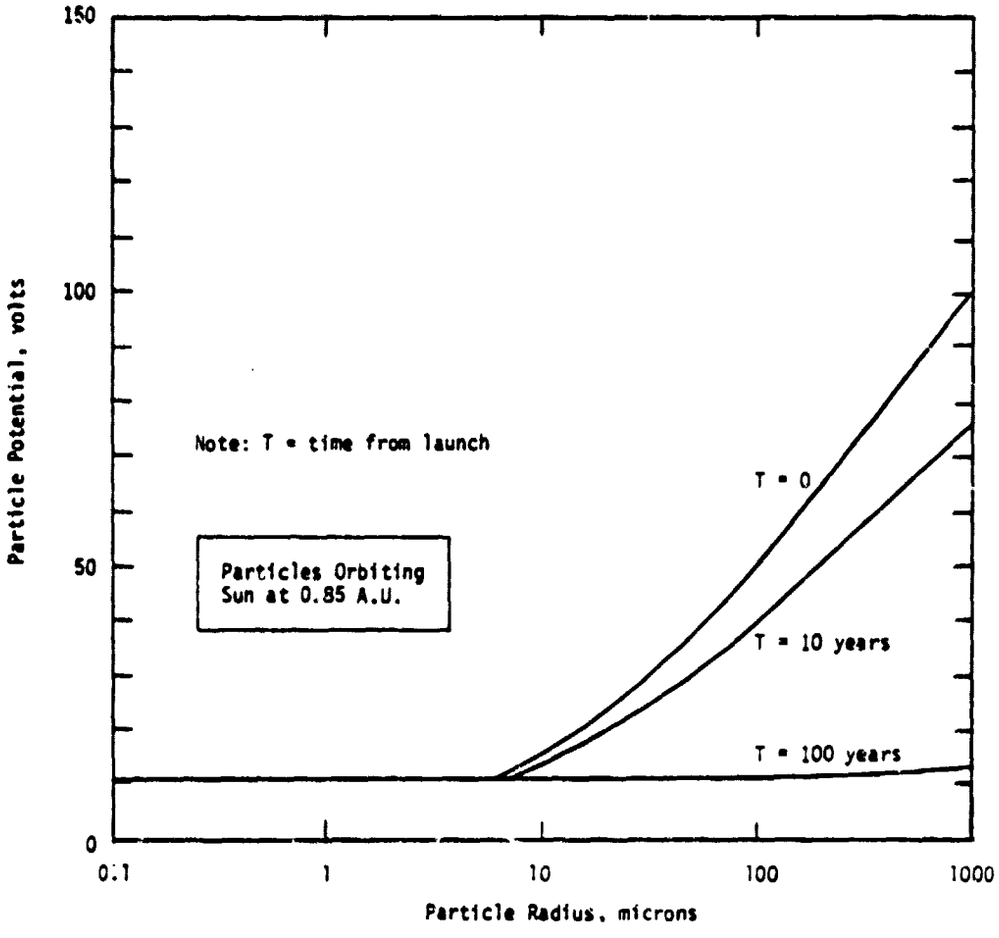

FIGURE 6-7. EQUILIBRIUM POTENTIAL OF SMALL RADIOACTIVE PARTICLES (PW-4b CERMET)

The electromagnetic Lorentz force per unit mass acting on a charged particle is given by

$$\underline{A}_{\ell} = (q/mc)\ (\underline{v} \times \underline{B}) \qquad (12)$$

where $m = 4/3\ r_p^3$ is the particle mass, c is the velocity of light, $\underline{v}$ is the velocity vector, and $\underline{B}$ is the magnetic field vector. For this problem the appropriate v is the addition of the solar wind and orbital velocities and the appropriate $\underline{B}$ is the solar magnetic field. A simplified estimate of the magnitude of the Lorentz acceleration can be made by considering the radial velocity direction where the solar wind speed greatly dominates the orbital speed. Taking $\rho = 6.7$ g/cm^3, V = 11 volts, and B = 3 x 10^{-5} gauss, the Lorentz acceleration is calculated from $A_\ell = 5.23 \times 10^{-11}/r_p^2$ in cgs units. Hence, a 1-micron particle (10^{-4} cm) would experience an acceleration of 5 x 10^{-3} cm/s^2; by comparison, the solar gravity at 0.85 A.U. is 0.82 cm/s^2. The inverse-square relationship makes it obvious that only particles smaller than a few microns would be perturbed significantly by the Lorentz force, even if the equilibrium potential on larger particles is much higher than 11 volts. This implies, as will be seen shortly, that radioactivity is of little importance in the orbit changes induced by electromagnetic effects.

The solar magnetic field is three-dimensional and time-varying on a scale short compared to the orbit period. The in-plane sector structure of the field changes sign on a time scale of several weeks while the out-of-plane structure due to turbulence in the solar wind changes sign on a time scale of days. Since this situation is best described by a random force process, the effect will be to randomly scatter the orbit elements of the particle about their mean value. In the absence of any other forces, the mean elements are unaffected and maintain their initial values.* The interaction with other forces is treated later.

An approximate analytical theory for this scattering or diffusion process has been developed by Consolmagno.[6-9] The mean-square change in semimajor axis, eccentricity, and inclination are determined by a set of complicated but manageable equations expressed in terms of the particles' initial orbit elements, size and density, and electric potential. These equations are not to be repeated here, but it may be useful to give the reduced expressions for the special case of a circular orbit near the plane of the solar equator. Taking V = 11 volts and transforming to a convenient set of units, the standard deviation or RMS (root mean square) values of the changes in a, e and i are given by

$$\sigma_a = (4.76 \times 10^{-2}/r_p^2 \rho)\, a_0^{0.5} t^{0.5} \quad \text{A.U.} \qquad (13)$$

$$\sigma_e = (1.69 \times 10^{-2}/r_p^2 \rho)\, a_0^{-0.5} t^{0.5} \qquad (14)$$

$$\sigma_i = (4.31/r_p^2 \rho)\, a_0^{-0.5} t^{0.5} \quad \text{degrees} \qquad (15)$$

with the particle radius (r_p) in microns, density (ρ) in g/cm^3, semimajor axis (a_0) in A.U. and time (t) in years. For example, over a period of 100 years, a 1-micron particle of density 6.7 g/cm^3 released in a 0.85 A.U., the circular orbit would experience a random perturbation of its orbit as measured

* This is only a supposition.

by RMS changes of 0.07 A.U. in semimajor axis, 0.03 in eccentricity and 7° in inclination.

The amount of scattering is seen to be proportional to the square root of time and inversely proportional to the square of the particle size. Figure 6-8 shows the semimajor axis scattering as a function of these parameters. The solid lines are calculated from Equation (13) and apply to particles which are not radioactive or which are derived from waste more than 100 years old. The dashed lines account for the radioactivity effect starting with newly processed waste at T = 0 and allowing the equilibrium potential to decay as shown in Figure 6-7. For the assumed initial orbit at 0.85 A.U., encounters with Earth or Venus are possible if the RMS Δa changes by more than 0.04 A.U. Only very small particles with radii less than 10 microns diffuse to this stability limit in less than 1 million years. The charge contribution due to radioactivity is seen to be of little consequence and can practically be ignored in the subsequent analysis.

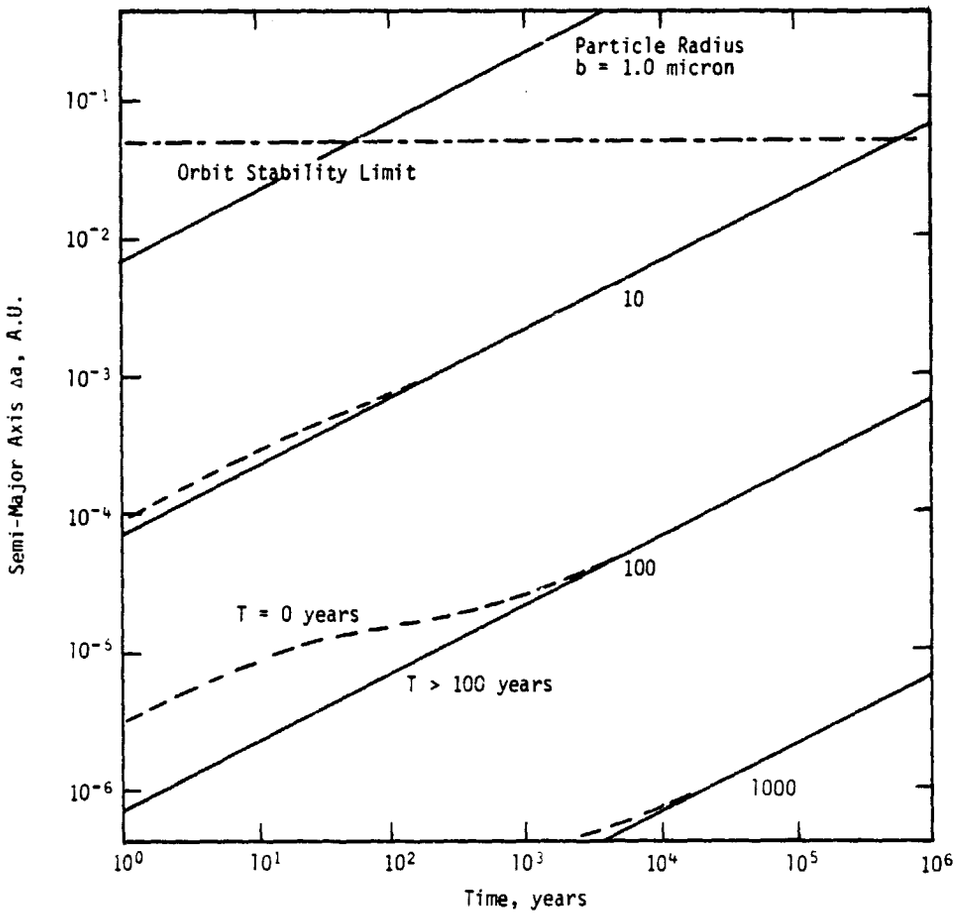

FIGURE 6-8. LORENTZ SCATTERING OF CHARGED DUST PARTICLES (PW-4b CERMET, a_0 = 0.85 A.U.)

6.1.2.4 Combined Poynting-Robertson and Lorentz Effects

It is necessary to know both the mean orbital elements of particles subjected to the Poynting-Robertson effect and the RMS change in the same parameters due to Lorentz scattering, to calculate the mass-time distribution of small particles that may be perturbed into Earth-crossing orbits and captured. Some insight concerning these competing forces may be gained by comparing Equations (8) and (13). Specifically, what is the limiting particle radius for which the RMS Lorentz change in semimajor axis equals one-third of the total Poynting-Robertson drift? The appropriate expression is $r_p^{3/2} = 3.48(a_0/\rho)^{1/2}$ which, for $a_0 = 0.85$ A.U., and $\rho = 6.7$ g/cm^3, is evaluated at $r_p = 1.15$ microns. Hence, Poynting-Robertson drift can be expected to dominate the motions in the inner solar system of all small particles larger than several microns, but Lorentz scattering can maintain significant numbers of submicron- and micron-sized particles against loss by Poynting-Robertson orbit collapse.

Figure 6-9 illustrates a snapshot time history of the combined effect of these two perturbing forces on semimajor axis. Lorentz scattering is shown as a time-varying Gaussian-like spread about a time-varying mean value due to Poynting-Robertson drift. If the initial condition is a circular orbit at 0.85 A.U., then eventually the distribution spreads outward to cross the Earth's orbit which lies in the distance range 0.98 to 1.02 A.U. There exists some low probability of Earth capture (reentry) during the interval of time when a particle orbit is within this 0.04 A.U. region. For any single particle, this time interval can be calculated by first determining the area (probability) of the Gaussian distribution encompassing this crossing region as a function of time, and then integrating this probability over the Poynting-Robertson lifetime. This value of Δt associated with Earth crossing risk is then used to calculate the probability of Earth reentry for that particle. Finally, the reentry probability is integrated over the size distribution of particles to determine the mass fraction of small particles expected to return to Earth. Orbit eccentricity changes, not shown in the simplified illustration of Figure 6-9, were accounted for in the computational procedure which generated the results described in the next subsection.

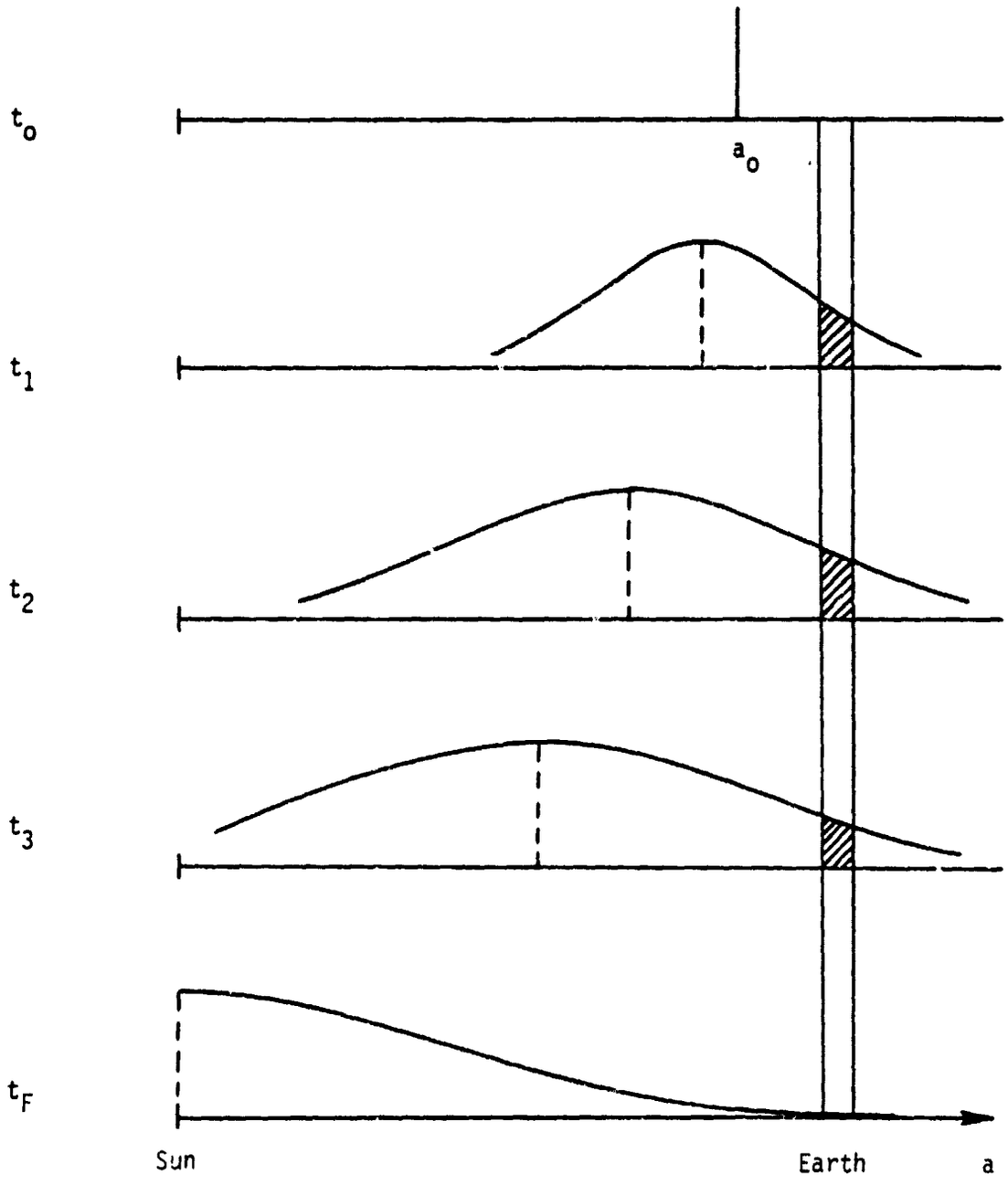

FIGURE 6-9. SNAPSHOT OF COMBINED EFFECTS DUE TO POYNTING-ROBERTSON DRIFT AND LORENTZ SCATTERING

6.1.3 Mass-Time Distributions and Earth Interception

The evolutionary distribution of small particle mass with time after payload breakup, and the fraction of total mass falling on each of the inner planets (Mercury, Venus, and Earth) has been calculated for a set of eight different initial conditions. These eight cases derive from combinations of the following conditions:

(1) Calcine and Cermet Waste Forms
(2) Nominal Storage Orbits at 0.85 A.U. and 1.19 A.U.
(3) Circular and Elliptical Initial Orbits.

The two waste forms have very different particle size distributions if breakup occurs; and therefore, one can expect different dispositions of the total mass in small particles. The 1.19 A.U. circular orbit between Earth and Mars has been discussed in previous studies as a candidate destination. Results here show that the reference 0.85 A.U. destination was the better choice, at least from the perspective of breakup effects. The circular initial orbit represents the case of payload breakup any time after achieving the nominal stable orbit, whereas the elliptical initial orbit represents a breakup event occurring before or at the start of the circularization propulsive maneuver. All initial orbits are assumed to be inclined by 1° relative to the ecliptic plane.

Figure 6-10 shows the mass-time distribution of calcine small particles for initially circular orbits at both 0.85 A.U. and 1.19 A.U. distance from the sun. As expected, the shape of the curves correlates closely with the calcine particle size distribution (see Figure 6-1). For the 0.85 A.U. case, the resulting disposition stated as a fraction of the total initial mass is as follows: (a) 0.001 percent falls on Earth; (b) 0.2 percent falls on Venus; (c) 0.01 percent falls on Mercury; and (d) 99.8 percent survives to the close vicinity of the sun. The mean time for the material return to Earth is about 800 years after the payload breakup event. Of the particles surviving to the sun, 12 percent of the mass arrives within 5000 years, 44 percent within 10,000 years, and 92 percent within 100,000 years after payload breakup. It is expected that the surviving mass will be ejected quickly toward the outer solar system by the solar wind and radiation pressure forces following vaporization, sputtering and/or photoionization. During the ejection process, which occurs at different times for individual particles, the probability of interception and capture of charged particles by the Earth's magnetosphere is very small--less than three chances in a million. Furthermore, only a fraction of the captured ions would subsequently drift into the atmosphere. Hence it appears that less than 0.0015 percent of the total mass of the "blown apart" calcine waste would ever return to Earth. This is only 75 grams for a 5000 kg payload and should be of little or no consequence.

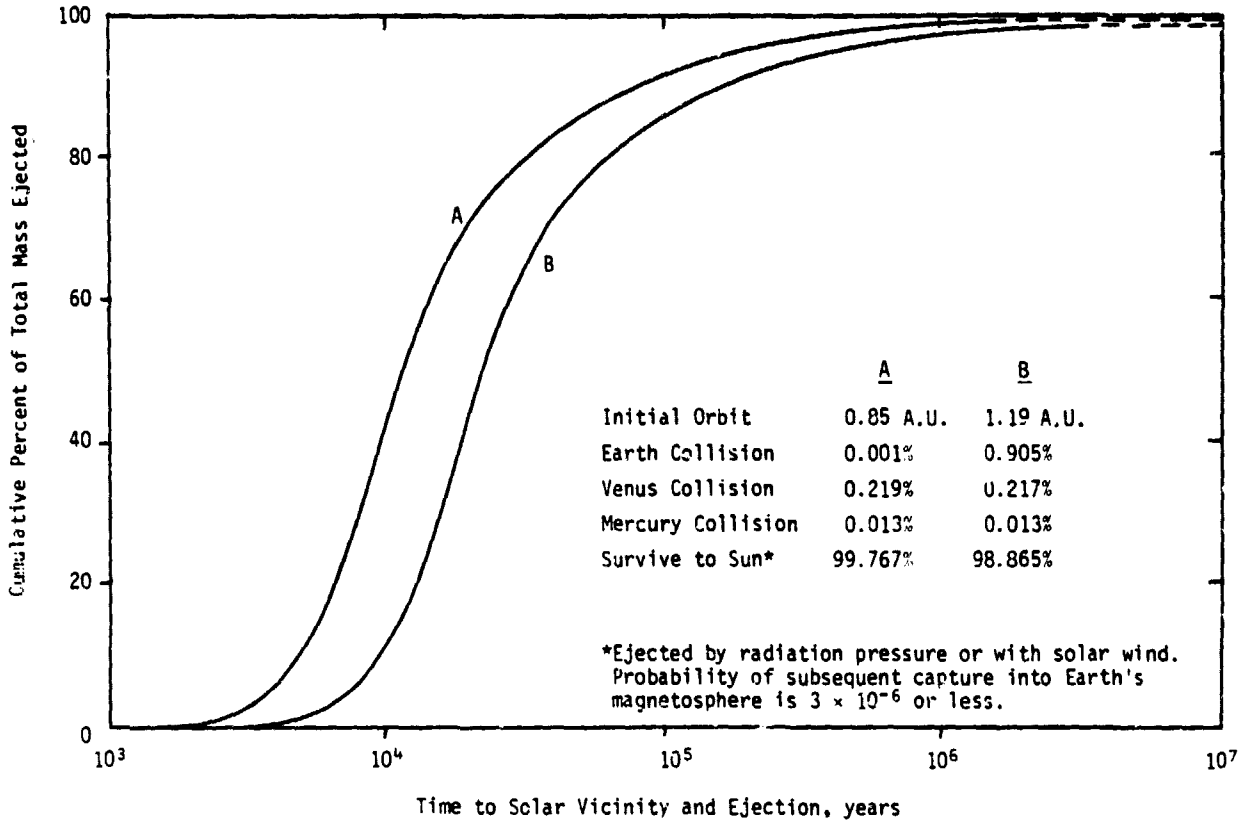

FIGURE 6-10. DISPOSITION OF SMALL PARTICLE MASS DISTRIBUTION (CALCINE WASTE FORM) UNDER POYNTING-ROBERTSON AND LORENTZ FORCES, INITIALLY CIRCULAR ORBITS INCLINED 1° TO ECLIPTIC PLANE

Curve B in Figure 6-10 applies to an initial circular orbit at 1.19 A.U. In this case, because Earth's orbit is first crossed as the particles spiral inward, the material that could be expected to return to Earth increases to 0.9 percent of the total mass. The mean time to Earth return is about 3000 years after the payload breakup event. Approximately the same mass fraction as before falls on Venus and Mercury, and almost 99 percent of the waste material would be eliminated. The median time of the Poynting-Robertson lifetime is 20,000 years, or twice as long as for the 0.85 A.U. case.

Mass disposition results for cermet waste particles in initially circular orbits are shown in Figure 6-11. The distribution curves in this case are strongly biased toward much longer Poynting-Robertson lifetimes since most of the fragmented mass resides in larger particle sizes (see Figure 6-1). In other words, the orbital changes imposed on the cermet particle distribution take place on a timescale about two orders of magnitude longer than that

for the calcine particle distribution. This leaves more time for the material to be swept up by the planets and the higher mass fractions shown reflect this fact. The return to Earth is about 0.1 percent for the 0.85 A.U. orbit and 6.7 percent for the 1.19 A.U. orbit. The mean time to Earth return is, respectively, 100,000 years and 45,000 years after the payload breakup event.

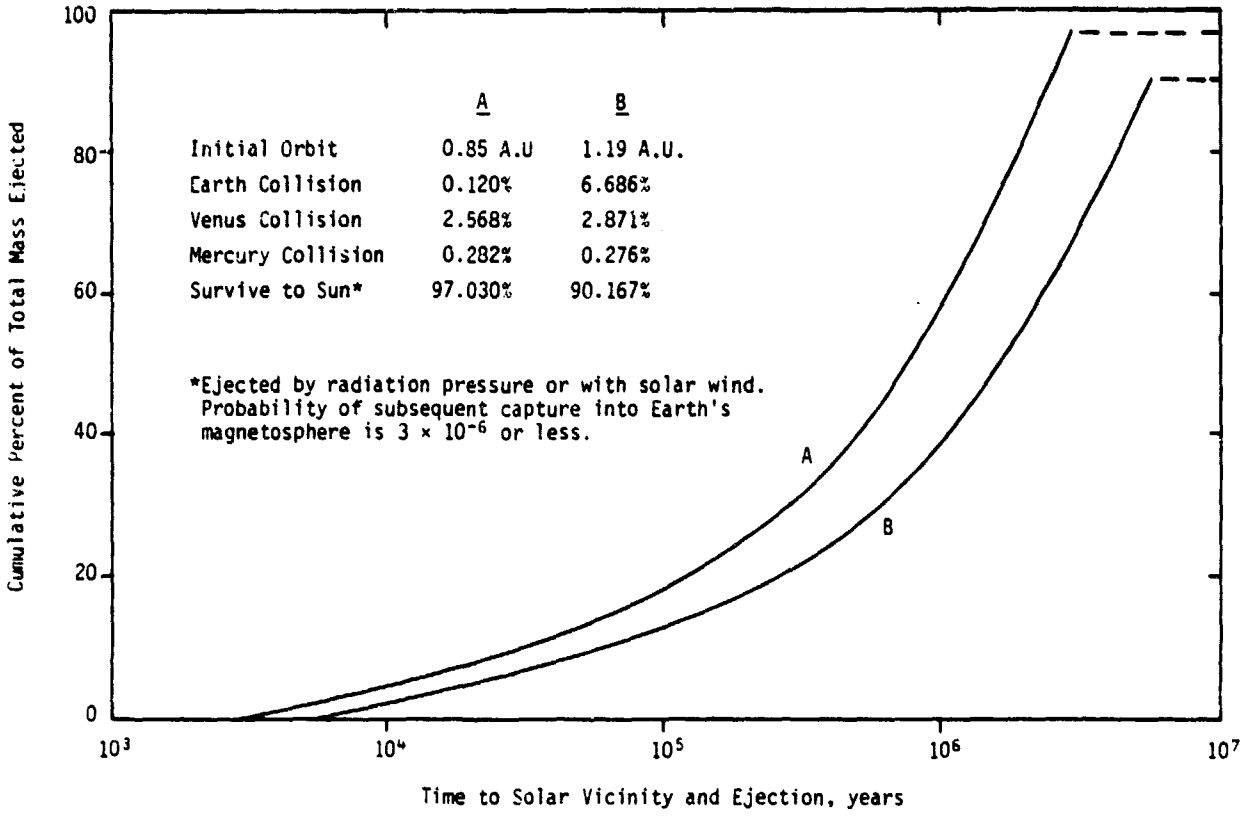

FIGURE 6-11. DISPOSITION OF SMALL PARTICLE MASS DISTRIBUTION (CERMET WASTE FORM) UNDER POYNTING-ROBERTSON AND LORENTZ FORCES, INITIALLY CIRCULAR ORBITS INCLINED 1° TO ECLIPTIC PLANE

Summary results for all eight cases, given in the table below, show the percentage of initial total waste mass (in small particle distribution) expected to return to Earth.

Initial Orbit, A.U.	Calcine Waste, percent	Cermet Waste, percent
0.85 x 0.85	0.001	0.120
0.85 x 1.00	0.353	3.450
1.19 x 1.19	0.905	6.686
1.19 x 1.00	2.260	12.940

A substantially higher return fraction results when the initial orbit at particle release is elliptical rather than circular. This is readily explained by the fact that the particles now start out in Earth-crossing orbits with no time delay needed for Poynting-Robertson or Lorentz forces to perturb them there. The worst case result is for cermet waste in a 1.19 x 1.00 A.U. orbit where the return fraction is 12.9 percent.

As a point of reference, if the package does not break up into small particles, then: (a) no mass returns to Earth from the stable 0.85 and 1.19 A.U. circular orbits; and (b) the long-term (10^6 year) probability of intact payload return is 21 percent for the 0.85 x 1.0 A.U. orbit and 15 percent for the 1.19 x 1.0 A.U. orbit. Hence, if the stable orbit is not attained because of deployment system failures and if there is no subsequent rescue attempt, the risk is reduced if the payload does break up into small particles.

It is important to place the results of the small particle effects analysis in perspective. The mass return fraction associated with a payload breakup event needs to be tagged with the probability of occurrence of such an event. For the reference waste cermet form, the threshold energy level of catastrophic fragmentation due to a 0.24 kg meteoriod impact would release only 0.2 percent of the total material in small particles. The probability of this threshold impact event is about 4E-09 per year. Complete fragmentation by a meteoriod mass of 30 kg is 6E-11 per year.

The data shown below assume a 5000 kg cermet payload placed in the nominally stable 0.85 A.U. circular orbit. The data show the probable amount of mass return to Earth as a function of time under the condition of immediate total fragmentation. For times up to 0.1 million years after fragmentation (or launch), the probable mass return is only 0.017 kg. The maximum mass return is 6 kg (0.12 percent of 5000 kg), but this requires a time interval of 3 million years.

Time After Fragmentation, Years	Probable Mass Return to Earth, kg
10^3	0.014
10^4	0.015
10^5	0.017
10^6	1.3
3×10^6	6.0 (Maximum)

With the assumption of a 5000 kg cermet payload in a 0.85 A.U. circular orbit, the consequences of material release, distributed over time in orbit, are given below. An integrated release rate of 1.6E-06 kg/year applies in this case; i.e., the probable material release by meteroid impact over 1 million years is only 1.6 kg. Since the probable amount of mass return to Earth is a small fraction of the mass released, this amount is quite negligible even up to several million years after launch. The probable maximum of 6 kg requires an interval of 3 billion years.

Time After Fragmentation, Years	Prabable Mass Return to Earth, kg
2×10^3	4.5×10^{-9}
2×10^4	4.8×10^{-8}
2×10^5	5.4×10^{-7}
2×10^6	4.2×10^{-4}
3×10^9	6.0 (Maximum)

Unless evidence to the contrary is uncovered, we would conclude that program planners need not be concerned about the risk associated with small particle release from a cermet payload in solar orbit. A much more likely failure event is that the payload would not achieve the desired orbit because of vehicle system malfunction. In such a case a rescue mission could be attempted, and the chance of payload breakup during the relatively short time before rescue is virtually nil.

6.2 Rescue Mission Technology Assessment

Rescue mission capability is defined as the ability to send another propulsion system to rendezvous and dock with a failed payload in orbit and to place it at the desired destination, or at least to prevent its imminent reentry. The rescue concept evolved in previous studies of the space disposal option when it became clear that acceptably low risk levels could probably not be achieved otherwise. Assuming that there is sufficient time to make as many rescue attempts as necessary to achieve success, what this concept offers is redundancy on a mission level rather than on a system design level. This relieves the almost impossible burden of designing the extremely high system reliability that would yield the equivalent low risk.

There are three operational prerequisites to accomplish rescue. First, the payload must be intact, i.e., not have fragmented as a result of the failure mode. Second, the rescue vehicle must be adaptable to the situation it encounters, i.e., have the capability of rendezvous and payload recovery under all conceivable failure modes including passive and uncontrollable targets. Third, the rescue operations must be accomplished in an automated mode, or with minimal man-in-the-loop control, since it is unlikely that near future manned operations will extend to the high Earth orbits or solar orbits of concern here. Meeting these conditions will be a tall, but not impossible order. What will be required is careful pre-mission analyses of failure modes and responses, appropriate design of payload and rescue vehicle systems, and hardware technology readiness.

A preliminary examination of the rescue problem was made as part of last year's work on the space disposal option. Both Earth orbit[6-11] and solar orbit[6-3] rescue regimes were considered. These analyses focused on the range of possible failure orbits, rendezvous phasing orbit requirements with rescue time/ΔV trades, and rescue propulsion stage requirements. This type of work should be an ongoing activity in conjunction with changes or maturation of reference disposal concepts and vehicle system definition, but will not be addressed further here. Another aspect of the previous effort was an initial assessment of the state of the art in automated rendezvous and docking techniques and sensors. It was concluded that such operations, while not yet commonplace in the U.S. space program, are technically feasibly based on current technology if a cooperative rendezvous mode can be assured, i.e., functional subsystems on the target vehicle. In the absence of this, the problem was thought to be very difficult requiring certain advances in design and hardware technology.

The objective of the subtask discussed in this section is to provide a more detailed technology assessment of the (critical) automated rendezvous and docking phase of the rescue mission. Of particular interest is the case of noncooperative or only partially cooperative rendezvous due to failure of crucial payload vehicle subsystems such as communications and attitude control. The approach taken is to review and summarize the current status of the technology, including ongoing programs, as ascertained by a literature search and personal contact with NASA and contractor staff members working in this field. This information should provide a basis for new directives in supporting research and technology (SR&T) programs.

6.2.1 Rendezvous and Docking Operations

The rescue mission can be divided into several phases: (1) launch; (2) orbit transfer; (3) terminal rendezvous; (4) stationkeeping/reconnaissance; (5) final closure; and (6) docking or capture. These phases have distinctly different requirements with respect to execution times, propulsion, ground-based support and on-board sensors. Launch and orbit transfer requirements are closely linked to the spatial regime of rescue operations, i.e., Earth orbit or solar orbit. The remaining phases of interest here, beginning with terminal rendezvous, are also dependent on the operational regime but to a lesser extent.

The terminal rendezvous phase begins after the rescue vehicle is transferred to the near vicinity of the target vehicle* position, close enough for on-board sensor acquisition of the target. Orbital velocities of the two vehicles are nearly matched at this point. Using the relative position and velocity information, the target vehicle is then accurately guided to within about 100 meters from the target. Fundamental differences between Earth orbit and solar orbit rescue are likely to have the greatest impact on design implementation for this phase of the rendezvous/docking operations. This arises because of the wide difference in target acquisition range required for the two cases. Orbit determination and guidance delivery errors during the transfer phase are measured against much longer baseline distances for solar orbit rescue. The problem is not too severe in the situation of cooperative rendezvous where it can be assumed that the target is radio-tracked from Earth-based installations and its orbit accurately determined. A target acquisition range of 50 km, typical of Earth orbit operations, might have to be increased to 500 or 1000 km in solar orbit. This maximum range is still within the design range of RF rendezvous radars. In the noncooperative mode, one of the worst case situations envisioned is loss of Earth-based tracking of the target due to transponder failure. Knowledge of the target's position must then rely on a prediction based on the last orbit determination fix, and the accuracy of this prediction degrades with time. If this failure occurs in solar orbit then target position uncertainty could increase to many thousands of kilometers by the time the rescue vehicle gets there. Unconventional means of target detection other than active RF radar tracking need to be considered.

Assuming that the target can be acquired and that the terminal rendezvous phase is accomplished, the next step is reconnaissance of the target to ascertain its physical state and determine its attitude motion. A video (TV) sensor system would be most useful here. Pictures could be transmitted back to Earth initially, taking full advantage of man's attributes of recognition, correlation and decision. Alternatively, or in a complementary mode, the video signals and other attitude sensor inputs could be processed on-board the target vehicle. This capability will likely be needed anyway during the final closure and docking phases when fast time response is important, necessitating autonomy from ground control.

---

*The terms target vehicle and payload are used synonomously.

Assuming that the payload is intact as determined from inspection, a positive recovery decision would be made. The final closure and docking maneuvers are greatly simplified if the target vehicle is in an axis-stabilized attitude and its docking structure intact, i.e., cooperative. The rescue vehicle slowly approaches the target aligned with the proper docking orientation, and uses sensor data in a feedback control mode until the docking mechanism is activated and a secure latch obtained. Both 3-axis and spin-stabilized configurations can be implemented in the cooperative or partially cooperative modes. The main difficulty arises if the target is found to be in an uncontrollable tumbling state, especially if the tumbling rates are high. Appropriate responses to this possible situation, both in pre-mission design and operational flexibility, will be discussed.

6.2.2 Synopsis of Literature Review

Twelve contractor reports and conference papers dealing with the subject of space rendezvous and docking were reviewed. The work reported covered the period 1971-79, and was performed by four different organizations encompassing university research and large aerospace companies. The nature of this work includes conceptual analyses, technology surveys, and systems engineering. Applications include Earth orbit and interplanetary missions, manned and unmanned operations, and both cooperative and noncooperative flight modes. Although teleoperator control is the main subject in several cases, all reports treat some aspects of automated systems. A brief summary of this work which follows is collated by some sensible combination of the organization or researcher performing the work and chronological sequence. The purpose here is to place the references "out front," and then use this material in the technology assessment presented in later subsections which are structured by subject matter, e.g., sensor requirements and recovery/docking concepts.

Kaplan at Pennsylvania State University has been largely responsible for setting the groundwork of conceptual analysis and design for space systems capable of orbit rescue/retrieval of disabled, uncooperative vehicles. Much of this work deals with Space Shuttle or space station operations where man is involved in the control loop--at least from a distance. One of the earliest papers[6-12] identifies some of the problem areas and operational aspects of retrieving passive satellites and orbiting debris, and describes a conceptual teleoperator package for remotely capturing and despinning objects of small to moderate size. Included also is a mathematical treatment of the attitude control problem. A second paper[6-13] continued this type of analysis but with application to large vehicles in a disabled state. Recovery techniques and devices involving external torque application and internal energy dissipation mechanisms are described. More detailed treatment of the above work performed under a NASA grant can be found in the progress and final reports.[6-14 and 6-15] One energy dissipation method identified, internal mass motion, is the subject of a comprehensive analysis presented in an AIAA Journal article.[6-16] The complete equations of motion for an asymmetric rigid spacecraft containing a translatable mass are presented, and appropriate control law and system parameters are selected to minimize kinetic energy in transforming tumbling motion into a simple spin state. The final

two papers in this series treat different methods of external torque application. Control and stability problems associated with satellite capture by grappler arms are presented in the first of these papers[6-17], while the second[6-18] considers a novel method for eliminating angular momentum by use of water sprays directed at the tumbling satellite.

Martin Marietta Corporation has been active in this field since 1973 performing work under several NASA contracts and in-house research programs. As part of a comprehensive study of the planned Mars sample return mission, a preliminary design analysis and technology assessment was conducted for JPL on the problems of automated rendezvous and docking of two spacecraft in Mars orbit.[6-19] The navigation, guidance, and control aspects of (cooperative) rendezvous and docking phases are treated in detail, as well as the design requirements and error analysis of radar sensors. Another study for MSFC is directed at rendezvous and docking operations of the Space Tug in Earth orbit.[6-20] A total systems analysis approach is taken here to: (1) define the requirements, methods, mechanisms, components, and subsystems of alternative concepts; (2) synthesize and recommend the best manual, automated, and hybrid systems; and (3) provide plans for simulation/demonstration testing. Application emphasis in the Tug docking study is on passive, cooperative spacecraft of various types, sizes and orbital regimes. Another recent report is recommended as a reference source on most aspects of automated rendezvous and docking problems with application to both Earth orbital and planetary missions.[6-21] This is a comprehensive survey and assessment of the current state of the art, with emphasis on sensors rather than docking mechanisms, and includes detailed descriptions of alternative sensor techniques and design configurations for both existing and proposed hardware.

Northrop Services, Inc. conducted a series of contracted studies for MSFC which addressed the problem of recovery of spinning satellites by the proposed Space Tug. Reference 6-22 includes an executive summary of the early study phases (postdocking and soft-docking operations) and detailed documentation of the last phase of work (predocking operations). Postdocking analysis is concerned with attitude control and stability of coupled bodies over the time interval between contact and target despinning. The soft-docking analysis examines the performance requirements for docking with different spacecraft configurations, and evaluates several candidate docking mechanisms. The predocking analysis treats the final stages of target approach in terms of the requirements on chase vehicle maneuvers, sensor information, and attitude control. Results of a 12-degree-of-freedom digital simulation are presented.

The final reference[6-23] is a study performed by the Essex Corporation for MSFC to develop concepts for satellite-retrieval devices employed by teleoperator systems to be used in nominal Space Shuttle operations in Earth orbit. The scope of work and emphasis is on the hardware mechanisms of various types. Details of the physical configurations and mechanical operations are presented.

The references cited above comprise but a representative sample of the work performed in the U.S. over the past decade. Many additional data sources can be found in the list of references and bibliography of these reports. These include literature translations from the Soviets who have demonstrated autonomous rendezvous and docking with their Kosmos-series spacecraft. Another source not yet tapped is the (possibly) classified work of U.S. military space projects.

6.2.3 Rendezvous and Docking Sensors

The rescue vehicle obviously needs a variety of on-board sensors and subsystems to implement guidance and control functions during all phases of the rescue mission. Attitude and thrust vector control functions require components such as gyros, accelerometers, celestial body sensors, momentum devices, thruster actuators, and computation electronics. Such "standard" equipment is considered here as technologically available, although it is recognized that the selection of the specific configuration of components and their specifications is not a trivial engineering design problem. Attention will be focused instead on those sensors needed to implement the terminal rendezvous and docking phases of the mission, particularly when the target vehicle is disabled and not cooperative.

Generic data types needed to determine the state of relative motion between rescue and target vehicles, and the physical and attitude state of the target are listed below:

(1) Range
(2) Range rate
(3) Line-of-sight (LOS) angles
(4) LOS rates
(5) Video image.

Range and angle rates are obtained either directly as part of the sensor mechanization or derived by differentiation as part of the computational algorithm. Table 6-2 indicates possible sensor types that can provide the various data requirements, the applicable phases of operation, and whether noncooperative targets can be accommodated.

An RF radar system is invariably included in a list of candidate rendezvous sensors because the basic technology is so well-developed and there have been numerous, flight-proven aerospace applications. Possible implementations include pulse, pulse/doppler, and CW sensor modes. By appropriate design, the RF radar can be used to acquire the target at fairly long range and track the target during the rendezvous approach and closure phases with information provided on range, range rate, and LOS angles. Functional and cost-effective requirements for a unified sensor might dictate the use of a CW system which is not inherently limited at close range and therefore, could be employed for both rendezvous and docking operations. RF rendezvous radars are normally designed for cooperative mode operation where the target includes an active retroreflector (transponder) to turn around the signal, and the antenna

TABLE 6-2. RENDEZVOUS AND DOCKING SENSOR REQUIREMENTS

SENSOR TYPE	DATA	OPERATIONAL PHASE				
		LONG-RANGE ACQUISITION	TERMINAL RENDEZVOUS	RECONNAISSANCE	CLOSURE	DOCKING
IR Telescope	LOS	✓ NC	✓ NC			
RF Radar	Range Range Rate LOS Angles	✓	✓	✓ NC	✓ NC	✓
Scanning Laser Radar	Range LOS Angles		✓	✓	✓	✓
Laser Beam Illuminator	Pattern Recognition				✓	✓
Video (TV)	Image			✓ NC	✓ NC	✓ NC

NC = noncooperative target accommodation

response pattern is well defined. Passive skin tracking of the target is also possible, but there are limitations on maximum acquisition range and tracking accuracy depending on the target's cross-sectional area and the radar power and antenna size.

Characteristics of the rendezvous radar proposed in a Martin Marietta study[6-19] of a Mars sample return mission are given in Table 6-3. The design, based on technology used in the Apollo Lunar Module rendezvous radar, is a unified S-band PM/CW system which serves a multipurpose function for both rendezvous and docking. In the cooperative mode, it provides range, range rate, and angle data from a maximum unambiguous range of 750 km down to a minimum docking range of 3 m. Other RF radar systems that have been considered[6-21] for rendezvous/docking operations, possibly with some modification of existing hardware, including Teledyne/Ryan's Viking Terminal Descent and Landing Radar (FM-CW phase monopulse), Cubic Corporations's CR-100/Electronic Location Finder III (FM-CW interferometer), and Hughes' Integrated Radar and Communication System (FM-CW amplitude monopulse).

Scanning laser radar systems have also been proposed for short-range applications (<50 km). Nominally, corner reflectors are placed on the target to passively return the signal for acquisition and tracking purposes. Two such devices have been under development in recent years, but neither has yet reached a state of technology readiness for space rendezvous/docking operations. The more advanced of the two is a low-powered Ga/As laser which could have application in cooperative mode operations. Relative location of the target is determined by measuring the range and LOS angles, while rates are

determined by differentiation. Range is found from the laser pulse propagation time from the transmitter to the target and back; resolution accuracy is about 10 cm. Target attitude information is determined by measuring the range and LOS angle to four retroreflectors mounted on the target in a known orientation. A laser beamwidth of 0.1 deg is scanned over a 30-degree field-of-view in the acquisition phase. Beam steering is accomplished by a piezoelectric-driven mirror and an image dissection technique. The second device is a high-powered CO_2 laser whose development for MSFC was apparently stopped in 1974. A potential advantage of the CO_2 laser is noncooperative mode application due to its capability for skin-track ranging. It should be noted, however, that neither laser radar was ever considered for the kind of long-range target acquisition function that might be required for noncooperative rendezvous in solar orbit.

TABLE 6-3. RENDEZVOUS RF RADAR CHARACTERISTICS

System Parameters	
Frequency	S-Band
Radar Type	CW
Radar Mode	Automatic
Modulation	PM (819 kc Subcarrier, 4 Minor Tones)
Radar Power	0.3 W (Solid State)
Maximum Range	750 km
Minimum Range	3 m
Radar Antenna	Traveling Wave Array
Angle Track Method	Phase Monopulse
Transponder Power	0.15 W (Solid State)
Transponder Antenna	Cassegrain
Coherence Ratio	220/239
Error Summary	
Range Error (Bias)	3 m
Range Error (Random)	
R < 65 km	<3 m
R = 750 km	750 m
Range Rate Error (Bias)	5 cm/s
Range Rate Error (Random)	5 cm/s
Angle Error (Bias)	1.5 mrad
Angle Error (Random)	
R < 10 km	<0.05 mrad
R = 750 km	3.2 mrad

The possibility of using an IR sensor for long-range acquisition arises because the nuclear waste payload is inherently a "hot" body against the space background. The surface temperature of the reference 5000 kg cermet payload (PW-4b) is estimated to be about 500 C. Calculations were made as part of this study to determine if there is any merit to this suggestion.

Results are given in Figure 6-12 which illustrates the trade-off between maximum acquisition range, target temperature, and IR sensor characteristics. The two IR systems considered are based on characteristics of the Infrared Astronomical Satellite (IRAS) and the Shuttle Infrared Telescope Facility (SIRTF). Both are cooled telescopes as required for low background noise and low detector noise. SIRTF is the more capable system because of its lower noise equivalent power, longer integration time, and larger collector optics. Of course, this instrument is much too massive to be included in the rescue vehicle payload. A sensor of similar design but with much smaller collector optics could possibly be carried into deep space.

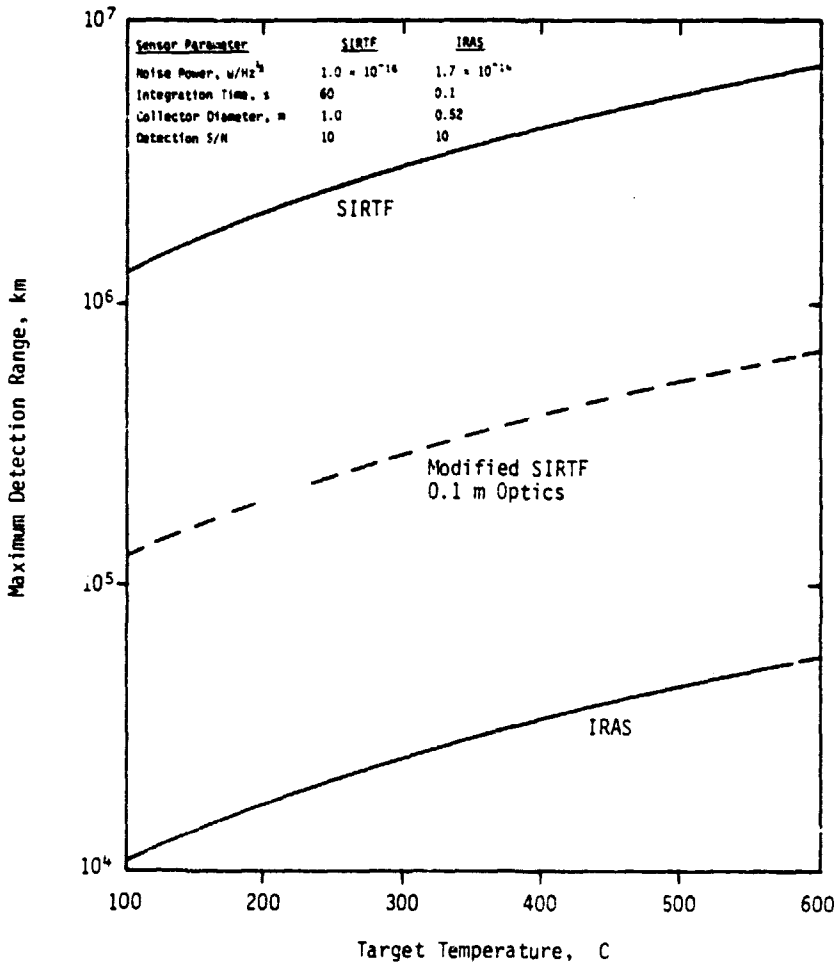

FIGURE 6-12. IR DETECTION OF NUCLEAR WASTE PAYLOAD IN SPACE

One might first inquire as to whether these IR sensors could detect a waste payload from Earth orbit. The maximum range for SIRTF varies from 1.5 x 10^6 km (0.01 A.U.) to 4.5 x 10^6 km (0.03 A.U.) as the target temperature increases from 100 C to 400 C. The detection range for IRAS is about two orders of magnitude less, i.e., 12,000 to 37,000 km. Thus, while Earth-based IR detection of a payload in solar orbit is practically out of the question, a disabled payload in Earth orbit might be found given some rough knowledge of its location and sufficient time for searching a predetermined, finite area of the sky. For solar orbit rescue, the IR sensor would have to be carried on-board the rescue vehicle, but long search times could be afforded. A modified SIRTF-type sensor with 0.1 m optics could have an acquisition range of 150,000 to 450,000 km depending on the target temperature--far greater than RF radars with practical limitations on transmitter power. IR detection seems to warrant further study with more detailed attention to target signature characteristics (relative to stellar background) and search methods.

An optical sensor of some type could be very useful for short-range operation during target inspection and final closure to docking. Visual cues from the target are certainly possible in the cooperative or partially cooperative modes of operation. This could take the form of patterned lights (active) or patterned reflective strips (passive). One possible sensor concept[6-22] is a continuous laser beam which illuminates the reflective strips placed, for example, on the docking port. Estimation of the docking port orientation can be determined through analysis of the reflected signal whose magnitude is a function of the beam incidence angle. It is not known whether there has been any practical development of such a concept.

Target imaging by standard vidicon systems or charge couple device (CCD) sensors currently being developed is another, and perhaps more practical, approach toward obtaining direct optical data. Illumination aids, such as spotlights or strobe lighting provided by the rescue vehicle, might be necessary. Processing of the images received for purposes of attitude determination and range computation is hardly a trivial job if done in a real-time autonomous mode of operation. However, high data rate computation could be performed by a dedicated video microprocessor integral with the sensor subsystem. This allows the general purpose on-board digital computer to provide only a supervisory function to the video system while performing its main function of guidance algorithm evaluation and generation of commands to the vehicle attitude control system. Also, unlike planetary science TV pictures, full frame resolution is probably not required for purposes of docking control, leaving room for data compression techniques to be used. An automated video system of this type cannot be classified as existing technology, but some basic work has been initiated [6-21] and should probably be continued.

6.2.4 Recovery (Docking) of Tumbling Vehicles

Under nominal or ideal conditions of space rescue operations, the nuclear waste payload will still be attached to the SOIS propulsion stage through some type of dual docking structure interface. Attitude control, most

likely 3-axis stabilization, is assumed to be still functional and provided by the SOIS, even if its propulsion system has failed, e.g., in solar orbit. Rescue in Earth orbit is most likely caused by failure of the OTV stage; it is assumed that the failed OTV can be jettisoned. The rescue vehicle contains whatever new propulsion elements are necessary, proceeds to recover the payload via the nominal docking mechanism, and goes about its business of completing the disposal mission. No particularly new technology problems are involved here since design of docking structures and mechanisms is a fairly evolved engineering practice at present. What happens, however, if the above ideal scenario does not occur and the payload (target vehicle) is not attitude-stabilized? Such failure mode events should be taken into account in the nominal design of the recovery concept and docking mechanisms in order to enhance the probability of successful rescue.

Table 6-4 lists several concepts suggested for accomplishing the recovery of spinning or tumbling vehicles. The various control techniques generally fall into two categories: (A) energy dissipation mechanisms and (B) external torque mechanisms. Energy dissipation refers to action taken by (active or passive) or on (external) the target vehicle causing a general tumbling motion to be damped into a spin-stabilized motion from which capture or docking can then be implemented. Examples of dissipation mechanisms include: (1) internal linear mass motion (active method); (2) various types of fluid, mechanical, or structural dampers (passive method); and (3) viscous fluid sprays (external method). The second category, external torque concepts, involves action taken solely by the rescue vehicle to implement capture or docking from a general state of tumbling motion. The two main examples in this case are: (1) a chase vehicle "glommer" which senses and matches the target motion, docks in this configuration, and then detumbles; and (2) a chase vehicle "grappler" which senses the motion, grips and detumbles the target vehicle, and then captures or docks with it.

In terms of engineering design requirements, the energy dissipation concepts impose a low-to-moderate burden on the target vehicle and a moderate-to-high burden on the rescue vehicle. Note that the rescue vehicle must now have the capability to dock with a spin-stabilized target in addition to, or in place of, the nominal axis-stabilized docking maneuver. The external torque concepts place no burden on the target but a high burden on the rescue vehicle, especially if these maneuvers must be performed remotely in an automated mode. The judgement here is that the "glommer" technique would be inordinately complex unless the tumbling rates are very low. Not only is it difficult to accurately measure another body's attitude motion when the rates are high, but the simultaneous control of flight path and attitude motion during the docking closure maneuvers is also quite difficult.

Detumbling by grappler arms or similar external torque devices has been under study in Space Shuttle-related programs. A number of different concepts have been proposed. Special end effectors and multiple degrees of freedom are often required of the grappling mechanisms. Probably, no general procedure is best for all satellites. The design drivers are clearly the target's mass, dimensions and specific hardware configuration, and the type and rate of tumbling motion expected. The proposed Shuttle applications have mostly involved teleoperator systems in Earth orbit with Shuttle crew participation. Performing such a function remotely in solar orbit, where limitations

surely exist on the size and weight of grapple mechanisms that can be brought there, would probably be very difficult. Perhaps the problem would be more tractable if the spherical waste payload were released from the SOIS stage.

TABLE 6-4. CONCEPTS FOR RECOVERY (DOCKING) OF TUMBLING VEHICLES

Momentum-Control Techniques	Target Vehicle Burden	Rescue Vehicle Burden
A. Energy Dissipation Mechanisms Capture in Spin-Stabilized Motion		
Active - Internal Mass Motion	Moderate	Moderate
Passive - Fluid Ring Dampers Pendulum Dampers Spring-Mass Dampers Flexible Structures	Low	Moderate
External - Viscous Fluid Sprays	None	High
B. External Torque Mechanisms Capture in General Tumbling Motion		
Chase Vehicle "Glommer" - Sense/Match Motion - Hard Dock - Detumble	None	High
Chase Vehicle "Grappler" - Sense Motion - Grip/Detumble - Hard Dock	None	High

A suggestion by R. Burns of MSFC bears further thought and analysis. Consider a rocket-powered harpoon, perhaps laser-guided, that is fired at some C.G. area on the target containing a guidance aid (reflector) and an impact pad. The induced translational motion will draw out the tether which is later pulled in to the rescue vehicle with the harpoon serving as an axle of rotation and a docking probe. Residual angular momentum might then be dissipated against a friction pad cradle. The general idea of harpooning the target has been considered by others in "blue sky" discussions, but apparently no backup analysis has been done to verify concept feasibility.

The external fluid spray mechanism[6-18] for energy dissipation seemed quite intriguing since action is safely taken "at a distance" on a generally noncooperative target. Based on laboratory experiments involving liquid jets exhausting into a vacuum, the idea here is to spray water at a tumbling object. Accumulation of water on the object forms into ice and the added mass absorbs angular momentum which is then carried away as the ice sublimes, thus slowing the object. Analytical investigation was applied to a range of target masses in low Earth orbits initially spinning at 30 rpm in order to estimate the control response history and the mass of water required. Results showed that despin times for 98 percent reduction in angular momentum ranged from several minutes to several hours for satellite masses up to 800 kg, and that the mass of water required ranged from several hundred to several thousand kilograms depending crucially on the water accumulation or sticking fraction. Thus, while this concept may be viable for despinning small satellites using large quantities of liquid apropos to Shuttle payload capability in Earth orbit, it does not appear to be viable from a weight standpoint for our application of despinning large vehicles in interplanetary space.

A movable mass control system on-board the target has been shown to be a viable energy dissipation concept.[6-16] The mass track should be placed as far as possible from the vehicle center of mass and oriented parallel to the maximum inertia axis. Larger control masses and displacement amplitudes generally result in better performance. Tumbling motion can be stabilized into simple spin within a few hours using a control mass of about 1 percent of the target vehicle mass. The main disadvantages of this method of energy dissipation are the relatively complex control system required and the potential failure of active mechanisms. Since longer control time can be afforded in the present application, a simpler and more reliable approach might be the use of passive energy dissipation devices such as fluid ring, pendulum or structural dampers which are automatically activated if the vehicle enters a state of tumbling motion.

6.2.5 Assessment Summary/SR&T Requirements

The implementation of automated rendezvous and docking operations as would be required for rescue of disabled nuclear waste payloads can by no means be viewed as an easy problem. This technology is in its early stages. However, there is no need to prove "off-the-shelf" availability of such systems today. What is needed is reasonable confidence that this capability can be developed in the near future, and an implementation plan to assure this development. Automated rendezvous and docking technology will surely be an essential requirement to carry out planned programs in the coming Shuttle era and in planetary exploration. An optimistic view would hold that waste payload rescue will be the beneficiary of these preceding programs. On the other hand, depending on the timescale and relative urgency, it could be the driver for such developments.

Cooperative, unmanned rendezvous between two spacecraft can be accomplished with current technology. The demonstration of this by the U.S. is

simply a matter of priorities, funding, and engineering design. Once this is accomplished there should be a steady progression to rendezvous and recovery of targets that have not been predesigned to aid these operations, i.e., partially cooperative or noncooperative targets.

If rescue capability is necessary in nuclear waste disposal, then it follows that cooperative rendezvous must not be relied on as the only mode of rescue operations. Fallback options must exist in the event of failure of target vehicle's communication link or attitude control capability. The following classification of rescue scenarios along with possible design criteria will place some perspective on the problem:

Class 1 Rescue. Cooperative rendezvous and docking is the nominal mode of operation and is reflected in the design of both rescue and target vehicles. Some level of redundancy is built in the target's subsystems to assure high reliability of nominal function.

Class 2 Rescue. Failure has occurred in the target's communications tracking link and/or 3-axis stabilization function. In the first instance, the rescue vehicle employs a backup sensor mode during the terminal rendezvous phase to acquire the target at long range, e.g., IR or higher powered RF radar. Possibly the target can aid this search by automatically deploying devices or material to increase its RF target cross section. In the second failure instance, the target automatically reverts to backup energy dissipation devices to convert tumbling motion into spin-stabilized motion. The rescue vehicle design accommodates docking with a spinning target as a backup mode. The target vehicle likewise accommodates this mode by design.

Class 3 Rescue. The target vehicle is completely noncooperative as a result of failure or absence of backup systems. The rescue vehicle is designed to accommodate all possible contingencies and still capture the target.

It is clear that each of these scenarios, ordered by increasing technical difficulty, will drive the design configuration of both rescue and target vehicle systems in different ways. Premature selection of fallback options may even affect the viability of the entire rescue concept. Trade-offs need to be made regarding questions of: (1) technology feasibility and development risk; (2) cost implications; (3) system reliability; and (4) rescue policy and ground rules related to acceptable level of risk of not succeeding. The data base that would eventually allow such trade-offs to be made needs to be improved. It is recommended that future study activity on the space disposal concept address this objective some place in the statement of work for both NASA in-house planning efforts and contracted systems engineering efforts.

In specific areas of supporting research and technology, the following directions are indicated:

1. Sensor Technology

a. Long-Range Target Acquisition Device--conceptual design and analysis of candidate sensors (e.g., IR or RF) that could locate

a passive target at ranges exceeding several thousand kilometers.

b. Automated Video Trackers--a phased development program to include data requirements definition, algorithm development, component design, laboratory breadboarding and testing, and flight tests.

2. Docking/Capture Technology

a. Energy Dissipation Mechanisms--a conceptual design study and analysis of candidate mechanisms (on-board target vehicle) for backup attitude control. Study input is current definition of waste payload/SOIS configuration. Study output is data base on derived system requirements, control response, estimated development cost and risk, and comparative evaluation.

b. External Torque Mechanisms--study scope similar to above but confined to techniques and devices (on-board rescue vehicle) for capture of unstable targets.

6.3 References

6-1. Friedlander, A. L., et al., "Aborted Space Disposal of Hazardous Material: The Long-Term Risk of Earth Reencounter," SAI-1-120-676-T8, Science Applications, Inc., Rolling Meadows, Illinois (February 1977).

6-2. Friedlander, A. L., et al., "Analysis of Long-Term Safety Associated with Space Disposal of Hazardous Material," SAI-1-120-676-T11, Science Applications, Inc., Schaumburg, Illinois (December 1977).

6-3. Friedlander, A. L., and Davis, D. R., "Long-Term Risk Analysis Associated with Nuclear Waste Disposal in Space," SAI-1-120-062-T12, Science Applications, Inc., Schaumburg, Illinois (December 1978).

6-4. Bonner, W. F., et al., "Spray Solidification of Nuclear Waste," BNWL-2059, Battelle Northwest Laboratories, Richland, Washington (August 1976).

6-5. Fujiwara, A., et al., "Destruction of Basaltic Bodies by High-Velocity Impact," Icarus, Vol. 31, No. 2 (June 1977).

6-6. Wall, J. K., "The Meteoroid Environment Near the Ecliptic Plane," The Zodiacal Light and the Interplanetary Medium, NASA SP-150 (1967).

6-7. Biermann, L., "Theoretical Considerations of Small Particles in Interplanetary Space," The Zodiacal Light and the Interplanetary Medium, NASA SP-150 (1967).

6-8. Burns, J. A., Lamy, P. L. and Soter, S., "Radiation Forces on Small Particles in the Solar System," Icarus, Vol. 40, No. 1 (October 1979).

6-9. Consolmagno, G., "Lorentz Scattering of Interplanetary Dust," Icarus, Vol. 38, No. 3 (June 1979).

6-10. Williams, A. C., "The Electric Potential of Particles in Interplanetary Space Released from a Nuclear Waste Payload," AM-PHY-201-01, Alabama A&M University, Normal, Alabama (October 1979).

6-11. Edgecombe, D. S., Rice, E. E., Miller, N. E., Yates, K. R., and Conlon, R. J., "Evaluation of the Space Disposal of Defense Nuclear Waste - Phase II," Vol. II, Battelle's Columbus Laboratory, Columbus, Ohio (January 1979).

6-12. Kaplan, M. H., "The Problem of Docking with a Passive Orbiting Object Which Possesses Angular Momentum," presented at the 22nd Congress of IAF, Brussels, Belgium (September 1971).

6-13. Kaplan, M. H., "Despinning and Detumbling Satellites in Rescue Operations," presented at the 23rd Congress of IAF, Vienna, Austria (October 1972).

6-14. Kaplan, M. H., "Dynamics and Control of Escape and Rescue from a Tumbling Spacecraft," Second Semi-Annual Progress Report on NASA Grant NGR 39-009-210, Pennsylvania State University, College Park, Penn. (June 1972).

6-15. Snow, W. R., et al., "A Module of Automatic Dock and Detumble (MADD) for Orbital Rescue Operations," Astronautics Research Report 73-3, Pennsylvania State University, College Park, Penn. (April 1973).

6-16. Edwards, T. L. and Kaplan, M. H., "Automatic Spacecraft Detumbling by Internal Mass Motion," AIAA Journal, Vol. 12, No. 4, pp. 496-502 (April 1974).

6-17. Kaplan, M. H. and Nadkarni, A. A., "Control and Stability Problems of Remote Orbit Capture," Mechanism and Machine Theory, Vol. 12, pp. 57-64 (1977).

6-18. Kaplan, M. H. and Freesland, D. C., "Use of Water Sprays in Space Rescue and Retrieval Operations," IAF-A-76-09, presented at the 27th Congress of IAF, Anaheim, California (October 1976).

6-19. Scofield, W. T., "A Feasibility Study of Unmanned Rendezvous and Docking in Mars Orbit," Report MCR 74-244, Martin Marietta Corp., Denver, Colorado (July 1974).

6-20. "Space Tug Docking Study," NASA CR-144240, Martin Marietta Corp., Denver, Colorado (March 1976).

6-21. Schappell, R. T., et al., "Study of Automated Rendezvous and Docking Technology," MCR-79-611, Martin Marietta Aerospace, Denver, Colorado (October 1979).

6-22. "Recovery of Spinning Satellites," TR-1777, Northrop Services, Inc., Huntsville, Alabama (March 1977).

6-23. Pruett, E. C., et al., "Development of Concepts for Satellite Retrieval Devices," H-79-04, Essex Corporation, Huntsville, Alabama (February 1979).

7.0 PROGRAM PLANNING SUPPORT ANALYSIS

The objective of the program planning support analysis (Task 5) was to assist NASA/MSFC and ONWI in program planning and to provide appropriate input data for generating and continued updating specific working documents. Section 7.1 discusses the activity related to the preparation of the Concept Definition Document (see Reference 7-1 and/or Section 2.0 of this report); Section 7.2 reviews the work done in developing the 4-year program plan[7-2] for the space option.

Section 7.3 discusses the "preferable" licensing approach for space disposal of nuclear waste. This approach and specific areas of application of licensing were developed based on Battelle's experience, review of the licensing section of last year's report[7-3] by NRC and ONWI personnel, review of JPL's work (Reference 7-4), recent discussions with NRC personnel, and review of the Interagency Review Group report on nuclear waste disposal. The discussion includes a projected systems development flow chart (updated from last year's report) illustrating the sequence and timing of various licensing events and their relation to other activities such as policy development and environmental impact assessments.

Section 7.4 presents a discussion of the requirements for supporting research and technology (SR&T) for the space system. Five SR&T areas are summarized in terms of status, justification, technical plan, resource requirements and target schedule. The five SR&T areas are: (1) waste concentration processes; (2) waste partioning processes; (3) waste form thermal and mechanical accident response; (4) remote automated rendezvous and docking; and (5) deep ocean recovery. Additional details regarding the SR&T related to rescue mission technology can be found in Section 6.2 of this report.

Section 7.5 discusses the anticipated requirements for flight and system component testing. An approach to testing is presented, along with a listing of specific suggested tests and schedule. Test activities have been broken down into two phases: (1) tests required to determine concept feasibility (as outlined in the program plan) and those required to demonstrate the required safety prior to implementation of the space option for disposal of nuclear waste.

7.1 Concept Definition Document

The Concept Definition Working Group, made up of BCL, SAI, and NASA/MSFC personnel, held meetings and telephone conferences throughout the study activity. The product of this interaction is known as the Concept Definition Document (CDD). It contains the "Reference" space option concept scenario upon which most of the conceptual and trade studies are based (see Section 2.0). Other options within the space option have been considered, studied, and are listed in the CDD. Working draft Concept Definition Documents were issued three times during the year (August 10, 1979; September 25, 1979; and January 23, 1980) under NASA/MSFC cover. The two significant format/content changes in this document, over those generated during the Phase II study, were: (1) the inclusion of a section discussing an advanced disposal concept, employing the SPS-based heavy lift launch vehicle (HLLV); and (2) the inclusion of a safety requirements section. The significant changes to the reference concept over last year's CDD[7-5] are:

- Waste Mix - commercial waste has replaced defense waste as the primary waste mix for space disposal
- Waste Form - The ORNL iron/nickel-based cermet matrix has replaced calcine powder
- Launch Vehicle - For each mission, the single Uprated Space Shuttle has replaced the dual standard Space Shuttle Launch.

The current CDD is contained, fairly much intact, in Section 2.0 of this technical report.

7.2 Concept Definition and Evaluation Program Plan

The activity reported here is a continuation of the program planning activity that began during the Phase II study effort (see Appendix B, Volume III, of Reference 7-3). Seven different drafts of a 4-year program plan for determining the feasibility of the space option were prepared by BCL for NASA/MSFC and ONWI. Early drafts considered information from last year's study and new input from NASA/MSFC and ONWI (July 13, 1979 and August 24, 1979). The preliminary rough draft of the Concept Program Plan (CPP), dated August 24, 1979, was reviewed and improved during September as several review meetings were held with a number of BCL staff members regarding the work breakdown structure for the proposed study activity and the contents of the task write-ups. Also, each individual estimated government manpower (including DOE laboratory support) and contracted research, based upon the description of the program. The resource estimates from each individual were then discussed in group sessions and general consensus was reached. Typical or average values were then used in the draft program plan that was provided to MSFC/ONWI on September 17, 1979. After review of ONWI, MSFC, BCL, and the newly formed space disposal DOE/NASA Ad Hoc Coordinating Group*, the draft plan was revised in mid-October.

Review and discussions among the parties involved continued through November, December and January. On January 28, 1980, the BCL final revision was submitted to NASA/MSFC and ONWI. That draft identified the following program objectives:

- Risk - To identify and quantify the risk benefits that may be achieved through use of space disposal of certain radioactive wastes as an augmentation for geologic waste disposal.

- Cost - To establish the costs of the space disposal augmentation for a reference risk level. Also, to establish the incremental costs of risk improvement.

The work breakdown structure for the January 28, 1980, plan is shown in Figure 7-1 and the overview of the schedule is provided in Figure 7-2. For other details concerning the plan the reader is referred to Reference 7-2.

---

*Note: The purpose of this group was to coordinate program planning for the space option. The group is made up of personnel from ONWI, NASA/MSFC, Sandia, Savannah River Laboratories, NUS Corporation, Battelle Northwest Laboratories, Applied Physics Laboratory and DOE/Headquarters.

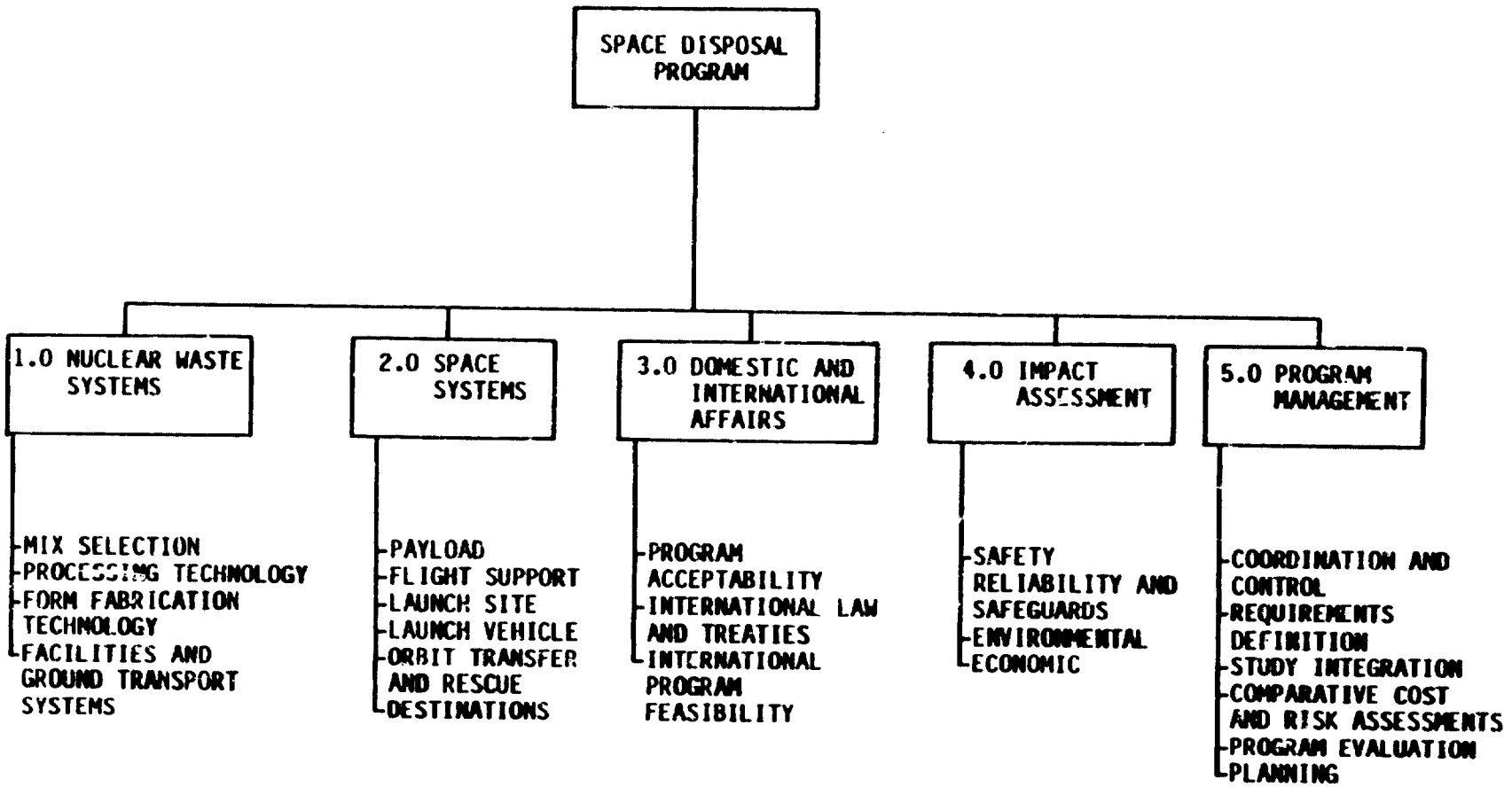

FIGURE 7-1. WORK BREAKDOWN STRUCTURE FOR SPACE OPTION PROGRAM PLAN

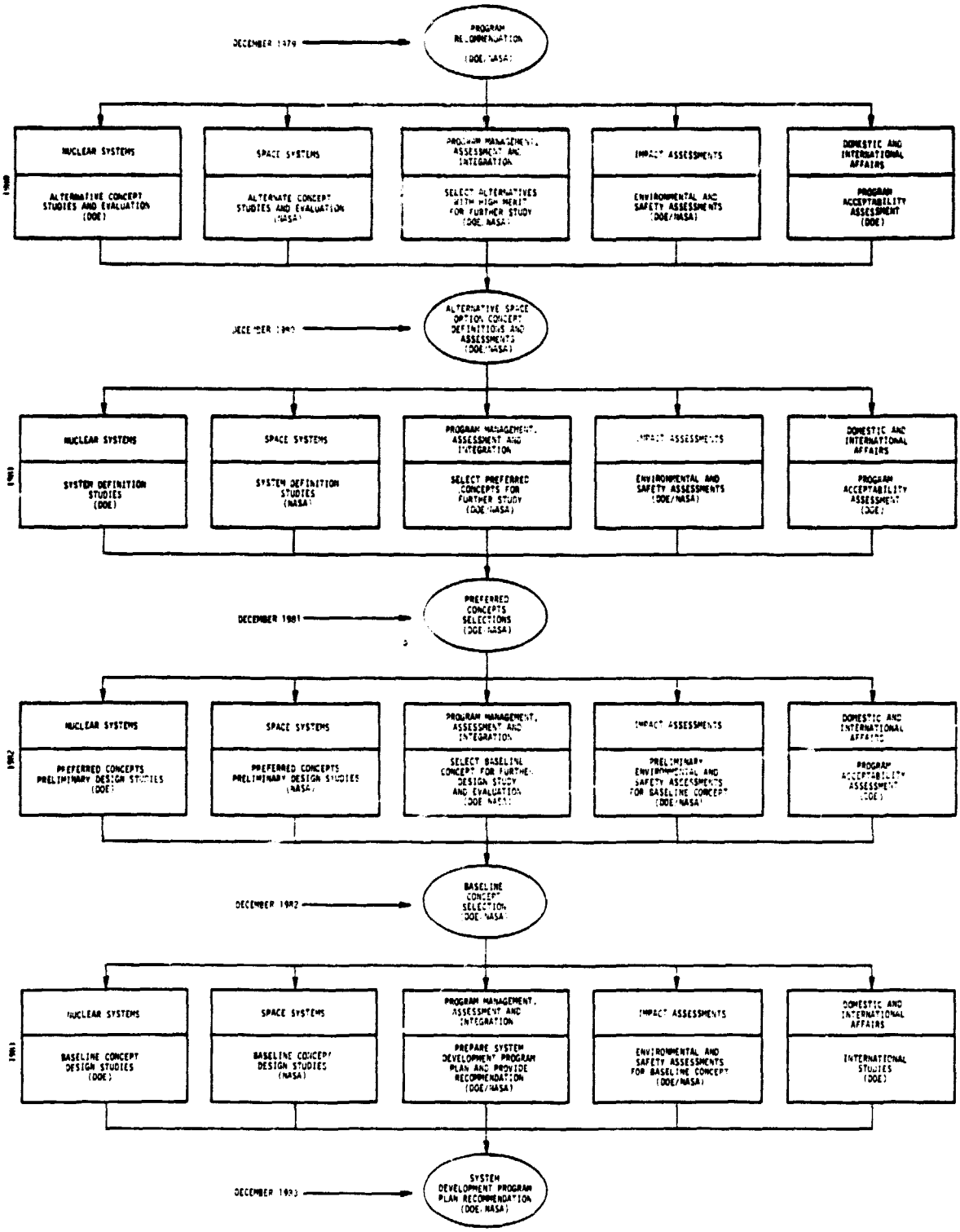

FIGURE 7-2. OVERVIEW SCHEDULE FOR SPACE OPTION PROGRAM PLAN

C-4

7.3 Licensing Requirements Definition

The space augmentation of high-level waste (HLW) disposal will require the development of new processes and construction of new facilities. These processes and facilities will be used to retrieve the waste from its currrent storage location, prepare the waste mix for space disposal, prepare the waste form for packaging and shipping, prepare the waste payload for placement in the Uprated Space Shuttle vehicle (see Section 2.0), launch the waste payload into Earth orbit, and transfer it to solar orbit using an OTV/SOIS. These activities can logically be divided into two major systems: (1) the retrieval, waste treatment, and waste form and payload fabrication system at the waste processing facility sites; and (2) the payload preparation and launch system at the launch site.

The purpose of this discussion is to address the licensing and policy questions that must be answered before proceeding with the space disposal option. The discussion presents first a general conceptual outline of the problem and procedure. The specific licensing questions on specific systems are then addressed. The criteria development requirement is discussed, as are the data requirements and the policy decisions that must be addressed.

The material contained in this section has been developed through a consideration of existing regulatory practices, likely future changes in these practices, and the unique nature of space disposal. Discussions with appropriate personnel at the United States Nuclear Regulatory Commission and the Jet Propulsion Laboratory (JPL) were most helpful.(7-6 and 7-7) Considerable use was made of the recent reports of the Interagency Review Group (IRG) (7-8) and 7-12), the JPL report(7-4), and other recent publications (7-9,7-10,7-11

7.3.1 Overview

The four primary areas of concern in developing the space disposal option are:

(1) The development and construction of the waste treatment and payload fabrication preparation facilities
(2) The development and construction of the launch site facilities
(3) The development of standards, criteria, and regulations for the space disposal option
(4) The major policy decisions required to allow the space option to proceed.

The interaction of these major areas is shown in Figure 7-3. The requirements for environmental impact statements and NRC licenses are included in the figure since an NRC license is expected to be required for all systems of HLW disposal.(7-6)

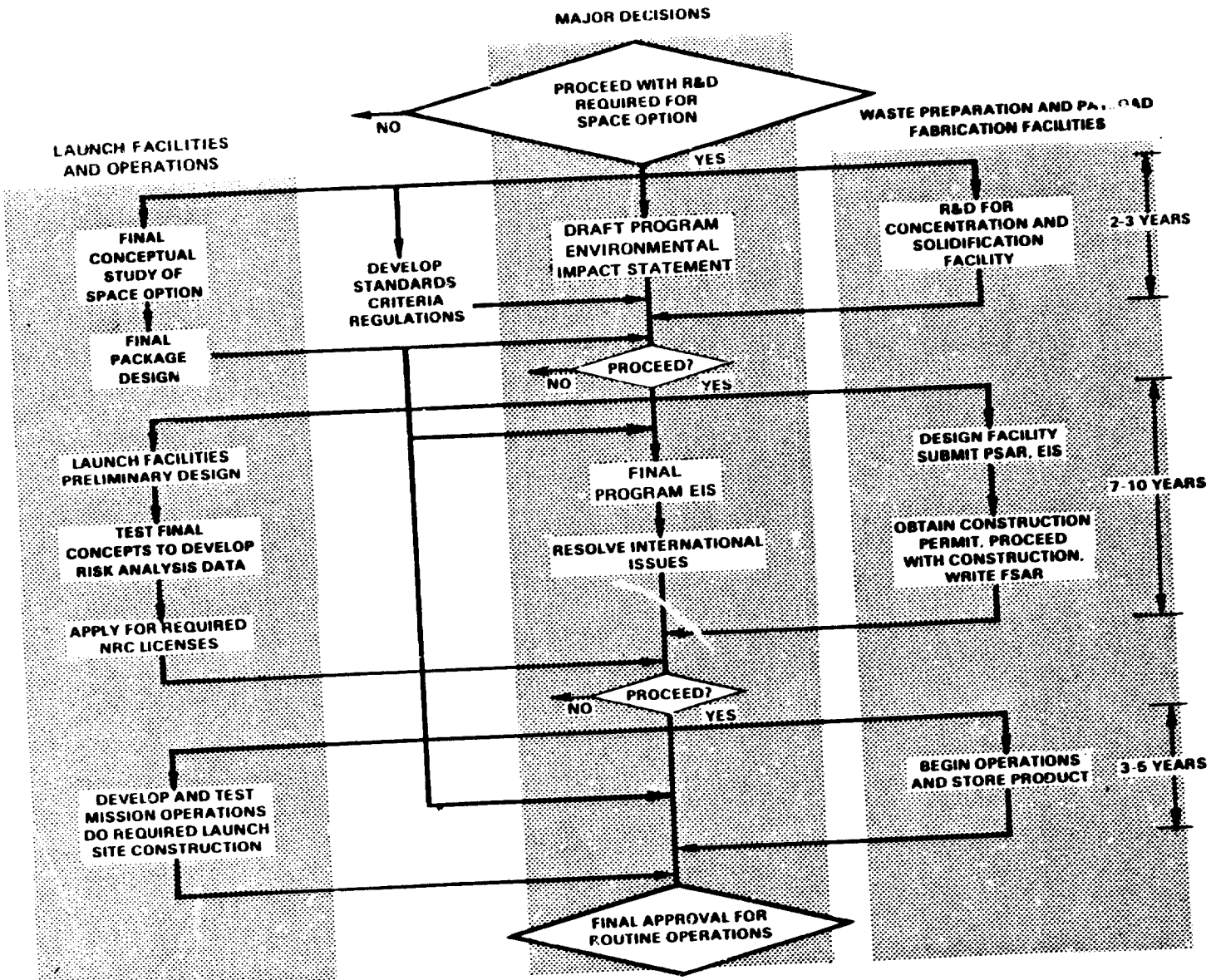

FIGURE 7-3. INTERACTION OF LICENSING WITH OTHER MAJOR DECISION AREAS

Since NRC licensing is assumed to be required, the question of the type of license and the regulations required is addressed for each system. Since current regulations may address a concept in one manner while new or changing regulations may be different, the question of licensing is somewhat speculative, but as many options as possible will be covered in the discussion.

Several major policy decisions will be required at different steps along the way. These become points at which "go, no go" decisions are made. If a decision is made to continue investigation (expected at the end of 1983) of the space disposal option, a draft environmental impact statement for the space disposal program will be required. At the same time, the development of standards, criteria, and regulations can begin. The development of the standards, criteria, and regulations will be a continuing process during the development of the space option. The regulations will have an important impact on the licensing requirements for the overall system.

Also, since the retrieval, concentration of defense waste, partitioning of commercial waste, and preparation of the waste form will be required, research and development of techniques for these operations should proceed (see Section 7.4). Retrieval, for example, will be required for any HLW disposal method requiring movement of the waste. The most novel or different part of the space option is the concentration requirement and perhaps even some chemical or isotopic partioning of the waste material.

The ground transportation of the loaded waste containers from the payload fabrication facility to the launch site requires no special licenses or analysis beyond those required by current regulations. The shipping container can be built to the standard requirements given in 10 CFR 71.(7-13)* Regulations such as 10 CFR 71 are constantly changing so the standard criteria may be different from those now in effect, although no major changes are anticipated.

The launch site facilities present a totally new problem as far as regulation and criteria are concerned. This problem is discussed in the section on the launch site.

7.3.2 Waste Treatment and Payload Fabrication Facilities

The waste treatment and payload fabrication facilities include the system for recovery of the wastes from storage, processing the waste, preparing an acceptable waste form, and loading the waste in a specified

---

*Existing United States Nuclear Regulatory Commission (NRC) regulations are quoted frequently in this section. 10 CFR 71 refers to Part 71, Title 10, Code of Federal Regulations - Energy. See Reference 7-13 for full title.

container. This system would be very much like the systems anticipated to be used in standard fuel reprocessing plants. Since these facilities must be integrated with each other, it is expected that they will be contained in a single building or complex of buildings and be licensed as a single system. The criteria for the payload would be specified by the environmental and technological considerations of the disposal operation.

The waste treatment and payload fabrication facilities must have facilities for storage of loaded waste containers (payload). It is unlikely that the most efficient method of operation will produce the product at a rate identical to the shipping and ultimate disposal rate. These facilities are similar to the waste handling operations envisioned for the commercial fuel reprocessing plant. It is normally expected that the design, licensing and construction of such a plant would take 7 to 10 years. However, it should be noted that no licensed facility of this type is now in operation.

Since the defense HLW is stored at DOE sites, it is expected that the waste treatment and payload fabrication facilities would be built at the site where the waste is located. The facilities would be owned by DOE and likely be operated by a DOE contractor. Currently, such DOE owned contractor operated facilities do not require NRC operating licenses or construction permits; however, this discussion is concerned with the types of licenses which may be required. Current discussion concerning the Waste Isolation Pilot Plant does not include licensing of the processing facility, only the repository. Regardless, similiar types of documents are required for DOE facilities anyway.

The disposal of commercial HLW will require all the processing facilities to have NRC licenses. Since current policy does not allow reprocessing, these plants would be special waste preparation facilities.

7.3.2.1 NRC Licensing

Since the waste treatment and payload fabrication facilities are much like a fuel reprocessing plant, such facilities could be licensed under regulations written in 10 CFR 50.* Additional requirements not presently contained in the regulations could be added as an additional Appendix to 10 CFR 50. Also, if safeguard requirements are needed, these are written in 10 CFR 73.

The facilities would go through the standard licensing process, with a construction permit first being obtained, and finally an operating license. Both preliminary and final safety analysis reports would be required and the appropriate reviews would be carried out by the NRC. Specific procedures would be dependent on the regulations in force at the time of application.

---

*See footnote, page 7-8, or Reference 7-13.

7.3.2.2 Environmental Impact

The National Environmental Policy Act of 1969 (NEPA) requires that an environmental impact statement (EIS) be filed for major Federal actions significantly affecting the quality of the human environment. These procedures are given in 10 CFR 51. It is expected that DOE would file an environmental report as part of their licensing application. The environmental impact statement would be prepared by NRC.

7.3.2.3 Criteria

Criteria for several parts of the waste processing system will have to be developed. These may include such items as allowable specific activity, payload container surface temperature, and heat flux, contents accountability requirement and many others. The criteria determined for the solidified waste will probably be determined by the requirements of the disposal system (see Sections 2.5 and 3.3). Specific criteria for the operations will include allowable gaseous releases, personal exposures, radiation dose limits of processing equipment, liquid radioactive release limits, and others.

Since several aspects of the system are not unique to the space disposal option, the criteria for these aspects can be obtained from or developed in conjunction with the other options for HLW disposal. Unique aspects such as concentration to higher specific activities, and possibly chemical and/or isotopic separation, waste form, and containerization will require the development of criteria independent of other programs.

The development of data required for statements of criteria will probably be carried out by contractors working on the space option, but the final criteria to be used in the system safety analysis will be specified by the NRC.

7.3.3 Overland Shipment

The overland shipment of the waste payload containers from the waste treatment and payload fabrication facilities to the launch site are not addressed in any detail here. Regulations for radioactive materials shipments currently exist and shipping containers and casks can be licensed under the applicable regulations, 10 CFR 71. Note, however, that the NRC does not currently license DOE casks, but DOE casks are built to NRC licensing requirements. It is expected that the NRC, sometime in the future, will license all shipping containers for radioactive materials.

The development and licensing of a shipping cask will take 3 to 5 years. Although this type of license is standard, the changing regulations are requiring new types of testing to prove the integrity of casks.

7.3.4 Launch Site Facilities and Operations

The launch site facilities include the Nuclear Payload Preparation Facility (NPPF), a ground transport system, and launch vehicle system including the mission operations and recovery system. These facilities will be the same for defense or commercial HLW. The launch facilities are viewed as a site with a radioactive materials license and the launch system as a transport vehicle carrying a licensed transportation payload.

The Interagency Review Group[7-8] has recommended that the NRC license all facilities for the long-term storage of radioactive waste. The question of the NRC licensing of a specified place in space must be addressed if that place is considered a facility for long-term storage of radioactive waste.

If a specific disposal site, such as the lunar surface, were selected as a space disposal site then the site would likely be licensed as any terrestrial site. However, it is expected that a solar orbit would not be licensed but specific criteria would be specified which the solar orbit would have to meet.

As for the waste processing facility, the launch site will likely be owned by the government and the question of NRC licensing NASA facilities must also be addressed. To be consistent with the previous discussion, in this discussion it is assumed that the NRC may license NASA facilities. It must be assumed that NASA would apply similar criteria to launch site facilities and operations even if NRC licensing were not a question.

7.3.4.1 Licensing

The licensing of a facility for possession and handling of radioactive material and the licensing of a container for shipping materials are the methods currently used in the regulations. Operations at the NPPF are expected to be simpler than those carried out in many hot cells. The ground transport at the launch site could be allowed under the special nuclear materials license granted under 10 CFR 70. Containers used for launch site ground transport by a licensee do not have to be licensed if the container is not moved on public roads or off the site. The licensee must, however, comply with the radioactivity release and exposure regulations of 10 CFR 20. If the fissile and fertile material content is below allowable limits, a license could be obtained under 10 CFR 33 since all the material handled could be considered by-product material. This licensing process is the same as is currently used for many radioactive materials operations including privately owned and operated hot cell facilities which can handle rather large quantities of spent fuel. The 10 CFR 70 license and 10 CFR 33 licenses specify the quantities of radionuclides the licensee may possess while the licensee must also comply with other health and safety regulations such as 10 CFR 20, and safeguards regulations in 10 CFR 73. However, government owned radioactive material is handled under DOE regulations which are essentially parallel to the NRC regulations.

By looking at the launch vehicle as a simple transport vehicle, such as a plane or truck, the current procedure, as applied, would be to license the payload for shipment in the Shuttle. This type of procedure was followed for the PAT-1 (Plutonium Air Transport Package - see Section 7.5 for discussion). Obviously, a new set of design criteria would have to be set up so that the payload and its contents would perform as intended under anticipated accident conditions such as a launch accident or unplanned reentry. The payload could be licensed under 10 CFR 71, which would have been amended to satisfy the criteria for space transport.

The licensing process would have to be examined closely since the types of licenses involved in this option normally do not involve the degree of public participation involved in 10 CFR 50 licenses. An extra effort would be needed regarding policy and environmental impact to assure public participation in the decision-making process, or the license proceeding would have to assure such participation.

7.3.4.2 Environmental Impact

An environmental report would be required for the handling of significant amounts of radioactive materials at the launch site. Also, the potential environmental impacts of the credible accidents during mission operations would also have to be examined. The environmental impact statement would be prepared by the NRC based on the environmental report filed by DOE/NASA as part of the license request.

7.3.4.3 Criteria

The criteria for the launch facility and operation could be a major factor in determining economic feasibility of the space option. These criteria would likely include specific limits on allowed radioactive release due to accidents and limits on the variation of the ultimate solar orbit of the waste payload. The level of risk will surely be a very important factor. The criteria on mission operations will have to be set up so that the consequences from most credible accidents will be extremely small. The entire concept may not be socially acceptable if any credible accident has severe consequences.

The possible impact of criteria on the design of system and mission operations should be examined early in the program so that potential design concepts can be examined. Therefore, criteria should be developed as soon as possible.

7.3.5 Major Policy Questions

Several major policy decision points will occur during the development of the space option. The first of these is a decision to proceed with the research and development required for the space option. If this decision is positive, the research required to develop the waste treatment processes, waste forms, and payload fabrication should proceed. Also, the standards, criteria, and regulations should be drafted. In conjunction with this, a draft environmental impact statement for the program must be prepared. A conceptual study of the space option should be made as well as conceptual designs of the total payload system to be carried into space on board the launch vehicle.

Based on the information obtained, the actual construction of waste treatment and payload facilities could begin. The preliminary design of NPPF could be prepared to comply with the criteria already set up. A final program EIS on space isolation would be prepared and international issues would be identified and resolved. The discussion and resolution of international questions is critical since final disposal would not be on U.S. territory. One solution may be to make space disposal operations an international venture; that is, to allow all nations to use this method for radioactive waste disposal. Testing of systems such as reentry and rescue systems must be carried out. These tests would allow a quantification of risk and consequences.

The next decision would be to develop and test the complete mission operation. Required launch site facility construction would begin and final testing be completed. These would lead to the final approval of routine space disposal operations.

7.3.6 Test Program Requirements

The major goal of the test program (see Section 7.5) would be to quantify and minimize the risk involved in space disposal option. Severe accidents which could lead to potentially unacceptable consequences should be simulated using actual hardware to aid design and to show that the accident consequences are indeed known and acceptable. These may include such things as testing reentry and recovery of payloads, subjecting payload systems to fires and explosions, and other credible accidents. The credibility of the space option will be dependent on the results of these tests. The specific requirements for testing are described in more detail in Section 7.5.

7.3.7 Summary and Conclusions

The isolation of HLW in space will require the development of two major systems; first, a facility for the recovery, waste processing, waste form preparation, and fabrication of HLW payloads, and second, launch site facilites (e.g., NPPF) and mission operations. These systems may be licensed in some manner by the NRC depending on government policy with respect to

defense wastes. All systems for the disposal of commercial waste are expected to be licensed by the NRC. The development of good standards, criteria, and regulations will play a key role in the development and use of the space option. While licensing may not be pacing item in the development of the space option the licensing process can be expected to lengthen the time expected to put the option into operation. Finally, a clear quantification and minimization of risk and consequences will be required.

It should be possible to establish a program in such a manner that will lead to vali., technically sound and socially acceptable decisions concerning the space option.

7.4 Supporting Research and Technology Requirements

This section defines the required technology developments that will have to be undertaken as a part of the supporting research and technology (SR&T) program for space disposal of nuclear waste. Each of the developments is summarized in terms of its status, justification, technical plan, resource requirements, and target schedule.

A distinction needs to be made between technology developments and design problems. Many elements of the space disposal system (OTV, SOIS, reentry vehicle, container, ejection system, etc.) do not currently exist, and would need to be designed, developed, and tested. However, none of these developments would necessarily require the creation of any new technology. As an example, the OTV would use hydrogen/oxygen liquid propellants. The technology for these propellants is well developed and systems using them have been built and flown operationally (e.g., Centaur, Saturn-IVB). This discussion concentrates on those areas where such technology is not presently available and needs to be developed as part of the overall program.

It has been stated that space disposal of nuclear waste is primarily an engineering problem, based largely on existing technology. This statement is substantiated by this discussion. Only five primary areas of technology development have been identified. The five areas are:

- Waste concentration processes (defense waste)
- Waste partitioning processes (commercial waste)
- Waste form thermal and physical response
- Remote automated rendezvous and docking
- Deep ocean recovery.

7.4.1 Waste Concentration Processes (Defense Waste)

7.4.1.1 Status

Defense nuclear waste exists in large quantities of dilute materials in storage at three different sites in the United States. Preliminary treatment processes have been defined for the Hanford wastes which would be suitable for terrestrial disposal, but which would not give adequate concentration for space disposal. Processes for further concentration have been defined, but are based on laboratory scale experiments and have not been verified as applicable in the scale envisioned. Further definition and demonstration of these proposed processes is required.

7.4.1.2 Justification

The number of booster flights required to dispose of defense nuclear waste is directly related to the degree of concentration achievable. Unless adequate concentration can be achieved, the number of flights required may be prohibitive. It is expected that the cost of concentration will increase in proportion to the degree of concentration required. Therefore, there is probably an intermediate level of concentration that minimizes overall cost (see below).

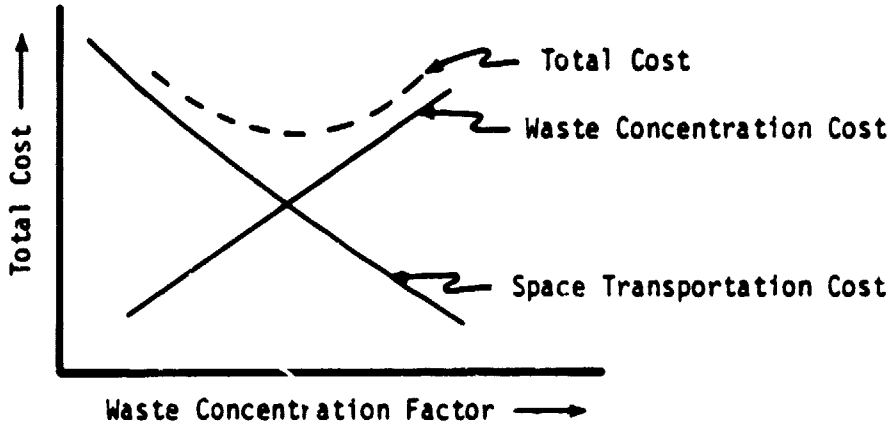

Better understanding of the potential waste concentration processes are required to determine this minimum cost point.

7.4.1.3 Technical Plan

Concentration processes need to be developed for Hanford, Savannah River, and Idaho defense waste. For Hanford waste, a process based on dissolution in molten caustic followed by treatment with nitric acid may be feasible and adequate for treatment of four of the five types of sludge stored there. The generally insoluble zirconium sludge may be soluble in molten caustic, and removal of significant amounts of inert materials would require development of a new (not yet defined) concentration process. Adequate concentration could probably be achieved if a caustic/nitric acid concentration process was developed. Development of a process for the zirconium sludge would allow additional concentration and would provide a margin in case of problems with the other process. For Savannah River waste, a single process involving successive washing with caustic and oxalic acid has been proposed and should be developed and demonstrated. For Idaho Falls waste, a method for dissolving the calcined waste must be developed. Dissolution chemistry has been under development at Idaho Falls, and a process involving dissolution with nitric acid and molten sodium bisulphate has been proposed. This process or an alternative needs to be developed and demonstrated.

7.4.1.4 Resource Requirements

Development and demonstration of the various concentration processes described above are estimated to require significant commitment of resources. It is expected that approximately $ 1 M will be required to reach a point where decisions regarding the feasibility of space disposal of defense waste could be made with confidence.

7.4.1.5 Target Schedule

Because of the significance of achievable concentration on the overall feasibility of space disposal of defense waste, concentration technology development should be initiated as soon as possible. The projected schedule is as follows:

1st Year	2nd Year	3rd Year	4th Year
$ 100 K	$ 200 K	$ 400 K	$ 300 K

7.4.2 Waste Partitioning Processes (Commercial Waste)

7.4.2.1 Status

Partitioning of nuclear wastes to separate critical radionuclides for special disposal, such as transmutation or space disposal, has been under study for some time. Methods of separation have been examined for elements such as iodine, strontium, cesium, technetium, and the actinides and lanthinides. Laboratory and pilot plant tests of these processes have been carried out to different degrees of demonstration. None of these processes can be considered fully developed.

7.4.2.2 Justification

The fundamental premise is that space disposal of nuclear waste can be used to supplement geologic disposal by removing particularly troublesome radionuclides from the biosphere. The problem radionuclides are those that have one or more of the following characteristics

(1) Very long lifetimes
(2) High radiotoxicity
(3) High mobility in release paths
(4) Rapid uptake into food cycles
(5) High short-term heating rates

For space disposal to be feasible, and to aid in making proper choice of radionuclides for space disposal, it must be demonstrated to what degree each problem radionuclide can be separated from the high-level nuclear waste.

7.4.2.3 Technical Plan

The DOE program on waste partitioning needs to be revitalized. Primary emphasis should be placed on methods for increasing the degree of recovery and on examining the feasibility of extending laboratory type processes to large scale operations. Emphasis also needs to be placed on defining processes that are simple, of low risk, and reliable.

7.4.2.4 Resource Requirements

The resources required to develop partitioning technology to the point where decisions regarding space disposal can be made with confidence is difficult to estimate. It appears likely that the cost will be at least several million dollars. For initial planning purposes, the cost over a 4-year period has been estimated at $ 3 M, with a strong possibility that additional resources could be required as the SR&T program progresses.

7.4.2.5 Target Schedule

The SR&T for the partioning process needs to proceed on an orderly schedule, therefore, a somewhat uniform spread of funding over the 4-year period is proposed, with the awareness that later year funding could need to be increased over what is shown, as further information develops and particular problems are encountered. Thus, the projected schedule is as follows:

1st Year	2nd Year	3rd Year	4th Year
$ 500 K	$ 500 K	$ 1000 K (+)	$ 1000 K (+)

7.4.3 Waste Form Thermal and Physical Response

7.4.3.1 Status

A preliminary evaluation of potential nuclear waste forms has been accomplished and the reference form selected (cermet-- see Section 3.1). Some of the evaluated waste forms are well-developed, while others have received less attention. Further definition of the characteristics of certain attractive waste forms is required, particularly regarding thermal and physical characteristics, such as dispersion and the formulation of inhalable particles under high temperature reentry environments, and land or ocean impact.

7.4.3.2 Justification

Accident analyses indicate that the waste payload may be subjected to severe environments which could lead to release of nuclear waste (see Section 4.3). The health effects (see Section 5.3) of these accidents could be reduced significantly if the waste form were resistant to dispersion and contained a minimum amount of small inhalable particles.

7.4.3.3 Technical Plan

Waste forms with the desirable characteristics need to be developed and tested on a laboratory scale. The dispersion and particle formulation processes will need to be examined under three conditions:

(1) Exposure to high temperature environments over an extended period, simulating on- or near-pad fires
(2) Exposure to high-velocity, high-temperature gas flows, simulating reentry from orbit
(3) Exposure to very high dynamic loads simulating land and water impact.

In the first case, small samples of the waste forms need to be exposed directly to the thermal environment, simulating waste in an exposed state due to container breachings from mechanical (e.g., fragment impact) or thermal (melting) causes. For the second case, small samples of the waste forms need to be exposed to high-speed, high-temperature gas flows in a hypersonic tunnel with high stagnation temperature capabilities. For the third case, waste samples need to be subjected to high impact loads in a ballistic range against both water and solid (e.g., granite) targets. In each case, the waste melting and/or dispersion rates and the resulting particle size distributions need to be determined for each candidate waste form.

7.4.3.4 Resource Requirements

Funding of $ 200 K to $ 300 K would probably be required, for each of the three types of tests identified, depending upon the number of forms to be tested.

7.4.3.5 Target Schedule

Testing of the possible waste forms needs to proceed relatively early in the program since the results of this testing will affect the environmental impact assessment, determination of program risk, and will influence public and governmental confidence in the feasibility of space disposal. Because of the experimental nature of the programs, peak expenditures are expected in the middle of the program. The projected schedule, is shown below.

1st Year	2nd Year	3rd Year	4th Year
$ 100 K	$ 250 K	$ 250 K	$ 200 K

7.4.4 Remote Automated Rendezvous and Docking

7.4.4.1 Status

Various portions of the contingency plans (see Section 2.6) for space disposal of nuclear waste would require a remote rendezvous and docking capability (e.g., rescue of a payload from an unplanned orbit). NASA has never conducted an automated rendezvous and docking. However, the Soviets have conducted numerous automated dockings in near-Earth orbits, and some proposed NASA planetary missions (e.g., Mars surface sample return) could require distant automated rendezvous and docking. Although some of the hardware elements required for this operation may already exist (e.g., transponders, aircraft-type search radars) a complete demonstrated technology base does not exist.

7.4.4.2 Justification

Demonstrated system safety will be a key requirement for obtaining public acceptance of any nuclear waste disposal approach. For space disposal, the ability to work around unplanned events or accidents will be the key to such safety. A remote rendezvous and docking capability will be an essential element of the space disposal safety approach.

7.4.4.3 Technical Plan

Current studies of remote rendezvous and docking for nuclear waste payload recovery (see Section 6.2) have identified three key problems:

(1) Location of a passive waste payload in Earth or solar orbit
(2) Determination of waste payload attitude and dynamic motion following coarse rendezvous
(3) Reducing the angular momentum of tumbling, noncooperative waste payloads.

Resolution of these problems will require four SR&T developments in two generic areas. These are:

(1) Sensors
   (a) Development of a long range target aquisition device (IR or RF) that could detect a passive payload at ranges exceeding several thousand kilometers.
   (b) Development of an automated tracker that can process and analyze video images of the waste payload.

(2) Docking/Capture Technology
   (a) Development of passive angular momentum dampers to stabilize waste payloads with failed attitude control systems.
   (b) Investigation of external torque application devices that could be carried by the rescue vehicle and used to reduce waste payload angular motions.

7.4.4.4 Requirements

The requirements in each of the four SR&T areas are:

(1) Sensors
   (a) Conceptual design and analysis of candidate RF or IR sensors to indicate feasibility of long range aquisition.
   (b) Software development and laboratory assembly of microprocessor and other hardware elements to permit laboratory demonstration of approach feasibility.

(2) Docking/Capture Technology
   (a) Conceptual design, analysis, and (where possible) laboratory demonstration of candidate approaches to indicate concept feasibility and to scope cost, mass and system performance.
   (b) Same as 1 (a) above.

It is difficult to project the resources that might ultimately be required for this area. Based on the perceived complexity of each task, the funding is projected as $ 300 K for 1(a), $ 800 K for 1(b), $ 300 K for 2(a), and $ 500 K for 2(b), or a total of $ 1.9 M.

7.4.4.5 Target Schedule

The projected SR&T activities involving documentation should have expenditures during the middle of the program. Therefore, the projected funding is as shown below.

SR&T Area	1st Year	2nd Year	3rd Year	4th Year
1(a)	$ 75 K	$ 75 K	$ 75 K	$ 75 K
1(b)	100 K	200 K	300 K	200 K
2(a)	75 K	75 K	75 K	75 K
2(b)	100 K	150 K	150 K	100 K
Total	$ 350 K	$ 500 K	$ 600 K	$ 450 K

7.4.5 Deep Ocean Recovery

7.4.5.1 Status

The ability to reach the deepest portions of the ocean floor has been demonstrated in undersea research programs. The ability to remove or recover objects from the ocean floor has been demonstrated as a part of undersea resource utilization and Naval undersea rescue programs. Therefore, the recovery of waste payloads from a known location in the ocean, following an aborted launch can be considered as an existing technology. However, development of special subsmersible systems for this specific application might be required. The key technology requirement is to be able to locate the aborted payload relatively accurately and promptly. If such location is prompt and accurate, survival of the payload in the ocean environment is reduced to a design problem of insuring adequate container strength to survive the pressures encountered during impact and at maximum depths. Corrosion of the container should not be a problem if the recovery is prompt.

7.4.5.2 Justification

Acceptance of space disposal of nuclear waste by the government and the public will require demonstration of adequate safety during launch. A major part of this demonstration will be to show that nuclear waste payloads will survive and can be recovered safety following aborted launches or launch system accidents. Recovery of a payload from the ocean floor will be a requirement of this demonstration, and is an area requiring some specific SR&T activities.

7.4.5.3 Technical Plan

There is a current capability to detect impacting warheads through the DOD missle impact detection system. This system uses hydrophonic detection of a small detonation charge activated at impact, or failing that, detects the impact splash noise. This system has limited range, and cannot detect impacts in arbitary locations. The feasibility of establishing a wider range net and the trade-offs involved in reducing the possible range of impacts through launch trajectory selection (e.g., equatorial launch site and zero-degree inclination parking orbit) need to be examined. Ary required increases in detector range and sensitivity need to be identified.

An impact detection system can provide a coarse indication of payload location. For recovery, a finer grid detection capability will probably also be required. An omnidirectional sonar beacon on board the payload may be required. Methods for providing such a beacon in a failsafe mode (e.g., using a piezoelectric power beacon activated by the pressure at depth) need to be defined and demonstrated.

7.4.5.4 Requirements

Examination of the use of a system similar to the missle impact detection system and identification of trade-offs and possible additional SR&T development is projected to require $ 200 K. The identification and demonstration of a possibly activated sonar beacon is projected to require $ 250 K, for a total funding of $ 450 K.

7.4.5.5 Target Schedule

The study of the detection net should be completed early so that any additional SR&T tasks identified can be undertaken. The beacon demonstration program should proceed over the full 4-year time span to allow proper testing. The project funding schedule is as shown below:

	1st Year	2nd Year	3rd Year	4th Year
Detection test	$ 100 K	$ 100 K	---	---
Passive beacon	50 K	75 K	75 K	50 K
	$ 150 K	$ 175 K	$ 75 K	$ 50 K

7.5 Safety Test Requirements

The unique nature of the space option for disposing of nuclear waste and the possible high concern over possible releases of nuclear waste material in the event of accidents (especially launch accidents) is expected to lead to an extensive requirement for testing. Normal subsystem testing is not included in the discussion that follows; only testing related to critical safety problems is presented. Safety testing that is expected to be accomplished, prior to carrying out actual disposal missions, includes: (1) materials characterization tests; (2) scale model response tests; (3) full-scale ground-based subsystem response tests; (4) flight tests of specific hardware items; and (5) qualification flight tests of the entire space disposal mission, both small and large scale. This section documents the brief review of previous safety testing activities for nuclear payloads, identifies the types of accidents and environments that are possible, presents a discussion of existing facilities that could be employed for certain tests, and develops a preliminary two-phase plan for safety testing for the space option.

7.5.1 Background

Section 4.1 of this report briefly reviews the safety philosophy and type of tests that have been performed for space nuclear payloads. To summarize, space nuclear payloads (power sources) have been tested such that there is high confidence that the payload will survive an accident event without any major release of radioactive material. The following paragraphs briefly discuss the testing approaches for the NASA/Lewis Research Center space option concept, Radioisotope Thermal-electric Generators (RTG's), General Purpose Heat Source (GPHS), and the Plutonium Accident Resistant Container (PARC). Emphasis has been placed on the latter, because it is most recent and because of the previous treatment of the others in Section 4.1.

During the space option studies of the early 1970's, LeRC performed ground impact and shrapnel tests for its spherical containment system [7-14 through 7-18]. Most of the impact tests (into concrete and soil) were conducted at Sandia Laboratories. The shrapnel tests were conducted by Physics International.[7-18] Results from these efforts indicate that a nuclear waste payload can be designed to survive the severe environments expected.

The Viking safety report[7-19] provides useful information regarding the safety analysis procedure, the type of tests performed, and the results of those tests. The types of safety tests that were performed for the Viking RTG system are listed below:

- Vibration
- Graphite oxidation
- Blast overpressure
- Fragment impact
- Liquid-propellant fire
- Solid-propellant fire
- Impact on granite
- Drop tests
- Reentry heating (plasma tunnel)
- Heat-transfer measurements
- Force and moments measurements

Also, safety tests for the space option for nuclear waste disposal are expected to include the above. The Viking safety report called for more in-depth methods of predicting the dynamic structural response to blast, fragment and impact, as well as, better definition of probability distributions for environment magnitudes for a given accident.

The preliminary accident environments (assumed for space launch) for the GPHS are defined by Reference 7-20 and include consideration of blast overpressure, fragments (shrapnel), solid propellent fire, impact, and reentry (including ablation and thermal stress). Of the five mentioned, the first four must be considered as occurring in sequence.(7-21) Also, in the GPHS design, no credit is given to the presence of auxiliary equipment for protection. During reentry, no more than one-half the minimum thickness of the reentry protection member is allowed to ablate.(7-20)

A recent United States Public Law (94-79; August 9, 1975) restricts the air shipment of plutonium. This law reads, in part, that no plutonium (except for very small quantities of material in medical devices) may be air transported until the NRC (U.S. Nuclear Regulatory Commission) ". . .has certified that a safe container has been developed and tested which will not rupture under crash and blast testing equivalent to the crash and explosion of a high-flying aircraft. . . ." Although there were problems of translating the general language of the law to technically meaningful definitions, very severe accident-modeling criteria were developed by the NRC, which also engaged Sandia Laboratories in the development of a transportation package that would acceptably survive those new criteria. Both the new criteria and the new package were presented for approval to the Advisory Committee for Reactor Safeguards and the National Academy of Engineering's Ad Hoc Committee on the Air Transport of Plutonium.(7-22)

The NRC criteria became a document defining those measures necessary to qualify and certify a package for the air transport of plutonium; this is referred to as the Qualification Criteria. The Qualification Criteria essentially consists of a test program with supporting rationale and stringent acceptance standards. The rationale embodies a maximum credible accident approach, with very severe single-event accident elements applied sequentially to the same package. Also, certain individual tests are included as well as a requirement to conform to existing regulations.

That portion of the program performed at Sandia bears the acronym "PARC" for Plutonium Accident Resistant Container. The PARC project resulted in the development of the PAT-1 (Plutonium Air Transportable) Package. The package was designed concurrently with and in response to the Qualification Criteria and survives the sequential and individual tests of both the new and old criteria and meets the applicable acceptance standards in each case.

The Qualification Criteria are summarized in Tables 7-1 and 7-2; Table 7-1 defines the test program of new sequential and individual tests, and also summarizes the tests of the existing regulations, 10 CFR 71.(7-13) Table 7-2 summarizes the acceptance criteria, essentially comprising three requirements: containment, shielding, and criticality.

In response to the Qualification Criteria (see Table 7-1), a package was designed, analyzed, and developed.[7-23] The resulting PAT-1 package is 62 cm (24.5 in.) OD, 108 cm (42.5 in.) in length, and weighs approximately 227 kg (500 lb) when loaded. Externally, it resembles a 65-gallon commercial stainless steel process vessel. The PAT-1 package comprises an AQ-1 (Air Qualified Model 1) overpack TB-1 containment vessel, and PC-1 product can.[7-23]

TABLE 7-1. QUALIFICATION CRITERIA FOR THE PLUTONIUM AIR TRANSPORT PACKAGE

Type of Test	Criteria
Sequential Tests	
Impact	• 129 m/s (422 fps; 250 KTS) perpendicular to flat unyielding target; most severe orientation
Crush	• 310 kN (70,000 lb) through 5.1 cm (2 in.) wide steel bar; most severe location
Puncture	• 227 kg (500 lb) steel probe dropped 3 m (10 ft); most severe location
Slash	• 45 kg (100 lb) steel angle dropped 46 m (150 ft); twice onto package tilted at 45°
Fire	• Engulfed in large JP-4 fire for 1 hour; left to self-extinguish
Submersion	• Under 1 m (3 ft) of water for 8 hours
Individual Tests	
Hydrostatic	• 4.1 MPa (600 psi) for 8 hours [411 m (1350 ft) depth]
Terminal Velocity Free Fall	• Test required if terminal velocity is more than 250 KTS
10 CFR 71 Tests	
Normal	• Heat, cold, pressure, vibration, water spray, 1.2-m (4 ft) drop, penetration, compression
Accident	• 9-m (30 ft) drop, puncture, fire, submersion

Source: Reference 7-22.

TABLE 7-2. ACCEPTANCE CRITERIA FOR THE PLUTONIUM AIR TRANSPORT PACKAGE

Requirement	Criteria
Plutonium Containment	• Release must be < IAEA A2 weekly quantity following test sequence of new criteria • "No release" from double containment following 10 CFR 71 normal or accident conditions measured as a leak rate --ANSI N 14.5: 10^{-7} cm^3/s -- or as actual loss of surrogate: less than 10^{-8} g, by fluorimetry
Shielding	• Normal transport - 49 CFR 173 requires that external radiation be limited to: 10 mrem/hr at 1 m (3 ft), and 200 mrem/hr at surface • Postaccident - 10 CFR 71 requires that external radiation, following the more severe tests of the new criteria, be limited to: 1000 mrem/hr at 1 m (3 ft)
Criticality	• Undamaged single packages and large arrays must be subcritical per 10 CFR 71 • Arrays of damaged packages must be subcritical per 10 CFR 71, following the more severe tests of the new criteria

Source: Reference 7-22.

Table 7-3 summarizes the tests conducted at Sandia Laboratories and indicates that five PAT-1 packages were subjected to a similar sequential test series, with the initial impact tests oriented so as to encompass five different orientations of top, top corner, side, bottom corner, and bottom. The crush, puncture, slash, fire, and immersion tests that follow were essentially identical for all packages, with the application point of each test being chosen to produce the most damaging cumulative effect on each package. Table 7-3 also includes the individual hydrostatic test required by the Qualification Criteria, and high and low temperature engineering development impact tests, applied as the first test in a sequential series. Before the tests, each package was loaded with a finely divided surrogate UO_2 powder and helium gas. The results show that no uranium oxide escaped as indicated by a fluorimetric test with a detection capability of 10^{-8}g. Also, only very small helium leak rates were detected through the containment vessel seals.

TABLE 7-3. SUMMARY OF QUALIFICATION TESTS FOR THE PLUTONIUM AIR TRANSPORT PACKAGE (PAT-1)

Impact Orientation	Impact Vel. ⊥ to Unyielding Target (fps)	Crush 70,000 (lb)	Puncture 5000 (ft-lb)	Slash 15,000 (ft-lb)	Fire 2300°F 60 Minutes	Immersion	Uranium Detection $\geq 10^{-6}$ g	Post-Test Air Leakage (cm^3/s)
Top 0°	442	√	√	√	√	√	none	$< 4.6 \times 10^{-6}$
Top Corner 30°	451	√	√	√	√	√	none	$< 4.5 \times 10^{-5}$ probably $\sim 1.7 \times 10^{-7}$
Side 90°	445	√	√	√	√	√	none	1.4×10^{-6}
Bottom Corner 150°	443	√	√	√	√	√	none	$< 5.5 \times 10^{-6}$
End 180°	466	√	√	√	√	√	none	1.8×10^{-6}

Individual Test: 600 psig hydrostatic: 8 hours - No detectable water leakage; $< 10^{-10}$ cm^3/s

Other Requirements: Impact at -40°F -- 2.4×10^{-6} cm^3/s result
Impact at 200°F -- 7×10^{-8} cm^3/s result

Source: Reference 7-22.

Based upon the above discussions and the consideration that NRC may eventually license the nuclear waste package for space disposal (see Section 7.3), stringent safety criteria for the space option are expected. The safety criteria to be developed for the nuclear waste package for space disposal will depend upon the details of the mission, the type of launch vehicle employed, the waste mix and waste form. Preliminary safety requirements for the space option are given in Sections 2.5 and 3.3 of this report.

7.5.2 Accident Identification and Environment Definition

The safety criteria to be developed for the space option must consider the potential magnitude and probability of occurrence of accidents. Table 7-4 presents a listing of possible accidents that could occur during the total space disposal mission. The type of accidents considered today to be the most important to insuring safety are:

(1) On-pad Vehicle Explosion and Fire
(2) In-flight Vehicle Explosion, Fire and Impact
(3) Reentry of Payload
(4) Ocean Impact of Payload
(5) Land Impact of Payload
(6) Loss of Active Cooling for Extended Periods

TABLE 7-4. IDENTIFIED ACCIDENTS FOR CONSIDERATION IN ACCIDENT ENVIRONMENT CHARACTERIZATION

Ground Handling Accidents	Vehicle On-Pad and Ascent Accidents	Orbital Operations Acccidents
• Shipping Container/Car Derailment	• Vehicle Fallback/Tipover/Tower Collision	• Accidental Ignition of Ejection Motors
• Shipping Container Fire	• High Velocity Vehicle Impact on Land/Water	• Loss of Payload Cooling
• Cooling System Failure	• Orbiter Crashes on Land/Water	• Collisions Between Payload and Another Object - OTV/SOIS - Orbiter - Spacecraft - Space Debris - Meteors
• Reentry Vehicle Propellant Fire	• Payload Descends to Ocean Floor After System Failure	
• Drop Loaded Container in NPPF	• Vehicle or Orbiter Collides with Another Aircraft	
• Drop Loaded Reentry Vehicle in NPPF	• Vehicle Explodes at Altitude W/WO Command Destruct	
• Outside Intrusion (Flying Vehicles, Natural)	• Abnormal Reentry of Reentry Vehicle	• Critically Inaccurate OTV Burn (Direction/Duration) Resulting in Reentry
• Transporter Accident	• Reentry Vehicle Impacts on Land/Water Surfaces After Ejection From Orbiter	• OTV Explosion
• Drop Loaded Reentry Vehicle at/in RSS	• Accidental Ignition of Payload Ejection Motor(s)	• SOIS Explosion
• Accidental On-Pad Vehicle Explosion/Fire During/After Propellant Loading	• Loss of Payload Cooling	• Communications Failure Resulting in Reentry
• Accidental Ignition of Ejection Motor(s)		• Payload Descends to Ocean Floor
• Loss of Payload Cooling		• Lunar Collision
		• Rescue Mission Failure

Note: No consideration is given in this table to accident probability. Some events listed are extremely unlikely, while others would be expected to occur during a space disposal program.

For the reference space disposal concept (see Sections 2.3 and 2.4) the severe environments for Events 1 through 3 are treated in Sections 4.2 and 4.3 of this report; ocean environment and aspects of ocean recovery are discussed in Reference 7-3 and Section 7.4, respectively; terminal velocity for a reentering payload and soil and granite impact considerations for large spheres are briefly discussed in Sections 4.3.2.1 and 4.1.3, respectively; and recovery time for a safe active cooling loss event is presented in Section 3.4.5.

7.5.3 Environmental Test Facilities

This section reviews some of the environmental test facilities that appear to be appropriate for the space option Concept Definition and Evaluation Program[7-2] and a Space Option Development Program (a plan for which is expected to be prepared in 1983 or 1984). Most of the discussion presented in this section is based upon a visit to Sandia Laboratories in November 1979, interviews with BCL staff who have been involved in the RTG/GPHS Programs, and reviews of various other documents (see Section 4.1).

For major large-scale environmental testing of the survivability of nuclear waste payloads, Sandia Laboratories appears well suited. Reference 7-24 presents the details of test facilities that can be used on a small and large scale to simulate the environments listed below:

- Acceleration
- Climatic
- Shock
- Impulse
- Static Loading
- Vibration
- Explosive
- Reentry (simulation)
- Electromagnetic
- Underwater.

Figure 7-4 provides a pictorial overview of the environmental test facilities at the Sandia Coyote Canyon Test Complex. Other test facilities exist at Livermore California, and at Holloman AFB (35,000-ft test track).

The unique capabilities of interest at Sandia are the two rocket sled track facilities (2000 and 5000 feet long), the Aerial Cable Facility, the Radiant Heating Facility, and the Blast Tunnel Facility. The rocket sleds ($10 to $20 K per test) could be used to simulate impact on various types of surfaces (granite, soil, etc.), but they could also be used for fragment (shrapnel) penetration tests (at a much cheaper per test cost). Any reasonable velocity and acceleration can be generated. The large Aerial Cable Facility, as it currently exists, can accommodate up to roughly 500 kg at a velocity of the order of 300 m/s. To go to a full-scale test of a nuclear waste container at terminal velocity, perhaps four new cables would have to be installed, or it may even be possible to use fewer, but stronger Kevlon fiber/steel cables. The cost for this development has been estimated to be on the order of $1 M. This facility has been used previously to investigate a sphere's impact on soil (see Section 4.1.3). The Radiant Heating Facility can be employed to simulate predicted thermal environment as a function of time, by inputting the proper heating curve data. The heating is accomplished by

FIGURE 7-4. OVERVIEW OF ENVIRONMENTAL TEST FACILITIES AT SANDIA COYOTE CANYON TEST COMPLEX

regulating the electrical power to radiant-heat emitters. The facility can deliver heat fluxes up to 4500 kW/m^2(400 Btu/ft^2-s) and has a rise-time to full power of 2 seconds. The Blast Tunnel, with roughly a 2 m diameter at the exit could provide side-on overpressures of about 200 N/cm^2(300 psi). It is likely, that only slightly scaled down payloads could be tested with the current facility at this pressure level.

Capabilities of interest that exist, but are not believed to be unique to Sandia, are: the liquid fuel fire pits, facilities for generating moving fragments, and the sounding rocket capability for atmospheric reentry testing.(7-25) Although these type of tests require remote areas, it is believed that other laboratories do not have adequate space to carry out the tests.

The Los Alamos Scientific Laboratory (LASL) is currently managing the General Purpose Heat Source (GPHS) Program and has done a considerable amount of work for previous RTG programs. For the GPHS Program, LASL is simulating both the impact and solid propellant fire environments for the GPHS, which is assumed to be flown into space on the Space Shuttle vehicle (see References in Section 4-1). Tests are being performed with surrogate waste forms at various specified thermal conditions. Generally speaking, LASL has the facilities capable for smaller scale testing.

It is expected that full-scale flight tests or simulated tests in ground-based facilities will be necessary for the space disposal mission. Historically, it has been possible to perform selective simulation tests in ground-based facilities to provide the aerodynamic data necessary to verify and/or compare the aerodynamic performance of various designs. It is believed that three types of aerodynamic testing should be considered. They are: aerodynamic stability, aerodynamic heating, and ablation. The amount of testing required will depend on the data available for the particular payload geometries and materials being considered. Preliminary results of the trajectory analyses such as those presented in Section 4.3 are useful in determining the flow regimes of importance and to determine the simulated test conditions. Facilities are available to produce environments that closely simulate the flight conditions anticipated during reentry. Included in this category are wind tunnel, shock tunnel, rocket exhaust, and high-speed test track facilities. Each of these types of facilities normally have operating envelopes which correspond to portions of the reentry flight regimes of interest. Facilities needed for these types of tests exist at NASA/Ames Research Center, NASA Langley Research Center, Edwards Air Force Base, Lockheed, Wright Patterson Air Force Base, ARO, Inc., and Sandia.

7.5.4 Safety Tests Anticipated During 4-Year Space Option Study

The safety related testing anticipated during the proposed 4-year Concept Definition and Evaluation Program is expected to involve only critical components of the conceptual space disposal system. Only those safety tests required to reduce the uncertainty in risk are appropriate during the 4-year

study program. The Draft Concept Definition and Evaluation Program Plan for Space Disposal of Nuclear Waste[7-2], identifies areas of safety testing for the space disposal concept. During the fourth year, safety testing of "critical payload features" are to be performed (WBS-4.1, Safety, Reliability and Safeguards) for the baseline concept. It is difficult to predict in detail, what tests would be performed for "critical payload features", because the baseline concept is yet to be defined and the system safety requirements have not been finalized. However, the launch and reentry aspects of the space disposal concept are not likely to change significantly between the reference concept (as defined in Sections 2.3 and 2.4 of this report) and the baseline concept to be defined in the fourth year of the program.

Risk associated with launch accidents, regardless of the type of nuclear waste that is disposed of in space, will be of utmost importance in determining feasibility. Certainty in payload survival is essential to the concept. Therefore, safety tests of protection system concepts, where material components are exposed to the expected sequential environments of the on- or near-pad booster failure are likely to be performed. The sequential tests are envisioned to include consideration of the accident environments specified in Section 2.5.1.3 of this report. Protection systems that should be tested are only those that need a significant improvement in performance confidence level. Protection systems, in general, include: thermal protection; insulation; impact shield; radiation shield; primary container; and the waste form itself. Scale-model testing of these system components appears to be appropriate. The physical and chemical characteristics of materials proposed for use in protection systems may also have to be determined to greater confidence level.

Risk associated with inadvertent reentry of nuclear waste payloads, depending upon the baseline concept, is also expected to remain an important part of the space option risk. Aerodynamic heating, ablation and thermal shock tests, associated with worst-case reentry environments (see Reference 7-26), may be necessary for scale-model system concepts. Again, only tests that would resolve uncertainty in risk for the space option, should be conducted. In addition to the consideration of testing of payload protection systems, the response of the "baseline" surrogate waste form to reentry environments may also be required. The consequences of a reentry accident depends not only upon how much of the waste form might be released in the upper atmosphere, but also upon the particle size distribution. Because of the manner in which a waste form may be released (melting), an actual test involving a surrogate waste form may be the only way to obtain confidence in the health risk prediction. Tests to measure scale-model payload response include the use of hypersonic and supersonic wind tunnels, and the use of liquid rocket engine plume facilities (mostly for thermal shock).

Should the risk/benefit analysis, conducted for the space option at the end of the 4-year study, indicate that the space system deserves further serious consideration, then additional safety testing will be required. The next section describes the testing anticipated for a development program.

7.5.5 Safety Testing for Development Program

Three categories of tests are anticipated during the development program for the space option: ground-based tests, flight tests of specific items, and qualification flight tests. A number of specific tests for each category are identified below. Additional test items are expected to be identified as the program evolves.

7.5.5.1 Ground-Based Tests

As discussed in Section 7.3, Licensing Requirements, the primary licensing emphasis is expected to be on insuring the survivability of the container under a wide range of potential accident conditions. Most of these accident conditions can be simulated in ground tests; therefore, compliance can be demonstrated thereby. Based on the data in Sections 2.5 and 4.2, ground tests to demonstrate container survival is expected. Sequential testing is likely to be a requirement. The exact conditions under which tests would be conducted would likely be defined as a part of the licensing criteria process discussed in Section 7.3 and identified in Figure 7-3. The actual tests would be conducted during the period prior to the application for license from the NRC, and the test results would be included in the supporting data accompanying the license application. Additional tests might need to be conducted during the license application hearing period to resolve specific NRC concerns.

Demonstrations of container survival during reentry will likely require actual flight test drops from the Shuttle Orbiter. The waste payload will be too large to allow reentry testing under simulated upper atmospheric conditions in existing supersonic and hypersonic tunnels. However, preliminary testing of subscale payload models for various portions of the reentry environment can and should be conducted. Such tests would give preliminary evidence of payload survival and could be used to define the likely severest cases to allow actual flight tests to be reduced to the minimum needed.

A second set of expected ground-based tests would involve the waste form rather than the containment systems. As previously indicated, resistance to dispersion and the potential for formulation of inhalable particles are expected to be the major criteria for selection of the final waste form. An extensive set of tests is expected to be conducted as a part of this selection process, and to demonstrate that the final waste form has the desired characteristics. These tests will probably be conducted in a low-density, high-stagnation-temperature hypersonic or supersonic wind tunnel facility, with special facilities for collection of the portions of the waste form samples eroded by the gas flow.

The third set of expected ground tests concerns the transportation and handling of the nuclear waste prior to launch. A number of potential accidents in the ground transportation and payload handling phase of disposal operations are identified in Table 7-4. It is expected that tests will be required to demonstrate payload intact survival under these various conditions

(e.g., ground transport delay combined with loss of primary cooling, dropping of the payload in the NPPF). Further, since the performance of the transporting and payload handling crews will affect overall system safety, a series of special tests could be conducted to test operator awareness and preparation.

7.5.5.2 Subsystem Flight Tests

A number of specific subsystems will need to be flight tested separately prior to an overall flight demonstration of the entire waste disposal system. Three subsystems are likely to receive specific attention: payload protection, payload cooling system operation, and remote rendezvous/docking. Each of these is discussed below.

The survival of the payload will need to be demonstrated under several conditions. At present, it is expected that at least three flight tests would be required.*

(1) Reentry of the payload plus reentry vehicle from low Earth orbit
(2) Reentry of waste container alone (no reentry vehicle but with some thermal protection) from low Earth orbit (shallow reentry simulating OTV failure shortly after ignition start)*
(3) Same as (2), but with a steep reentry path simulating a seriously misdirected OTV burn.*

The third test would require attaching a velocity package (probably a large solid propellant motor) to the waste container to provide the simulated OTV velocity increment. The tests would be designed to demonstrate container survival and/or to detect any container breach and associated surrogate waste form dispersion.

The consequences of a failure of the cooling system, while the waste payload is in the "insulated" reentry vehicle, have not yet been determined. Currently, it is anticipated that internal waste form melting would occur for high-level waste payloads. Operational safety procedures and operational subsystem reliability could be verified and carried out piggyback on other Space Shuttle missions.

The third set of special flight tests would be of the remote rendezvous and docking capabilities with an uncooperative mockup payload. This is discussed in detail in Sections 6.2 and 7.4. The OTV and a simulated payload would be the primary test items. The tests would require only one Shuttle launch. The required rescue mission simulation would take place in low Earth orbit. Rendezvous and docking would likely use a man-in-the-loop system with continuous control. A simulated deep space rendezvous and docking would be carried out by employing an on-board autonomous system. Both capabilities could be demonstrated in one flight test.

*Note: Current reference concept assumes protection removed at Earth orbit; if protection is carried all the way to destination Item (2) would be eliminated from consideration and Item (3) would be conducted for the reentry vehicle.

7.5.5.3 Qualification Test Flights

Prior to final operating license approval, it is expected that several qualification flight tests of the entire space disposal system will be required. The tests would be designed to demonstrate the nominal disposal mission profile. Early tests could involve reduced waste form masses; later, after confidence is gained "fully loaded" payloads could be used. It is likely that the disposal system will also have to demonstrate its ability to correct unexpected subsystem failures. In qualification flight tests, this would likely take the form of several planned simulated subsystem failures or anomalies. These failures would be known to the program test managers, but not to the flight control personnel responsible for conducting the test flight. Successful demonstration of the mission profile while overcoming the unexpected anomalies would be a major step in satisfying NRC and other regulatory requirements and in increasing public confidence in space disposal.

7.5.6 Development Program Test Schedule

The schedule for development testing should be correlated with the licensing and overall decision schedule shown in Figure 7-3. The primary test period will be during the 7 to 10 year period following the decision to begin major development of the space-based waste disposal system. Some of the ground-based testing would need to occur prior to this period, and the qualification flight tests would be conducted in the 3 to 5 year period of final development prior to initiation of disposal operations.

7.6 References

7-1. "Concept Definition Document for Nuclear Waste Disposal in Space," a working document, NASA/Marshall Space Flight Center, Huntsville, Alabama (January 23, 1980).

7-2. "Concept Definition and Evaluation Program Plan, 1980-1983," an ONWI working document, The DOE Office of Nuclear Waste Isolation, Columbus, Ohio (January 28, 1980).

7-3. Edgecombe, D. S., Rice, E. E., Miller, N. E., Conlon, R. J., Yates, K. R., "Evaluation of Space Disposal of Nuclear Waste--Phase II," Battelle's Columbus Laboratories, Columbus, Ohio (January, 1979).

7-4. English, T. D., Lees, L., and Divita, E., "Space Augmentation of Military High-level Waste Disposal," JPL Publication 79-45, Jet Propulsion Laboratory, Pasadena, California (May 1979).

7-5. Edgecome, D. S., Priest, C. C., et al., "Concept Definition Document for the Space Disposal of Nuclear Waste," Battelle's Columbus Laboratories, Columbus, Ohio (October 1978).

7-6. Edgecombe, D. S., and Kok, K. D., "Review of JPL Final Report on Nuclear Waste in Space," BCL-SNWD-MM-78-8, Battelle's Columbus Laboratories, Columbus, Ohio (November 20, 1978).

7-7. Edgecombe, D. S., and Kok, K. D., "Review of Possible Licensing Requirements for Space Disposal of Nuclear Waste with NRC Personnel," BCL-SNWD-MM-78-9, Battelle's Columbus Laboratories, Columbus, Ohio (November 20, 1978).

7-8. Deutch, J. M., et al., "Report to the President by the Interagency Review Group on Nuclear Waste Management," TID-28817 (Draft) (October 1978).

7-9. English, T. D., "An Analysis of the Back End of the Nuclear Fuel Cycle with Emphasis on High-level Waste Management," JPL 77-59, Vol. I & II, Jet Propulsion Laboratory, Pasadena, California (August 12. 1977).

7-10. Boyle, R. R., "Licensing of High-Level Radioactive Waste Repositories," Waste Management Contractor's Conference, Berkeley Springs, West Virginia (September 17-20, 1978).

7-11. Smith, C. V., Jr., "Licensing Procedures for Geologic Repositories for High-Level Wastes," United States Nuclear Regulatory Commission, Washington, D.C. (June 30, 1978).

7-12. "Review of Criteria for Packaging Plutonium for Transport by Air," NUREG/CR-0428, National Academy of Sciences, Washington D.C. (1978).

7-13. United States Nuclear Regulatory Commission, Rules and Regulations, Title 10, Part 71, Code of Federal Regulations - Energy (September, 1978).

7-14. Puthoff, R. L., "High Speed Impact Tests of a Model Nuclear Reactor Containment System," NASA TM X-67856, NASA/Lewis Research Center, Cleveland, Ohio (June 1971).

7-15. Puthoff, R. L., and Dallas, T., "Preliminary Results on 400 Ft/Sec Impact Tests of Two 2-Foot Diameter Containment Models for Mobile Nuclear Reactors," NASA TM X-52915, NASA/Lewis Research Center, Cleveland, Ohio (October 1970).

7-16. Puthoff, R. L., "A 1055 Ft/Sec Impact Test of Two Foot Diameter Model Nuclear Reactor Containment System Without Fracture," NASA TM X-68103, NASA/Lewis Research Center, Cleveland, Ohio (June 1972).

7-17. Puthoff, R. L., "A 810 Ft/Sec Soil Impact Test of a 2-Foot Diameter Model Nuclear Reactor Containment System," NASA TM X-68180, NASA/Lewis Research Center, Cleveland, Ohio (December 1972).

7 18. Seifert, K., and Wilhoit, D., "Nuclear Waste Containment Vessel Impact Study," PIFR-444 Volume II--Experimental Program, prepared by Physics International Company, San Leandro, California for NASA/Lewis Research Center, Cleveland, Ohio (July 1973).

7-19. "SNAP 19/Viking Final Safety Analysis Report," Vol. I and II, ESD-3069-15, Teledyne Isotopes, Energy Systems Divisions, Timonium, Md. (August 1974).

7-20. "Safety Specification for Plutonium-238 Developmental Heat Sources, NRA-3," Division of Nuclear Research and Applications, Energy Research and Development Administration, Washington, D. C. (April 1977).

7-21. Snow, E. C., and Zocher, R. W., "General-Purpose Heat Source Development, Phase I--Design Requirements," LA-7385-SR, Los Alamos Scientific Laboratory, at the University of California (1977).

7-22. Anderson, J. A., "Plutonium Accident Resistant Container Project," SAND 78-0724 (Revised), Sandia Laboratories, Albuquerque, N.M. (September 1978).

7-23. Anderson, J. A., Duffey, T. A., Dupree, S. A., and Nilson, R. H., "PARC (Plutonium Accident Resistant Container) Program Research, Design, and Development," NUREG/CR-0030, SAND 76-0587, RT, Sandia Laboratories, Albuquerque, N. M. (July 1978).

7-24. "Environmental Test Facilities," Sandia Laboratories, Albuquerque, N.M. (November 1977).

7-25. Rollstin, L. R., and Fellerhoff, R. D., "Aeroballistic and Mechanical Design and Development of the Talos-Terrier-Recruit (TATER) Rocket System with Flight Test Results," SAND 74-0440, Sandia Laboratories, Albuquerque, N.M. (February 1976).

7-26. Pardue, W. M., "Heat Source Component Development Program," Quarterly Reports, Battelle's, Columbus Laboratories, Columbus, Ohio (October 1976 - January 1979).

8.0 CONCLUSIONS

This section summarizes a few of the general conclusions that have been reached as a result of this Phase III study. The conclusions listed below have been organized by task activity:

Payload Characterization (Task 1)

- The ORNL iron/nickel/copper-based cermet waste form has been judged, at this point in time, to be the most suitable waste form for the space disposal of high-level nuclear waste.
- ^{90}Sr and ^{137}Cs contribute significantly to the internal heating problems associated with the space disposal mission.
- Proposed thermal limits for the waste form restrict the size of the cermet form to 8 to 9 MT per payload when considering the PW-4b waste mix.
- For commerical high-level waste, the neutron dose becomes significant for large payloads (> 5 MT).
- For an unshielded 5.5 MT commerical high-level waste payload, an operating distance of greater than 1 km is required to maintain a dose level to the crew of less than 2 rem/hour; the similiar operating distance for an unprotected defense waste payload is less than 20 meters.
- Radiation shielding provided to the crew by Space Shuttle Orbiter structure is considered to be negligible.

Safety Assessment (Task 2)

- The on-pad catastrophic failure of an Uprated Space Shuttle (liquid rocket boosters replacing the solid rocket boosters) is likely to have significantly less severe thermal accident environments than the standard Space Shuttle.
- Because of its very short duration (less than 15 seconds), the fireball resulting from the on-pad catastrophic failure of almost any liquid propellant booster is considered to be virtually unimportant when compared to the possible long-term residual fires.
- Because of the large uncertainty in the fragment (shrapnel) environment data base, caution must be taken in using the data.

- The simulated reentry of the reentry vehicle (RV) showed that the RV should survive with adequate margins; the terminal velocity for the reference vehicle is 110 m/s.

- Under certain reentry conditions it is likely that the unprotected stainless steel container wall will melt away and allow the release of the cermet waste form material to the atmosphere.

- If the thermally unprotected waste container is cool enough prior to reentry and is made to spin or rotate during reentry, no release of waste is expected.

- For the case of an inadvertant reentry of the unprotected waste container (5 MT waste form) the predicted terminal velocity is excessive (365 m/s.)

- Calculations show that the thermal protection provided by the reentry vehicle in the event of a catastrophic Uprated Space Shuttle vehicle failure is adequate, even if the thermal protection system and insulation were lost in the initial explosion.

- For the same degree of payload protection, the total risk of a space disposal program carried out by the HLLV versus the Uprated Space Shuttle is approximately equal.

- The use of a HLLV provides the opportunity to significantly increase protection and decrease the event and total program risk for a similar launch cost.

Health Effects Assessment (Task 3)

- The simplified ORIGEN dilution hazard index is not adequate to determine which radionuclides should be disposed of in space.

- The results from the pathway model assessment indicate that Te and the actinides are appropriate for space disposal.

- Resuspension of fallout particles does not contribute significantly to the dose commitment resulting from an upper atmosphere release of small particles.

- The health effects resulting from a credible release scenario for a thermally unprotected container are significant. The consequences would be worldwide; changes in the reference concept are necessary.

Long-Term Risk Assessment (Task 4)

- For the reference container and cermet waste form, the probability of total fragmentation into small particles as a result of meteoroid impact is 6×10^{-11} per year.
- If small (less than 1000 microns) radioactive particles are released in the 0.85 A.U. circular solar orbit as a result of a total payload fragmentation event (e.g., meteorid impact), the amount of waste form mass expected to return to the Earth over a 3 million year period is a maximum of 6 kg.
- If rescue capability is necessary in nuclear waste disposal, then the design of both rescue vehicle and pay oad vehicle systems must accommodate noncooperative rendezvous and docking operations in addition to the nominal cooperative mode.
- Although automated noncooperative rescue is not presently at a stage of technology readiness, preliminary work in this area gives reasonable confidence that this capability can be developed in the near future.

Program Planning Support Analysis (Task 5)

- An approach to the licensing of space disposal has been developed. It would likely involve NRC licensing of the waste processing and payload fabrication facilities, the Nuclear Payload Preparation Facility at KSC, nuclear waste payload, and possibly the space destination (if lunar surface).
- Five SR&T development activities to support nuclear waste disposal in space are expected to be required. These are: defense waste concentration, commercial waste partitioning, waste form thermal and physical response, remote automated rendezvous and docking, and deep ocean recovery.
- A preliminary safety test plan for the space option was developed. It considers materials characterization tests, scale model response tests, full scale ground tests, flight tests and qualification flight tests. Only tests required to reduce uncertainty in risk are appropriate for the early testing phase. Details of the development testing are expected at the end of the proposed 4-year study.

9.0 RECOMMENDATIONS

Prior to any development or implementation decision on space disposal of nuclear waste, important issues problems will have to be addressed by DOE and NASA. Some specific programmatic and design recommendations resulting from the current Phase III study are summarized below:

Programmatic Recommendations

- The Concept Definition and Evaluation Program Plan, that was developed as a part of this study effort, should be implemented (DOE).*
- Supporting research and technology (SR&T) efforts in the areas of defense waste concentration (DOE), commercial waste partitioning (DOE), waste form thermal and physical response (DOE), remote automated rendezvous and docking (NASA), and deep ocean recovery (NASA) should be implemented.
- Pathway hazard model work should be performed, to determine within the reasonable bounds, the radionuclides which, if removed from the mined repository and shipped to space, provide the best long-term risk benefit. Preliminary indications are that technetium and the actinides should be considered for space disposal (DOE).
- The containment requirements and safety specifications developed during this study for the space disposal option should be updated and revised as new information becomes available (DOE).
- A safety index similar to that used for radioactive space power sources should be developed for the space option of nuclear waste disposal (DOE).
- An experimental program for fragmentation of propellant tanks is required to reduce uncertainty in all space nuclear payload safety assessments (NASA).
- ORNL should continue to perform research on the cermet waste form (DOE).
- The techniques of separation of strontium and cesium from the PW-4b reference waste mix should be evaluated (DOE).
- A study evaluating consequences of an inadvertent loss of payload cooling for extended periods, either on the ground or in space, should be conducted (NASA).

*Note: Parenthetic notation after each recommendation indicates prime agency responsibility.

- There does not appear to be any strong reason for program planners to be concerned about the risk associated with small particle release in solar orbit (NASA).

Design Recommendations

- Any future concepts for space disposal should consider the application of carbon/carbon thermal reentry protection for the container and waste form (NASA).
- The stainless steel wall container material should be replaced with a material (e.g., Ti, Nb etc.) having high structural integrity and a higher melting point (NASA).
- Provisions should be made to insure spinning of the unprotected waste container as a result of an inadvertant reentry (NASA).
- The reference waste mix for space disposal should include the removal ($\geq$ 90%) of cesium and strontium from PW-4b (DOE).
- During mission operations, significant heat producing nuclear waste payloads should be kept as cool as possible; this will likely reduce the consequences from a catastrophic system failure (NASA).
- The concept of integrating defense and commercial waste into a single payload to minimize cooling and shielding requirements should be evaluated (NASA).
- A detailed analysis needs to be performed for actinide payload concepts (DOE).
- The fabrication of large waste forms, by employing various technologies, should be investigated further (DOE).
- Continued study of employing adequate thermal, radiation, and impact protection systems for HLLV payloads, such that they are carried all the way to the final destination are warranted (NASA).
- The design implications of keeping protection systems all the way to a particular space destination requires further study (NASA).

APPENDIX A

ACRONYMS AND ABBREVIATIONS

APPENDIX A
ACRONYMS AND ABBREVIATIONS

Å	angstroms
ACS	attitude control system
ALARA	as low as reasonably achievable
AMAD	activity median aerodynamic diameter
ANPPF	Advanced Nuclear Payload Preparation Facility
APL	Applied Physics Laboratory, Md.
ARL	Ames Research Center, NASA's
A.U.	astronomical unit
atm	atmospheres
ATO	abort-to-orbit
AOA	abort-once-around
BCL	Battelle's Columbus Laboratories, Columbus, Ohio
BIPS	Brayton Isotope Power System
BNWL	Battelle-Northwest Laboratories, Richland, Washington
B.O.	burnout mass
B.R.	burn rate
C	degrees centigrade
CDD	Concept Definition Document
C_3	twice the energy per unit mass
CANDU	Canadian deuterium uranium reactor
CBGS	confined by ground surface tests
CBM	confined by missile
cc	cubic centimeters (cm^3)
c.g.	center of gravity

CFR	Code of Federal Regulations
Ci	Curies
μCi	micro-Curies
cm	centimeters
COE	center of explosion
COR	contracting officers representative
CPIA	Chemical Propulsion Information Agency
CW	continuous wave
DOE	U.S. Department of Energy
DOT	U.S. Department of Transportation
dpm	disintegrations per minute
EIS	environmental impact statement
EOTV	Electric Orbit Transfer Vehicle (SPS's)
EPA	Environmental Protection Agency (U.S.)
ERDA	U.S. Energy Research and Development Administration
ESATA	Executive Subroutines for Afterheat Temperature Analysis (Westinghouse)
esu	electrostatic units
ET	Space Shuttle's External Tank
EVA	extravehicular activity in space
FM	frequency modulation
FWPF	fineweave pierced fabric
g	grams
gal	gallons (U.S.)
G.I.	gastrointestinal (tract)
GPHS	General Purpose Heat Source
GWe	gigawatts electric

HARC	Human Affairs Research Centers (Battelle)
He	helium
HLLV	heavy lift launch vehicle
HLW	high-level waste
HTGR	high-temperature gas-cooled reactor
Hz	Hertz
ICRP	International Commission on Radiological Protection
IR	Infrared
IUS	Inertial Upper Stage
JSC	NASA's Johnson Space Center, Houston
K	degrees Kelvin
kg	kilogram
kJ	kiloJoule
km	kilometer
KSC	Kennedy Space Center, Florida
kW	kilowatt
L	lymph
LASL	Los Alamos Scientific Laboratory, California
LCC	Launch Control Center (Shuttle's at KSC)
LeRC	NASA's Lewis Research Center, Cleveland
LH_2	liquid hydrogen
LOS	line-of-sight
LOX	liquid oxygen
LM	thoracic lymph
LMFBR	liquid metal fast breeder reactor
LRB	Liquid Rocket Booster (Uprated Shuttle)

LWR	light water reactor
m	meters
mm	millimeters
μm	micrometers
$M_{B.O.}$	mass at stage burn out
M_p	propellant mass
mrem	millirem
m/s	meters per second
MLP	Mobile Launch Platform (Shuttle's at KSC)
MT	metric tons
MTHM	metric tons of heavy metal (uranium charge to the reactor)
MMH	monomethyl hydrazine
MPC	maximum permissible concentration
MSFC	NASA's Marshall Space Flight Center, Huntsville, Alabama
MWD/T	megawatt days per ton
N	Newtons
NC	non-cooperative
N/cm^2	Newtons per square centimeter
n. mi.	nautical mile
N_2O_4	nitrogen tetroxide
NTO	nitrogen tetroxide
NASA	National Aeronautics and Space Administration
NEP	nuclear electric propulsion
NPPF	Nuclear Payload Preparation Facility
NRC	Nuclear Regulatory Commission
O/F	oxidizer to fuel ratio

OMS	Orbital Maneuvering System (Shuttle)
ONWI	Office of Nuclear Waste Isolation (DOE's)
ORNL	Oak Ridge National Laboratory, Tennessee
OTV	Orbit Transfer Vehicle
P	pulmonary
PAT	plutonium air transport (package)
PL	payload
POTV	Personnel Orbit Transfer Vehicle (SPS's)
rem	roentgen equivalent, man
RCS	Reaction Control System (Shuttle)
RETAC	Reentry Thermal Analysis Code (BCL's)
RF	radio frequency
RP-1	rocket propellant number 1 (kerosene)
RSS	Rotating Service Structure (Shuttle)
RTG	radioisotope thermal electric generator
RTLS	return-to-landing-site
RV	Reentry Vehicle
s	seconds
SAI	Science Applications, Inc., Schaumburg, Illinois
SAR	Safety Analysis Report
SEP	solar electric propulsion
S.L.	sea-level
SOIS	Solar Orbit Insertion Stage
SPS	Space Power Station
SR&T	supporting research and technology
SRB	Solid Rocket Booster (Shuttle)

SS	Space Shuttle
SSME	Space Shuttle Main Engine
SSP	solar sail propulsion
STS	Space Transportation System
$\dot{T}$	rate of temperature change with time
ΔT	change in temperature
TB	tracheobronchial
TBD	to be determined
V	change in velocity
VAB	Vertical Assembly Building (Shuttle's at KSC)
VPF	Vertical Processing Facility
W	watt
WCF	waste concentration factor
yr	year

APPENDIX B

METRIC/ENGLISH UNIT CONVERSION FACTORS

APPENDIX B
METRIC/ENGLISH UNIT CONVERSION FACTORS

To convert	into	multiply by
atmospheres (atm)	pounds per square inch (psi)	14.70
atmospheres (atm)	pounds per square ft (psf)	2116.8
calories (cal)	British thermal units (Btu)	3.9685×10^{-3}
calories per gram (cal/g)	British thermal units per pound (Btu/lb)	1.80
centimeters (cm)	inches (in)	0.3937
centimeters (cm)	feet (ft)	3.281×10^{-2}
centimeters (cm)	yards (yd)	1.094×10^{-2}
cubic centimeters (cm^3)	cubic inches (in^3)	0.0610
cubic meters (m^3)	cubic feet (ft^3)	35.32
cubic meters (m^3)	gallons (gal)	264.2
degrees Centigrade (C)	degrees Fahrenheit (F)	1.8 C + 32*
degrees Kelvin (K)	degrees Rankine (R)	1.8
grams (g)	pounds (lb)	2.205×10^{-3}
kilograms (kg)	pounds (lb)	2.205
kilometers (km)	statute miles (mi)	0.6214
kilometers (km)	nautical miles (n.mi.)	0.540
kilometers (km)	feet (ft)	3281
kilowatts (kW)	Btu per hour (Btu/hr)	3413
meters (m)	inches (in.)	39.37
meters (m)	feet (ft)	3.281
meters (m)	yards (yd)	1.094

*NOTE: Multiply by 1.8 and then add 32.

To convert	into	multiply by
meters per second (m/s).	feet per second (ft/s).	3.281
metric tons (MT)	pounds (lb)	2205
metric tons (MT)	tons (T).	1.102
micrometers (μm)	meters (m).	1.0×10^{-6}
Newtons (N).	pounds force (lb_f).	0.2248
Newtons per cm^2 (N/cm^2).	pounds per square inch (psi). .	1.4504

APPENDIX C

TECHNICAL DATA FOR CONTAINMENT REQUIREMENTS

APPENDIX C
TECHNICAL DATA FOR CONTAINMENT REQUIREMENTS

In the definition of containment requirements (see Section 3.3), limits are in the form of generic terms (e.g., melting temperature, yield strength). To apply these limits to actual design configurations, it is necessary to define them in terms of specific data. Tables C-1 through C-3 contain temperature, mechanical, and nuclear limit data for the current reference concept. Unknown information is noted as TBD (to be determined). Data for chemical limits are not available at this writing. As the reference concept evolves, additional technical input for containment requirements should be developed and revised, as appropriate.

TABLE C-1. CONTAINMENT REQUIREMENT TEMPERATURE LIMITS, C

MATERIAL	FABRICATION	MELTING	CREEP	NDTT[c]
CERMET (Fe-Ni)	1200	1450	—	—
SS (304L)	—	1450	427[b]	—
NIOBIUM[a]	—	2420	—	-120[d]
TUNGSTEN[a]	—	3430	—	340[d]
GRAPHITE (ABLATION)	TBD	TBD	TBD	TBD
URANIUM	—	1130[d]	TBD	0-10[d]
LEAD	—	326[d]	TBD	TBD
ALUMINUM	—	582[d]	TBD	TBD

NOTES: (a) REQUIRE ADDITIONAL CLADDING TO OFFSET HIGH TEMPERATURE CHEMICAL INTERACTIONS
(b) ASME CODE, SECTION III, APPENDIX III, PARAGRAPH III-2110, 1974 EDITION
(c) NIL DUCTILITY TRANSITION TEMPERATURE
(d) MARK'S HANDBOOK, 7TH ED., 1967, P. 6-114

TABLE C-2. CONTAINMENT REQUIREMENT MECHANICAL LIMITS(a), N/CM^2

MATERIAL	YIELD(b)	ULTIMATE(b)	DYNAMIC
SS (304L)	20,700(c)	51,700(c)	TBD
NIOBIUM	24,100(f)	31,000(d)	TBD
TUNGSTEN	—	12,400-413,800(e)	TBD
ALUMINUM	28,000(e)	31,000(e)	700-6000 (HONEYCOMB)
URANIUM	17,000-31,000(e)	41,000-69,000(e)	TBD
LEAD	800-950(e)	1600-2100(e)	TBD
GRAPHITE (ABLATION)	TBD	TBD	TBD

NOTES: (a) MECHANICAL STRENGTH IS A FUNCTION OF TEMPERATURE AND LOADING RATE
(b) STATIC, ROOM TEMPERATURE
(c) ASME CODE, 1974 ED., SECTION III, SUBSECTION NA, TABLE I-1.2
(d) MARK'S HANDBOOK, 7TH ED., 1967, P. 6-114
(e) MARK'S HANDBOOK, 7TH ED., 1967, P. 6-10
(f) METAL'S REFERENCE BOOK, 5TH ED., 1976, P. 1258

TABLE C-3. CONTAINMENT REQUIREMENT NUCLEAR LIMITS

MATERIAL	CRITICALITY	DISPERSION
CERMET (Fe-Ni)	$K_{eff}<0.95$	TBD
SS (304L)	—	TBD
NIOBIUM	—	TBD
TUNGSTEN	—	TBD

APPENDIX L

EFFECTS OF CERMET METAL ON SHIELDING REQUIREMENTS

APPENDIX D
EFFECTS OF CERMET METAL ON SHIELDING REQUIREMENTS

The ORNL cermet waste form incorporates the radioactive waste within a metallic phase as a means of immobilizing the waste. The prime candidate for the metallic phase is an alloy similar to a Hastelloy, which is chiefly composed of iron, nickel, copper, and molybdenum. This waste form concept was compared to two others with different metallic phases to determine the effect on radiation shield requirements. The two optional metallic phases were molybdenum and tantalum. The comparison was made with the same source term (30 year-old commercial waste) on an equal waste mass basis, using the Los Alamos Scientific Laboratory QAD shielding code (LA-3572, April 1967). The QAD code is useful in predicting gamma dose rates. The neutron dose rate component was assumed to be constant for all cases. Although a more accurate method could be used to calculate dose rates, the use of QAD is believed adequate since only a comparative assessment was necessary.

Table D-1 presents a summary of the waste form mass, shielding mass, and their total for each cermet metal phase candidate. These results illustrate the effects of changing the metallic phase in the waste form. By adding a higher density metal to the waste material the total waste form mass increases, because the waste material requires the same volume of metallic phase, regardless of density. A higher density material is generally a more efficient gamma shield. Therefore, the self-shielding characteristic of the metallic phase results in a smaller uranium shield requirement for the higher density metals. Nevertheless, the combined total mass of the cermet waste form and the uranium shield increases as the metal phase density increases. From a standpoint of low payload mass, a more efficient waste form will employ the lower density metallic phase. However, from the standpoint of an unshielded container radiation dose, a higher density cermet metal phase produces lower surface dose rates.

TABLE D-1. EFFECT OF CERMET METAL PHASE ON SHIELDING DOSE

	Composition of Metal Phase	Bulk Density, g/cc	Cermet Mass[a], kg	Uranium Shield Mass,[b] kg	Payload Total Mass[c], kg
Reference	55% Fe 15% Ni 18% Cu 13% Mo	6.70	5500	4200	9,700
Alternate-1	100% Mo	7.72	6340	3910	10,200
Alternate-2	100% Ta	10.30	8460	3070	11,530

NOTES: (a) Equal waste mass (3230 kg) per payload sphere, homogeneous mixture based on 58.7% waste loading for reference case, 30 year-old commercial waste.
(b) QAD shielding code, dose at 1 m from surface = 2 rem/hr.
(c) Includes only waste form and uranium mass.

APPENDIX E

THERMAL MODEL FOR SPACE ENVIRONMENT

APPENDIX E
THERMAL MODEL FOR SPACE ENVIRONMENT

This appendix describes the model used in the thermal analysis for the payload waste form and container, in a steady state space environment. The model assumes conduction, convection, and radiation modes of heat transfer for spherical geometry. The waste form is the sole heat source; solar radiation was neglected (a secondary effect). The relationship between the maximum waste temperature and the environment temperature is:

$$T_W = \Delta T_W + \Delta T_C + \Delta T_S + T_\infty \quad (E\text{-}1)$$

where: T_W = Waste form temperature,

ΔT_W = Waste form gradient = $(qr_w^2)/(6k_w)$, C (E-1)

ΔT_C = Container gradient = $(qr_c t)/(6k_c)$, C

ΔT_S = Space gradient = $(qr_c)/(3h_r)$, C

T_∞ = Environment temperature = 3 K (deep space)

q = Waste form volumetric heat generation, W/m^3

r_w = Waste form outer radius, m

k_w = Waste form conductivity, W/m-C

r_c = Container mean radius, m

k_c = Container conductivity, W/m-C

h_r = Surface heat transfer coefficient, W/m^2-C

It was assumed that no gap existed between the waste form and container surfaces. Furthermore, the container gradient (Tc) is small in comparison with the other terms and is neglected. The remaining unknown variable in Equation E-1 is the surface heat transfer coefficient, h_r. For a gray body in black surroundings, neglecting the space environment temperature (3K), this coefficient is approximately:

$$h_r \approx \varepsilon \sigma T_S^3$$

where: ε = the container surface emissivity

σ = the Stephan-Boltzmann constant.

Given the data in Table 3-21 and the above relationships, the waste center and surface temperatures for various payload masses were calculated (see Table 3-22). The assumption to neglect the container wall gradient results in an underestimate of less than 5 percent for the largest waste mass payload temperature.

APPENDIX F

MODIFIED PW-4b COMMERCIAL HIGH-LEVEL WASTE MIX

APPENDIX F
MODIFIED PW-4b COMMERCIAL HIGH-LEVEL WASTE MIX

The heat generation rate for the reference commercial high-level waste mix (PW-4b) is sufficiently high to cause the waste form and container temperature limits to be exceeded for the large spherical payloads. Two reasonable ways of achieving a lower heat generation rate are: (1) remove the heat producing elements from the mix; and (2) allow the waste to decay to a level of lower activity, before disposing of the waste in space. Table F-1 presents the results for these two scenarios. The Modified PW-4b waste mix has been chosen to reduce the heat generation rate thus allowing acceptable temperatures for normal conditions in the 9.5 MT cermet waste form payload being considered for the advanced space disposal concept (see Section 2.8). Also, the use of this mix for the reference concept allows increased safety margins when loss of cooling occurs.

The major heat sources in ten-year old high-level waste are ^{90}Sr, ^{134}Cs, ^{137}Cs, and their decay products ^{90}Y, and ^{137m}Ba. The proposed modified waste mix considers the removal of 90 percent of the strontium and cesium from the liquid high-level waste in the initial waste treatment process. Removal of yttrium and barium is unnecessary because of their short half-lives. Removal of these elements to this degree will reduce the heat output of the high-level mix to 24 percent of that of the reference PW-4b mix. This reduced heat generation (4.63 W/kg) was used in the thermal analysis for the 9.5 MT waste form payload (see Section 3.4.5).

The gamma source strength of the strontium and cesium nuclide decay chain was compared to the total contribution of the PW-4b waste. The effect of removing 90 percent of the strontium and cesium from PW-4b does not yield a proportional decrease in the gamma source strength. Rather, the modified source is only 65 percent less. Assuming this reduction in gamma source strength and maintaining the neutron source, the required uranium thickness for a 9.5 MT waste mass payload is about 6.3 cm (includes the shielding contribution from 2.54 cm of steel) to reduce the dose rate to 2 rem/hr at 1 m.

TABLE F-1. PW-4b WASTE MIX HEAT REDUCTION CONSIDERATIONS

Isotope	Reference (Disposal After 10 Years)	Remove 90 Percent Sr & Cs	Remove 99 Percent Sr & Cs	Dispose After 25 Yr	Dispose After 37.5 Yr	Dispose After 50 Yr	Dispose After 100 Yr
			Watts Per MTHM				
Sr-90	91.1	9.1	0.9	63.8	47.4	35.5	10.0
Y-90	410	41	4.1	287	213	160	45.1
Cs-134	90	9	0.9	0.0	0.0	0.0	0.0
Cs-137	165	16.5	1.6	117	89.1	66	21.4
Ba-137	371	37.1	3.7	263	200	148	48.2
Pm-147	50.6	50.6	50.6	1.0	0.0	0.0	0.0
Eu-154	39.3	39.3	39.3	9.8	3.1	0.0	0.0
Am-241	15	15	15	15	15	15	15
Cm-244	103	103	103	70(a)	50(a)	40(a)	35(a)
Total	1335	321	219	826.6	617.6	464	174.7
Percent of Reference	100	24	16	62	46	35	13

(a) Estimated

APPENDIX G

THERMAL MODEL FOR AUXILIARY COOLING

APPENDIX G
THERMAL MODEL FOR AUXILIARY COOLING

This Appendix describes a steady-state thermal model used for calculating the temperatures for the payload waste form, container, radiation shield, and reentry vehicle in an Earth environment. The model includes conduction, convection, and radiation heat transfer where applicable, and assumes a spherical geometry for all components. The model developed also includes consideration of gap temperature gradients. Auxiliary cooling is assumed to be available uniformly over the surface of the primary container. This model was applied in Section 3.4.5 to determine minimum auxiliary cooling requirements. No attempt at a cooling system design is made.

The relationship between the waste form center temperature and the waste form surface temperature is directly proportional to the decay heat:

$$T_w = \frac{q r_w^2}{6 k_w} + T_s \qquad \text{(G-1)}$$

where T_w = Waste form center temperature
T_s = Waste form surface temperature
q = Waste form volumetric heat generation rate
r_w = Waste form radius
k_w = Waste form conductivity.

The total heat generated, qV (where V is the payload waste form volume), must be either transmitted through the payload system boundaries or actively be removed by means of auxiliary cooling. For conduction in spherical geometry, the heat transferred is given by:(G-1)

$$q = \frac{4\pi k r_o r_i (T_s - T_\infty)}{r_o - r_i}$$

and for a thin shell,

$$q = \frac{4\pi k \bar{r}^2 (T_s - T_\infty)}{t}$$

For the high-level waste container problem here, therefore, we have:

$$q = \frac{4\pi\ (T_s - T_\infty)}{R_c + R_{c,gap} + R_s + R_{s,gap} + R_R + R_\infty} \qquad \text{(G-2)}$$

where R_c = Thermal resistance of container = $(t_c)/(r_c^2 k_c)$

$R_{c,gap}$ = Thermal resistance of container/shield gap = $(1/r_c)^2 (t/k + 1/h)_{gap}$

R_s = Thermal resistance of shield = $(ts)/r_s^2 k_s)$

$R_{s,gap}$ = Thermal resistance of shield/reentry vehicle gap = $(1/r_s)^2 (t/k + 1/h)_{gap}$

R_R = Thermal resistance of reentry vehicle = $(t_R)/r_R^2 k_R)$

R_∞ = Thermal resistance of Earth environment = $1/(r_T^2 h_\infty)$

t = Material thickness
k = Material conductivity
h = Surface heat transfer coefficient
r = Radius.

The procedure used to calculate the auxiliary cooling requirements is as follows:

(1) Choose the desired waste form center or surface temperature.
(2) Calculate T_s (or T_w) from Equation G-1.
(3) Calculate the heat transferred through payload system to ambient, using Equation G-2.
(4) Calculate auxiliary cooling (equals heat generated minus heat transferred to ambient).

In the actual computations for Section 3.4.5, the thermal resistances through the various metal walls (i.e., container, shield, and reentry vehicle) were neglected because they are small in comparison to the gaps, insulating materials, and ambient resistances. For the principal gaps assumed (between container and shield, and shield and reentry vehicle), the heat transfer is a combination of conduction, and convection and radiation. The latter components were assumed to be constant, 14.2 W/m^2-C, representing gap convection and radiation heat transfer, as previously determined in the Battelle Phase II Study.(G-2) The gap conductivity was assumed to be that of air, at a temperature of 315 C, equal to 0.043 W/m-C, with an assumed gap thickness of 0.15 cm.

The reentry vehicle thermal resistance was assumed to consist of the insulation conductivity. A representative value of 0.035 W/m-C was assumed for MIN-K insulating material, having a thickness of 2.54 cm. The surface heat transfer coefficient (convection and radiation in air) was assumed from the Phase II effort (11.4 W/m^2-C).(G-2)

Since detailed designs are not required at this stage of the concept definition, representative values were assumed to determine the approximate temperatures for the various payloads. Minor differences in detailed conceptual design information will not affect the conclusions reached during this study.

References

G-1. Kreith, F., Principles of Heat Transfer, 2nd ed., International Textbook Co., Scranton, Pa. (1967).

G-2. Edgecombe, D. S., Rice, E. E., Miller, N. E., Yates, K. R., and Conlon, R. J., "Evaluation of the Space Disposal of Defense Nuclear Waste--Phase II," Volume II, Battelle's Columbus Laboratories, Columbus, Ohio (January 1979).

APPENDIX H

CALCULATION OF FIREBALL TEMPERATURE, HEAT FLUX AND DIAMETER

APPENDIX H

CALCULATION OF FIREBALL TEMPERATURE, HEAT FLUX AND DIAMETER

This appendix describes the equations and data that were used to calculate the fireball temperature and surface heat flux (as a function of time) resulting from postulated fireballs of the Space Shuttle, the Uprated Space Shuttle, and HLLV. The results of these calculations and many of the assumptions are presented in Section 4.2.1. The Bader "Liquid-Propellant Rocket Abort Fire Model" (Reference H-1) was employed here, with modifications appropriate for the vehicles. Solutions to the fireball energy equation for the two time regions of interest (the time from ignition, $t = 0$, until the time the liquid propellants have all been consumed, $t = t_b$, and the time, $t = t_b$, until the fireball stem lifts off the ground, $t = 1.5 \times t_b$ --see Figure 4-1) are presented below. Also, a discussion of fireball diameter is presented.

Temperature and Heat Flux Calculations for $t \leq t_b$

The energy equation (Equation 10 of Reference H-1) for the fireball is derived by equating the rate of internal energy change and expansion work of the fireball to the difference between the rate of energy added by fuel (propellant) addition and the rate of energy loss by radiation, as shown below:

$$Rh_r - \varepsilon\sigma AT^4 = \frac{d(Wh_p)}{dt} \qquad \text{(H-1)}$$

where:

- R = Constant Rate of Fuel Addition
- $h_r = h_{reactants}$ = Specific Enthalpy of Formation for propellants (defined as h_{in} in Reference H-1)
- ε = Fireball Emissivity
- σ = Stefan-Boltzmann constant
- A = Fireball Surface Area

T = Fireball Temperature

W = Mass of Fireball (W_b = total mass of propellants)

h_p = $h_{products}$ = Specific Enthalpy of Formation for Fireball (defined as h_{FB} in Reference H-1)

t = time (defined as τ in Reference H-1).

Equation (H-1) can be rearranged as:

$$Rh_r = \varepsilon\sigma AT^4 + W\frac{dh_p}{dt} + h_p\frac{dW}{dt} \quad , \tag{H-2}$$

but, $\frac{dW}{dt}$ is equal to R, the constant rate of fuel addition. Thus, we can rewrite Equation (H-2) as:

$$R\,(h_r - h_p) = \varepsilon\sigma AT^4 + W\frac{dh_p}{dT}\cdot\frac{dT}{dt} \quad . \tag{H-3}$$

The surface area of the fireball, A, can be expressed in terms of the density, ρ , rate of fuel addition, R, and time, t. The surface area of the spherical fireball is defined as:

$$A = 4\pi r^2 \quad , \tag{H-4}$$

where r is the radius of the fireball. However, the density of the fireball at any given time can be expressed as:

$$\rho = \frac{\text{Mass}}{\text{Volume}} = \frac{W}{\frac{4}{3}\pi r^3} = \frac{Rt}{\frac{4}{3}\pi r^3} \quad . \tag{H-5}$$

Therefore, the radius of the fireball can be expressed as:

$$r = \left(\frac{3Rt}{4\pi\rho}\right)^{1/3} \quad ; \tag{H-6}$$

and thus the surface area of the fireball is:

$$A = 4\pi\left(\frac{3Rt}{4\pi\rho}\right)^{2/3} \quad . \tag{H-7}$$

Also, from the equation of state:

$$P = \rho RT \quad , \tag{H-8}$$

where:

P = Pressure
R = Gas Constant
T = Temperature.

Equation (H-7) can be rewritten as:

$$A = 4\pi \left(\frac{3RtRT}{4\pi P}\right)^{2/3} \qquad \text{(H-9)}$$

Substituting Equation (H-7) into Equation (H-3) and noting that R = W/t, we arrive at a first order, non-linear differential equation:

$$\frac{dT}{dt} = \left[(h_r - h_p) - St^{2/3}T^{14/3}\right]\left[\frac{1}{t}\right]\left[\frac{1}{dh_p/dT}\right] , \qquad \text{(H-10)}$$

where:

$$S = 4\pi\epsilon\sigma \left(\frac{3R}{4\pi P}\right)^{2/3} R^{-1/3} . \qquad \text{(H-11)}$$

The relationships between h_p and T for the Space Shuttle, Uprated Space Shuttle, and the HLLV propellants were presented in Section 4.2.1.2 of this report. The table below presents data calculated for h_p and T.

T,K	Vehicle		
	Space Shuttle	Uprated Space Shuttle	HLLV
	hp, cal/g		
2000	--	-2258	-2234
2100	-1844	-2176	-2154
2200	-1752	-2084	-2063
2300	-1653	-1977	-1958
2400	-1542	-1851	-1834
2500	-1414	-1698	-1682
2600	-1261	-1512	-1499
2700	-1073	-1288	-1278
2800	-836.5	-1034	-1027
2900	-540.6	-725.6	-722.3
3000	-178.0	-391.6	-393.4
3100	251.9	-28.88	-36.93
3200	739.6	355.0	339.6
3300	--	751.4	727.7

Note: These data are plotted in Figures 4-2, 4-3, and 4-4 of Section 4.2.1.2.

These data were fitted to fifth order polynomials of the form:

$$h_p = B_0 + B_1T + B_2T^2 + B_3T^3 + B_4T^4 + B_5T^5 ,$$

with

$$\frac{dh_p}{dT} = B_1 + 2B_2T + 3B_3T^2 + 4B_4T^3 + 5B_5T^4 .$$

For h_p, in units of cal/g, and T, in degrees K, the constants are as follows:

Constant	Space Shuttle	Uprated Space Shuttle	HLLV
B_0	+1.79040E+05	+6.86817E+03	+5.44953E+03
B_1	-3.65130E+02	-3.02094E+01	-2.73145E+01
B_2	+2.91226E-01	+3.34755E-02	+3.11942E-02
B_3	-1.14824E-04	-1.70831E-05	-1.62001E-05
B_4	+2.23578E-08	+4.12726E-09	+3.95964E-09
B_5	-1.71028E-12	-3.74386E-13	-3.62049E-13

The values of h_r were computed using: (1) the heats of formation as given in Reference H-2 for liquid hydrogen and liquid oxygen, at their normal boiling points; (2) RP-1, at 25 C; and (3) the propellant mole ratios particular to each vehicle. The values of h_r for these assumptions are given in Table 4-3.

To obtain the value of S (see Equation H-11) we must first define certain constants and determine the value of R, the constant rate of fuel (propellant) addition.

For a spherical Space Shuttle fireball under the influence of atmospheric pressure (P = 1.0 atm), the average density of the gases at the time of liftoff ($t = t_b$) can be approximated by assuming, for temperature, the value of 2991 K (see Section 4.2.1.2). From the equation of state, Equation (H-8), we have:

$$\rho = \frac{P}{RT} = \frac{(1.0 \text{ atm})}{0.082 \frac{\text{m}^3\text{-atm}}{\text{kg-mole K}} \times \frac{\text{kg-mole}}{14.006 \text{ kg}} \times (2991 \text{ K})}$$

Thus,

$$\rho = 0.05714 \text{ kg/m}^3 \ (0.003565 \text{ lb}_m/\text{ft}^3) \quad .$$

From Equation (H-6) and W = R x t, the radius for the Space Shuttle fireball at the time of liftoff ($t = t_b$) is given as:

$$r_b = \left(\frac{3}{4\pi\rho}\right)^{1/3} W_b^{1/3} \quad . \tag{H-14}$$

$$r_b = 1.61 \ W_b^{1/3} \text{ (when } W_b \text{ is in kg)}$$

or

$$[r_b = 4.063 \ W_b^{1/3} \text{ (when } W_b \text{ is in lb}_m\text{)}]$$

Reference H-1 defines the relationship between the time of liftoff, t_b, and the fireball radius at that time, r_b. This is given as:

$$t_b = \left(\frac{3r_b}{g}\right)^{1/2} \quad , \tag{H-15}$$

where, g is the acceleration of gravity, 9.8 m/s^2. After substituting Equation (H-14) into the above relationship we arrive at:

$$t_b = 0.702 \ W_b^{1/6} \text{ (when } W_b \text{ is in kg)}$$

or

$$[t_b = 0.615 \ W_b^{1/6} \text{ (when } W_b \text{ is in lb}_m\text{)}] \quad . \tag{H-16}$$

Since the constant rate of fuel (propellant) addition, R, is given as:

$$R \text{ (kg/s)} = \frac{W}{t} = \frac{W_b}{t_b} = \frac{W_b}{0.702 \ W_b^{1/6}} \quad . \tag{H-17}$$

We have:

$$R = 1.425 \ W_b^{5/6} \text{ (when } W_b \text{ is in kg)}$$

or

$$[R = 1.626 \ W_b^{5/6} \text{ (when } W_b \text{ is in lb}_m\text{)}] \quad .$$

For the case of the Space Shuttle, W_b = 7.12 E+05 kg (1.57 E+06 lb_m), we arrive at:

$$R = 1.074 \text{ E+05 kg/s}$$
$$r_b = 144 \text{ m}$$
$$t_b = 6.63 \text{ s.}$$

Therefore, the Space Shuttle fireball is expected to lift off the ground at 6.63 seconds after the initial fire and is expected to have a diameter of approximately 288 m. Reference H-1 indicates that the time of stem liftoff (see Figure 4-1) is given as 1.5 x t_b; thus, the stem is expected to lift off the ground at 9.95 seconds after the initial fire. The value of S is calculated using Equation (H-11).

Substituting in values for S, h_r and using Equations (H-12) and (H-13) to substitute for h_p and (dh_p/dT), Equation (H-10) was then integrated numerically by computer using the Runge-Kutta-Gill method. Battelle's IRKG and RKG Routines were employed. The resulting data are plotted in Figures 4-5, 4-6, and 4-7 of Section 4.2.1.2 for each vehicle.

Temperature and Heat Flux Calculations for $t_b < t < 1.5\ t_b$

The energy equation used for $t < t_b$ (See Equation H-1) is modified by the assumption that there is no more chemical heat added and the mass of the fireball is constant ($W = W_b$). This results in:

$$-\varepsilon\sigma A T^4 = W_b \frac{dh_p}{dt} = W_b \frac{dh_p}{dT} \cdot \frac{dT}{dt} \quad ; \tag{H-18}$$

rearranging, and substituting using Equation (H-9) for A we arrive at:

$$\frac{dT}{dt} = -S' \left[T^{14/3}\right]\left[t^{2/3}\right]\left[\frac{1/dh_p}{dT}\right] \quad , \tag{H-19}$$

where:

$$S' = \frac{4\pi\varepsilon\sigma}{W_b}\left(\frac{3R^2}{4\pi\rho}\right)^{2/3} \quad . \tag{H-20}$$

By employing Equation (H-13), giving the relationship between dh_p/dT and T, the value of S' is determined. The values of S and S' that were used in the calculations are given below, both in English and metric units. Also, other important parameters used in the calculation are given.

Parameter	Space Shuttle	Space Shuttle	HLLV
Metric Units			
$\mathcal{R}$,$(m^3\text{-atm})/(kg\text{-}K)$	0.00585	0.00393	0.00389
ρ,kg/m^3	0.05714	0.08319	0.08416
W_b,kg	0.712E+06	1.79E+06	6.14E+06
r_b,m	144.	173.	259.
t_b,s	6.630	7.267	8.902
t_bx1.5,s	9.945	10.900	13.354
S/σ,$(m^2\text{-}s^{1/3})/(g\text{-}k^{2/3})$	3.31E-06	1.92E-06	1.35E-06
S'/σ,$m^2/(g\text{-}K^{2/3}\text{-}s^{2/3})$	4.98E-07	2.64E-07	1.52E-07
English Units			
$\mathcal{R}$,$(lb_f\text{-}ft)/(lb_m\text{-}R)$	110.33	74.12	73.27
ρ,lb_m/ft^3	0.003565	0.005190	0.005251
W_b,lb_m	1.57E+06	3.95E+06	13.54E+06
r_b,ft	472.	566.	851.
t_b,s	6.630	7.267	8.902
t_bx1.5,s	9.945	10.900	13.354
S/σ,$(ft^2\text{-}s^{1/3})/(lb_m\text{-}R^{2/3})$	10.920E-03	6.344E-03	4.468E-03
S'/σ,$ft^2/(lb_m\text{-}R^{2/3}\text{-}s^{2/3})$	16.455E-04	8.7292E-04	5.0186E-04

Equation (H-19) was then integrated numerically by computer using the Runge-Kutta-Gill method. The resulting data are shown in Figures 4-5, 4-6, and 4-7 in Section 4.2.1.2.

Fireball Diameter

The predicted fireball diameters as a function of time for the three vehicles of interest are shown in Figure 4-8 of Section 4.2.1.2. These

relationships were generated by evaluating the following equation (also see Equation 6) which relates the diameter of the fireball to the density and the mass of the fireball:

$$d = 2xr = 2\left(\frac{3W}{4\pi\rho}\right)^{1/3} \qquad \text{(H-21)}$$

The values of density (assuming the molecular weight at the initial conditions), , and fireball mass, W, were calculated as a function of time. For values of time greater than t_b, a constant value of fireball mass was used. A decrease in fireball size for $t > t_b$ is due to the large amount of radiation being emitted from the fireball, thus cooling it and increasing its density.

Reference H-3 provides relationships between the maximum fireball diameter and total propellant for the propellant combinations considered here. These relationships were developed from experimental data. The relationships, modified to reflect diameter in meters, are as follows:

$$\begin{array}{cc} \underline{LO_2/LH_2} & \underline{LO_2/RP\text{-}1} \\ d(m) = 4.390\ W_b^{0.306} & d(m) = 3.933\ W_b^{03.16} \quad \text{(when } W_b \text{ is in kg)} \\ \left[d(ft) = 11.05\ W_b^{0.306}\right. & \left. d(ft) = 10.05\ W_b^{0.316} \quad \text{(when } W_b \text{ is in lb)}\right] \end{array} \qquad \text{(H-22)}$$

For the Space Shuttle case, W_b = 7.12 E+05 kg, the predicted maximum fireball diameter, d, is 265 m. This value is shown in Figure 4-11 in Section 4.2.1.2, and good agreement with the Bader Model is observed. The predicted fireball maximum diameters for the Uprated Space Shuttle and HLLV are, based upon Equation H-22 for LO_2/RP-1, 372 and 549 m, respectively. The analytical Bader Model predicts slightly lower values than these. In looking back to the data used to develop the correlations given above(H-3), the predicted values are well within the data envelope.

References

H-1. Bader, B. E., Donaldson, A. B., and Hardee, H. C., "Liquid-Propellant Rocket Abort Fire Model," AIAA Journal of Spacecraft, Vol. 8, No. 12 (December 1971).

H-2. Rowe, J. R., "Properties and Performance of Liquid Rocket Propellants," Aerojet Liquid Rocket Company, Sacramento, California (May 1975).

H-3. Gayle, J. B. and Bransford, J. W., "Size and Duration of Fireballs from Propellant Explosions," NASA TMX-53314, NASA/Marshall Space Flight Center, Huntsville, Alabama (August 4, 1965).

APPENDIX I

FRAGMENT VELOCITY DISTRIBUTION

APPENDIX I

FRAGMENT VELOCITY DISTRIBUTION

NASA CR-134538[I-1] reports pooled data (data from several tests) for initial fragment velocities for the CBM (confined by missile) and CBGS (confined by ground surface, typically a drop test) for LO_2/LH_2 and LO_2/RP-1 propellants in Table X (see Table I-1). The report concludes that the data are best represented by a log-normal distribution. NASA CR-134906,[I-2] in Figures 4-46 (see Figure I-1) and 4-47 (see Figure I-2) shows a log-normal discribution for the CBM cases, with the correlation line passing through the appropriate mean value. The data for the LO_2/LH_2 CBM case from NASA CR-134538, Table X (Table I-1), and the correlation line from NASA CR-134906 Figure 4-46 (Figure I-1) are plotted in Figures I-3 and I-4. It is evident from Figure I-3 that the data do not fit a log-normal distribution. Further, fitting these data to a log-normal distribution results in overestimating the fragment population in the high velocity tail and underestimating the population in the low velocity tail. In Figure I-4, the data and correlation line are shown on (normal) probability paper. It is evident that the data from Table X (Table I-1) fit the normal distribution to a quite good approximation (both the LO_2/LH_2 and LO_2/RP-1 data are shown). Table I-2 compares the normal and log-normal predictions for various velocity percentiles. As indicated, the use of the log-normal distribution predicts much higher velocities at the higher percentiles than the normal distribution.

TABLE I-2. COMPARISON OF NORMAL AND LOG-NORMAL VELOCITY DISTRIBUTIONS*

Percentile	Normal Velocity Distribution ft/s	Normal Velocity Distribution m/s	Log-Normal Velocity Distribution ft/s	Log-Normal Velocity Distribution m/s
10	50	15	180	55
20	270	82	280	85
50	670	200	650	200
90	1280	390	2230	680
95	1460	445	3200	975
99	1780	543	6400	1950

*Note: Data taken from Figures I-3 and I-4, for CBM, LO_2/LH_2 tank explosions.

TABLE I-1. PERCENTILES, MEANS AND STANDARD DEVIATIONS FOR GROUPED VELOCITY DATA (fps)

Percentiles	CBM LO_2/LH_2	CBM LO_2/RP-1	CBGS LO_2/LH_2	CBGS LO_2/RP-1
10	105.8	290.0	170.0	160.1
20	228.6	414.3	219.2	262.3
30	393.3	536.8	289.3	316.8
40	541.8	714.2	345.1	364.9
50	642.0	822.8	459.4	388.3
60	821.4	973.3	594.3	431.2
70	915.0	1096.3	728.8	498.5
80	1102.7	1216.8	897.7	573.4
90	1249.3	1405.6	1169.9	790.5
Estimated Mean*	6.464	6.713	6.129	5.962
Estimated Standard Deviation*	.9875	.6313	.7715	.6387

*Log Normal Distribution, to base e. To convert to fps, take anti-logarithm

Source: NASA CR 134538, Reference I-1.

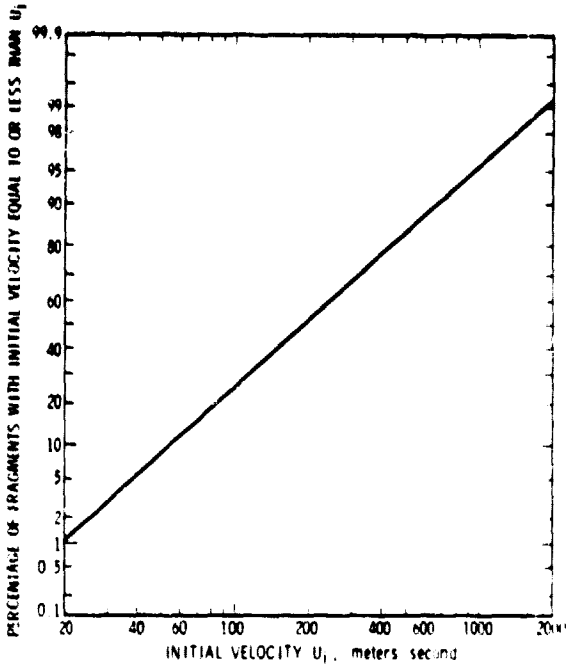

FIGURE I-1. INITIAL VELOCITY DISTRIBUTION, CBM, LO_2/LH_2

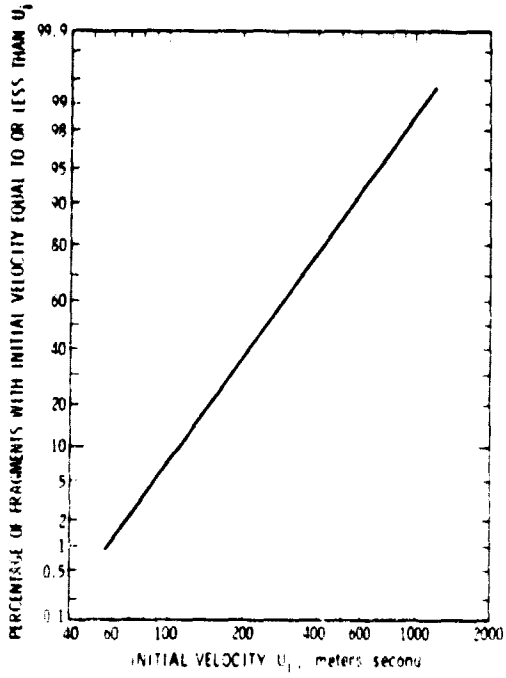

FIGURE I-2. INITIAL VELOCITY DISTRIBUTION, CBM, $LO_2/RP\text{-}1$

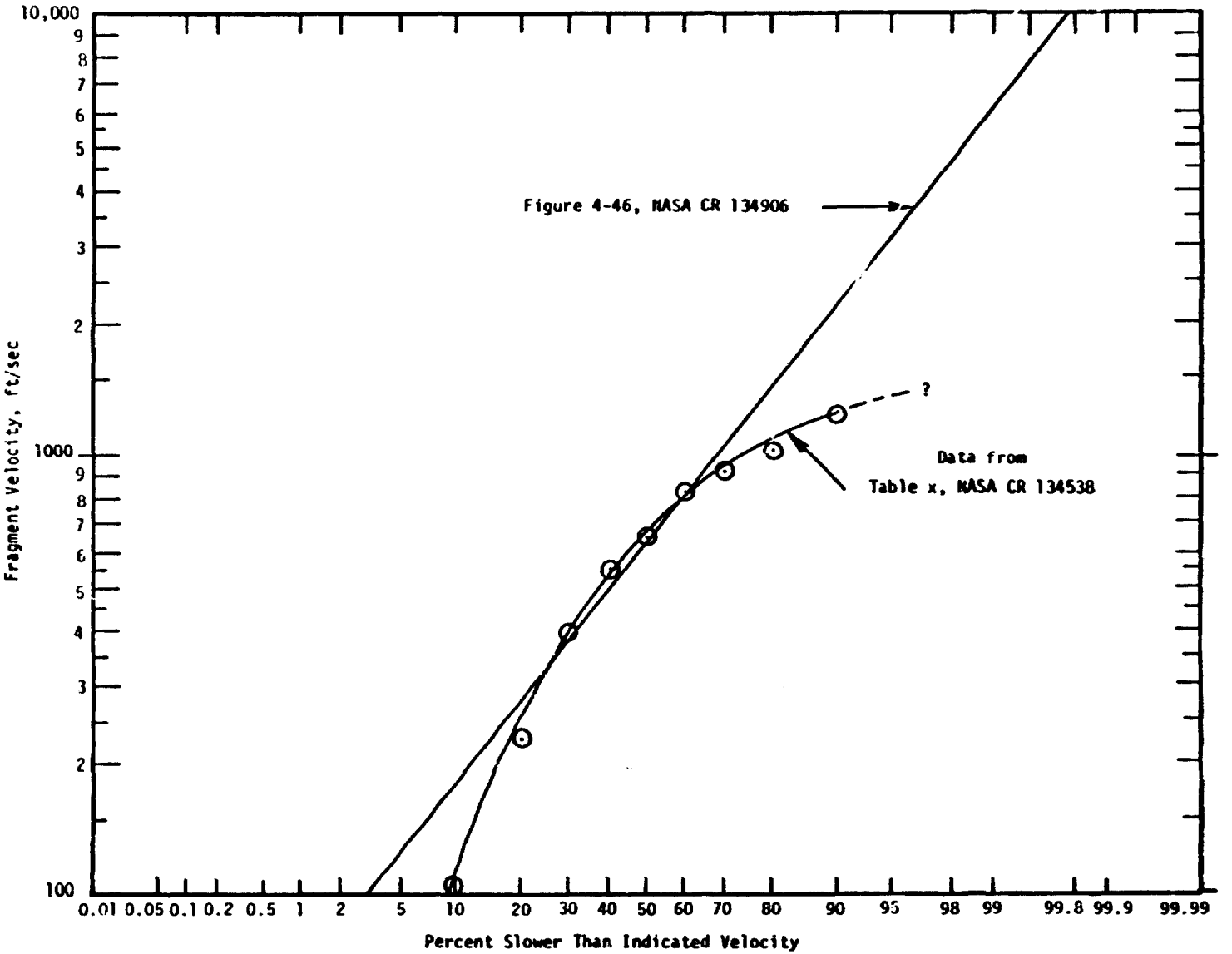

FIGURE I-3. FRAGMENT VELOCITY DISTRIBUTIONS CONFINED BY MISSILE (CBM), LO_2/LH_2

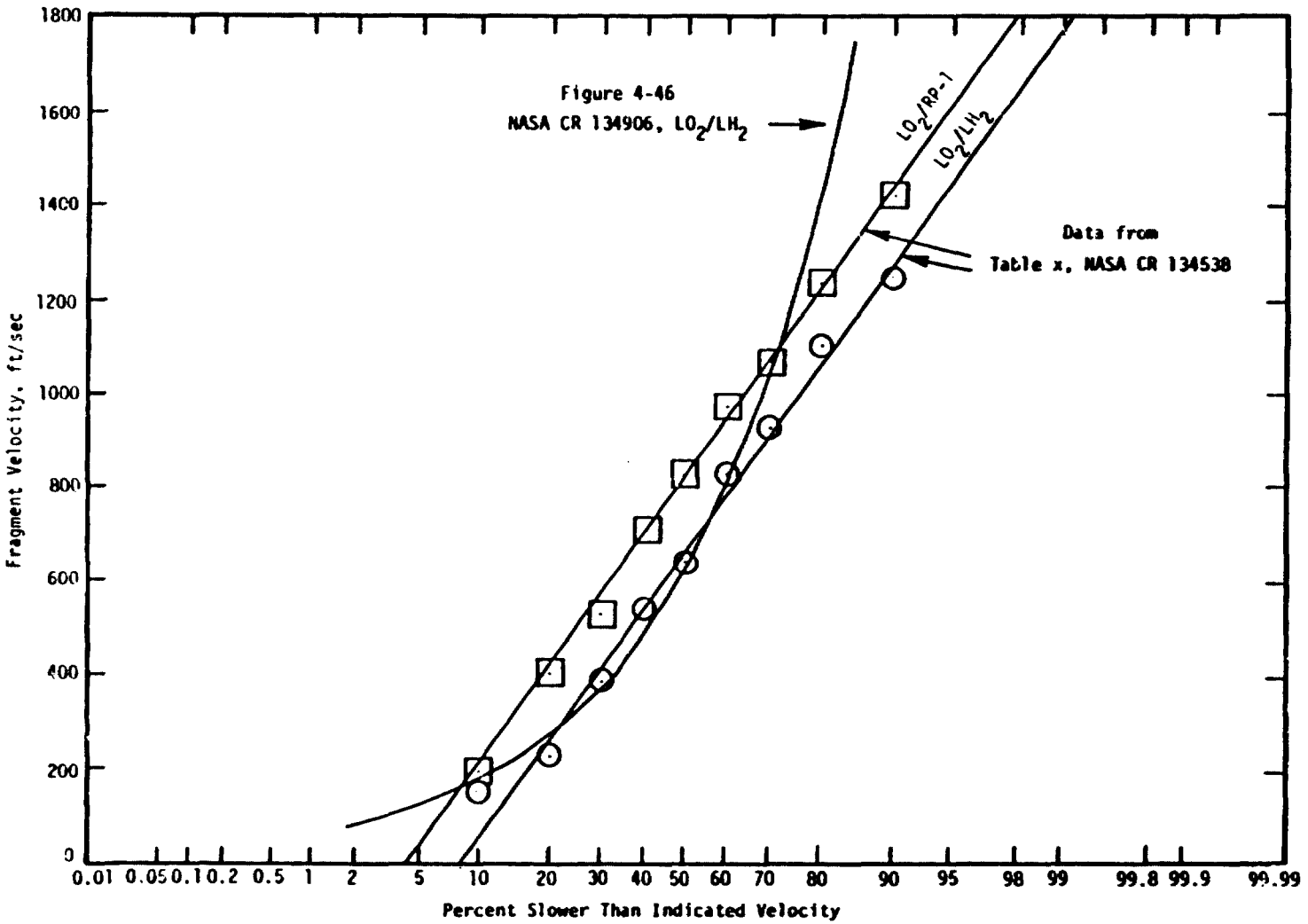

FIGURE I-4. FRAGMENT VELOCITY DISTRIBUTIONS CONFINED BY MISSILE (CBM)

In spite of the good fit of the available CBM data to a normal distribution, the real distribution cannot be normal. This is because the normal distribution has tails extending to + and - infinity, and as defined here, the velocities cannot be negative. The log-normal distribution, in which the logarithms of the variable are distributed normally, is free from this problem, as the logarithm of zero is $-\infty$. Hence the log-normal distribution is convenient for, often chosen for, and often provides a good fit to distributions extending from zero to $+\infty$. Either distribution encounters the difficulty of producing a very high velocity tail extending to $+\infty$, while physically the fragment velocities must be limited to finite values (related to the velocity of the detonation or blast wave causing the fragments). In practical application of the log-normal distributions, the tail extending to $+\infty$ is ignored, and this causes little trouble provided the population in the neglected tail is small. The same approach can be taken when using the normal distribution, and again, if the population in the negative tail is small, no serious problem is encountered.

In the case here (Figure I-4) the lines require that 5 to 10 percent of the fragments have negative velocities, a population that can hardly be considered small. Therefore, it is necessary to consider the reason we wish to fit the available data to a standard distribution. The reason is that we wish to manipulate the data in a convenient, compact form, and most importantly that we wish to extrapolate the data into the high velocity region. In this respect, it is our opinion that using the log-normal distribution leads to a serious overestimation of the population in the high velocity tail. Even though the real distribution cannot be normal, the very good fit of the higher velocity populations to the normal distribution make it definitely preferable for extrapolating into the high velocity region.

It should also be noted that the method of securing the fragment velocity data (reductions from photographs) was undoubtedly selective. Probably only the larger fragments were observed, and it is possible that very slow fragments were obscured by the fireball, smoke, and dust accompanying the explosion, and that very fast fragments might fail to appear on two frames, or might fail to leave a recognizable image due to smear.

References

I-1. Baker, W. E., et al., "Assembly and Analysis of Fragmentation Data for Liquid Propellant Vessels," NASA CR-13458, Prepared by Southwest Research Institute, San Antonio, Texas for NASA/Lewis Research Center, Cleveland, Ohio (January 1969).

I-2. Baker, W. E., et al., "Workbook for Predicting Pressure Wave and Fragment Effects of Exploding Propellant Tanks and Gas Storage Vessels," NASA CR-134906, prepared by Southwest Research Institute, San Antonio, Texas for NASA/Research Center, Cleveland, Ohio (November 1975).

APPENDIX J

REENTRY THERMAL ANALYSIS CODE (RETAC)

APPENDIX J

REENTRY THERMAL ANALYSIS CODE (RETAC)

The Reentry Thermal Analysis Code (RETAC) consists of a family of subprograms primarily directed toward reentry heating which can be combined in various ways to best simulate the specific problem under consideration. It is being upgraded almost continually both with improvements in existing subprograms and with the addition of new subprograms. Figure J-1 shows a general layout of the currently operational RETAC subprograms. They are, in general, divided into four areas: environment description, thermochemical response of materials, mechanical response of materials, and heat conduction. The heat conduction is coupled to the thermochemical and mechanical responses by moving boundary logic and a feedback of nose radius change and wall temperature to the aeroheating subroutine. Shape change feedback to the ground test environment and trajectory subprograms have been incorporated in certain cases. The link between the environment and material response includes gas boundary-layer blocking effects and surface temperature. In addition to the subprograms shown, a special subprogram can provide a simulation of internal vaporizing reservoirs with subsequent flow through a porous structure to the surface.

It should be noted that not all possible combinations of subprograms have been run to date; in fact, some programming changes are generally necessary when a new combination is first run. However, these changes generally are minor and, as experience has been gained in the use of RETAC on various problems, they are proceeding quite smoothly. This is in line with the basic philosophy of RETAC development which is to build a family of fairly simple subprograms which can then be combined in a flexible manner to fit the specific problem. As many direct interactions of pertinent phenomena as possible are incorporated. To remain flexible, an explicit finite difference method of solution is employed for the heat conduction equation.

Four alternate methods of calculating internal conduction are presently available. Multilayer, one-dimensional computations may be carried out with combined series-and-parallel heat flow paths to simulate certain two- and even three-dimensional effects. While these techniques are still used for certain problems, they have definite limitation. Therefore, alternate approaches have been developed which are a general two-dimensional axisymmetric subprogram and a three-dimensional (r, θ, z) subprogram. A two-dimensional moving boundary scheme has been developed to remove material and predict shape change.

The aerodynamic heating subroutine is essentially the original subroutine developed for RTG reentry studies. Gas gap radiation has been added for superorbital conditions, however. The aerodynamic heating subroutine calculates heating to the reentry body on the basis of local properties (pressure, temperature), configuration, and reentry mode. Either existing internal (to the program) equations can be employed, or trajectory data supplied from the 3-degree-of-freedom or 6-degree-of-freedom computer

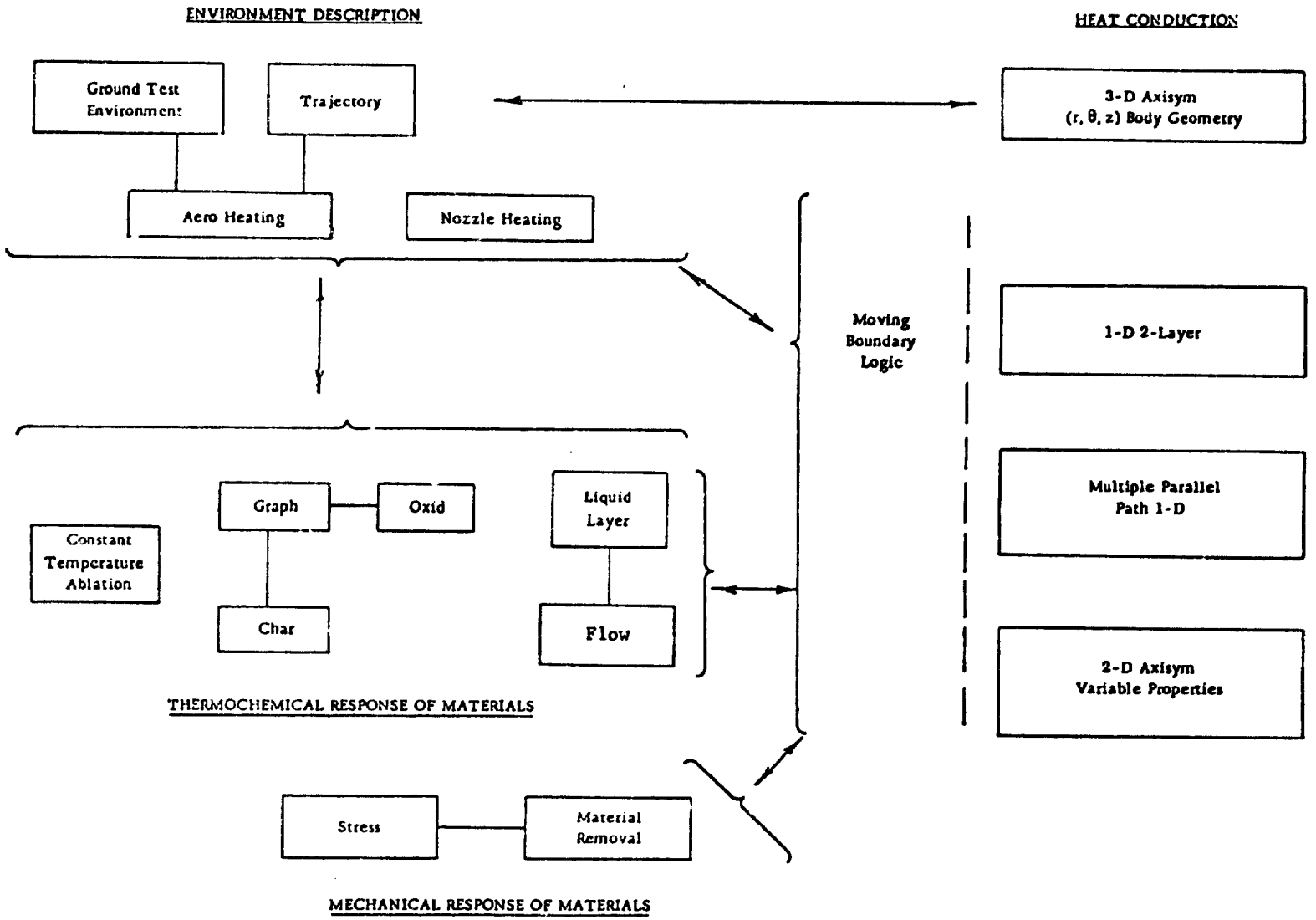

FIGURE J-1. GENERAL LAYOUT OF REENTRY THERMAL ANALYSIS CODE (RETAC)

program via punched-card input. In the aeroheating subprogram, heat transfer correlations covering free molecular theory, transition theory, and boundary layer theory are used. Coupling of the aeroheating calculations with the ablation and heat conduction analyses provides for calculation of the reentry shield surface temperature(s). Cooling of the reentry body during the latter portion of reentry is, therefore, automatically included in the analysis.

The GRAPH ablation subroutine essentially uses the general aerothermal model, which includes the reaction rate-controlled regime, the diffusion-controlled regime, and sublimation regime. The model includes continuous transitions between the regimes and also predicts when the transition occurs. It has also been modified for other oxidation processes such as tungsten oxidation.

Another ablation model used in the program is a constant temperature phase change with mass removal. This can be used for surface melting or processes such as Teflon ablation. By allowing this model to simulate the pyrolysis boundary movement and gas evolution and combining it with subprogram GRAPH at the surface of the carbon char, CHAR, a subprogram for charring ablators, has also been developed and used. An alternate method for handling charring ablators is also available in which a pyrolysis zone is defined by specifying the properties including density as a function of temperature. The rate of gas evolution is obtained by determining the rate of change of the density of the material remaining. A time delay for the gases to reach the surface can also be included.

A generalized thermomechanical response model can be used in which the subroutine OXID calculates the mass loss in the reaction rate- or diffusion-controlled regimes and the phase change ablation model takes over when a specified temperature is reached. This generalized model can ablate through layers of different materials. It can also be used in place of the GRAPH subroutine with sublimation handled in the phase change model.

The FLOW subroutine calculates the flow through a porous structure from an arbitrary number of internal reservoirs. The porosity between each reservoir and various surface locations is specified as input. The subroutine calculates the pressure within each reservoir by vapor pressure and continuity relationships and then obtains the pressure differences to the various surface locations using the external pressure distribution. The changing distances between the reservoirs and the surface locations are also recalculated as the surface recedes. The final result is a distribution of ejected flow along the surface. The heat transfer between the flowing fluid and the porous matrix can be added to the energy equation in the conduction program.

The liquid layer subprogram provides a detailed description of the dynamics of a liquid layer on an axially symmetric reentry body surface. The liquid layer is coupled into the external flow by shear and surface vaporization. It is coupled to the solid body by the liquid injection rate and distribution, surface temperature distribution, and body shape. For parametric studies, this subprogram can be run separately from RETAC.

The mechanical response of materials is predicted by a subprogram STRESS in which any of a variety of models can be used. This is then coupled with material removal logic by some assumed failure criterion. This material removal is then linked to the heat conduction by the same moving boundary logic that is used for thermomechanical material removal. At the present time, only one-dimensional stress subprograms have been linked directly with the heat conduction. However, two-dimensional thermal stress calculations have been made using two-dimensional temperature profiles generated by RETAC, so the extension to a two-dimensional linked model is relatively straightforward.